

Electronic Thesis and Dissertation Repository

---

6-25-2020 10:00 AM

## Thermo-catalytic Decarboxylation of Fatty Acids and Real-World Derivatives Towards Liquid Fuels

Shaun J. Fraser, *The University of Western Ontario*

Supervisor: Charpentier, Paul, *The University of Western Ontario*

A thesis submitted in partial fulfillment of the requirements for the Master of Engineering Science degree in Chemical and Biochemical Engineering

© Shaun J. Fraser 2020

Follow this and additional works at: <https://ir.lib.uwo.ca/etd>

 Part of the [Catalysis and Reaction Engineering Commons](#)

---

### Recommended Citation

Fraser, Shaun J., "Thermo-catalytic Decarboxylation of Fatty Acids and Real-World Derivatives Towards Liquid Fuels" (2020). *Electronic Thesis and Dissertation Repository*. 7247.  
<https://ir.lib.uwo.ca/etd/7247>

This Dissertation/Thesis is brought to you for free and open access by Scholarship@Western. It has been accepted for inclusion in Electronic Thesis and Dissertation Repository by an authorized administrator of Scholarship@Western. For more information, please contact [wlsadmin@uwo.ca](mailto:wlsadmin@uwo.ca).

## Abstract

The production of green diesel through waste fats and oils is a promising route to producing renewable transportation fuels that are energy dense, have low oxygen content, low nitrogen content, and possess excellent cold flow properties. However, producing green diesel can be expensive, as most methods use expensive noble metals catalysts such as platinum or palladium, use expensive hydrogen gas, and/or use pyrolysis and thermal cracking to reduce hydrocarbon chain length and lose energetic carbon-hydrogen bonds. This thesis studies the continuous thermo-catalytic decarboxylation of fatty acids and their derivatives to create liquid transportation fuels using an inexpensive  $\text{MoO}_x/\text{Al}_2\text{O}_3$  catalyst with no addition of hydrogen gas to produce hydrocarbons with minimal cracking.  $\text{MoO}_x/\text{Al}_2\text{O}_3$  catalyst was found to decarboxylate oleic acid up to 99% at 375 °C and decarboxylate stearic acid up to 99% at 390 °C. A feedstock of 50:50 oleic:stearic acid processed at 375°C and 3.5 h residence time had a minimum decarboxylation of 90 %, heptadecane selectivity of 55 %, and a liquid yield of 86 %. The addition of glycerol and ethanol to the reaction, which is thought to undergo reforming, lowered the necessary reaction temperature for stearic acid from 375 °C to 390 °C. Changing the reaction solvent from steam to toluene, without added glycerol/ethanol, lowered the necessary reaction temperature for stearic acid from 390 °C to 375 °C. A third-party fuel analysis confirmed that product from the process was suitable as a commercial diesel fuel, which makes this a possible route for green diesel production.

Keywords: decarboxylation, fatty acids, green diesel, thermochemical, green solvent

## Summary for Lay Audience

The use of fossil fuels is associated with the emission of greenhouse gases and therefore, global warming. A greenhouse gas increases the amount of heat our atmosphere is able to retain and effectively increases average global temperatures, helping to cause global warming. When fossil fuels are burned for energy, they produce carbon dioxide (CO<sub>2</sub>), a gas known to be a potent greenhouse gas. An increase in global average temperatures is correlated to an increase in droughts, larger category storms, and other adverse environmental events. Decreasing the use of fossil fuels for energy is essential for reducing the impact of global warming.

Biofuels are renewable and CO<sub>2</sub> neutral alternatives to fossil fuels. Biofuels are carbon neutral because the CO<sub>2</sub> that is absorbed by the biomass is equal to the CO<sub>2</sub> that is released when the fuel is burned. When fossil fuels are burned, the CO<sub>2</sub> is sourced from underground reserves that result in a net positive amount of CO<sub>2</sub> in the atmosphere.

There are several challenges associated with producing a biofuel that has properties that are ideal for our current engines, climates, and infrastructure. Promising biomass sources for biofuels are waste fats and oils such as corn distiller's oil, yellow grease, and brown grease. These sources are composed of molecules that have long hydrocarbon chains with oxygen atoms at the head of the chain. The removal of these oxygen atoms from fats and oils improves fuel properties and makes these biofuels look and behave more akin to diesel, jet fuel, and gasoline. Decarboxylation, which uses a catalyst for the removal of the oxygen atoms in the form of CO<sub>2</sub>, is a promising method for production of liquid transportation fuels.

This thesis explored the potential of MoO<sub>x</sub>/Al<sub>2</sub>O<sub>3</sub> catalysts for the continuous production of green diesel from corn distiller's oil, oleic acid, and stearic acid. By modifying reaction conditions such as temperature, pressure, residence time, and additives, fuel was produced that was deemed suitable as diesel.

## Co-Authorship Statement

The experimental works, product analysis and catalyst characterizations were performed by Shaun Fraser in collaboration with Dr Anil Jhavar and Dr Muhammad B.I. Chowdhury under the guidance of Prof. Paul Charpentier. Dr William Z. Xu and David Hiscott assisted with analysis. The draft of this manuscript was written by Shaun Fraser and reviewed by Prof. Paul A. Charpentier.

## Acknowledgments

I would like to acknowledge the guidance and support provided by Dr. Paul Charpentier throughout the studies of my Master's degree. His endless discussions and directions have guided me to success and will continue to do so. I would also like to thank Dr. Paul Charpentier for his support outside his office, and for the tasty walleye caught on his boat.

My special thanks to Dr Anil Kumar Jhawar, without whom, this thesis would have been impossible. With the hundreds of hours spent together, you have taught me superior critical thinking skills and how to think as a scientist. While you have given me valuable tools and delicious Indian food, I regret I was only able to increase your blood pressure and give you hundreds of pages of a thesis to edit.

My continued thanks to Dr Muhammad B.I. Chowdhury, Dr. William Z. Xu, and Devin Machin for their excellent support, knowledge, and helpful discussions during my time here. I would also thank all my colleagues in Prof. Charpentier's Lab for their help in many ways and just being overall incredible people who I am glad to have met.

To my parents Colette and Joe, thank you for supporting me so I was able to pursue this degree. Thank you for teaching me to be curious and to appreciate learning.

To my significant other, Caitlin, thank you for your patience and your help during my graduate studies. After our multiple travels back and forth from Toronto, I hope to never use a greyhound bus again.

## Table of Contents

Abstract .....	ii
Summary for Lay Audience .....	iii
Co-Authorship Statement.....	iv
Acknowledgments.....	v
Table of Contents .....	vi
List of Tables .....	x
List of Figures.....	xi
Chapter 1 .....	1
1. Literature Review .....	1
1.1. Introduction.....	1
1.2. Biofuels.....	3
1.3. Lipid and FA based Biofuels .....	7
1.3.1. Biodiesel .....	7
1.3.2. Green Diesel.....	9
1.4. Deoxygenation Processes .....	12
1.4.1. Decarboxylation.....	12
1.4.2. Hydrogenation.....	13
1.5. Catalysts.....	15
1.6. Reaction Atmosphere.....	23
1.7. Feedstocks.....	24
1.8. Solvents.....	25
1.8.1. Water as a Reaction Medium .....	26
1.8.2. Supercritical Water .....	27

1.8.3. Subcritical Water .....	30
1.8.4. Steam.....	31
1.9. Catalyst Deactivation and Regeneration.....	32
1.10. Research Objectives.....	33
1.11. References.....	34
Chapter 2.....	53
2. Continuous Thermocatalytic Decarboxylation of Stearic Acid, Oleic Acid, and Corn Distiller's Oil with a MoO <sub>x</sub> Catalyst.....	53
2.1. Abstract.....	53
2.2. Introduction.....	54
2.3. Materials and Methods .....	58
2.4. Results and Discussion .....	62
2.4.1. Determination of Fatty acid content by FTIR.....	62
2.4.2. Parametric studies for the decarboxylation of oleic and stearic acid.....	64
2.4.3. Investigation of Chain Length by GC-FID.....	71
2.4.4. Decarboxylation and Product Analysis by Alkene Content in Fatty Acids.....	78
2.4.5. Decarboxylation of CDO .....	82
2.4.6. NMR of Products .....	87
2.4.7. Catalyst Characterization.....	89
2.5. Conclusions.....	100
2.6. References.....	101
Chapter 3.....	120
3. Effects of Reaction Solvent and Added Hydrogen Donor to the Continuous Thermo-catalytic Decarboxylation of Fatty Acids into Liquid Hydrocarbons.....	120
3.1. Abstract.....	120
3.2. Introduction.....	121

3.3. Materials and Methods .....	125
3.4. Results and Discussion .....	126
3.4.1. Addition of Ethanol and Glycerol into Decarboxylation Process.....	126
3.4.2. Solvent Comparisons .....	131
3.4.3. GC-FID .....	134
3.4.4. NMR of products .....	144
3.4.5. Regenerated Catalyst .....	146
3.4.6. Catalyst Characterization .....	147
3.5. Conclusions.....	160
3.6. References.....	161
Chapter 4.....	180
4. Catalyst-Free Hydrogenation of Fatty Acids and Corn Distiller’s Oil in Subcritical Water and Subsequent Decarboxylation to form Liquid Hydrocarbons .....	180
4.1. Abstract.....	180
4.2. Introduction.....	181
4.3. Materials and Methods .....	183
4.4. Results and Discussion .....	185
4.4.1. NMR Studies.....	185
4.4.2. FTIR Decarboxylation Studies .....	190
4.5. Conclusions.....	192
4.6. References.....	193
5. Conclusions and Recommendations .....	212
5.1. General Conclusions.....	212
5.2. Recommendations and Future Work .....	213
Appendix A.....	216

Curriculum Vitae ..... 223

## List of Tables

Table 1.1 List of the main green diesel producers in operation in 2020.....	10
Table 1.2 Comparison of conversion and liquid yield for green diesel and deoxygenation of oils and fatty acids in the literature .....	19
Table 2.1 Third Party fuel quality testing on 5 h collection product. Run conditions were 3.5 h residence time and a temperature of 390 °C. ....	85
Table 2.2.2. Surface Areas, Pore Volumes, and Pore Sizes of Selected Catalysts .....	90
Table 2.3 Relative weights of products on catalyst surfaces measured by TGA.....	93
Table 3.1 N <sub>2</sub> Physisorption of Catalyst surface properties .....	148
Table 3.2 Table of Thermogravimetric analysis data of spent catalysts, quantified based on combustion and evaporation temperatures.....	151
Table 4.1 Parametric study conditions and results of the saturation of oleic acid with subcritical water.....	187
Table A.5.1 Stearic acid feed processed at 390 °C with a 3.5 h residence time, product quantities over time.....	217
Table A.5.2 Stearic acid feed processed at 390 °C with 10 % glycerol and a 3.5 h residence time, product quantities over time .....	219

## List of Figures

Figure 1.1 Transportation Energy Fuel Share of Demand, Reference Case. Biofuels include ethanol and biodiesel blended with petroleum products. (National Energy Board, 2016). .....	2
Figure 1.2 Common and representative fatty acids .....	4
Figure 1.3 Comparison of biofuel production costs. White dots indicate cost values for exemplarily concepts by Deutsches Biomasseforschungszentrum (DBFZ) database .....	6
Figure 1.4 Representative transesterification reaction of a TGA reacting with an alcohol (methanol) to form FAMES and glycerol.....	8
Figure 1.5 Decarbonylation, decarboxylation, and hydrodeoxygenation reaction pathways. ..	9
Figure 1.6 Decarboxylation reaction for fatty acids. ....	12
Figure 1.7 Phase diagram of water in Celsius and MPa .....	27
Figure 1.8 Water density as a function of temperature and pressure (Castello & Fiori, 2011) .....	28
Figure 1.9 Water's dielectric constant as a function of temperature and pressure (Castello & Fiori, 2011) .....	29
Figure 2.1 1) Decarbonylation, 2) decarboxylation, and 3) hydrodeoxygenation reaction pathways. ....	55
Figure 2.2 Continuous plug-flow reactor setup used for the decarboxylation of fatty acids and oils. Oils and fatty acids used in this study are pumped via an oil pump and water via the water pump. They are mixed by a mixing valve and continue towards the fixed bed reactor. After reaction the effluent reaches a separator which separates gases and liquids. The final product is collected and then separated from the water solvent via separatory funnels. All lines in this process are heated to prevent solidification and pressure increases due to plugging.....	59

Figure 2.3 Decarboxylation over time of oleic acid at 375 °C, at 2.5 h (■) and 3.5 h (×) residence times. Time on the x-axis corresponds to reaction run time. For example, 180 minutes corresponds to the product that was collected from the condensers at the 180 minute mark during the course of the continuous process. .... 65

Figure 2.4 Decarboxylation over time of stearic acid at 375 °C at 3.5 h (■) and 5 h (×) residence times ..... 66

Figure 2.5 Decarboxylation over time of stearic acid at 390 °C at 2.5 h (■) and 3.5 h (×) Residence Times ..... 67

Figure 2.6 Decarboxylation over time of stearic acid at 400 °C at 2.5 h (■), 3.5 h (×), and 5 h (●) residence times ..... 68

Figure 2.7 Decarboxylation over time of oleic (■) and stearic acid (×) at 375 °C at 3.5 h residence time. .... 69

Figure 2.8 GC-FID fractions of oleic acid at 375°C and 3.5h res. time (black) and stearic acid at 375°C and 3.5 h res. time (white). The reaction time for both samples was 5 h..... 72

Figure 2.9 GC-FID fractions of stearic acid processed at 375 °C and 3.5 h res. time (black) and stearic acid at 375 °C and 5 h res. time (white)..... 73

Figure 2.10 Product fractions of stearic acid at 375 °C (white), 390 °C (grey), and 400 °C (diagonal lines)..... 74

Figure 2.11 Product fractions of stearic acid processed at 400 °C at residence times of 2.5 h (black), 3.5 h (white), and 5 h (diagonal lines)..... 75

Figure 2.12 Stearic acid feed processed at 390 °C with a 3.5 h residence time, product quantities over time. Percent heptadecane in black and all other products not including heptadecane in white. 76

Figure 2.13 Decarboxylation of mixtures of oleic and stearic acid. 0:100 oleic:stearic (■), 10:90 (×), 25:75 (✱), 50:50 (+), and 100:0 (●)..... 78

Figure 2.14 Product hydrocarbon fractions of mixtures of stearic and oleic acid. 0:100 oleic:stearic (grey), 10:90 (white), 25:75 (striped), 50:50 (dotted), and 100:0 (black). .....	80
Figure 2.15 Percent decarboxylation over time of CDO at 375 °C in water (●), oleic acid in water at 375 °C (×), and stearic acid at 375 °C (■) all with residence times of 3.5 h. ....	82
Figure 2.16 GC-FID fractions of products formed from oleic acid in water at 375 °C (black) and CDO in water at 375 °C (white). All experiments were run at 375 °C and 3.5 h residence time. ....	83
Figure 2.17 <sup>1</sup> H NMR spectra of (a) oleic acid, (b) stearic 375 °C 3.5h, (c) stearic 390 °C 3.5 h (4 h collection point), (d) stearic 390 °C 3.5 h (8 h collection point), (e) stearic 400 °C 3.5h. ....	87
Figure 2.18 TGA analysis of spent catalyst processed with stearic acid feed under 390 °C and a residence time of 3.5 h. TGA (TG) signal corresponds to the left axis while the derivative of the TGA signal (DT) corresponds to the right axis. ....	91
Figure 2.19 Temperature Programmed Reduction of fresh (grey) and spent (black) MoO <sub>x</sub> /Al <sub>2</sub> O <sub>3</sub> catalysts. ....	95
Figure 2.20 XRD spectra of fresh (solid line) and spent (dashed line) MoO <sub>3</sub> catalysts. There is no indication of graphitic coke (14.8 and 28.6 °) in the spent catalyst .....	96
Figure 2.21 XPS spectra for Mo/Al <sub>2</sub> O <sub>3</sub> catalysts. Spectrum on the left is of a fresh catalyst, spectrum on the right is a spent catalyst that was used with stearic acid at 375 °C and 3.5 h residence time. ....	97
Figure 2.22 NH <sub>3</sub> TPD of spent (grey) and fresh (black) MoO <sub>x</sub> /Al <sub>2</sub> O <sub>3</sub> catalysts.....	98
Figure 3.1 Percent decarboxylation over time in a PFR of stearic acid at 375°C with a residence time of 3.5 h (●). The impact of added glycerol (×) or ethanol (■) at the same conditions.....	127
Figure 3.2 Percent decarboxylation over time in a PFR of stearic acid at 390 °C (●) and a residence time of 3.5 h. The impact of additions of ethanol (■) and glycerol (×) are shown.....	128

Figure 3.3 Percent decarboxylation over time in a PFR of stearic acid at 400 °C (✕) and a residence time of 3.5 h. The impact of the additions of ethanol ( ) is shown..... 129

Figure 3.4 Percent decarboxylation over time in a PFR of oleic acid at 375 °C (■) and a residence time of 3.5 h. The impact of the addition of ethanol (✕) is shown ..... 130

Figure 3.5 Percent decarboxylation over time in a PFR of oleic acid at 375 °C in water (★), in water with ethanol (✕), in toluene (■) and oleic acid processed with no solvent (●) all with residence times of 3.5 h..... 131

Figure 3.6 Percent decarboxylation over time in a PFR of stearic acid at 375 °C in water (★), in toluene as a solvent at 375 °C (✕), stearic acid at 390 °C in water (■), and in toluene as a solvent at 390 °C (●) all with residence times of 3.5 h. .... 132

Figure 3.7 GC-FID fractions of products formed from stearic acid (black), stearic acid with 10 % w/w glycerol (white), and stearic acid with 10 % w/w ethanol (striped). All experiments were run at 375 °C and 3.5 h res. time. .... 135

Figure 3.8 GC-FID fractions of products formed from stearic acid with 10 % w/w ethanol (black) and stearic acid without any added ethanol (white). All experiments were run at 390 °C and 3.5h res. time..... 136

Figure 3.9 GC-FID fractions of products formed from stearic Acid with 10 % w/w ethanol (black) and stearic acid without any added ethanol (white). All experiments were run at 400 °C and 3.5 h res. time..... 137

Figure 3.10 GC-FID fractions of products formed from oleic acid with 10 % w/w ethanol (white) and oleic acid without any added ethanol (black). All experiments were run at 375 °C and 3.5 h res. time..... 138

Figure 3.11 GC-FID fractions of products formed from oleic acid in toluene at 375 °C (black), oleic acid with no added solvent (white), and oleic acid processed in water (striped). All experiments were run at 375 °C and 3.5 h res. time. .... 140

Figure 3.12 GC-FID fractions of products formed; stearic acid processed in water with 10 % ethanol at 375 °C (black), stearic acid in toluene at 375 °C (white), stearic acid processed in water with 10 % ethanol at 390 °C (striped), and stearic acid processed in toluene at 390 °C. All experiments were run with 3.5 h res. time. ....	141
Figure 3.13 Stearic acid feed processed at 390 °C with a 3.5 h residence time, product quantities over time. Percent heptadecane in black and all other products not including heptadecane in white. ....	142
Figure 3.14 <sup>1</sup> H NMR spectra of (a) oleic acid, (b) oleic acid 375 °C 3.5 h 10% ethanol, (c) oleic acid 375 °C 3.5 h, (d) stearic 375 °C 3.5 h 10% glycerol, and (e) stearic 375 °C 3.5 h. ....	144
Figure 3.15 Decarboxylation over time of CDO with a fresh catalyst (■) and CDO processed with in-situ regenerated catalyst (×).....	146
Figure 3.16 NH <sub>3</sub> TPD of MoO <sub>3</sub> /Al <sub>2</sub> O <sub>3</sub> Catalysts. In situ regenerated fresh catalyst (dashed), spent catalyst (grey), and freshly prepared catalyst (black).....	152
Figure 3.17 H <sub>2</sub> TPR profile of fresh (grey), spent (black), and regenerated (dashed) MoO <sub>x</sub> /Al <sub>2</sub> O <sub>3</sub> catalysts .....	154
Figure 3.18 XPS spectra for Mo/Al <sub>2</sub> O <sub>3</sub> catalysts. Details for each catalyst conditions can be found in each spectrum .....	156
Figure 3.19 XRD spectra of fresh gamma alumina MoO <sub>x</sub> catalyst (solid line), calcined gamma alumina (dashed and dotted line), regenerated gamma alumina MoO <sub>x</sub> catalyst (grey), and calcined theta alumina (dashed). ....	158
Figure 4.1 NMR spectrum of corn distiller's oil .....	186
Figure 4.2 <sup>1</sup> H NMR spectrum of corn distiller's oil processed under subcritical water conditions of 325 °C with a 2.5 h residence time with a water to oil ratio of 1:5. ....	186
Figure 4.3 Plot of saturation yield by residence time for oleic acid processed under temperatures of 330 °C (green), 350 °C (blue), and 360 °C (red). ....	189

Figure 4.4 Decarboxylation of saturated CDO feed at 375 °C, 500 psi and 3.5 h space time	190
Figure 4.5 Horizontal (■) vs vertical (×) decarboxylation at 375 °C, 500 psi, and 3.5 h space times	191

# Chapter 1

## 1. Literature Review

### 1.1. Introduction

Warming of the world's climate is unmistakable, and since the 1950s, many of the observed changes have been unprecedented. The atmosphere and ocean have warmed, the amount of snowfall and ice have diminished, and the sea level has risen (IPCC, 2013, 2014). The human-activity related release of greenhouse gases (GHGs) such as CO<sub>2</sub>, water vapour, N<sub>2</sub>O, and methane have been identified as causes of the increase in average global temperatures (IPCC, 2013). Most greenhouse gases released into the atmosphere are from the electricity and transportation sectors, and constitute 34 % and 27 % of total emissions, respectively (EPA, 2012). The International Energy Agency (IEA) forecasted that the emissions of CO<sub>2</sub> from the transportation sector would increase by 92 % between 1990 and 2020 and an estimated 8.6 billion metric tons CO<sub>2</sub> to be released into the atmosphere from 2020 to 2035 (Chapman, 2007), (Gorham, 2002). In Canada, petroleum product use will continue to grow for at least the next two and a half decades, and fossil fuels will remain the dominant source of energy.

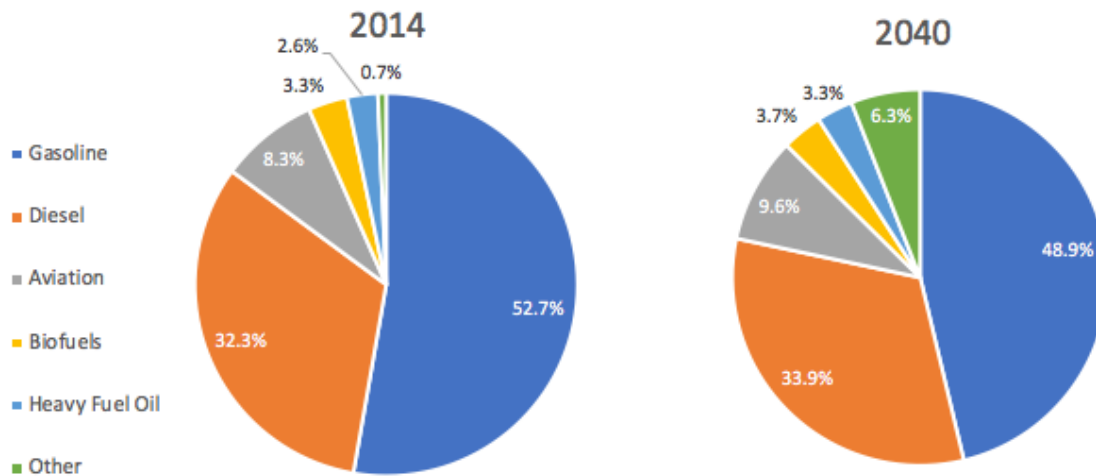


Figure 1.1 Transportation Energy Fuel Share of Demand, Reference Case. Biofuels include ethanol and biodiesel blended with petroleum products. (National Energy Board, 2016).

Diesel fuel is projected to increase in Energy Fuel share in the transport sector from 32.3% to 33.9% from 2014 to 2040 (National Energy Board, 2016). By 2040 Canadian crude oil production is projected to reach 5.7 MMb/d, 41 % higher than 2015 levels. A combination of consumer demand for petroleum products and political targets for reduced CO<sub>2</sub> emissions (Paris Agreement) will make renewable biofuels a key commodity of the future.

## 1.2. Biofuels

Biofuels are typically sourced from three major feedstocks; lignocellulosic, amorphous sugars, and triglycerides (Demirbas, 2009). Lignocellulosic biomass is a widely available feedstock consisting of rigid cellulose fibers, hemicelluloses, and lignin (Somerville, Youngs, Taylor, Davis, & Long, 2010). Lignocellulosic biomass comprises 35–50% cellulose, 20–35% hemi-cellulose, and 10–25% lignin. Cellulose is the main component of lignocellulosic biomass, and as such, it is thought that approximately half of all organic carbon in the biosphere exists as cellulose (Somerville et al., 2010; Zhou, Xia, Lin, Tong, & Beltramini, 2011). Even with the high abundance of this feedstock, the low energy density of cellulose does not permit the production of cheap fuels and value-added chemicals (Bell, Gates, Ray, & Thompson, 2008). Amorphous sugars are simple sugars and starches and may suffer the same energy density issues as ligno-cellulosics, but this may not be their largest issue. Amorphous sugars can also be consumed as food and may cause prices for these foods to increase as the use of these feedstocks increase (Babcock, 2012). However, this type of feedstock has more value as food than fuel. This can create serious economic impediments for the sale and distribution of these fuels (Condon, Klemick, & Wolverton, 2015).

The final feedstock category is triglyceride-based fats and oils. Triglycerides (TGAs) are the main constituent of vegetable oils, are easily transported and processed due to being liquid, and have energy densities similar to that of diesel (Button, 2010). Oils are composed of glycerol and the fatty acids, typically in a 1:3 molar ratio of glycerol to fatty acids (FAs). FAs are carboxylic acids with long aliphatic chain tails, which can contain one, multiple, or no alkene bonds. Palmitic, stearic, and lauric acid are saturated fatty acids with no alkene bonds. Unsaturated FAs contain alkene bonds, examples of which included oleic acid (1 C=C), linoleic acid (2 C=C's), and linolenic acid (3 C=C's). Various FAs can be seen in Figure 2.1 below.

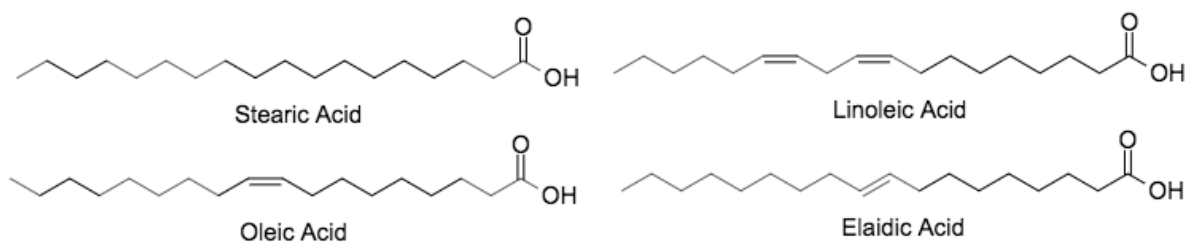


Figure 1.2 Common and representative fatty acids

Bio-Oils from FAs and TGAs have multiple potential sources from which they can be harvested. Fuels can be produced from edible fuel oils such as corn oil, but stated previously, many negative socio-economic outcomes may come from using food as fuel (Condon et al., 2015). To prevent these issues, non-edible plant seed oils may be used, such as jatropha tree (*Jatropha curcas*), karanja (*Pongamia pinnata*), mahua (*Madhuca indica*), castor bean seed (*Ricinus communis*), neem (*Azadirachta indica*), rubber seed tree (*Hevea brasiliensis*), etc (Demirbas, 2009). These seed oils may use land that is considered unproductive and not interfere with traditional farmlands, and will not exacerbate the food vs fuel debate (Sahoo, Das, Babu, & Naik, 2007). However, plants like the karanja are mostly cultivated and harvested in tropical and sub-tropical regions (India, 2014).

TGA and FA feedstocks can potentially be sourced from algal oils. Algal biofuels are seen as an attractive source because of their minimal environment and freshwater impacts, high flash points, and can be produced in both salt-water and wastewater (J. Yang et al., 2011), (Dinh, Guo, & Sam Mannan, 2009), (Demirbas, 2011). Compared to plants such as *Jatropha*, algae boast a growth rate of 20-30 times faster (Demirbas & Fatih Demirbas, 2011). Algae can produce 7-31 times more oil than palm oil and 250 times the amount of oil per acre as soybeans (Shay, 1993). Like non-edible seed oils, it does not conflict with food for land use (Paul Abishek, Patel, & Prem Rajan, 2014).

Waste cooking oil can be a renewable feedstock for liquid fuel production. During cooking, oils can hydrolyze and degrade into different compounds such as polymers, volatiles, FFA, and other degradation products. The content of FAs, TGAs, water, and other by-products significantly alter the biodiesel conversion process, which can be costly (Knothe, 2007). In fact, quality

properties of waste oils (presence of polymers, volatiles, FFAs, water etc.) may be more problematic than those from vegetable oils (Abbas et al., 2016).

Overall, many factors determine what feedstocks may be ideal for biomass to biofuel conversion. Economic factors such as supply, demand, cost, cost of storage etc. For TGA feedstocks, properties such as density, stability, oil saturation content, free fatty acid content, and various other chemical and physical characteristics play major roles in product quality. One of the principle factors that determines the viability of TGAs as a feedstock is their market price. When producing biodiesel from TGAs, the largest input cost to the process is the seed oil feedstock itself (Wan Omar & Saidina Amin, 2011). One strategy to decrease the biodiesel production cost is to use cheaper and nonedible vegetable oils (jatropha and camelina oil), animal fats, and waste oils as feedstocks. However, these low-cost feedstocks usually contain significant quantities of Free Fatty Acids and water, which can deactivate biodiesel catalysts, increase costs related to product separation, and decrease overall product yield (Jiménez-López, Jiménez-Morales, Santamaría-González, & Maireles-Torres, 2011) ,(Junhua Zhang, Chen, Yang, & Yan, 2010). Despite these costs, TGAs and Free Fatty Acids still have much potential and have some of the lowest costs among all three types of feedstocks (lignocellulosic, amorphous sugars, TGAs), as seen in Figure 1.3 (Müller-Langer, Majer, & O’Keeffe, 2014).

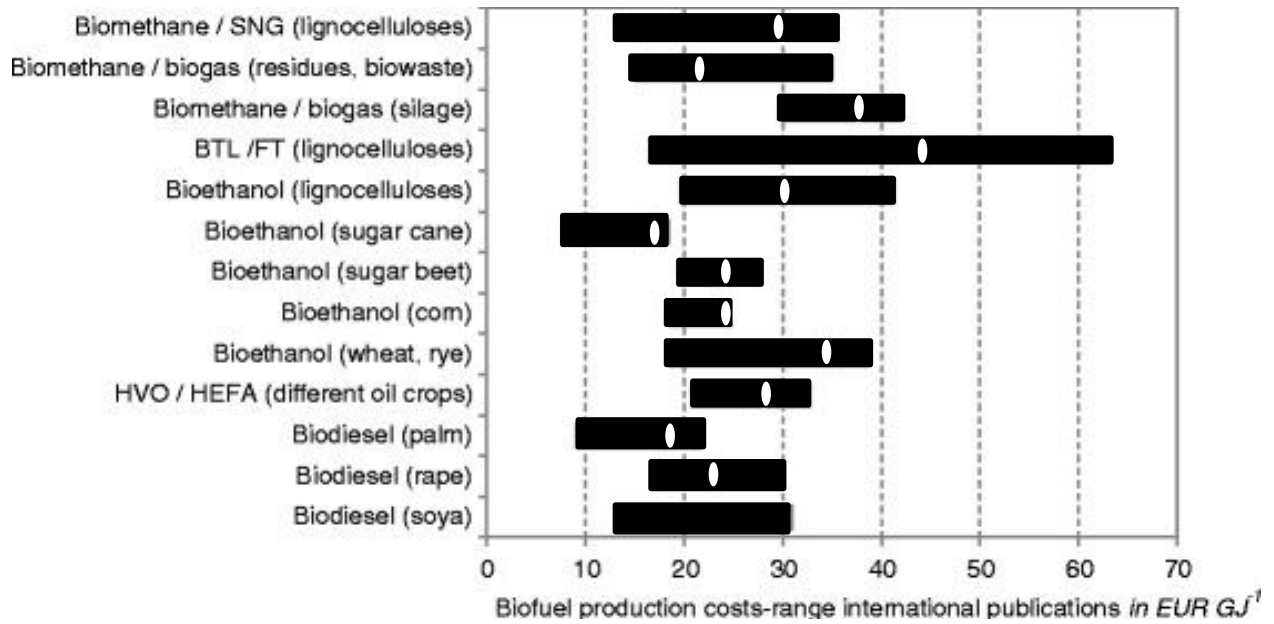


Figure 1.3 Comparison of biofuel production costs. White dots indicate cost values for exemplarily concepts by Deutsches Biomasseforschungszentrum (DBFZ) database

## 1.3. Lipid and FA based Biofuels

Lipid and FA based biofuels are most commonly produced in the form of biodiesel or green diesel. These fuels require no change in current diesel infrastructures or modifications to current engines. These properties are among some of the reasons why there is much interest in these two transportation fuels.

### 1.3.1. Biodiesel

While seed and vegetable oils are very energy dense and have low viscosities, they cannot be directly used as fuel. They contain free fatty acids, phospholipids, sterols, water, and other impurities which can lead to clogging of the engine and degradation of the engine (Sawangkeaw & Ngamprasertsith, 2013). To counteract these issues, purification and modification of the oils is essential. Transesterification, pyrolysis and emulsification are processes used to convert the plant oils into biofuels. However, transesterification is the most common process, which produces biodiesel.

The global biodiesel market value stood at USD 36.42 billion in 2019 and is projected to grow at a healthy compound annual growth rate of 4.7% towards 2025 (Adroit Market Research, 2019). While some European markets are phasing out diesel and other combustion engines (IEA, 2020), biodiesel use is growing in markets such as USA and Brazil (Adroit Market Research, 2019).

Biodiesel is comprised of Fatty Acid Methyl Esters (FAME) which are produced from transesterification. Transesterification is the process of exchanging the organic group R'' of an ester with the organic group R' of an alcohol (Otera, 1993). This process of creating biodiesel FAMEs can be seen in

Figure 1.4. Glycerol is a by-product of this reaction.

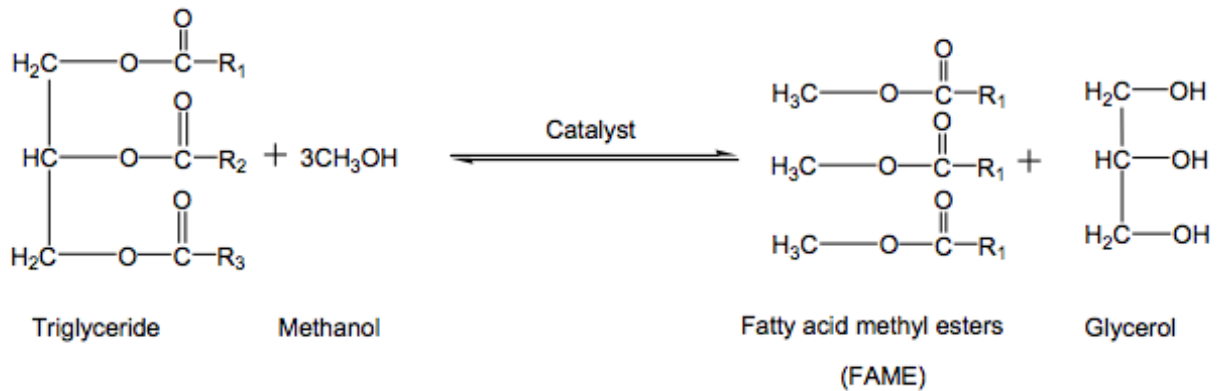


Figure 1.4 Representative transesterification reaction of a TGA reacting with an alcohol (methanol) to form FAMES and glycerol

Methanol is the most common alcohol used due to its relatively low cost, but ethanol, propanol, and butanol can also be used (Ramadhas, Jayaraj, & Muraleedharan, 2005). Acid and base catalysts can be used for this reaction; however, basic catalysts have been found to have higher yields compared to acidic catalysts. The most common basic catalysts for this process are KOH and NaOH. It has been found that higher percentages of FFAs reduce the overall yield for biodiesel, and so this must be selected for when choosing feedstocks. Since KOH and NaOH are homogeneous catalysts, separation and neutralization of the catalyst and separation of the product is challenging which leads to material loss, decreased yields, and increased production costs (Di Serio et al., 2007).

Biodiesel as a renewable transportation fuel has many merits and advantages. With minor modifications to the feedstock, the biodiesel process creates a product with similar fuel properties to diesel, has very low SO<sub>x</sub> emissions, and requires little alteration of storage infrastructure and engines (Müller-Langer et al., 2014). Biodiesel has its fair share of disadvantages as well. Traditional petroleum-derived diesel comprises about 75% saturated hydrocarbons and 25% aromatic hydrocarbons (Chou, Riviere, & Monteiro-Riviere, 2002), whereas biodiesel is comprised of FAMES which contain multiple oxygen molecules. The oxygen atoms contained in the esters contribute to higher viscosities, higher cloud points, and higher acid values than petroleum diesel. These properties are far more detrimental in cold climates, such as Canada (Centeno, Laurent, & Delmon, 1995). Additionally, Biodiesel has much higher NO<sub>x</sub> emissions,

lower oxidative stability and poor cold flow properties compared to conventional diesel, leaving much to be desired (Lin, Zhu, & Tavlarides, 2014).

### 1.3.2. Green Diesel

Green diesel is a fuel comprising of diesel-like hydrocarbons which have similar combustion properties to diesel. Green diesel can be produced from TGAs and FAs in mainly 3 routes; decarbonylation, decarboxylation, and hydrodeoxygenation (Jęczmionek & Porzycka-Semczuk, 2014). Figure 1.5 shows these reaction pathways for stearic acid.

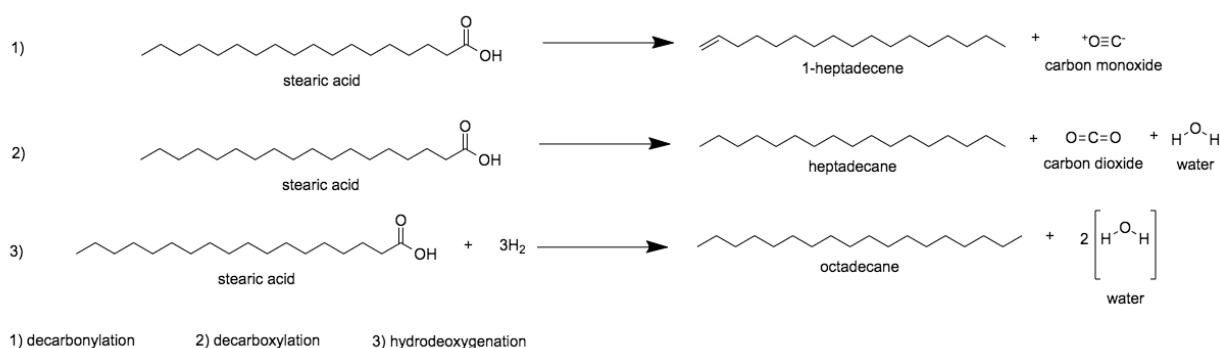


Figure 1.5 Decarbonylation, decarboxylation, and hydrodeoxygenation reaction pathways.

The main goal of these sets of reactions is total deoxygenation of the TGAs and FAs. By reducing the oxygen content of the fuel one can create a suitable drop-in diesel fuel. By comparison to biodiesel, the removal of oxygen increases the oxidative stability, lowers specific gravity, increases cetane number (an indicator of the combustion speed of diesel fuel and compression needed for ignition) and improves cold flow properties (Hoekman, 2009). As green diesel is sourced from renewable TGAs and FAs, it should be a carbon neutral fuel with a high energy density that is fully compatible with existing diesel engines. Table 1 shows the main green diesel producers in operation in 2018 (Douvartzides, Charisiou, Papageridis, & Goula, 2019).

Table 1.1 List of the main green diesel producers in operation in 2020

Company	Location	Feedstocks	Capacity	Technology
Neste	The Netherlands	Vegetable oil and waste animal fat	1,000,000 ton/year	Hydrodeoxygenation
Neste	Singapore	Vegetable oil and waste animal fat	1,000,000 ton/year	Hydrodeoxygenation
Diamond Green Diesel	USA	Non-edible vegetable oils and fats	900,000 ton/year	Hydrodeoxygenation
UOP/Eni	Italy	Vegetable oils, animal fats, used cooking oils	780,000 ton/year	Hydrodeoxygenation
Neste	Finland	Vegetable oil and waste animal fat	380,000 ton/year	Hydrodeoxygenation
Altair Fuels	USA	Non-edible natural oils and agricultural waste	130,000 ton/year	Hydrodeoxygenation
UPM Biofuels	Finland	Crude tall oil	100,000 ton/year	Hydrodeoxygenation
Forge	Canada	Waste fats and oils	26,600 ton/year	Thermal cracking/pyrolysis

UOP/ENI green diesel hydroprocessing technology is an example of the hydrodeoxygenation process. UOP has been operating in Italy since 2009. In the UOP/ENI process, vegetable oil (soybean/rapeseed/palm oil) is fed to the reactor under pressure of H<sub>2</sub> at the desired reaction temperature. The process uses the hydrodeoxygenation reaction to form green diesel. The product is then separated and sent to fractionation. Valuable products (propane,

naphtha, and diesel) are then separated from the heavier fractions. Forge Hydrocarbons creates green diesel, jet fuel, and gasoline through the thermal cracking of waste fats and oils. They do not use any hydrogen or catalyst, but obtain a mixture of products (Asomaning, Mussone, & Bressler, 2014).

The products from green diesel production can also be used as feed material to produce bio-jet fuel. Kim et al. describe a two-stage process utilizing Pt supported on nanocrystalline large-pore BEA zeolite in which deoxygenated triglycerides undergo hydrocracking to form bio-jet fuel (M. Y. Kim, Kim, Lee, Lee, & Choi, 2017). The production of bio-jet fuel is important especially due to the phasing out of combustion engines in the coming decades (IEA 2020). Iceland, Ireland, Israel, Netherlands, Slovenia, and Sweden have all pledged to begin phasing out combustion engines by 2030, and Canada, France, Singapore, and Sri Lanka have a proposed commencement of 2040 (IEA 2020). However, cracking to produce bio-jet fuel has disadvantages, as hydrocracking can result in over-cracking and therefore produce low yields of jet-fuel-range alkanes and high yields of out-of-jet fuel range hydrocarbons which have lower economic value than diesel or jet fuel (W. C. Wang & Tao, 2016).

## 1.4. Deoxygenation Processes

Hydrodeoxygenation (HDO) is a hydrogenolysis process for removing oxygen from oxygen containing compounds. In the case of TGAs and FAs to green diesel, the oxygen is contained in the Carboxylic acids and esters. The HDO reaction typically occurs at temperatures from 300-600°C, under high H<sub>2</sub> gas pressure, and in the presence of a catalyst (Bell et al., 2008). Typical HDO catalysts are sulfided NiMo or CoMo supported on gamma alumina (Topsøe, Clausen, & Massoth, 2012). Reaction conditions will differ depending on the various physico-chemical properties of the feedstocks (Bell et al., 2008). While HDO green diesel has many benefits over biodiesel (Cold flow, energy density, oxidative stability) the main drawback is the costly input of H<sub>2</sub> gas.

### 1.4.1. Decarboxylation

The decarboxylation reaction involves the removal of a Carboxylic Acid group and the release of CO<sub>2</sub>. Some carboxylic acids readily decarboxylate in the presence of heat. Δ<sup>9</sup>-tetrahydrocannabinolic acid (THC) converts to Δ<sup>9</sup>-Tetrahydrocannabinol by half in 2 minutes at a temperature of 140°C (Perrotin-Brunel et al., 2011). While THC will readily decarboxylate, this is not the case with larger alkanolic acids. Therefore, FAs require more energy to facilitate decarboxylation (March, 2009). For FAs, the reaction proceeds as in Figure 1.6.

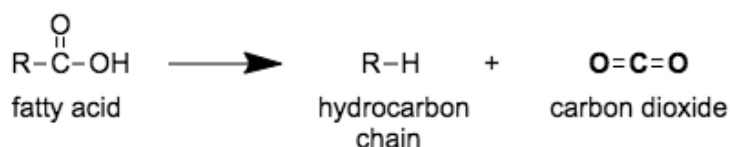


Figure 1.6 Decarboxylation reaction for fatty acids.

As stated, FAs require more energy to undergo decarboxylation than other compounds. Na et al. (Na et al., 2010) found that oleic acid would decarboxylate with a catalyst of MgO loaded on hydrotalcites at a temperature of 400 °C. Solid-like products were formed in the reaction at 350 °C, due to the competing saponification reaction when using this catalyst.

While both hydrodeoxygenation (HDO) and decarboxylation will produce deoxygenated hydrocarbons from FAs and TGAs, decarboxylation is more advantageous than HDO. H<sub>2</sub> gas input is only necessary to saturate alkene bonds in decarboxylation, and therefore has less consumption of expensive H<sub>2</sub> gas. This reduces capital expenditure and operational expenditure for the production of green diesel hydrocarbons through decarboxylation (Bell et al., 2008). The CO<sub>2</sub> emitted from this process can theoretically be captured, separated, purified, and sold.

The decarboxylation of C<sub>18</sub> fatty acids such as stearic and oleic acid will result in the production of heptadecane. Heptadecane is a C<sub>17</sub> aliphatic hydrocarbon that can be used in diesel fuel and in paraffin waxes, electrical insulation, and lubricating oils (Swick, Jaques, Walker, & Streicher, 2014). This chemical is flexible as a fuel and a value-added product.

Cracking often occurs during the decarboxylation process. These cracked products from decarboxylation can be of similar sizes of chain lengths of jet fuel (Itthibenchapong, Srifa, Kaewmeesri, Kidkhunthod, & Faungnawakij, 2017). Jet fuel exhibits a range of carbon chain length of mainly C<sub>10</sub>-C<sub>14</sub> (Chou et al., 2002).

## 1.4.2. Hydrogenation

Fatty acids and oils come in many different forms that vary in chain length and unsaturation content. These parameters can decrease or increase the overall reaction rates for deoxygenation processes. While saturated fatty acids will follow the decarboxylation pathway to produce straight chain alkanes with a high selectivity, unsaturated fatty acids will first hydrogenate into saturated fatty acids and then decarboxylate (Fu, Lu, & Savage, 2011a). While unsaturated products tend to saturate during the decarboxylation process, Yeh et al. (Yeh, Hockstad, Linic, & Savage, 2015) found that feedstocks with higher proportions of carbon-carbon double bonds decrease the catalytic activity and selectivity towards decarboxylated products. In addition to reduced activity,

Snare et al. (Mathias Snåre, Kubičková, Mäki-Arvela, Eränen, & Murzin, 2006) attributed decarboxylation catalyst deactivation to the quantity of unsaturated products which led to catalyst coking for Ru/C and Rh/C catalysts. It appears that for these specific processes, higher saturation content feedstocks are preferred.

One can decrease the unsaturation content in fatty acids and oils by either sourcing more saturated oils and fatty acids (grease, palm oil, lauric acid, stearic acid) or by subjecting unsaturated feedstocks to hydrogenation processes. At industrial conditions,  $100 < T < 200$  °C and  $14.5 < P_{H_2} < 145$  psi, polyunsaturated fatty acids are hydrogenated. This selectivity increases with increasing temperature and decreases with hydrogen pressure. Common heterogeneous catalysts in the margarine industry are often nickel-based, but expensive platinum and palladium also have good hydrogenation rates (Cheng, Dowd, Easson, & Condon, 2012; Coenen, 1986). Palladium has several advantages over nickel such as; lower contamination, lower hydrogenation temperatures, low amounts of *trans*-isomers, and can be regenerated many times (Savchenko & Makaryan, 1999).

## 1.5. Catalysts

Thermal decarboxylation of fatty acids and their esters have low yields of O<sub>2</sub>-free products at temperatures lower than 400°C (Päivi Mäki-Arvela, Kubickova, Snåre, Eränen, & Murzin, 2007). Without a catalyst, it was found that the thermal decarboxylation of stearic acid leads to 5% conversion in a semi-batch reactor under an inert helium atmosphere at 300 °C and 87 psi (Mathias Snåre et al., 2006). An effective catalyst for this process is necessary to increase the reaction rate and economize the process overall. Chemical manufacturing processes will utilize catalysts not only for increasing reaction rate, but also for selectivity of products. Selectivity of products is particularly useful for contouring processes towards added value chemicals.

Various supported monometallic catalysts such as Pd, Pt, Ru, Mo, Ni, Rh, Ir, and Os have been used for deoxygenation/decarboxylation of fatty acids and their esters. These metals have been supported on activated carbon, Al<sub>2</sub>O<sub>3</sub>, ZrO<sub>2</sub>, SiO<sub>2</sub>, and Zeolites, (Fu, Lu, & Savage, 2011b; M. Snåre, Mäki-Arvela, Simakova, Myllyoja, & Murzin, 2009). Catalyst supports are generally used to keep the active metal phase highly dispersed, increase reaction rates, increase separability of product from catalyst, and improve stability of the catalyst (Sakata, Tamaura, Imamura, & Watanabe, 2006). Catalyst support properties other than porosity, tortuosity (ratio of the diffusivity in free space to the diffusivity in the porous medium), and other mass transfer related characteristics can impact catalyst activity. Catalyst support surface acidity contributes to product cracking and coking of the catalyst (Huang et al., 2009). Hengst et al. (Hengst, Arend, Pfütznerreuter, & Hoelderich, 2015) also demonstrated that an acidic catalyst enhanced the deoxygenation and cracking of free fatty acids into liquid hydrocarbons. This property was also found by the Charpentier group (Hossain, Chowdhury, Jhawar, Xu, Biesinger, et al., 2018) in the comparison of acidity and activity of Mo/Al<sub>2</sub>O<sub>3</sub>, MgO/Al<sub>2</sub>O<sub>3</sub>, and Ni/Al<sub>2</sub>O<sub>3</sub> catalysts. Activated carbon supports have also been used in the deoxygenation of FAs to hydrocarbons, and have been found to have effective reaction rates and reduced rates of coking and fouling (W. Scaroni, Jenkins, & Walker, 1985), (Hossain, Chowdhury, Jhawar, Xu, & Charpentier, 2018). However, catalyst regeneration is problematic with carbon supports. When deactivation is related to the coking of the catalyst, the catalyst is heated under air at temperatures >600 °C to burn the coke from the catalyst

(Kern & Jess, 2005). Activated carbon supports are consumed from this process, but regeneration methods involving KOH as a chemical activating agent are currently under investigation.

Snåre et al. (Mathias Snåre et al., 2006) have screened various catalysts for their activity towards decarboxylation at 300 °C with a He pressure of 87 psi, and found the catalyst reactivities are in order of Pd>Pt>Ni>Rh>Ir>Ru>Os. Noble metal catalysts have some of the highest hydrodeoxygenation yields, but they are in short supply and therefore very costly (Fu, Lu, et al., 2011b), (M. Snåre et al., 2008). This cost coupled with fast deactivation has given rise to research into the development of more affordable catalysts (Santillan-Jimenez & Crocker, 2012). When considering monometallic catalysts in general, Peng et al. (B. Peng, Zhao, Kasakov, Foraita, & Lercher, 2013) performed deoxygenation of palmitic acid under H<sub>2</sub> and inert environments and concluded that for monometallic catalysts, a source for disassociated hydrogen protons on the catalyst surface is required to provide adequate results. Wu et al. (Wu et al., 2016) studied the decarboxylation of stearic acid over Ni/C in an inert atmosphere and the results indicated that the Ni/C catalysts completely converted stearic acid to oxygen-free products with 80% of heptadecane selectivity at 370 °C. To have the same catalytic performances, the decarboxylation reaction over Ni/C is performed 70 °C higher in temperature than for the Pd/C catalysts. Similar results in the literature show the further need for monometallic catalyst development. Miao et al. (Miao et al., 2016) found 64.2% conversion of palmitic acid to liquid paraffins (C8-C15) by hydrothermal deoxygenation using Ni/ZrO<sub>2</sub> catalyst. Robin et al. (Robin, Jones, & Ross, 2017) studied the hydrothermal processing of lipids into a mixture of alkenes and aromatics using transition metal (molybdenum, chromium, cobalt and iron) doped HZSM-5 and MoZSM-5. They also found that lipids high in poly-unsaturations promote cross-linking and heavier molecular weight products, which are undesirable by-products (Robin et al., 2017). Itthibenchapong et al. (Itthibenchapong et al., 2017) achieved jet fuel-like hydrocarbons from palm kernel oil using Ni-MoS<sub>2</sub>/γ-Al<sub>2</sub>O<sub>3</sub> catalysts. They showed that while transition metals such as Ni have good catalytic activity, Nickel loses its catalytic activity quickly compared to Pd and Pt, which have already been stated to have quick deactivation in the literature (Santillan-Jimenez & Crocker, 2012).

Bimetallic catalysts have also been tested for the deoxygenation of fatty acids. Loe et al. (Loe et al., 2016) studied the deoxygenation of stearic acid over alumina-supported bimetallic Ni-Cu and Ni-Sn catalysts. The reactions were performed at two temperatures, 260 °C and 300 °C,

with 290 psi of H<sub>2</sub> with a residence time of 1.5 h. Stearic acid conversion increased from 92 % over 20 wt % Ni/ Al<sub>2</sub>O<sub>3</sub> to 98 % over 20 wt % Ni-5 wt % Cu/Al<sub>2</sub>O<sub>3</sub> at 300 °C, with an increase of C<sub>17</sub> selectivity from 66 % to 79 %. It is suggested that this is due to Cu enhancing the reducibility of Ni and suppressing coking and cracking reactions.

Hydrodesulfurization catalysts such as CoMoS and NiMoS catalysts have shown good activity and are cheaper than noble metals such as palladium and platinum. However, leaching of the sulfur may deactivate the catalyst and possibly contaminate fuel products (Kubička & Horáček, 2011). Kubička et al. (Kubička & Horáček, 2011) found that continuous addition of dimethyldisulfide to a CoMoS/  $\gamma$ -Al<sub>2</sub>O<sub>3</sub> catalyst slowed deactivation, as it acted to help prevent sulfur removal from the catalyst.

Addition of metal oxides to Pt/Alumina catalysts have shown to increase activity of hydrodeoxygenation. Darbha et al. (Janampelli & Darbha, 2018) have shown that promotion of hydrodeoxygenation activity of Pt/Alumina catalysts activities are in the order of; MoO<sub>x</sub> > ReO<sub>x</sub> > WO<sub>x</sub> > SnO<sub>x</sub>. The Charpentier group (Hossain, Chowdhury, Jhawar, Xu, Biesinger, et al., 2018) have shown deoxygenation activity with MoO<sub>x</sub> supported on  $\gamma$ -Al<sub>2</sub>O<sub>3</sub>, without any noble metals. It has been demonstrated that acidic catalysts are preferable for enhancing decarboxylation, and therefore a MoO<sub>x</sub> catalyst was used by Hossain et al. as a low cost comparative to Pd (Hossain, Chowdhury, Jhawar, Xu, & Charpentier, 2018), (Hengst et al., 2015).

The savage group (Fu, Lu, et al., 2011b) and others have made significant advances showing the utility of using supercritical water for decarboxylation, but several challenges of these methodologies remain. The challenges are; the use of expensive platinum and palladium-based catalysts, use of relatively small 2-4 ml reactors, and the use of model compounds and feeds. In order to produce hydrocarbons from FAs in an economical and industrial scale, testing must be conducted in continuous processes, on real-world feedstocks, with affordable and effective catalysts.

Table 1.2 which was adapted from Hossain et al 2018 (Hossain et al., 2018) shows catalysts studied in the literature for production of green diesel through deoxygenation processes, as compared by reactor conditions, conversion, and liquid yield.



Table 1.2 Comparison of conversion and liquid yield for green diesel and deoxygenation of oils and fatty acids in the literature

Catalyst	Feed Material	Mode of Operation	Operating Conditions	Conversion (%)	Liquid yield (%)	Product yield or selectivity (%)
NiMo/ $\gamma$ -Al <sub>2</sub> O <sub>3</sub> and NiMoS <sub>2</sub> / $\gamma$ -Al <sub>2</sub> O <sub>3</sub> (Guzman, Torres, Prada, & Nuñez, 2010)	crude palm oil	continuous	350 °C, H <sub>2</sub> atmosphere, 2 h <sup>-1</sup> of LHSV (pilot scale)	100	~100	n/a
NiMoS <sub>2</sub> / $\gamma$ -Al <sub>2</sub> O <sub>3</sub> (Srifa et al., 2014)	refined palm kernel oil	continuous	330 °C, H <sub>2</sub> atmosphere, 1 h <sup>-1</sup> of LHSV	100	~89	>95.5 ( <i>n</i> -alkane yield)
NiMoS <sub>2</sub> / $\gamma$ -Al <sub>2</sub> O <sub>3</sub> (Kubička & Kaluža, 2010)	food grade rapeseed oil	continuous	280 °C, H <sub>2</sub> atmosphere, 0.25–4 h of contact time (V/F)	80–100	>90	n/a
Mo/ $\gamma$ -Al <sub>2</sub> O <sub>3</sub> (Hossain, Chowdhury, Jhavar, Xu, Biesinger, et al., 2018)	oleic acid	continuous	375 °C, hydrothermal conditions, 4 h of space time	91	71	18.3 (heptadecane selectivity)
Pd/mesoporous C (Päivi Mäki-Arvela et al., 2011)	tall oil fatty acid	batch	350 °C, H <sub>2</sub> atmosphere, 5.5 h of reaction time	59	n/a	91 (selectivity of heptadecane and heptadecene)
Pd/SiO <sub>2</sub> (Ford, Immer, & Lamb, 2012)	lauric acid	batch	300 °C, H <sub>2</sub> atmosphere, 4 h of reaction time	100	n/a	96 ( <i>n</i> -undecane yield)

Pd/Al <sub>2</sub> O <sub>3</sub> (Ford et al., 2012)	lauric acid	batch	300 °C, H <sub>2</sub> atmosphere, 4 h of reaction time	100	n/a	94 ( <i>n</i> -undecane yield)
Pd/C (Rozmysłowicz et al., 2012)	lauric acid	batch	300 °C, H <sub>2</sub> atmosphere, 5 h of reaction time	65	58.4	91 ( <i>n</i> -undecane selectivity)
Pt/ZIF-67/zeolite 5A (Liqui Yang & Carreon, 2017a)	lauric acid	batch	320 °C, 2 h of reaction time, CO <sub>2</sub> atmosphere	95	n/a	93.5 ( <i>n</i> -undecane selectivity)
Pt/ZIF-67/zeolite 5A (Liqui Yang & Carreon, 2017a)	palmitic acid	batch	320 °C, 2 h of reaction time, CO <sub>2</sub> atmosphere	95	n/a	91.7 (pentadecane selectivity)
Ni/ZrO <sub>2</sub> (Miao et al., 2016)	palmitic acid	batch	300 °C, H <sub>2</sub> atmosphere in the presence of H <sub>2</sub> O, 6 h of reaction time	88.2	66.8	30.2 (pentadecane yield)
Ni/ZrO <sub>2</sub> (Miao et al., 2016)	palmitic acid	batch	300 °C, H <sub>2</sub> atmosphere, 6 h of reaction time	88	61	30.2 (pentadecane yield)
Pd/CNT (Ding et al., 2015)	palmitic acid	batch	260 °C, H <sub>2</sub> atmosphere, 4 h of reaction time	93.3	n/a	85.4 (pentadecane selectivity)
MoO <sub>2</sub> /CNT (Ding et al., 2015)	palmitic acid	batch	260 °C, H <sub>2</sub> atmosphere, 4 h of reaction time	100	n/a	15.4 (pentadecane selectivity)

Pt/C (Fu, Lu, & Savage, 2010)	palmitic acid	batch	290 °C, hydrothermal conditions, 6 h of reaction time	90	90	98 (pentadecane selectivity)
Pd/C (Fu et al., 2010)	palmitic acid	batch	370 °C, hydrothermal conditions, 3 h of reaction time	n/a	n/a	63 ± 5 (pentadecane yield)
AC (Fu, Shi, Thompson, Lu, & Savage, 2011)	palmitic acid	batch	370 °C, hydrothermal conditions, 3 h of reaction time	33 ± 13	n/a	58 ± 4 (pentadecane selectivity)
AC (Fu, Shi, et al., 2011)	oleic acid	batch	370 °C, hydrothermal conditions, 3 h of reaction time	80 ± 4	n/a	7 ± 1 (heptadecane selectivity)
Pt/zeollite 5A (Liqiu Yang, Tate, Jasinski, & Carreon, 2015)	oleic acid	batch	320 °C, 2 h of reaction time, H <sub>2</sub> atmosphere	98.7	~100	72.6 ± 2 (heptadecane selectivity)
Pt/ZIF-67/zeollite 5A (Liqiu Yang et al., 2015)	oleic acid	batch	320 °C, 2 h of reaction time, CO <sub>2</sub> atmosphere	100	~100	90.5 ± 1.3 (heptadecane yield)
Pt-Ga-MOF (L. Yang, Ruess, & Carreon, 2015)	oleic acid	batch	320 °C, 2 h of reaction time, H <sub>2</sub> atmosphere	92	~84	21.5 (heptadecane selectivity)
Pt/SAPO (Ahmadi, Macias, Jasinski, Ratnasamy, & Carreon, 2014)	oleic acid	batch	325 °C, 2 h of reaction time, H <sub>2</sub> atmosphere	98	n/a	32 (heptadecane yield)

Pt-MoOx/ZrO <sub>2</sub> (Janampelli & Darbha, 2019)	oleic acid	batch	260 °C, 1 h of reaction time, H <sub>2</sub> atmosphere,	83	n/a	85.6 (C18 selectivity)
Ru/C (Jing Zhang, Huo, Li, & Strathmann, 2019)	stearic acid	batch	330 °C, hydrothermal conditions with added glycerol, 1 h of reaction time	89.1	66	66 (liquid hydrocarbons )

## 1.6. Reaction Atmosphere

The reaction atmosphere can change the types of reactions that occur and can prioritize one type of deoxygenation reaction over others. Yang et al. (Liqiu Yang & Carreon, 2017b) explored the deoxygenation of oleic acid with a Pt/ZIF67 membrane/zeolite 5Å bead catalyst under three different atmospheres; H<sub>2</sub> (reducing), N<sub>2</sub> (inert), and a CO<sub>2</sub> (oxidizing) atmosphere. A 90% heptadecane yield with a small octadecane yield (0.26%) was achieved in the CO<sub>2</sub> atmosphere, 75% heptadecane with 0.82% octadecane in N<sub>2</sub> environment, and an octadecane yield of 17.6% with a heptadecane yield of 80% was achieved in the H<sub>2</sub> atmosphere. The presence of H<sub>2</sub> gas pushed more hydrodeoxygenation to occur, and the lack of H<sub>2</sub> in both the N<sub>2</sub> and CO<sub>2</sub> atmospheres indicated decarboxylation to be the dominant reaction.

Decarboxylation does not require H<sub>2</sub> in order to progress, however, many have found that the addition of H<sub>2</sub> improves yield into desirable alkanes, saturating the alkene bonds in reactants. Saturating these alkene bonds are important, as it has been demonstrated that alkenes in gasoline may lead to an increase in reactive olefins in exhaust gases, which can be carcinogens (“Olefin by-product may be carcinogenic,” 2010). It is simultaneously desirable to limit the concentration of olefins in green diesel products and to limit the expensive input of H<sub>2</sub> gas.

To reduce the costly input of H<sub>2</sub> gas while limiting the concentration of carcinogenic alkenes combust-products, Hossain et al. (Hossain et al., 2017) and Fu et al. (Fu, Shi, et al., 2011) accomplished the hydrogenation and deoxygenation of oleic acid into heptadecane by producing *in situ* H<sub>2</sub> via the water gas shift reaction using activated carbon as a catalyst and as a source of H<sub>2</sub>. Other instances of converting unsaturated fatty acids into saturated hydrocarbon products have also been demonstrated (Na et al., 2010),(Holliday, King, & List, 1997). Glycerol and ethanol have been reported to undergo aqueous phase reforming to produce *in-situ* H<sub>2</sub> gas (Wen, Xu, Ma, Xu, & Tian, 2008), (Cruz, Ribeiro, Aranda, & Souza, 2008).

## 1.7. Feedstocks

The type of oil or FA feedstock used for the deoxygenation reaction can have a significant impact on the process. Yeh et al. (Yeh et al., 2015) converted almost 100% of oleic acid with a 35% molar yield of heptadecane over PtSnx/C catalyst at 350 °C and 2 h residence time. At the same temperature and residence time, 80% conversion of linoleic acid (C<sub>18</sub>, 2 alkene bonds) was obtained. The product comprised of 15% molar yield of heptadecane. The reaction of stearic acid provided 90% conversion with a 60% molar yield of heptadecane. The authors reported that feedstocks with increasing degrees of alkene content had decreased the catalytic activity and selectivity towards the decarboxylated products.

Chain length of the FAs have a strong impact on catalytic performance. FA conversion increases with chain length from C<sub>10</sub>-C<sub>18</sub> (Ford et al., 2012), and the selectivity to hydrocarbon decreases at the same time, (Mohite, Armbruster, Richter, & Martin, 2014) due to the higher propensity of long-chain fatty acids to undergo cracking. There does appear to an ideal chain length for maximum performance, as Maki-Arvela et al. (Päivi Mäki-Arvela et al., 2007) found that the initial reaction rate of Behnic Acid (C<sub>21</sub>) (0.36 mmol/min-gcat) was lower than that of stearic acid (C<sub>18</sub>) (0.63 mmol/min-gcat) using a commercial Pd/C catalyst in dodecane at 300°C under 5% H<sub>2</sub> balanced with Argon for 6h.

## 1.8. Solvents

In many accounts, it appears that in order for decarboxylation reactions to produce alkanes, a solvent must be present (Fu, Lu, et al., 2011a), (Päivi Mäki-Arvela et al., 2007). This suggests that an ideal solvent may possibly participate in the reaction on the catalyst surface or prevents competition for H<sub>2</sub> between solvent and reactants. An n-dodecane solvent is has shown lower decarboxylation activity compared to n-decane and mesitylene (Gosselink, Hollak, et al., 2013). Mesitylene may improve rates as it can act as a hydrogen acceptor in the decarboxylation reaction due to its unsaturations. Meanwhile, n-decane has a lower dehydrogenation capability than n-dodecane, which may have contributed to a higher degree of decarboxylation than n-dodecane (Gosselink, Hollak, et al., 2013). Another explanation for the change in activity is that solvents with lower boiling points may improve activity, as both mesitylene and decane have lower boiling points than dodecane (P. Mäki-Arvela, Snåre, Eränen, Myllyoja, & Murzin, 2008).

Water may also be used as a solvent for decarboxylation. Hossain et al. (Hossain et al., 2017) and Fu et al. (Fu, Lu, et al., 2011a) both used subcritical water as a solvent to demonstrate the production of hydrocarbons from C12 to C17, and C8 to C15 respectively. Fu et al.'s results show that saturated fatty acids follow the decarboxylation pathway for producing straight chain alkanes with a high selectivity, while unsaturated fatty acids first hydrogenate into stearic acid and then decarboxylate into heptadecane.

A solvent's properties other than being an aqueous or organic solvent can be seen to have major impacts on decarboxylation activity. Physical properties of solvents such as density, viscosity, and boiling point are important parameters to consider. Immer and Lamb (Immer, Kelly, & Lamb, 2010) demonstrated the impact of the vapor pressure of the solvent on the partial pressure of hydrogen. A lower vapor pressure of high boiling point solvent can cause the partial pressure of hydrogen to increase, which inhibits decarboxylation. Also, the use of excess amount of solvent can decrease the rate of decarboxylation due to volume expansion of the solvent.

### 1.8.1. Water as a Reaction Medium

Each year, more than twenty million tons of waste from organic solvents are released into the atmosphere. This can and has led to detrimental effects such as the pollution of the environment and the depletion of the ozone layer (Jutz, Andanson, & Baiker, 2011). In addition to environmental damage, the WHO published that a quarter of diseases occur as a result of long-term exposure to environmental pollutants and solvents (WHO, 2016). One of the main aims of the field of Green Chemistry is the reduction or replacement of toxic and damaging solvents with safer alternatives (Jessop, 2011).

Water is sometimes known as the ‘universal solvent’ and is crucial for most industrial processes. At the same time, water is abundant and non-toxic, and can be a reactant, solvent, or catalyst. This makes water an excellent solvent for a large variety of industrial processes. Water can also shift its properties depending on its phase regime, which allows one to tune various properties (density, dielectric constant, ionic product).

## 1.8.2. Supercritical Water

Figure 1.7 shows the phases of water at various pressures and temperatures. Beyond temperatures of 374 °C at pressures beyond 22.1 MPa, water enters the supercritical regime. Supercritical water (SCW) blurs the lines of liquid and gases, as some of its physical properties are closer to those of a gas while some properties are closer to those of a liquid. Density, for example, varies as a function of temperature and pressure and differs greatly once a phase change occurs. Figure 1.8 shows water density drop when water changes from liquid to gas phase, based on a model generated with a Peng-Robinson equation of state (Castello & Fiori, 2011).

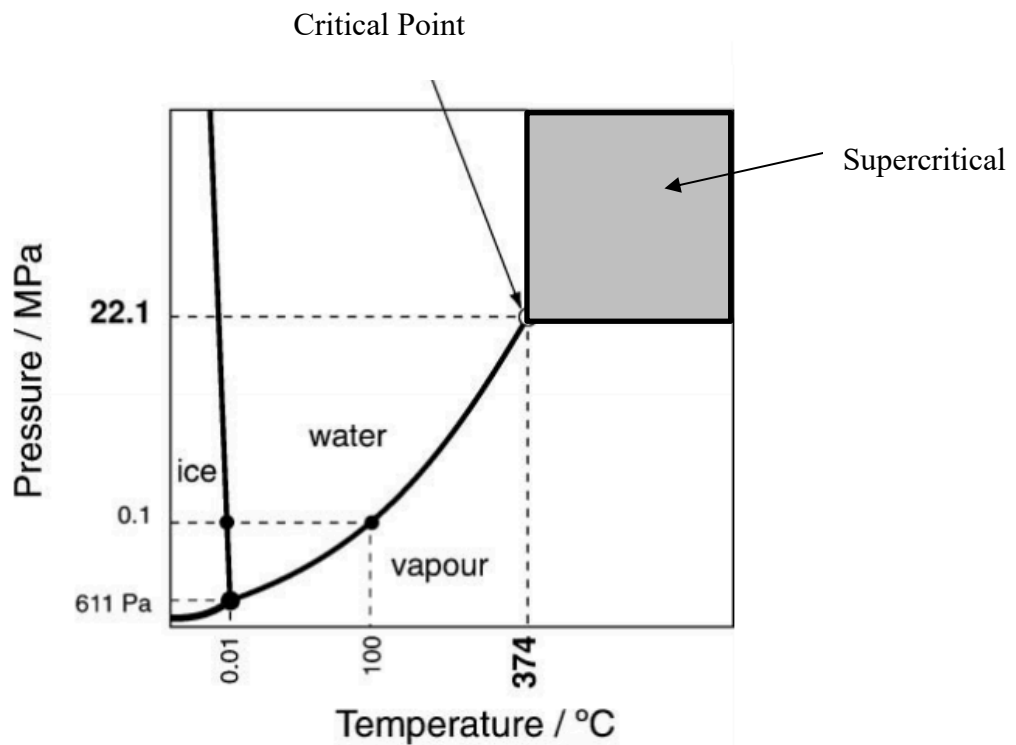


Figure 1.7 Phase diagram of water in Celsius and MPa

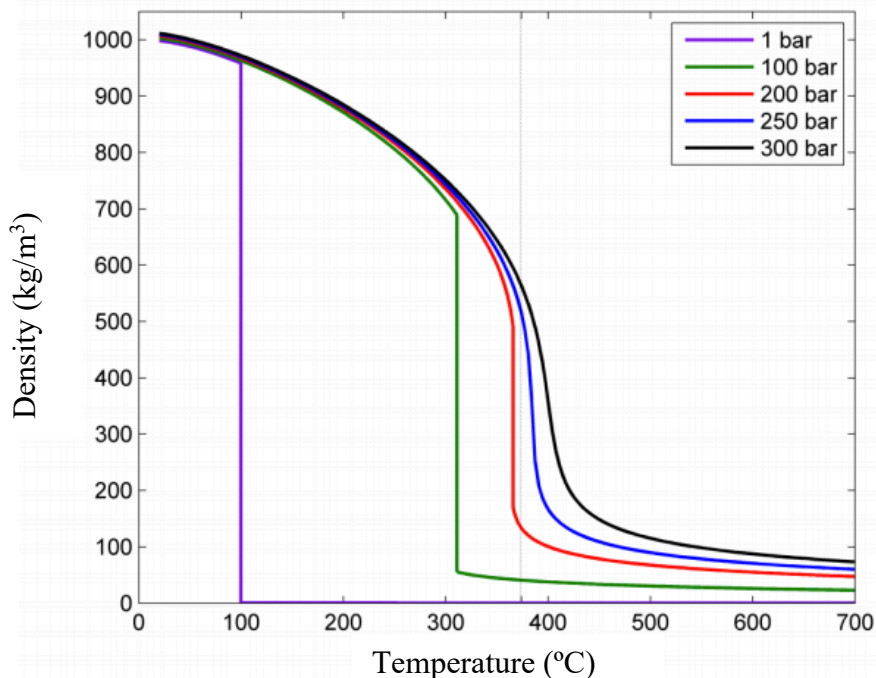


Figure 1.8 Water density as a function of temperature and pressure (Castello & Fiori, 2011)

While density is an important parameter for solvation and separation, a solvent’s dielectric constant directly relates to polarity, which describes a solvent’s ability to form a dipole. Solvents with dipoles have an affinity for solvating polar molecules, while non-polar molecules tend to be immiscible. Atmospheric room-temperature water has a high dielectric constant and is a highly polar molecule. However, as liquid water changes its phase to a gas, its dielectric constant decreases. This is because hydrogen bonding in water opposes an alignment from its dipole moment when an electric field is applied, and the strength of hydrogen bonding decreases with increasing temperatures (Castello & Fiori, 2011). As the strength of hydrogen bonding is decreased, so too does the dielectric constant. Figure 1.8 shows the relationship of water’s dielectric constant with regards to changes in temperature and pressure.

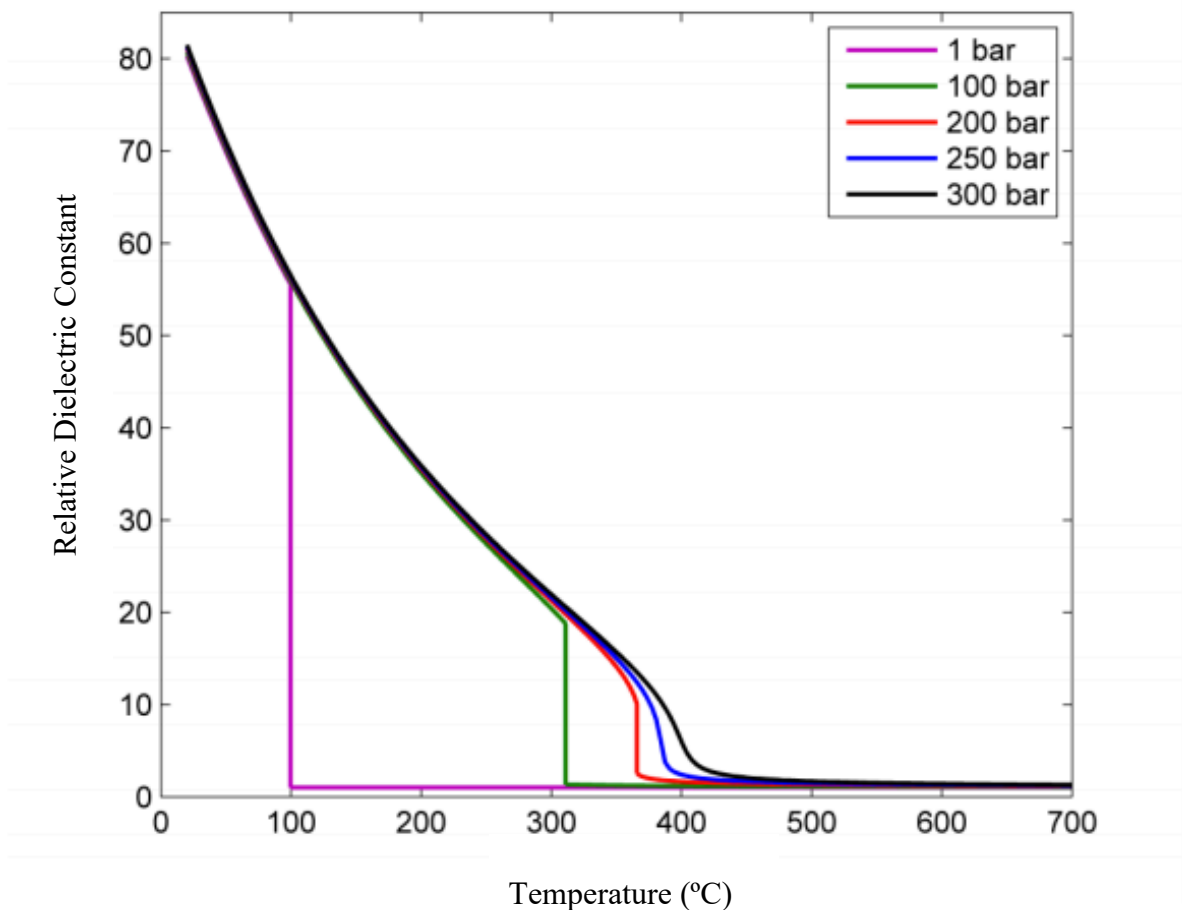


Figure 1.9 Water's dielectric constant as a function of temperature and pressure (Castello & Fiori, 2011)

The ability of water to reduce its dipole and reduce its polarity is important when processing lipid biomass. Lipids, oils, fatty acids, and their intermediates are non-polar, and having a good solvent for these compounds should theoretically increase reaction rates, reduce mass transfer limitations, and improve catalyst life.

### 1.8.3. Subcritical Water

While SCW is well-defined with specific conditions, there is no strictly specific definition of subcritical water. Fundamentally, subcritical water is not a physically defined state, as all water above the triple point and below the critical point is either liquid or gas. However, subcritical water is given a name that is separate to liquid water because there are unique properties of water at conditions just below the critical point. Mostly, the conditions of interest are above 200 °C and pressures sufficient to keep the water in liquid phase. Subcritical water has a density that lies between that of ambient and supercritical conditions. As stated previously, this is a determinant of solvation power for various compounds. The dielectric constant is quite low and has a higher ion product than ambient water or supercritical water. This means that water is more disassociated, and that any ionic reactions involving water molecules as reacting agents can be enhanced in a subcritical water environment (Westacott, Johnston, & Rossky, 2001).

Non-polar fats and oils are insoluble in ambient and room temperature water, but their miscibility increases in subcritical/supercritical water. This is because the dielectric constant of water lowers considerably in the sub/supercritical regime. In addition, fats or oils hydrolyze in hot and pressurized water to produce fatty acids. The major difference between pyrolysis and hydrothermal decarboxylation is that pyrolysis produces shorter chain length hydrocarbons whereas hot compressed water suppresses the degradation of fatty acids and produces longer chain hydrocarbons (Watanabe, Iida, & Inomata, 2006).

## 1.8.4. Steam

Steam reforming of natural gas is the most economical way of producing hydrogen gas (Steinberg & Cheng, 1989). Steam reforming of hydrocarbons is performed in fixed-bed reactors with nickel-based catalysts. Usually, the mixture of hydrocarbon and steam enters the catalyst bed at a temperature around 450 – 600 °C (Rostrup-Nielsen, Christensen, & Dybkjaer, 1998). Hydrocarbons other than natural gas are also processed for steam reforming, and natural plant oils can be too. The steam reforming of sunflower oil with a commercial nickel catalyst for the production of hydrogen was demonstrated by Marquovich et al. (Marquovich, Coll, & Montane, 2000) and 87% of stoichiometric potential of hydrogen was produced. Thermal cracking of the oil in the gas-phase was a competing process, especially above 650 °C where it converted fatty acids to a wide array of products, including ethylene and aromatics. Steam reforming of natural materials present in natural oils may help to provide hydrogen for decarboxylation.

Steam as a solvent may have additional performance over super and subcritical water due to the severity and causticity of super and subcritical water. Structure change and pore collapse of gamma alumina has been shown to happen when in aqueous environments that are > 200 °C (Ravenelle, Copeland, Kim, Crittenden, & Sievers, 2011). Yu et al. 114, (Yu & Savage, 2001) demonstrate a more than 20-fold reduction in specific surface area of metal oxide catalysts supported on  $\gamma$ -Al<sub>2</sub>O<sub>3</sub> when exposed to supercritical water conditions. High temperature subcritical and supercritical water can further increase the damage done to the catalyst. Other supports are non-ideal because acidity of the catalyst is a major contributor to decarboxylation rates (Huang et al., 2009), (Hengst et al., 2015), (Hossain, Chowdhury, Jhawar, Xu, Biesinger, et al., 2018).

## 1.9. Catalyst Deactivation and Regeneration

Decarboxylation occurs at relatively high temperatures and pressures, which can deactivate the catalyst in a number of ways. In general, catalyst deactivation occurs via;

- Poisoning of the catalyst (water in sulphided hydrodesulfurization catalysts)
- Metal Oxidation or reduction
- Metal leaching
- Physical fouling of catalyst pores (coking)
- Reduction of surface area by sintering of the active metal

Sulfur is a common catalyst poison, and any feedstocks with high sulfur content usually bind to the active metal and deactivate. Careful separation and removal of sulfur from feedstocks are generally the best solution to this form of deactivation. Several authors reported that metal oxidation (Toba et al., 2011) and metal leaching (Lestari et al., 2009) are insignificant for supported Pd catalysts. Deactivation of the catalyst due to metal sintering is largely impacted by reaction conditions and media. Pt/C and Pd/C catalysts undergo sintering in aqueous media during decarboxylation of fatty acids, but this may not cause a loss in catalytic activity (Fu et al., 2010). Instead, the loss in catalytic activity is thought to be poisoning due to the production of gases such as CO/CO<sub>2</sub>. Coking is also responsible for the deactivation of Pd/C catalysts (Päivi Mäki-Arvela et al., 2011).

## 1.10. Research Objectives

As biodiesel is non-ideal due to its low energy density, low oxidative stability, and poor cold flow properties, decarboxylation of lipid feedstocks can be an innovative solution to providing economical routes to green diesel. Although other groups have made significant advances showing the utility of using high temperature water (HTW) for decarboxylation, several challenges of their methodology remain: 1) use of expensive platinum-based catalysts; 2) use of small 2-4 ml fluidized reactors, 3) the lack of comparison of saturated vs unsaturated fatty acids in a continuous process, and 4) the lack of comparison of water to other solvents in a continuous system. The Charpentier group has already explored the decarboxylation of corn distiller's oil (CDO) in a continuous system, but additional reactor scaling up is still necessary is crucial to fill knowledge gaps for the development of a pilot plant.

This thesis conducted fundamental studies in the catalysis and reaction engineering with experimentation on a pre-pilot-scale (0.532" i.d. x 24" length) fixed bed plug flow reactor. It was explored how the addition of unsaturated feeds affects product quality by using model compounds. The impact of no solvent, toluene solvent, and steam solvents on the decarboxylation process were investigated. It was hypothesized that the addition of glycerol and ethanol to the process could reduce the reaction temperature conditions and improve product quality overall. This thesis also focused on the analysis of a cost-effective catalyst and its properties in its regenerated state. Understanding the decarboxylation mechanism, catalyst performance, impact of sacrificial ethanol/glycerol in various media requires further investigation in order to adopt this technology for commercialization.

## 1.11. References

- 11, A. D. –. (2011). Standard Test Method for Acidity in Aviation Turbine Fuel 1. *Annual Book of ASTM Standards*. <https://doi.org/10.1520/D3242-11>.This
- Abbas, J., Hussain, S., Iqbal, M. J., Nadeem, H., Qasim, M., Hina, S., & Hafeez, F. (2016). Oil industry waste: a potential feedstock for biodiesel production. *Environmental Technology (United Kingdom)*. <https://doi.org/10.1080/09593330.2016.1141997>
- Abdulkareem-Alsultan, G., Asikin-Mijan, N., Lee, H. V., Rashid, U., Islam, A., & Taufiq-Yap, Y. H. (2019). Review on thermal conversion of plant oil (Edible and inedible) into green fuel using carbon-based nanocatalyst. *Catalysts*. <https://doi.org/10.3390/catal9040350>
- Adroit Market Research. (2019). *Global Biodiesel Market Size 2019 by Feedstock (Vegetable Oil [Soybean oil, Canola oil, Other edible oils], Animal fats[Poultry, White grease, Tallow, Others]), by Application (Fuel[Automotive, Marines, Others], Power Generation, Others), by Region and Fo*. Dallas, TX.
- Afshar Taromi, A., & Kaliaguine, S. (2018). Hydrodeoxygenation of triglycerides over reduced mesostructured Ni/γ-alumina catalysts prepared via one-pot sol-gel route for green diesel production. *Applied Catalysis A: General*, 558(September), 140–149. <https://doi.org/10.1016/j.apcata.2018.03.030>
- Ahmadi, M., Macias, E. E., Jasinski, J. B., Ratnasamy, P., & Carreon, M. A. (2014). Decarboxylation and further transformation of oleic acid over bifunctional, Pt/SAPO-11 catalyst and Pt/chloride Al<sub>2</sub>O<sub>3</sub> catalysts. *Journal of Molecular Catalysis A: Chemical*. <https://doi.org/10.1016/j.molcata.2014.02.004>
- Al Alwan, B., Salley, S. O., & Ng, K. Y. S. (2015). Biofuels production from hydrothermal decarboxylation of oleic acid and soybean oil over Ni-based transition metal carbides supported on Al-SBA-15. *Applied Catalysis A: General*, 498, 32–40. <https://doi.org/10.1016/j.apcata.2015.03.012>
- Anon. (1974). FLAMMABLE AND COMBUSTIBLE LIQUIDS CODE 1973. *ANSI Stand.*

- Asomaning, J., Mussone, P., & Bressler, D. C. (2014). Thermal deoxygenation and pyrolysis of oleic acid. *Journal of Analytical and Applied Pyrolysis*. <https://doi.org/10.1016/j.jaap.2013.09.005>
- Babcock, B. A. (2012). The impact of US biofuel policies on agricultural price levels and volatility. *China Agricultural Economic Review*. <https://doi.org/10.1108/17561371211284786>
- Baltrusaitis, J., Mendoza-Sanchez, B., Fernandez, V., Veenstra, R., Dukstiene, N., Roberts, A., & Fairley, N. (2015). Generalized molybdenum oxide surface chemical state XPS determination via informed amorphous sample model. *Applied Surface Science*. <https://doi.org/10.1016/j.apsusc.2014.11.077>
- Behnejad, B., Abdouss, M., & Tavasoli, A. (2019). Comparison of performance of Ni–Mo/ $\gamma$ -alumina catalyst in HDS and HDN reactions of main distillate fractions. *Petroleum Science*. <https://doi.org/10.1007/s12182-019-0319-5>
- Bell, A. T., Gates, B. C., Ray, D., & Thompson, M. R. (2008). *Basic Research Needs: Catalysis for Energy*. <https://doi.org/10.2172/927492>
- Button, S. (2010). Biodiesel: Vehicle Fuel from Vegetable Oil. *Energy & Environment*. <https://doi.org/10.1260/0958-305x.20/21.8/1.1305>
- Castello, D., & Fiori, L. (2011). Supercritical water gasification of biomass: Thermodynamic constraints. *Bioresource Technology*. <https://doi.org/10.1016/j.biortech.2011.05.017>
- Centeno, A., Laurent, E., & Delmon, B. (1995). Influence of the support of CoMo sulfide catalysts and of the addition of potassium and platinum on the catalytic performances for the hydrodeoxygenation of carbonyl, carboxyl, and guaiacol-type molecules. *Journal of Catalysis*. <https://doi.org/10.1006/jcat.1995.1170>
- Chapman, L. (2007). Transport and climate change: a review. *Journal of Transport Geography*. <https://doi.org/10.1016/j.jtrangeo.2006.11.008>
- Charisiou, N. D., Baklavaridis, A., Papadakis, V. G., & Goula, M. A. (2016). Synthesis Gas Production via the Biogas Reforming Reaction Over Ni/MgO–Al<sub>2</sub>O<sub>3</sub> and Ni/CaO–Al<sub>2</sub>O<sub>3</sub>

- Catalysts. *Waste and Biomass Valorization*. <https://doi.org/10.1007/s12649-016-9627-9>
- Cheng, H. N., Dowd, M. K., Easson, M. W., & Condon, B. D. (2012). Hydrogenation of cottonseed oil with nickel, palladium and platinum catalysts. *JAOCs, Journal of the American Oil Chemists' Society*. <https://doi.org/10.1007/s11746-012-2036-8>
- Chou, C. C., Riviere, J. E., & Monteiro-Riviere, N. A. (2002). Differential relationship between the carbon chain length of jet fuel aliphatic hydrocarbons and their ability to induce cytotoxicity vs. interleukin-8 release in human epidermal keratinocytes. *Toxicological Sciences*. <https://doi.org/10.1093/toxsci/69.1.226>
- Choudhury, M. B. I., Ahmed, S., Shalabi, M. A., & Inui, T. (2006). Preferential methanation of CO in a syngas involving CO<sub>2</sub> at lower temperature range. *Applied Catalysis A: General*. <https://doi.org/10.1016/j.apcata.2006.08.008>
- Chowdhury, M. B. I., Hossain, M. M., & Charpentier, P. A. (2011). Effect of supercritical water gasification treatment on Ni/La 2O<sub>3</sub>-Al<sub>2</sub>O<sub>3</sub>-based catalysts. *Applied Catalysis A: General*. <https://doi.org/10.1016/j.apcata.2011.07.031>
- Clayton, C. R., & Lu, Y. C. (1989). Electrochemical and XPS evidence of the aqueous formation of Mo<sub>2</sub>O<sub>5</sub>. *Surface and Interface Analysis*. <https://doi.org/10.1002/sia.740140114>
- Coenen, J. W. E. (1986). Catalytic Hydrogenation of Fatty Oils. *Industrial and Engineering Chemistry Fundamentals*. <https://doi.org/10.1021/i100021a006>
- Condon, N., Klemick, H., & Wolverton, A. (2015). Impacts of ethanol policy on corn prices: A review and meta-analysis of recent evidence. *Food Policy*. <https://doi.org/10.1016/j.foodpol.2014.12.007>
- Corma, A., & Orchillés, A. V. (2000). Current views on the mechanism of catalytic cracking. *Microporous and Mesoporous Materials*. [https://doi.org/10.1016/S1387-1811\(99\)00205-X](https://doi.org/10.1016/S1387-1811(99)00205-X)
- Cruz, I. O., Ribeiro, N. F. P., Aranda, D. A. G., & Souza, M. M. V. M. (2008). Hydrogen production by aqueous-phase reforming of ethanol over nickel catalysts prepared from hydrotalcite precursors. *Catalysis Communications*.

<https://doi.org/10.1016/j.catcom.2008.07.031>

Demirbas, A. (2009). Political, economic and environmental impacts of biofuels: A review. *Applied Energy*. <https://doi.org/10.1016/j.apenergy.2009.04.036>

Demirbas, A. (2011). Biodiesel from oilgae, biofixation of carbon dioxide by microalgae: A solution to pollution problems. *Applied Energy*. <https://doi.org/10.1016/j.apenergy.2010.12.050>

Demirbas, A., & Fatih Demirbas, M. (2011). Importance of algae oil as a source of biodiesel. *Energy Conversion and Management*. <https://doi.org/10.1016/j.enconman.2010.06.055>

Den Otter, I. M. J. A. M. (1970). The Dimerization of Oleic Acid with a Montmorillonite Catalyst I: Important Process Parameters; Some Main Reactions. *Fette, Seifen, Anstrichmittel*. <https://doi.org/10.1002/lipi.19700720809>

Desikan, A. N., Huang, L., & Oyama, S. T. (1992). Structure and dispersion of molybdenum oxide supported on alumina and titania. *Journal of the Chemical Society, Faraday Transactions*. <https://doi.org/10.1039/FT9928803357>

Di Serio, M., Cozzolino, M., Giordano, M., Tesser, R., Patrono, P., & Santacesaria, E. (2007). From homogeneous to heterogeneous catalysts in biodiesel production. *Industrial and Engineering Chemistry Research*. <https://doi.org/10.1021/ie070663q>

Ding, R., Wu, Y., Chen, Y., Liang, J., Liu, J., & Yang, M. (2015). Effective hydrodeoxygenation of palmitic acid to diesel-like hydrocarbons over MoO<sub>2</sub>/CNTs catalyst. *Chemical Engineering Science*. <https://doi.org/10.1016/j.ces.2014.10.024>

Dinh, L. T. T., Guo, Y., & Sam Mannan, M. (2009). Sustainability evaluation of biodiesel production using multicriteria decision-making. *Environmental Progress and Sustainable Energy*. <https://doi.org/10.1002/ep.10335>

Dos Anjos, J. R. S., De Araujo Gonzalez, W., Lam, Y. L., & Frety, R. (1983). Catalytic decomposition of vegetable oil. *Applied Catalysis*. [https://doi.org/10.1016/0166-9834\(83\)80158-4](https://doi.org/10.1016/0166-9834(83)80158-4)

- Dou, B., Wang, C., Song, Y., Chen, H., & Xu, Y. (2014). Activity of Ni-Cu-Al based catalyst for renewable hydrogen production from steam reforming of glycerol. *Energy Conversion and Management*. <https://doi.org/10.1016/j.enconman.2013.10.067>
- Douette, A. M. D., Turn, S. Q., Wang, W., & Keffer, V. I. (2007). Experimental investigation of hydrogen production from glycerin reforming. *Energy and Fuels*. <https://doi.org/10.1021/ef060379w>
- Douvartzides, S. L., Charisiou, N. D., Papageridis, K. N., & Goula, M. A. (2019). Green Diesel: Biomass Feedstocks, Production Technologies, Catalytic Research, Fuel Properties and Performance in Compression Ignition Internal Combustion Engines. *Energies*. <https://doi.org/10.3390/en12050809>
- EPA. (2012). Chapter 3. Energy. In *Inventory of U.S. Greenhouse Gas Emissions and Sinks: 1990–2012*.
- Ford, J. P., Immer, J. G., & Lamb, H. H. (2012). Palladium catalysts for fatty acid deoxygenation: Influence of the support and fatty acid chain length on decarboxylation kinetics. *Topics in Catalysis*. <https://doi.org/10.1007/s11244-012-9786-2>
- Friedman, D., Masciangioli, T., & Olson, S. (2012). Replacing critical materials with abundant materials. In *The role of the chemical sciences in finding alternatives to critical resources - A workshop summary*.
- Fu, J., Lu, X., & Savage, P. E. (2010). Catalytic hydrothermal deoxygenation of palmitic acid. *Energy and Environmental Science*. <https://doi.org/10.1039/b923198f>
- Fu, J., Lu, X., & Savage, P. E. (2011a). Hydrothermal decarboxylation and hydrogenation of fatty acids over Pt/C. *ChemSusChem*. <https://doi.org/10.1002/cssc.201000370>
- Fu, J., Lu, X., & Savage, P. E. (2011b). Hydrothermal decarboxylation and hydrogenation of fatty acids over Pt/C. *ChemSusChem*, 4(4), 481–486. <https://doi.org/10.1002/cssc.201000370>
- Fu, J., Shi, F., Thompson, L. T., Lu, X., & Savage, P. E. (2011). Activated carbons for hydrothermal decarboxylation of fatty acids. *ACS Catalysis*.

<https://doi.org/10.1021/cs1001306>

Global EV Outlook 2020. (2020). In *Global EV Outlook 2020*. <https://doi.org/10.1787/d394399e-en>

Gollakota, A. R. K., Kishore, N., & Gu, S. (2018). A review on hydrothermal liquefaction of biomass. *Renewable and Sustainable Energy Reviews*. <https://doi.org/10.1016/j.rser.2017.05.178>

Gonçalves, A. A. S., Faustino, P. B., Assaf, J. M., & Jaroniec, M. (2017). One-Pot Synthesis of Mesoporous Ni-Ti-Al Ternary Oxides: Highly Active and Selective Catalysts for Steam Reforming of Ethanol. *ACS Applied Materials and Interfaces*. <https://doi.org/10.1021/acsami.6b15507>

Gorham, R. (2002). Air Pollution From Ground Transportation; An Assessment of Causes , Strategies and Tactics , and Proposed Actions for the International Community. In *The Global Initiative on Transport Emissions*.

Gosselink, R. W., Hollak, S. A. W., Chang, S. W., Van Haveren, J., De Jong, K. P., Bitter, J. H., & Van Es, D. S. (2013). Reaction pathways for the deoxygenation of vegetable oils and related model compounds. *ChemSusChem*. <https://doi.org/10.1002/cssc.201300370>

Gosselink, R. W., Stellwagen, D. R., & Bitter, J. H. (2013). Tungsten-based catalysts for selective deoxygenation. *Angewandte Chemie - International Edition*. <https://doi.org/10.1002/anie.201209809>

Guzman, A., Torres, J. E., Prada, L. P., & Nuñez, M. L. (2010). Hydroprocessing of crude palm oil at pilot plant scale. *Catalysis Today*. <https://doi.org/10.1016/j.cattod.2009.11.015>

Hengst, K., Arend, M., Pfützenreuter, R., & Hoelderich, W. F. (2015). Deoxygenation and cracking of free fatty acids over acidic catalysts by single step conversion for the production of diesel fuel and fuel blends. *Applied Catalysis B: Environmental*. <https://doi.org/10.1016/j.apcatb.2015.03.009>

Hoekman, S. K. (2009). Biofuels in the U.S. - Challenges and Opportunities. *Renewable Energy*.

<https://doi.org/10.1016/j.renene.2008.04.030>

Holliday, R. L., King, J. W., & List, G. R. (1997). Hydrolysis of Vegetable Oils in Sub- And Supercritical Water. *Industrial and Engineering Chemistry Research*.

<https://doi.org/10.1021/ie960668f>

Hossain, M. Z., Chowdhury, M. B. I., Jhavar, A. K., Xu, W. Z., Biesinger, M. C., & Charpentier, P. A. (2018). Continuous Hydrothermal Decarboxylation of Fatty Acids and Their Derivatives into Liquid Hydrocarbons Using Mo/Al<sub>2</sub>O<sub>3</sub> Catalyst. *ACS Omega*.

<https://doi.org/10.1021/acsomega.8b00562>

Hossain, M. Z., Chowdhury, M. B. I., Jhavar, A. K., Xu, W. Z., & Charpentier, P. A. (2018). Continuous low pressure decarboxylation of fatty acids to fuel-range hydrocarbons with in situ hydrogen production. *Fuel*. <https://doi.org/10.1016/j.fuel.2017.09.092>

Hossain, M. Z., Jhavar, A. K., Chowdhury, M. B. I., Xu, W. Z., Wu, W., Hiscott, D. V., & Charpentier, P. A. (2017). Using Subcritical Water for Decarboxylation of Oleic Acid into Fuel-Range Hydrocarbons. *Energy and Fuels*.

<https://doi.org/10.1021/acs.energyfuels.6b03418>

Huang, J., Jiang, Y., Marthala, V. R. R., Bressel, A., Frey, J., & Hunger, M. (2009). Effect of pore size and acidity on the coke formation during ethylbenzene conversion on zeolite catalysts. *Journal of Catalysis*. <https://doi.org/10.1016/j.jcat.2009.02.019>

Immer, J. G., Kelly, M. J., & Lamb, H. H. (2010). Catalytic reaction pathways in liquid-phase deoxygenation of C18 free fatty acids. *Applied Catalysis A: General*.

<https://doi.org/10.1016/j.apcata.2009.12.028>

India, B. (2014). *Millettia Pinnata*.

IPCC. (2013). Summary for policymakers. In *Climate Change 2014: Impacts, Adaptation, and Vulnerability. Part A: Global and Sectoral Aspects. Contribution of Working Group II to the Fifth Assessment Report of the Intergovernmental Panel on Climate Change*.

IPCC. (2014). Climate Change 2014: Summary for Policymakers. *Climate Change 2014: Impacts,*

*Adaptation and Vulnerability - Contributions of the Working Group II to the Fifth Assessment Report.* <https://doi.org/10.1016/j.renene.2009.11.012>

Itthibenchapong, V., Srifa, A., Kaewmeesri, R., Kidkhunthod, P., & Faungnawakij, K. (2017). Deoxygenation of palm kernel oil to jet fuel-like hydrocarbons using Ni-MoS<sub>2</sub>/γ-Al<sub>2</sub>O<sub>3</sub> catalysts. *Energy Conversion and Management*. <https://doi.org/10.1016/j.enconman.2016.12.034>

IUPAC. (2014). Compendium of Chemical Terminology 2nd ed. (the “Gold Book”). *Blackwell Scientific Publications, Oxford*. <https://doi.org/10.1351/goldbook.I03352>

Janampelli, S., & Darbha, S. (2018). Metal Oxide-Promoted Hydrodeoxygenation Activity of Platinum in Pt-MO<sub>x</sub>/Al<sub>2</sub>O<sub>3</sub> Catalysts for Green Diesel Production. *Energy and Fuels*. <https://doi.org/10.1021/acs.energyfuels.8b03588>

Janampelli, S., & Darbha, S. (2019). Highly efficient Pt-MoO<sub>x</sub>/ZrO<sub>2</sub> catalyst for green diesel production. *Catalysis Communications*. <https://doi.org/10.1016/j.catcom.2019.03.027>

Jęczmionek, Ł., & Porzycka-Semczuk, K. (2014). Hydrodeoxygenation, decarboxylation and decarbonylation reactions while co-processing vegetable oils over a NiMo hydrotreatment catalyst. Part I: Thermal effects - Theoretical considerations. *Fuel*. <https://doi.org/10.1016/j.fuel.2014.04.055>

Jeon, J. Y., Han, Y., Kim, Y. W., Lee, Y. W., Hong, S., & Hwang, I. T. (2019). Feasibility of unsaturated fatty acid feedstocks as green alternatives in bio-oil refinery. *Biofuels, Bioproducts and Biorefining*. <https://doi.org/10.1002/bbb.1979>

Jessop, P. G. (2011). Searching for green solvents. *Green Chemistry*. <https://doi.org/10.1039/c0gc00797h>

Jiménez-López, A., Jiménez-Morales, I., Santamaría-González, J., & Maireles-Torres, P. (2011). Biodiesel production from sunflower oil by tungsten oxide supported on zirconium doped MCM-41 silica. *Journal of Molecular Catalysis A: Chemical*. <https://doi.org/10.1016/j.molcata.2010.11.035>

- Jutz, F., Andanson, J. M., & Baiker, A. (2011). Ionic liquids and dense carbon dioxide: A beneficial biphasic system for catalysis. *Chemical Reviews*. <https://doi.org/10.1021/cr100194q>
- Katryniok, B., Paul, S., & Dumeignil, F. (2013). Recent developments in the field of catalytic dehydration of glycerol to acrolein. *ACS Catalysis*, 3(8), 1819–1834. <https://doi.org/10.1021/cs400354p>
- Kern, C., & Jess, A. (2005). Regeneration of coked catalysts - Modelling and verification of coke burn-off in single particles and fixed bed reactors. *Chemical Engineering Science*. <https://doi.org/10.1016/j.ces.2005.01.024>
- Kim, M. C., & Kim, K. L. (1996). A role of molybdenum and shape selectivity of catalysts in simultaneous reactions of hydrocracking and hydrodesulfurization. *Korean Journal of Chemical Engineering*. <https://doi.org/10.1007/BF02705881>
- Kim, M. Y., Kim, J. K., Lee, M. E., Lee, S., & Choi, M. (2017). Maximizing Biojet Fuel Production from Triglyceride: Importance of the Hydrocracking Catalyst and Separate Deoxygenation/Hydrocracking Steps. *ACS Catalysis*. <https://doi.org/10.1021/acscatal.7b01326>
- King, J. W., Holliday, R. L., & List, G. R. (1999). Hydrolysis of soybean oil: In a subcritical water flow reactor. *Green Chemistry*. <https://doi.org/10.1039/a908861j>
- Kirszensztejn, P., Przekop, R., Tolińska, A., & Maćkowska, E. (2009). Pyrolytic and catalytic conversion of rape oil into aromatic and aliphatic fractions in a fixed bed reactor on Al<sub>2</sub>O<sub>3</sub> and Al<sub>2</sub>O<sub>3</sub>/B<sub>2</sub>O<sub>3</sub> catalysts. *Chemical Papers*. <https://doi.org/10.2478/s11696-008-0104-1>
- Knothe, G. (2007). Some aspects of biodiesel oxidative stability. *Fuel Processing Technology*. <https://doi.org/10.1016/j.fuproc.2007.01.005>
- Kordouli, E., Sygellou, L., Kordulis, C., Bourikas, K., & Lycourghiotis, A. (2017). Probing the synergistic ratio of the NiMo/Γ-Al<sub>2</sub>O<sub>3</sub> reduced catalysts for the transformation of natural triglycerides into green diesel. *Applied Catalysis B: Environmental*, 209, 12–22. <https://doi.org/10.1016/j.apcatb.2017.02.045>

- Kubička, D., & Horáček, J. (2011). Deactivation of HDS catalysts in deoxygenation of vegetable oils. *Applied Catalysis A: General*. <https://doi.org/10.1016/j.apcata.2010.10.034>
- Kubička, D., & Kaluža, L. (2010). Deoxygenation of vegetable oils over sulfided Ni, Mo and NiMo catalysts. *Applied Catalysis A: General*. <https://doi.org/10.1016/j.apcata.2009.10.034>
- Lestari, S., Päivi, M. A., Bernas, H., Simakova, O., Sjöholm, R., Beltramini, J., ... Murzin, D. Y. (2009). Catalytic deoxygenation of stearic acid in a continuous reactor over a mesoporous carbon-supported pd catalyst. *Energy and Fuels*. <https://doi.org/10.1021/ef900110t>
- Lin, R., Zhu, Y., & Tavlarides, L. L. (2014). Effect of thermal decomposition on biodiesel viscosity and cold flow property. *Fuel*. <https://doi.org/10.1016/j.fuel.2013.10.034>
- Loe, R., Santillan-Jimenez, E., Morgan, T., Sewell, L., Ji, Y., Jones, S., ... Crocker, M. (2016). Effect of Cu and Sn promotion on the catalytic deoxygenation of model and algal lipids to fuel-like hydrocarbons over supported Ni catalysts. *Applied Catalysis B: Environmental*. <https://doi.org/10.1016/j.apcatb.2016.03.025>
- Luo, N., Fu, X., Cao, F., Xiao, T., & Edwards, P. P. (2008). Glycerol aqueous phase reforming for hydrogen generation over Pt catalyst - Effect of catalyst composition and reaction conditions. *Fuel*. <https://doi.org/10.1016/j.fuel.2008.06.021>
- Ma, X., Cui, K., Hao, W., Ma, R., Tian, Y., & Li, Y. (2015). Alumina supported molybdenum catalyst for lignin valorization: Effect of reduction temperature. *Bioresource Technology*. <https://doi.org/10.1016/j.biortech.2015.05.032>
- Madsen, A. T., Ahmed, E. H., Christensen, C. H., Fehrmann, R., & Riisager, A. (2011). Hydrodeoxygenation of waste fat for diesel production: Study on model feed with Pt/alumina catalyst. *Fuel*. <https://doi.org/10.1016/j.fuel.2011.06.005>
- Mäki-Arvela, P., Snåre, M., Eränen, K., Myllyoja, J., & Murzin, D. Y. (2008). Continuous decarboxylation of lauric acid over Pd/C catalyst. *Fuel*. <https://doi.org/10.1016/j.fuel.2008.07.004>
- Mäki-Arvela, Päivi, Kubickova, I., Snåre, M., Eränen, K., & Murzin, D. Y. (2007). Catalytic

- deoxygenation of fatty acids and their derivatives. *Energy and Fuels*.  
<https://doi.org/10.1021/ef060455v>
- Mäki-Arvela, Päivi, Rozmysłowicz, B., Lestari, S., Simakova, O., Eränen, K., Salmi, T., & Murzin, D. Y. (2011). Catalytic deoxygenation of tall oil fatty acid over palladium supported on mesoporous carbon. *Energy and Fuels*. <https://doi.org/10.1021/ef200380w>
- March, J. (2009). The decarboxylation of organic acid. *Journal of Chemical Education*, 40(4), 212.  
<https://doi.org/10.1021/ed040p212>
- Marquevich, M., Coll, R., & Montane, D. (2000). Steam Reforming of Sunflower Oil for Hydrogen Production. . *Industrial & Engineering Chemistry Research*.  
<https://doi.org/10.1021/ie9910874>
- Melero, J. A., Clavero, M. M., Calleja, G., García, A., Miravalles, R., & Galindo, T. (2010). Production of biofuels via the catalytic cracking of mixtures of crude vegetable oils and nonedible animal fats with vacuum gas oil. *Energy and Fuels*.  
<https://doi.org/10.1021/ef900914e>
- Miao, C., Marin-Flores, O., Davidson, S. D., Li, T., Dong, T., Gao, D., ... Chen, S. (2016). Hydrothermal catalytic deoxygenation of palmitic acid over nickel catalyst. *Fuel*.  
<https://doi.org/10.1016/j.fuel.2015.10.120>
- Miao, C., Marin-Flores, O., Dong, T., Gao, D., Wang, Y., Garcia-Pérez, M., & Chen, S. (2018). Hydrothermal Catalytic Deoxygenation of Fatty Acid and Bio-oil with in Situ H<sub>2</sub>. *ACS Sustainable Chemistry and Engineering*. <https://doi.org/10.1021/acssuschemeng.7b02226>
- Mo, N., & Savage, P. E. (2014). Hydrothermal catalytic cracking of fatty acids with HZSM-5. *ACS Sustainable Chemistry and Engineering*. <https://doi.org/10.1021/sc400368n>
- Mohite, S., Armbruster, U., Richter, M., & Martin, A. (2014). Impact of Chain Length of Saturated Fatty Acids during Their Heterogeneously Catalyzed Deoxygenation. *Journal of Sustainable Bioenergy Systems*. <https://doi.org/10.4236/jsbs.2014.43017>
- Müller-Langer, F., Majer, S., & O’Keeffe, S. (2014). Benchmarking biofuels—a comparison of

- technical, economic and environmental indicators. *Energy, Sustainability and Society*.  
<https://doi.org/10.1186/s13705-014-0020-x>
- Na, J. G., Yi, B. E., Kim, J. N., Yi, K. B., Park, S. Y., Park, J. H., ... Ko, C. H. (2010). Hydrocarbon production from decarboxylation of fatty acid without hydrogen. *Catalysis Today*.  
<https://doi.org/10.1016/j.cattod.2009.11.008>
- National Energy Board. (2016). Canada's Energy Future 2016 Energy Supply and Demand Projections to 2040.
- Ndubuisi, R. U., Sinichi, S., (Cathy) Chin, Y. H., & Diosady, L. L. (2019). Diesel Precursors Via Catalytic Hydrothermal Deoxygenation of Aqueous Canola Oil Emulsion. *JAACS, Journal of the American Oil Chemists' Society*. <https://doi.org/10.1002/aocs.12208>
- Nikolskaya, E., & Hiltunen, Y. (2018). Determination of Carbon Chain Lengths of Fatty Acid Mixtures by Time Domain NMR. *Applied Magnetic Resonance*.  
<https://doi.org/10.1007/s00723-017-0953-2>
- Olefin by-product may be carcinogenic. (2010). *Chemical & Engineering News*.  
<https://doi.org/10.1021/cen-v054n035.p008>
- Otera, J. (1993). Transesterification. *Chemical Reviews*. <https://doi.org/10.1021/cr00020a004>
- Paul Abishek, M., Patel, J., & Prem Rajan, A. (2014). Algae Oil: A Sustainable Renewable Fuel of Future. *Biotechnology Research International*. <https://doi.org/10.1155/2014/272814>
- Peng, B., Zhao, C., Kasakov, S., Foraita, S., & Lercher, J. A. (2013). Manipulating catalytic pathways: Deoxygenation of palmitic acid on multifunctional catalysts. *Chemistry - A European Journal*. <https://doi.org/10.1002/chem.201203110>
- Peng, J., Chen, P., Lou, H., & Zheng, X. (2009). Catalytic upgrading of bio-oil by HZSM-5 in sub- and super-critical ethanol. *Bioresource Technology*.  
<https://doi.org/10.1016/j.biortech.2009.02.007>
- Pereira, R. C. C., & Pasa, V. M. D. (2006). Effect of mono-olefins and diolefins on the stability of

automotive gasoline. *Fuel*. <https://doi.org/10.1016/j.fuel.2006.01.022>

Perrotin-Brunel, H., Buijs, W., Spronsen, J. Van, Roosmalen, M. J. E. V., Peters, C. J., Verpoorte, R., & Witkamp, G. J. (2011). Decarboxylation of  $\Delta^9$ -tetrahydrocannabinol: Kinetics and molecular modeling. *Journal of Molecular Structure*, 987(1–3), 67–73. <https://doi.org/10.1016/j.molstruc.2010.11.061>

Peterson, A. A., Vogel, F., Lachance, R. P., Fröling, M., Antal, M. J., & Tester, J. W. (2008). Thermochemical biofuel production in hydrothermal media: A review of sub- and supercritical water technologies. *Energy and Environmental Science*. <https://doi.org/10.1039/b810100k>

Pinto, J. S. S., & Lanças, F. M. (2006). Hydrolysis of corn oil using subcritical water. *Journal of the Brazilian Chemical Society*. <https://doi.org/10.1590/S0103-50532006000100013>

Popov, S., & Kumar, S. (2015). Rapid hydrothermal deoxygenation of oleic acid over activated carbon in a continuous flow process. *Energy and Fuels*. <https://doi.org/10.1021/acs.energyfuels.5b00308>

R. C. Archuleta. (1991). Non catalytic steam hydrolysis of fats and oils. *Montana State University*.

Ramadhass, A. S., Jayaraj, S., & Muraleedharan, C. (2005). Biodiesel production from high FFA rubber seed oil. *Fuel*. <https://doi.org/10.1016/j.fuel.2004.09.016>

Ravenelle, R. M., Copeland, J. R., Kim, W. G., Crittenden, J. C., & Sievers, C. (2011). Structural Changes of  $\gamma$ -Al<sub>2</sub>O<sub>3</sub>-Supported Catalysts in Hot Liquid Water. *ACS Catalysis*. <https://doi.org/10.1021/cs1001515>

Remón, J., Randall, J., Budarin, V. L., & Clark, J. H. (2019). Production of bio-fuels and chemicals by microwave-assisted, catalytic, hydrothermal liquefaction (MAC-HTL) of a mixture of pine and spruce biomass. *Green Chemistry*. <https://doi.org/10.1039/c8gc03244k>

Robin, T., Jones, J. M., & Ross, A. B. (2017). Catalytic hydrothermal processing of lipids using metal doped zeolites. *Biomass and Bioenergy*. <https://doi.org/10.1016/j.biombioe.2017.01.012>

- Rostrup-Nielsen, J. R., Christensen, T. S., & Dybkjaer, I. (1998). Steam reforming of liquid hydrocarbons. *Studies in Surface Science and Catalysis*. [https://doi.org/10.1016/s0167-2991\(98\)80277-2](https://doi.org/10.1016/s0167-2991(98)80277-2)
- Rozmysłowicz, B., Mäki-Arvela, P., Tokarev, A., Leino, A. R., Eränen, K., & Murzin, D. Y. (2012). Influence of hydrogen in catalytic deoxygenation of fatty acids and their derivatives over Pd/C. *Industrial and Engineering Chemistry Research*. <https://doi.org/10.1021/ie202421x>
- Sahoo, P. K., Das, L. M., Babu, M. K. G., & Naik, S. N. (2007). Biodiesel development from high acid value polanga seed oil and performance evaluation in a CI engine. *Fuel*. <https://doi.org/10.1016/j.fuel.2006.07.025>
- Sakata, Y., Tamaura, Y., Imamura, H., & Watanabe, M. (2006). Preparation of a new type of CaSiO<sub>3</sub> with high surface area and property as a catalyst support. In *Studies in Surface Science and Catalysis*. [https://doi.org/10.1016/S0167-2991\(06\)80924-9](https://doi.org/10.1016/S0167-2991(06)80924-9)
- Santillan-Jimenez, E., & Crocker, M. (2012). Catalytic deoxygenation of fatty acids and their derivatives to hydrocarbon fuels via decarboxylation/decarbonylation. *Journal of Chemical Technology and Biotechnology*. <https://doi.org/10.1002/jctb.3775>
- Savchenko, V. I., & Makaryan, I. A. (1999). Palladium catalyst for the production of pure margarine: Catalyst and new non-filtration technology improve production and quality. *Platinum Metals Review*.
- Sawangkeaw, R., & Ngamprasertsith, S. (2013). A review of lipid-based biomasses as feedstocks for biofuels production. *Renewable and Sustainable Energy Reviews*. <https://doi.org/10.1016/j.rser.2013.04.007>
- Scanlon, D. O., Watson, G. W., Payne, D. J., Atkinson, G. R., Egdell, R. G., & Law, D. S. L. (2010). Theoretical and experimental study of the electronic structures of MoO<sub>3</sub> and MoO<sub>2</sub>. *Journal of Physical Chemistry C*. <https://doi.org/10.1021/jp9093172>
- Shay, E. G. (1993). Diesel fuel from vegetable oils: Status and opportunities. *Biomass and*

*Bioenergy*. [https://doi.org/10.1016/0961-9534\(93\)90080-N](https://doi.org/10.1016/0961-9534(93)90080-N)

- Smits, G. (1976). Measurement of the diffusion coefficient of free fatty acid in groundnut oil by the capillary-cell method. *Journal of the American Oil Chemists' Society*, 53(4), 122–124. <https://doi.org/10.1007/BF02586347>
- Snåre, M., Kubičková, I., Mäki-Arvela, P., Chichova, D., Eränen, K., & Murzin, D. Y. (2008). Catalytic deoxygenation of unsaturated renewable feedstocks for production of diesel fuel hydrocarbons. *Fuel*, 87(6), 933–945. <https://doi.org/10.1016/j.fuel.2007.06.006>
- Snåre, M., Mäki-Arvela, P., Simakova, I. L., Myllyoja, J., & Murzin, D. Y. (2009). Overview of catalytic methods for production of next generation biodiesel from natural oils and fats. *Russian Journal of Physical Chemistry B*. <https://doi.org/10.1134/S1990793109070021>
- Snåre, Mathias, Kubičková, I., Mäki-Arvela, P., Eränen, K., & Murzin, D. Y. (2006). Heterogeneous catalytic deoxygenation of stearic acid for production of biodiesel. *Industrial and Engineering Chemistry Research*. <https://doi.org/10.1021/ie060334i>
- Somerville, C., Youngs, H., Taylor, C., Davis, S. C., & Long, S. P. (2010). Feedstocks for lignocellulosic biofuels. *Science*. <https://doi.org/10.1126/science.1189268>
- Song, C., Nihonmatsu, T., & Nomura, M. (1991). Effect of Pore Structure of Ni–Mo/Al<sub>2</sub>O<sub>3</sub> Catalysts in Hydrocracking of Coal Derived and Oil Sand Derived Asphaltenes. *Industrial and Engineering Chemistry Research*. <https://doi.org/10.1021/ie00056a008>
- Spevack, P. A., & McIntyre, N. S. (1992). Thermal reduction of molybdenum trioxide. *The Journal of Physical Chemistry*. <https://doi.org/10.1021/j100201a062>
- Srifa, A., Faungnawakij, K., Itthibenchapong, V., Viriya-empikul, N., Charinpanitkul, T., & Assabumrungrat, S. (2014). Production of bio-hydrogenated diesel by catalytic hydrotreating of palm oil over NiMoS<sub>2</sub>/γ-Al<sub>2</sub>O<sub>3</sub> catalyst. *Bioresource Technology*. <https://doi.org/10.1016/j.biortech.2014.01.100>
- Steinberg, M., & Cheng, H. C. (1989). Modern and prospective technologies for hydrogen production from fossil fuels. *International Journal of Hydrogen Energy*.

[https://doi.org/10.1016/0360-3199\(89\)90018-9](https://doi.org/10.1016/0360-3199(89)90018-9)

- Swick, D., Jaques, A., Walker, J. C., & Estreicher, H. (2014). Gasoline toxicology: Overview of regulatory and product stewardship programs. *Regulatory Toxicology and Pharmacology*. <https://doi.org/10.1016/j.yrtph.2014.06.016>
- Talebian-Kiakalaieh, A., Amin, N. A. S., & Hezaveh, H. (2014). Glycerol for renewable acrolein production by catalytic dehydration. *Renewable and Sustainable Energy Reviews*. <https://doi.org/10.1016/j.rser.2014.07.168>
- Teeter, H. M., Bell, E. W., O'Donnell, J. L., Danzig, M. J., & Cowan, J. C. (1958). Reactions of conjugated fatty acids. VI. Selenium catalysis, a method for preparing diels-alder adducts from cis,trans-octadecadienoic acid. *Journal of the American Oil Chemists' Society*, 35(5), 238–240. <https://doi.org/10.1007/BF02639835>
- Teeter, H. M., O'Donnell, J. L., Schneider, W. J., Gast, L. E., & Danzig, M. J. (1957). Reactions of Conjugated Fatty Acids. IV. Diels-Alder Adducts of 9,11-Octadecadienoic Acid. *Journal of Organic Chemistry*, 22(5), 512–514. <https://doi.org/10.1021/jo01356a010>
- Thommes, M., Kaneko, K., Neimark, A. V., Olivier, J. P., Rodriguez-Reinoso, F., Rouquerol, J., & Sing, K. S. W. (2015). Physisorption of gases, with special reference to the evaluation of surface area and pore size distribution (IUPAC Technical Report). *Pure and Applied Chemistry*. <https://doi.org/10.1515/pac-2014-1117>
- Thornton, T. D., & Savage, P. E. (1990). Phenol oxidation in supercritical water. *The Journal of Supercritical Fluids*. [https://doi.org/10.1016/0896-8446\(90\)90029-L](https://doi.org/10.1016/0896-8446(90)90029-L)
- Tian, Q., Zhang, Z., Zhou, F., Chen, K., Fu, J., Lu, X., & Ouyang, P. (2017). Role of Solvent in Catalytic Conversion of Oleic Acid to Aviation Biofuels. *Energy and Fuels*. <https://doi.org/10.1021/acs.energyfuels.7b00586>
- Toba, M., Abe, Y., Kuramochi, H., Osako, M., Mochizuki, T., & Yoshimura, Y. (2011). Hydrodeoxygenation of waste vegetable oil over sulfide catalysts. *Catalysis Today*. <https://doi.org/10.1016/j.cattod.2010.11.049>

- Topsøe, H., Clausen, B. S., & Massoth, F. E. (2012). Hydrotreating Catalysis. In *Catalysis*. [https://doi.org/10.1007/978-3-642-61040-0\\_1](https://doi.org/10.1007/978-3-642-61040-0_1)
- W. Scaroni, A., Jenkins, R. G., & Walker, P. L. (1985). Coke deposition on Co-Mo/Al<sub>2</sub>O<sub>3</sub> and Co-Mo/C catalysts. *Applied Catalysis*. [https://doi.org/10.1016/S0166-9834\(00\)84353-5](https://doi.org/10.1016/S0166-9834(00)84353-5)
- Wan, J., Cao, Y. D., Ran, R., Li, M., Xiao, Y., Wu, X. D., & Weng, D. (2016). Regeneration of sintered Rh/ZrO<sub>2</sub> catalysts via Rh re-dispersion and Rh–ZrO<sub>2</sub> interaction. *Science China Technological Sciences*. <https://doi.org/10.1007/s11431-016-6052-z>
- Wan Omar, W. N. N., & Saidina Amin, N. A. (2011). Optimization of heterogeneous biodiesel production from waste cooking palm oil via response surface methodology. *Biomass and Bioenergy*. <https://doi.org/10.1016/j.biombioe.2010.12.049>
- Wang, H., Lin, H., Feng, P., Han, X., & Zheng, Y. (2017). Integration of catalytic cracking and hydrotreating technology for triglyceride deoxygenation. *Catalysis Today*. <https://doi.org/10.1016/j.cattod.2016.12.009>
- Wang, W. C., & Tao, L. (2016). Bio-jet fuel conversion technologies. *Renewable and Sustainable Energy Reviews*, 53, 801–822. <https://doi.org/10.1016/j.rser.2015.09.016>
- Watanabe, M., Iida, T., & Inomata, H. (2006). Decomposition of a long chain saturated fatty acid with some additives in hot compressed water. *Energy Conversion and Management*. <https://doi.org/10.1016/j.enconman.2006.01.009>
- Wen, G., Xu, Y., Ma, H., Xu, Z., & Tian, Z. (2008). Production of hydrogen by aqueous-phase reforming of glycerol. *International Journal of Hydrogen Energy*. <https://doi.org/10.1016/j.ijhydene.2008.07.072>
- Westacott, R. E., Johnston, K. P., & Rossky, P. J. (2001). Stability of ionic and radical molecular dissociation pathways for reaction in supercritical water. *Journal of Physical Chemistry B*. <https://doi.org/10.1021/jp010005y>
- WHO. (2016). WHO | Air pollution. *World Health Organization*.

- Wu, J., Shi, J., Fu, J., Leidl, J. A., Hou, Z., & Lu, X. (2016). Catalytic decarboxylation of fatty acids to aviation fuels over nickel supported on activated carbon. *Scientific Reports*. <https://doi.org/10.1038/srep27820>
- Yang, J., Xu, M., Zhang, X., Hu, Q., Sommerfeld, M., & Chen, Y. (2011). Life-cycle analysis on biodiesel production from microalgae: Water footprint and nutrients balance. *Bioresource Technology*. <https://doi.org/10.1016/j.biortech.2010.07.017>
- Yang, L., Ruess, G. L., & Carreon, M. A. (2015). Cu, Al and Ga based metal organic framework catalysts for the decarboxylation of oleic acid. *Catalysis Science and Technology*. <https://doi.org/10.1039/c4cy01609b>
- Yang, Liqiu, & Carreon, M. A. (2017a). Deoxygenation of Palmitic and Lauric Acids over Pt/ZIF-67 Membrane/Zeolite 5A Bead Catalysts. *ACS Applied Materials and Interfaces*. <https://doi.org/10.1021/acsami.7b11638>
- Yang, Liqiu, & Carreon, M. A. (2017b). Effect of reaction parameters on the decarboxylation of oleic acid over Pt/ZIF-67membrane/zeolite 5A bead catalysts. *Journal of Chemical Technology and Biotechnology*. <https://doi.org/10.1002/jctb.5112>
- Yang, Liqiu, Tate, K. L., Jasinski, J. B., & Carreon, M. A. (2015). Decarboxylation of Oleic Acid to Heptadecane over Pt Supported on Zeolite 5A Beads. *ACS Catalysis*. <https://doi.org/10.1021/acscatal.5b01913>
- Yeh, T. M., Hockstad, R. L., Linic, S., & Savage, P. E. (2015). Hydrothermal decarboxylation of unsaturated fatty acids over PtSn<sub>x</sub>/C catalysts. *Fuel*. <https://doi.org/10.1016/j.fuel.2015.04.039>
- Yu, J., & Savage, P. E. (2001). Catalyst activity, stability, and transformations during oxidation in supercritical water. *Applied Catalysis B: Environmental*. [https://doi.org/10.1016/S0926-3373\(00\)00273-3](https://doi.org/10.1016/S0926-3373(00)00273-3)
- Zhang, Jing, Huo, X., Li, Y., & Strathmann, T. J. (2019). Catalytic Hydrothermal Decarboxylation and Cracking of Fatty Acids and Lipids over Ru/C. *ACS Sustainable Chemistry and*

*Engineering*. <https://doi.org/10.1021/acssuschemeng.9b00215>

Zhang, Junhua, Chen, S., Yang, R., & Yan, Y. (2010). Biodiesel production from vegetable oil using heterogenous acid and alkali catalyst. *Fuel*. <https://doi.org/10.1016/j.fuel.2010.05.009>

Zhao, C., Brück, T., & Lercher, J. A. (2013). Catalytic deoxygenation of microalgae oil to green hydrocarbons. *Green Chemistry*, *15*(7), 1720–1739. <https://doi.org/10.1039/c3gc40558c>

Zhou, C.-H., Xia, X., Lin, C.-X., Tong, D.-S., & Beltramini, J. (2011). Catalytic conversion of lignocellulosic biomass to fine chemicals and fuels. *Chemical Society Reviews*. <https://doi.org/10.1039/c1cs15124j>

## Chapter 2

### 2. Continuous Thermocatalytic Decarboxylation of Stearic Acid, Oleic Acid, and Corn Distiller's Oil with a MoO<sub>x</sub> Catalyst

#### 2.1. Abstract

The production of green diesel can be expensive, as most methods use expensive noble metals catalysts such as platinum or palladium and use hydrogen gas. In this work, we demonstrate a continuous hydrogen gas free thermocatalytic process for the decarboxylation of stearic and oleic acid with a MoO<sub>x</sub>/γ-Al<sub>2</sub>O<sub>3</sub> catalyst to produce diesel range hydrocarbons. Temperature (375-400 °C), residence time (2.5-5 h), and oleic:stearic acid ratios (0:100 – 50:50) were investigated as key factors for degree of decarboxylation. A sample containing the complete removal of the carboxylic group from stearic acid was achieved at 390 °C and a residence time of 3.5 h as confirmed by ATR-FTIR. 97% percent removal of the carboxylic group from oleic acid was achieved at 375 °C and a residence time of 3.5 h. The temperature at which 100% of stearic acid was decarboxylated was decreased from 390 °C to 375 °C by the addition of just 10% (w/w) of oleic acid. GC-FID results showed a high selectivity to heptadecane conversion with stearic acid, whereas products formed from oleic acid show lower heptadecane proportions and a higher proportion of cracked products. 100 % removal of carboxylic acid was demonstrated with corn distiller's oil at 375 °C and a residence time of 3.5 h. The GC-FID of the corn distiller's oil indicates large proportions of cracked products and a third-party fuel test analysis of our product shows that it is similar to petroleum diesel, which demonstrates the potential of this method as a commercial process.

## 2.2. Introduction

The production of green diesel instead of biodiesel (fatty acid alkyl esters) produced from triglycerides are considered one of the most promising routes for producing renewable transportation fuels and chemicals (Abdulkareem-Alsultan et al., 2019; Douvartzides et al., 2019). Fats and oils (containing triglycerides (TGA) and fatty acids (FA)) are currently used as renewable feedstocks to produce transportation fuels in the form of biodiesel (Katryniok, Paul, & Dumeignil, 2013; Paul Abishek et al., 2014),(Button, 2010), but they can also be repurposed to produce green diesel (Afshar Taromi & Kaliaguine, 2018; Fu, Lu, et al., 2011b; Zhao, Brück, & Lercher, 2013). Biodiesel is produced through transesterification, which does not remove oxygen from the feedstock. Because of this, biodiesel has lower oxidative stability, higher corrosivity, lower energy density, and worse cold flow properties than petroleum sourced diesel (M. Snåre et al., 2009). To avoid these undesirable fuel properties, one can instead produce green diesel via deoxygenation reactions to obtain fuel properties far more similar to petroleum diesel (Douvartzides et al., 2019).

Deoxygenation of FAs and TGAs typically occur via three pathways; decarbonylation, decarboxylation, and hydrodeoxygenation (Jęczmionek & Porzycka-Semczuk, 2014).

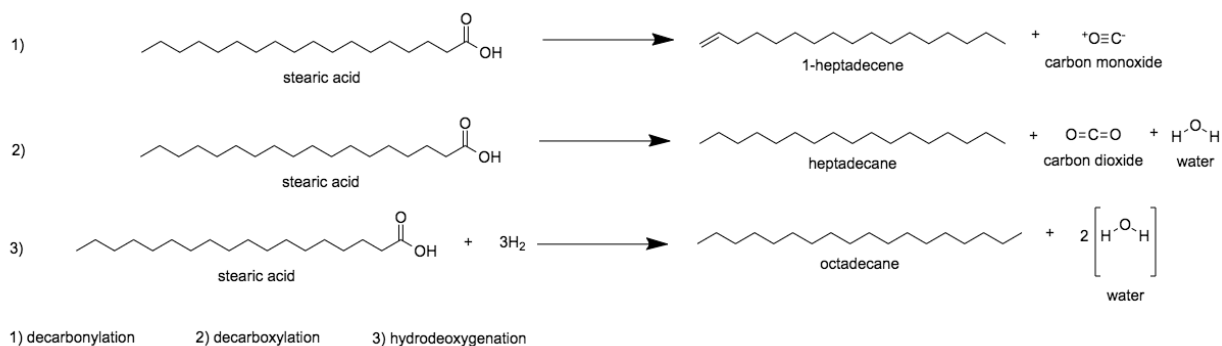


Figure 2.1 shows these reaction pathways for stearic acid.

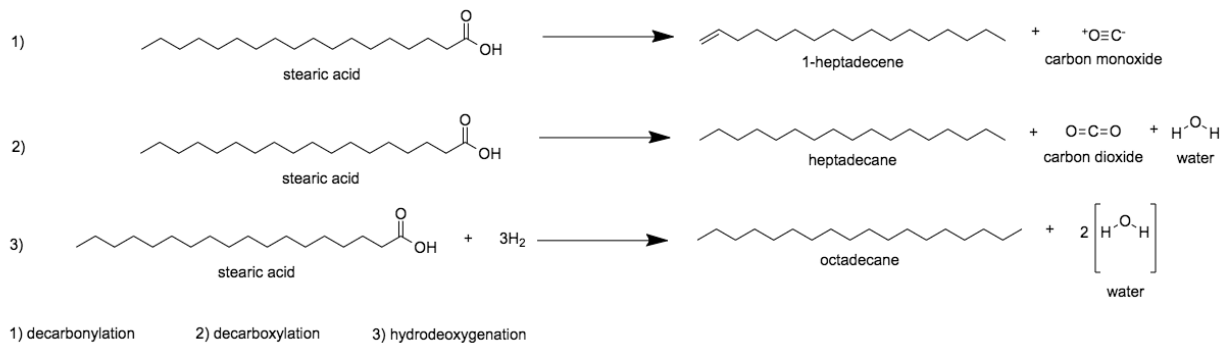


Figure 2.1 1) Decarbonylation, 2) decarboxylation, and 3) hydrodeoxygenation reaction pathways.

Out of all three pathways, only decarboxylation does not strictly require H<sub>2</sub> for the reaction to progress. Decarboxylation of stearic acid forms heptadecane, a C<sub>17</sub> aliphatic hydrocarbon that can be used in diesel fuel and in paraffin waxes, electrical insulation, and lubricating oils (Swick et al., 2014). This chemical is flexible as a fuel and a value-added product. For stearic acid undergoing decarboxylation at 300 °C, the reaction is slightly endothermic ( $\Delta H = 9.2$  kJ/mol) while decarbonylation is much more endothermic ( $\Delta H = 179.1$  kJ/mol) (Popov & Kumar, 2015). The addition of H<sub>2</sub> gas can reduce the endothermic requirements of decarbonylation ( $\Delta H = 48.1$  kJ/mol). Experimentally, it has been found that these pathways are not all independent, and addition of H<sub>2</sub> gas into most deoxygenation processes have been found to increase fuel/paraffin yields overall (Rozmysłowicz et al., 2012), (Gosselink, Stellwagen, & Bitter, 2013). However, H<sub>2</sub> is an expensive input for a process with already incredibly tight economic margins.

In order to reduce activation energies for decarboxylation, catalysts are used. Hydrodesulfurization catalysts have shown good decarboxylation activity and are cheaper than noble metal catalysts. However, leaching of the sulfur may deactivate the catalyst and possibly contaminate fuel products (Kubička & Horáček, 2011). Kubička et al. (Kubička & Horáček, 2011) found that continuous addition of dimethyldisulfide to a CoMoS/  $\gamma$ - Al<sub>2</sub>O<sub>3</sub> catalyst slowed deactivation, as it acted to help prevent sulfur removal from the catalyst. Addition of metal oxides to Pt/Alumina catalysts increase the activity of hydrodeoxygenation. Darbha et al. (Janampelli & Darbha, 2018) have shown that promotion of hydrodeoxygenation activity of Pt/Alumina catalysts is in the order of; MoO<sub>x</sub> > ReO<sub>x</sub> > WO<sub>x</sub> > SnO<sub>x</sub>.

Noble metals have been shown to be excellent catalysts for decarboxylation. However, noble metals are expensive and require costly H<sub>2</sub>. Therefore, the use of cheap transition metals is attractive. MoO<sub>x</sub> was shown by Darbha et al. to be a good transition metal oxide to combine with Pt in order to improve reaction rates. Hossain et al. (Hossain, Chowdhury, Jhavar, Xu, Biesinger, et al., 2018) have shown deoxygenation activity with MoO<sub>x</sub> supported on  $\gamma$ -Al<sub>2</sub>O<sub>3</sub>, without any noble metals added. The acidic nature of MoO<sub>x</sub>/ $\gamma$ -Al<sub>2</sub>O<sub>3</sub> enhances decarboxylation (Hengst et al., 2015), and is therefore a good catalyst to use and test (Hossain, Chowdhury, Jhavar, Xu, & Charpentier, 2018) as a low cost comparative to Pd/Pt (palladium can be up to 2500 times more expensive than molybdenum on a weight basis) (Friedman, Masciangioli, & Olson, 2012).

The MoO<sub>x</sub> catalyst, tested by the Charpentier group, showed comparatively good rates of decarboxylation of oleic acid for a non-noble metal catalyst in the absence of H<sub>2</sub> and in the presence of subcritical water. However, the products were much shorter than C<sub>17</sub> when deoxygenation rates were high. Cracking is likely the reason for the shortened chain lengths, as MoO<sub>x</sub> has been shown to be a cracking catalyst (Mo & Savage, 2014), (Song, Nihonmatsu, & Nomura, 1991).

Real-world green diesel feedstocks such as Corn Distiller's Oil (CDO), used cooking oils, waste animal fats, and brown and yellow grease will have various content of both saturated and unsaturated fatty acids. While there is much testing and comparison of deoxygenation of saturated vs unsaturated fatty acids, there appears to be a lack of data on mixed unsaturated and saturated feeds that more realistically resemble the composition of potential green diesel feedstocks. Further, there is a lack of data on larger scale continuous reactors using green solvents such as water to produce diesel-like hydrocarbons through deoxygenation processes. Therefore, while exploration of activity with oleic acid (Hossain, Chowdhury, Jhavar, Xu, & Charpentier, 2018) has been performed, it is of continuing interest to explore decarboxylation activity with fully saturated fatty acids with a low cost MoO<sub>x</sub>/ $\gamma$ -Al<sub>2</sub>O<sub>3</sub> catalyst.

It is hypothesized that saturated fatty acids may have similar activities to unsaturated feeds and may undergo less cracking due to the absence of an alkene bond that would otherwise be subjected to cracking (Corma & Orchillés, 2000). As unsaturation content may also increase the amount of feed cracking, it will produce more coke, and thus block catalyst pores and effectively

deactivate the catalyst. Hydrogen production from this cracking has been found to be negligible because the hydrogen is consumed to yield hydrocarbons and mainly water in the cracking of renewable raw materials (Melero et al., 2010).

In this present study, stearic acid and oleic acid were used as model compounds to investigate the impact of unsaturation content as well as temperature and residence time on the deoxygenation process using a continuous fixed bed plug flow reactor (PFR) with MoOx/ $\gamma$ -Al<sub>2</sub>O<sub>3</sub> as a catalyst. Steam was used as the reaction solvent instead of subcritical water because structural change and pore collapse of gamma alumina has been shown to occur when in aqueous environments that are >200 °C (Ravenelle et al., 2011). Yu et al. (Yu & Savage, 2001) demonstrate a more than 20-fold reduction in specific surface area of metal oxide catalysts supported on  $\gamma$ -Al<sub>2</sub>O<sub>3</sub> when exposed to supercritical water conditions. High temperature subcritical and supercritical water can further increase the damage done to the catalyst. Other supports are non-ideal because acidity of the catalyst is a major contributor to decarboxylation rates (Huang et al., 2009), (Hengst et al., 2015), (Hossain, Chowdhury, Jhavar, Xu, Biesinger, et al., 2018).

Characterization of fresh and spent catalysts was conducted using several techniques including N<sub>2</sub>- physisorption Brunauer–Emmett–Teller (BET) surface area and Barrett–Joyner–Halenda (BJH) pore size distribution, NH<sub>3</sub> temperature-programmed desorption (NH<sub>3</sub>-TPD), X-ray diffraction (XRD), O<sub>2</sub> pulse chemisorption, X-ray photoelectron spectroscopy (XPS), transmission electron microscopy (TEM), H<sub>2</sub> temperature-programmed reduction (H<sub>2</sub>-TPR), and scanning electron microscopy (SEM). Product quality was determined with FTIR for percent remaining carboxylic acid with the FTIR method correlated to values determined from acid value titrations. Product fractions were determined by GC-FID.

## 2.3. Materials and Methods

**Materials.** Stearic acid (95+%), oleic acid (90%), hexanes (ACS Grade), Toluene (ACS Grade), ammonium molybdate tetrahydrate  $(\text{NH}_4)_6\text{Mo}_7\text{O}_{24}\cdot 4\text{H}_2\text{O}$ , were obtained from Sigma-Aldrich, Canada, and are used as received. Corn distiller's oil was comprised of 12 % free fatty acids. When hydrolyzed, the total free fatty acids that make up the triglycerides is as follows; 12% palmitic acid, 29 % oleic acid, 56 % linoleic acid, 1 % linolenic acid, and 2% stearic acid.

Alumina ( $\gamma\text{-Al}_2\text{O}_3$ ) powder (Catalox SSCa 5/200) was obtained from SASOL. A compact ultrapure water system (EASY pure LF, Mandel Scientific Co., model BDI-D7381) was used to obtain deionized water (18.2 M $\Omega$ ).

**Catalyst Synthesis.**  $\text{MoO}_x$  supported on  $\gamma\text{-Al}_2\text{O}_3$  catalyst was synthesized using an incipient impregnation method (Chowdhury, Hossain, & Charpentier, 2011),(Choudhury, Ahmed, Shalabi, & Inui, 2006). Support material was calcined to 675 °C before impregnation. The larger surface area of the  $\gamma\text{-Al}_2\text{O}_3$  phase provides more active sites and therefore a more acidic catalyst (Hossain, Chowdhury, Jhavar, Xu, Biesinger, et al., 2018). To synthesize, 7.5 wt % loading of metal precursor was dissolved in deionized water equivalent to 120 vol % of pore volume of alumina (0.50 cm<sup>3</sup> /gm). The mixed support and metal precursor were then calcined into a muffle furnace at 675 °C at a ramp rate of 5 °C/min and then held for 4 h.

**Catalyst Testing.** 38 mL of fatty acid or CDO feedstock was added to the heated oil pump in the reactor setup shown in Figure 2.2. Flowrates of water and oil were calculated to use 38 mL

of oil material in 8 h with a residence time of 3.5 h. For residence times of 2.5 h and 5 h, flowrates of oil and water were changed so that the relative oil to water proportions and total oil added to the process stayed the same. Lines coming from the pumps were heated to 90 °C to ensure that stearic acid would not solidify within the lines. Pressures used in these studies were of autogenous conditions, which were ca. 50 psi. The main reactor body was 24 inches long and 0.532" ID, it was filled with 68 g of (1/8") ball bearings in the first phase of the reactor. The ball bearings were used as a pre-mixing and heating zone due because the furnace used has an effective heating length of about 12". The second half of the reactor, separated from the first half by quartz wool as a filter, was filled with 60 g of catalyst. From there, the product would exit the reactor and enter condensers/separators cooled to 7 °C by a chiller. If products in the condensers were solid, the condensers would be heated using a water bath to 45 °C and a heat gun, so as to recover the product. The product would then be contained in vials and/or centrifuge tubes awaiting analysis.

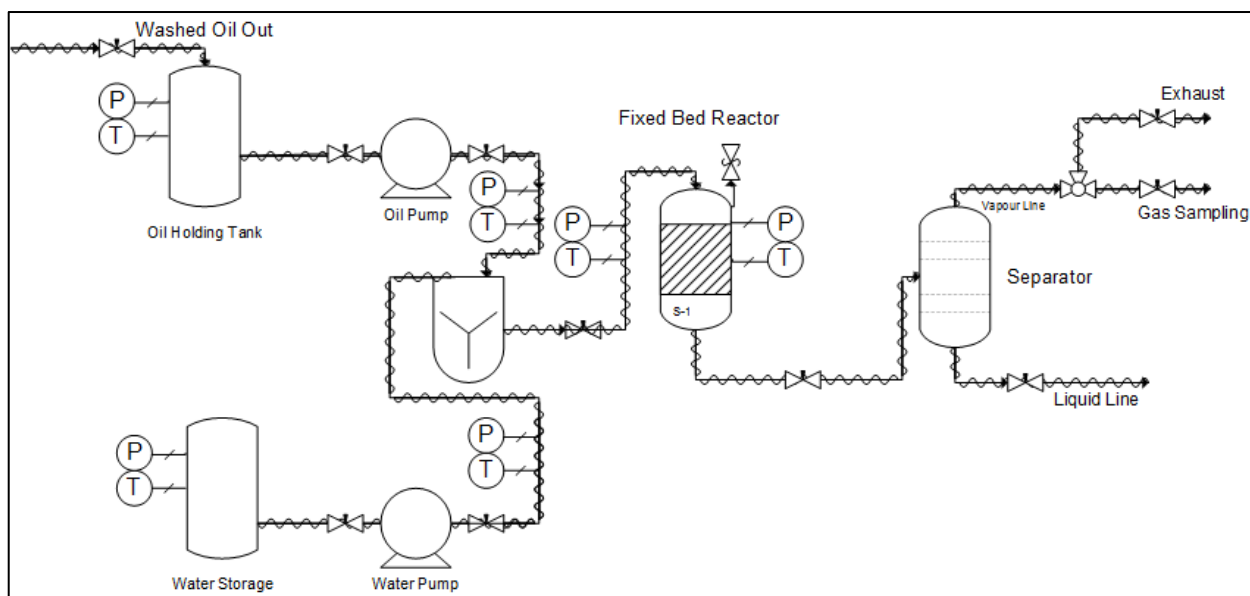


Figure 2.2 Continuous plug-flow reactor setup used for the decarboxylation of fatty acids and oils. Oils and fatty acids used in this study are pumped via an oil pump and water via the water pump. They are mixed by a mixing valve and continue towards the fixed bed reactor. After reaction the effluent reaches a separator which separates gases and liquids. The final product is collected and then separated from the water solvent via separatory funnels. All lines in this process are heated to prevent solidification and pressure increases due to plugging.

**Product Analysis.** Hydrocarbon product chain length was quantified using a Shimadzu GC-2014 equipped with a flame ionization detector and a capillary DB-5 Wax column (Agilent Technologies, Santa Clara, CA, USA) (dimension: 30 m × 0.250 mm × 0.25 μm, temperature limit: -60 to 325 °C). Helium, hydrogen, and helium-air were used as the carrier, flame, and makeup gas, respectively. Retention times of known standards of C<sub>8</sub>–C<sub>24</sub> saturated hydrocarbons and heptadecane (Restek Corporation, Bellefonte, Pennsylvania, USA) were used as internal standards to gauge the weights and lengths of hydrocarbons in the liquid product. Sample (1 μL) with a 10:1 split ratio was injected into the column. Product fractions were measured by the peak heights as the rising baseline of the chromatograph led to bias in calculating concentration by peak area. A second order calibration was used to predict product fraction concentrations. Calibrations were performed for n-alkanes from C<sub>9</sub> to C<sub>24</sub>. The calibrations for each n-alkane of a specific weight were applied to the unknown products in the similar regions of the chromatograph so as to quantify the fuel fractions. Injector and detector temperatures were retained at 200 and 250 °C, respectively. Infrared spectra (600–4000 cm<sup>-1</sup> with a resolution of 8 cm<sup>-1</sup> over 32 scans) of feedstock and liquid products were collected using an ATR–FTIR spectroscope (Nicolet 6700 FTIR, Thermo Scientific). <sup>1</sup>H nuclear magnetic resonance (NMR) spectra of reactant and product samples were recorded using a Varian Inova 400 spectrometer. Samples were dissolved in CDCl<sub>3</sub> and the chemical shifts were referenced to CDCl<sub>3</sub> (7.26 ppm). Third-party fuel quality analysis was carried out by InnoTech Alberta (Edmonton, Alberta) and cetane index, kinematic viscosity, oxygen content, nitrogen content, carbon %, hydrogen %, and flash point were tested.

Catalyst Characterization.

**N<sub>2</sub>-Physisorption:** A Tristar II 3020 (Micromeritics Instrument Corporation, Norcross, GA, USA) instrument was used to perform the BET surface area and BJH pore size distributions of the fresh and spent catalysts. Temperatures of analysis were conducted at -193 °C using 99.995% pure N<sub>2</sub> gas obtained from Praxair (Oakville, Canada). 150 mg of each catalyst sample was degassed under an N<sub>2</sub> atmosphere at 200 °C overnight before measurement.

**XRD Analysis:** Crystallinity of catalyst samples was analyzed using a Bruker D2 Phaser powder diffractometer over 2θ = 15–80° using a scan rate of 0.1°/min and Cu Kα radiation (λ for Kα is equal to 1.54059 Å).

**O<sub>2</sub> Pulse Chemisorption:** An Autochem II 2920 analyzer was used to determine the active particle diameter, the % metal dispersion, and the active metal surface area of catalyst samples using a series of 1 mL of O<sub>2</sub> pulses (5% O<sub>2</sub> balanced with He) injected into the catalyst sample at 400 °C. The catalyst sample was pretreated with a stream of He balanced with 10% H<sub>2</sub> (50 mL/min) and heated to 1000 °C to reduce the Mo metal before O<sub>2</sub> pulses were injected. Method was adapted from Desikan et al. (Desikan, Huang, & Oyama, 1992).

**NH<sub>3</sub>-TPD Analysis:** NH<sub>3</sub> TPD analysis was conducted using a Micromeritics Autochem II 2920 analyzer coupled with a thermal conductivity detector. Samples were pretreated at 400 °C @ 15 °C/min for 1 h under helium. The sample was then cooled from 400 to 100 °C using 10% NH<sub>3</sub> balanced with He (50 cm<sup>3</sup> /min) for another hour. NH<sub>3</sub> flow was then stopped and He (50 cm<sup>3</sup> /min) was flowed at 100 °C for 1 h to remove any adsorbed NH<sub>3</sub>. The temperature was then increased to 1000 °C @ 15°/min for desorption of NH<sub>3</sub> from the catalyst surface. The holding time at 1000 °C was 1 h. The acidity of the catalysts was calculated from the amount of NH<sub>3</sub> desorbed from the acid sites of the catalyst, measured by TCD.

**XPS Analysis:** The XPS analyses were carried out with a Kratos AXIS Supra spectrometer using a monochromatic Al K(alpha) source (15mA, 15kV). The instrument work function was calibrated to give a binding energy (BE) of 83.96 eV for the Au 4f<sub>7/2</sub> line for metallic gold and the spectrometer dispersion was adjusted to give a BE of 932.62 eV for the Cu 2p<sub>3/2</sub> line of metallic copper. The Kratos charge neutralizer system was used on all specimens. Survey scan analyses were carried out with an analysis area of 300 x 700 microns and a pass energy of 160 eV. High resolution analyses were carried out with an analysis area of 300 x 700 microns and a pass energy of 20 eV. Spectra have been charge corrected to the main line of the carbon 1s spectrum (adventitious carbon) set to 284.8 eV. Spectra were analyzed using CasaXPS software.

## 2.4. Results and Discussion

### 2.4.1. Determination of Fatty acid content by FTIR

The main deoxygenation reaction by the MoO<sub>x</sub>/Al<sub>2</sub>O<sub>3</sub> catalyst in water was shown by Hossain et al. (Hossain, Chowdhury, Jhawar, Xu, Biesinger, et al., 2018) to be decarboxylation. Hossain et al. measured the degree of decarboxylation by Fourier Transform Infrared Spectroscopy (FTIR). Percentage removal of -COOH group or degree of decarboxylation was calculated from the peak (1707 cm<sup>-1</sup>) areas of -COOH group in both reactants and liquid products. Before peak area calculation, the spectra were normalized to the 2920 cm<sup>-1</sup> peak and then a linear baseline correction was performed between 1670 cm<sup>-1</sup> and 1760 cm<sup>-1</sup> to encompass the entire ~1700 cm<sup>-1</sup> peak. After this pre-processing, % removal was calculated as below:

$$\begin{aligned} \% \text{ removal of } -\text{COOH (Degree of Decarboxylation)} = & \quad (2.1) \\ \frac{(\text{Initial peak area of } -\text{COOH in Feedstock}) - (\text{Peak area of } -\text{COOH in product})}{(\text{Initial peak area of } -\text{COOH in Feedstock})} & \\ \times 100 & \end{aligned}$$

This method of quantification was validated by correlation of values calculated to those found by ASTM D3242 - Standard Test Method for Acidity in Aviation Turbine Fuel (11, 2011). Samples collected during the course of the study were randomly sampled and subsequently measured for remaining fatty acid content by the acid value titration and the result of the calibration can be seen in Appendix 1.

A linear regression was performed on the reference values collected by acid Value titration as the independent variable and the values calculated by the FTIR method as the dependent variable. The linear equation and R<sup>2</sup> value were found to be:

$$y = 1.0127x + 1.4197, R^2 = 0.9824 \quad (2.2)$$

Root mean square error of prediction (RMSEP) was calculated by the equation as below:

$$RMSEP = \sqrt{\sum_{i=1}^n \frac{(\hat{y}_i - y_i)^2}{n}} \quad (2.3)$$

Based on this formula the RMSEP was found to be 3.04% degree of decarboxylation. Based on this standard error, a slope of nearly 1, and an  $R^2$  value of 0.98; it was found that the FTIR method is satisfactory for our purposes of predicting the quantity of remaining carboxylic acid in the product measured by the reference method.

## 2.4.2. Parametric studies for the decarboxylation of oleic and stearic acid

Parametric studies which varied temperature from 375– 400 °C and residence times (2.5 h – 5h) were conducted on feedstocks of oleic and stearic acid within a fixed bed plug flow reactor. We did not explore solvent to feed ratio as it was previously examined by the Charpentier group (Hossain, Chowdhury, Jhavar, Xu, Biesinger, et al., 2018) and had found larger ratios of water to oleic acid produced longer chain alkanes. Temperature and residence time are the two main parameters that impact decarboxylation rate and catalyst longevity. The degree of decarboxylation was assessed at different experimental conditions (Temp = 375 to 400°C, residence time = 2.5 h to 5 h) using 60 g of the 7.5 wt.% Mo/Al<sub>2</sub>O<sub>3</sub> catalyst. The decarboxylation of oleic acid was assessed at 375 °C and at residence times of 2.5 h and 3.5 h, and the reactions were run so as to process 38 mL of feedstock regardless of residence time. The decarboxylation over time of oleic acid at 2.5 h and 3.5 h is shown in

Figure 2.3. Time on the x-axis corresponds to reaction run time. For example, 180 minutes corresponds to the product that was collected from the condensers at the 180-minute mark during the course of the continuous process. Since it is a continuous process, residence time is the nomenclature used for the time that the feed material spends in the bed of the catalyst. It is evident that decarboxylation increased by 10-20% with when residence time increased from 2.5 h to 3.5 h. It appears that the decarboxylation of oleic acid at both 2.5 h and 3.5 h never reach steady state. However, the infrared measurement error (3 %) may help explain a portion of the lack of steady state. Another reason may be due to the changing nature of the catalyst through the extent of the reaction. Figure 2.22 shows the NH<sub>3</sub> TPD profile of fresh and spent catalyst and shows an increase in the number of strong acid sites within the spent catalyst. Steady state may not be reached in these runs as the mechanism of decarboxylation changes due to chemical changes in the catalyst.

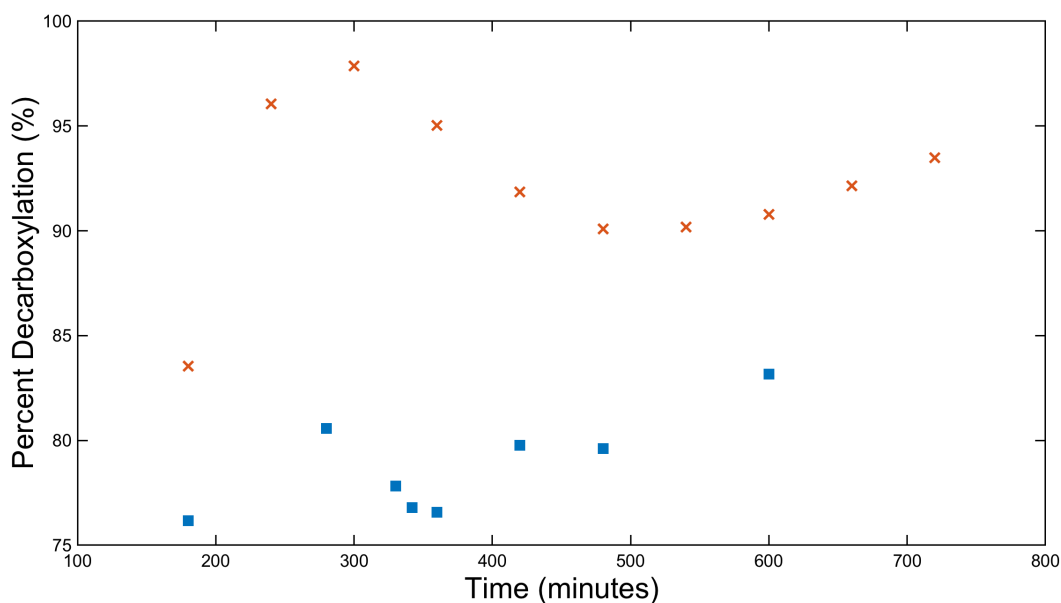


Figure 2.3 Decarboxylation over time of oleic acid at 375 °C, at 2.5 h (■) and 3.5 h (×) residence times. Time on the x-axis corresponds to reaction run time. For example, 180 minutes corresponds to the product that was collected from the condensers at the 180 minute mark during the course of the continuous process.

The  $\text{MoO}_x\text{-Al}_2\text{O}_3$  catalyst shows good activity over time at 375°C with oleic acid as a feedstock. While saturated and unsaturated fatty acids will both decarboxylate in the presence of a decarboxylation catalyst and hydrogen gas, Fu et al. (Fu, Lu, et al., 2011b) demonstrated that unsaturated fatty acids first undergo hydrogenation and subsequent decarboxylation. Therefore, one might suggest that fully saturated fatty acids should be a better feedstock, as they will progress straight to decarboxylation and prevent the formation of by-products such as dimer acids (Den Otter, 1970).

Figure 2.4 shows the percent decarboxylation over time of stearic acid at 375 °C with residence times of 3.5 h and 5 h.

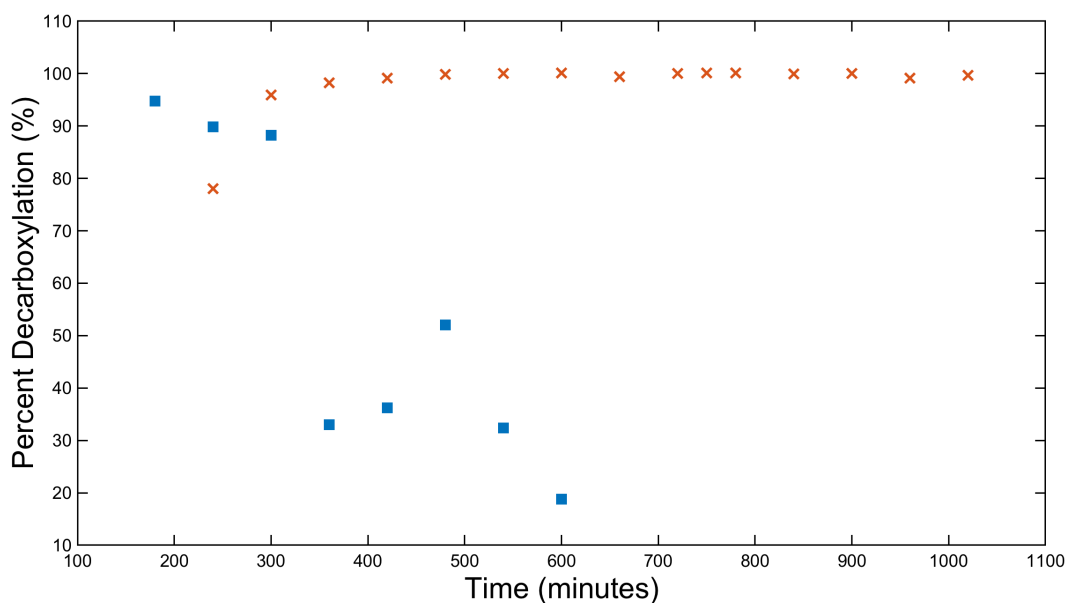


Figure 2.4 Decarboxylation over time of stearic acid at 375 °C at 3.5 h (■) and 5 h (×) residence times

From

Figure 2.4, one can see that the percent of decarboxylation of stearic acid at 375 °C and 3.5 h residence time is less than 50 %. The data for the 3.5 h run is quite variable, as the catalyst seems to lose activity after 300 minutes. The catalyst may be losing some catalytic property that is regenerated during the 5 h residence time run. The low conversion rate of stearic acid contradicts the proposed mechanism of saturation first occurring and then decarboxylation by Fu et al. (Fu, Lu, et al., 2011b) which used a noble metal catalyst and a H<sub>2</sub> environment. If saturation occurs first, as Fu et al. (Fu, Lu, et al., 2011b) demonstrated, and does not degrade the catalyst, then oleic and stearic acid should have identical activities. The discrepancy in results is perhaps due to the use of the non-noble metal catalyst, MoO<sub>x</sub> supported on Al<sub>2</sub>O<sub>3</sub>, and elimination of the use of external hydrogen. Increasing the residence time to 5 h at the same temperature generates products that are around 90 % decarboxylated (10 % carboxylic acid remaining). Since increasing the residence time creates a more decarboxylated product, then a reasonable increase of temperature might also increase better product reducing overall process time. To justify this hypothesis, we examined stearic acid decarboxylation at elevated temperature at 390 °C.

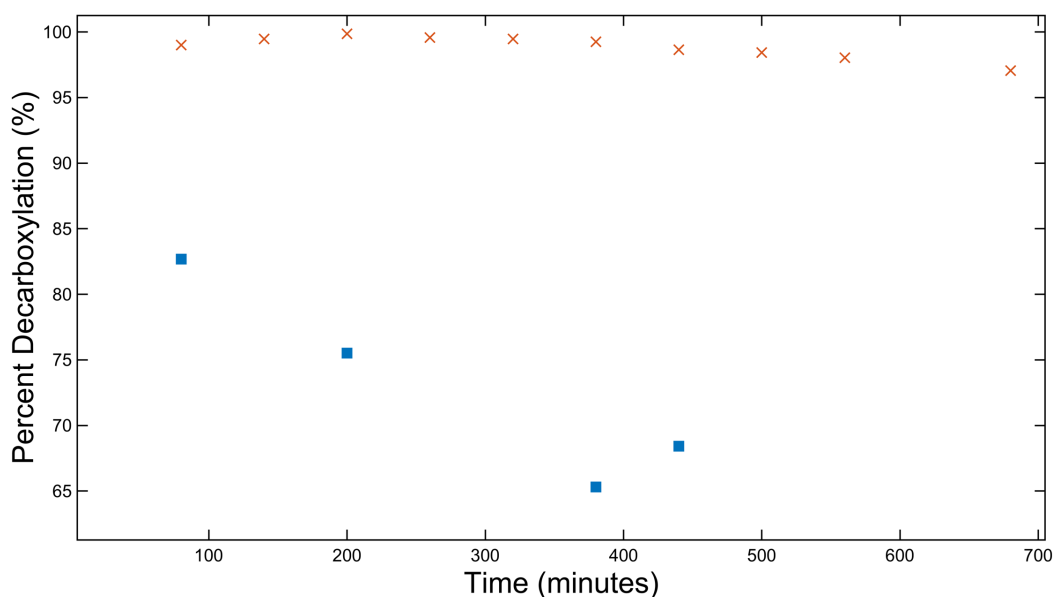


Figure 2.5 Decarboxylation over time of stearic acid at 390 °C at 2.5 h (■) and 3.5 h (x) Residence Times

From Figure 2.5, percent decarboxylation holds somewhat steady at nearly 100 % in 3.5 h residence time, but a significant deactivation and reduction in activity was observed with a 2.5 h residence time. However, the minimum percent decarboxylation at 390 °C and 2.5 h (~66 %) is much higher when compared with 375 °C and 3.5 h (< 20 %). An increase in temperature of 15 °C improves the degree of decarboxylation by a similar margin by increasing residence time by 2.5 h. Finally, we further increased temperature to 400 °C with three different residence times (2.5 h, 3.5 h, and 5 h). The results of these experimental runs are shown in

Figure 2.6. At 3.5 h and 5 h residence times there is negligible deactivation observed during the run. At 400 °C and 2.5 h residence time it is observed that the degree of deoxygenation is reduced significantly towards the end of the run. It may be possible that the heavier products are likely to accumulate in the reactor and travel more slowly than lighter fractions. Since mass transfer of the heavier products are low compared to the lighter products, with low residence time fresh feedstock might have hindered further desorption of products from the catalyst's surface. Eventually, heavier products might lead to the formation of coke at elevated temperatures, resulting in the catalyst's deactivation.

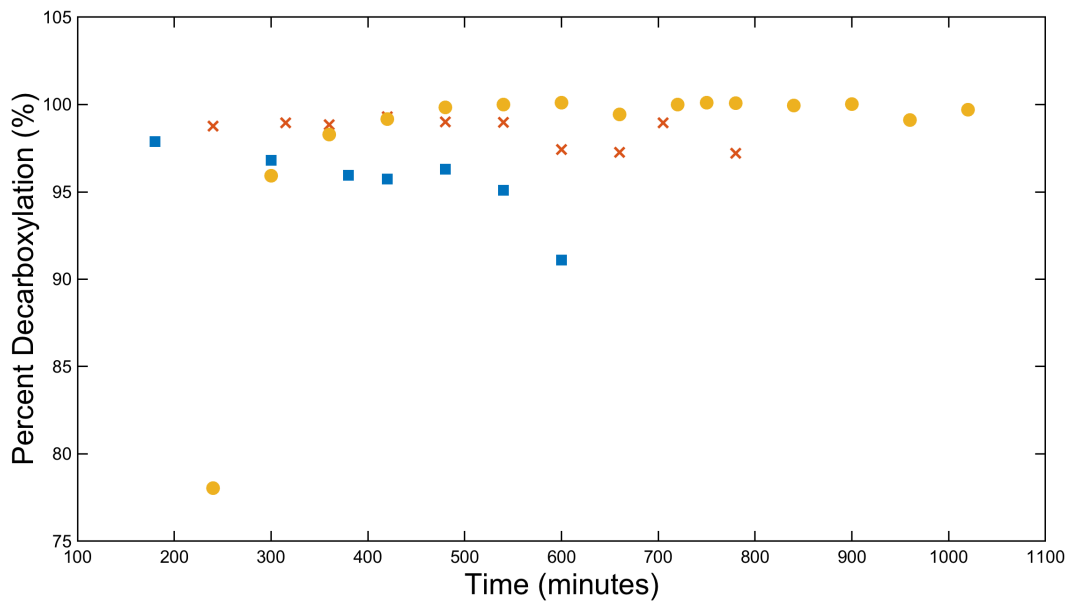


Figure 2.6 Decarboxylation over time of stearic acid at 400 °C at 2.5 h (■), 3.5 h (×), and 5 h (●) residence times

At 400 °C and 2.5 h residence time stearic acid has a lower overall decarboxylation compared to 3.5 and 5 h residence time. This shows a trend of deactivation, whereas there is no indication of deactivation for 3.5 h and 5 h. The 5 h reaction appears to reach steady state at approximately 420 minutes, which appears to be much longer than 2.5 h and 3.5 h take to reach steady state. Using 100% stearic acid in this process, the optimum conditions of the reaction is suggested to be 390 °C at 3.5 h residence time.

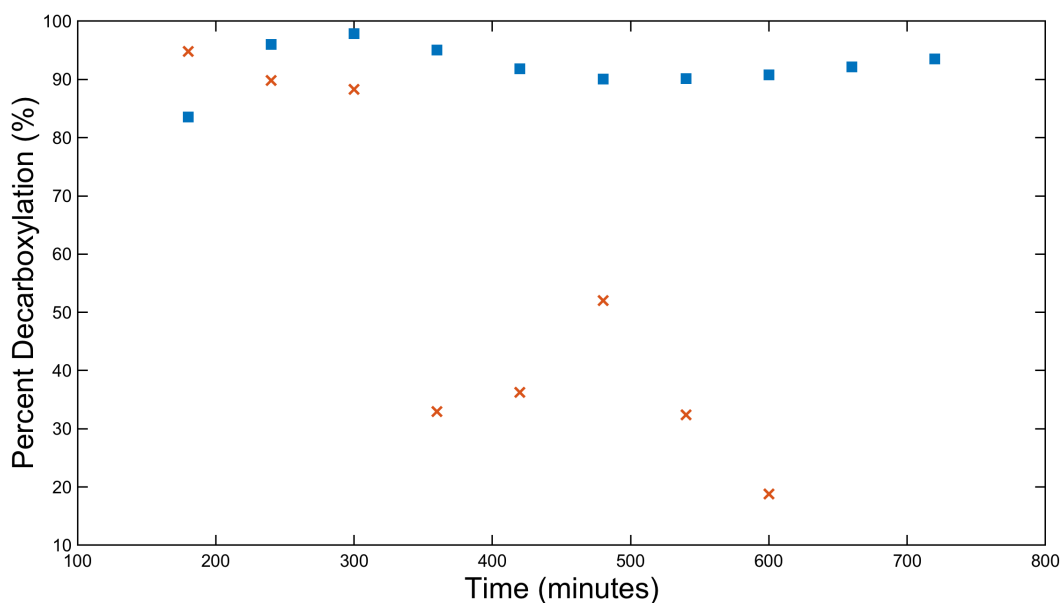


Figure 2.7 Decarboxylation over time of oleic (■) and stearic acid (×) at 375 °C at 3.5 h residence time.

When comparing optimal conditions of temperature and residence time between oleic and stearic acid decarboxylation, it is noted that stearic acid requires a temperature 15 °C more than oleic acid in order to achieve high yields of deoxygenated products. This comparison can be seen in Figure 2.7. Based on Hossain et al.'s (Hossain, Chowdhury, Jhavar, Xu, Biesinger, et al., 2018) work with an activated carbon catalyst, it was shown that decarboxylation follows pseudo-first order kinetics. According to the Arrhenius rule of thumb, most reaction rates will double for every 10 °C increase in temperature. This means that stearic acid has a reaction rate 2-4 times less than that of oleic acid. The reaction pathway may not be that oleic acid will first saturate and then decarboxylate as suggested by Fu et al. (Fu, Lu, et al., 2011b).

Based on this large discrepancy in reaction rates, we suggest there must be a property that differs between oleic acid and stearic acid that causes such changes in reaction rates. Oleic acid and stearic acid have near identical boiling points (360 °C and 361 °C, respectively), so this cannot effectively explain the difference in reaction rates. Oleic and stearic acid also have very similar molecular weight, as they differ by a pair of hydrogen atoms. If it is a mass transfer issue, then we would expect to see a large difference in the diffusion coefficient between the two feeds. In

groundnut oil, the diffusion coefficients at room temperature of oleic and stearic acid are  $(4.2 \pm 0.16)10^{-10}$  and  $(3.7 \pm 0.23)10^{-10}$  m<sup>2</sup>/s, respectively (Smits, 1976). While our study's reaction temperatures, pressures, and transport mediums are different than the conditions used to obtain the diffusion coefficients, we can see that the oleic and stearic coefficients are not greatly dissimilar at room temperature. This may indicate that the diffusion coefficients may not greatly diverge in value and remain similar to one another (oleic to stearic) at our study's conditions (375 °C – 400 °C). From this assumption, one might say the issue of reduced reaction rates may not be entirely due to reduced mass transfer.

Another property that differs between oleic and stearic acid is the presence of an alkene bond. Cracking of oleic and palmitic acids occur with increasing temperatures using HZSM-5 catalysts, which may reduce activation energies in a similar capacity to our MoO<sub>x</sub>/Al<sub>2</sub>O<sub>3</sub> catalyst, which has been shown to be a cracking catalyst (Mo & Savage, 2014), (Song et al., 1991). As cracking will release hydrogen, and hydrogen has been demonstrated to increase decarboxylation rates (Melero et al., 2010), this offers another explanation as to why decarboxylation progresses easier with oleic acid than stearic acid. However, it is unknown whether hydrogen is released in the form of molecular hydrogen gas, or as a proton or other “hydrogen equivalents” on the catalyst surface. Peng et al. (B. Peng et al., 2013) concluded that for monometallic catalysts, a source for disassociated hydrogen protons on the catalyst surface is required to provide adequate results. In addition, as deactivation appears to happen with decreased temperatures and residence times, this is further evidence that the current mode of decreased activity may not be physical fouling by the production of coke.

### 2.4.3. Investigation of Chain Length by GC-FID

While cracking can generate useful hydrogen that can facilitate decarboxylation (Mathias Snåre et al., 2006), it also shortens the aliphatic product lengths, consumes energetic carbon-hydrogen bonds, and forms coke on the surface of the catalyst.

Figure 2.8 shows the hydrocarbon product range from  $C_7$  to  $C_{24}$  formed from oleic acid (375 °C and a residence time of 3.5 h) and stearic acid (375 °C and 3.5 h). For clarification,  $C_9$  to  $C_{10}$  fractions would contain nonane up to but not including decane fractions. This is the pattern maintained among all GC-FID figures. Heptadecane is shown separately from the  $C_{17-18}$  group to demonstrate the selectivity of decarboxylation. There is a higher proportion of heptadecane with stearic acid as the feedstock as opposed to oleic acid (57% vs 20%, respectively) when processed at 375 °C. Oleic acid produces larger amounts of fractions smaller than heptadecane (49 %) vs stearic acid (13 %) which indicates a significant increase in cracking. oleic acid was demonstrated to decarboxylate more readily than stearic acid and the GC-FID shows that the oleic acid products are lower molecular weight hydrocarbons that have cracked more. The large amount of  $C_{22-24}$  in the stearic acid data is believed to be unreacted stearic acid based on running pure stearic acid. Stearic acid elutes at this time due to its carboxylic acid increasing its retention time in the column. Oleic acid also produces a larger proportion of fractions greater than heptadecane (31 %) than in stearic acid (7 %). This could be due to formation of smaller radicals from cracking that react with larger chain fractions to create larger molecular weight products (Teeter, O'Donnell, Schneider, Gast, & Danzig, 1957).

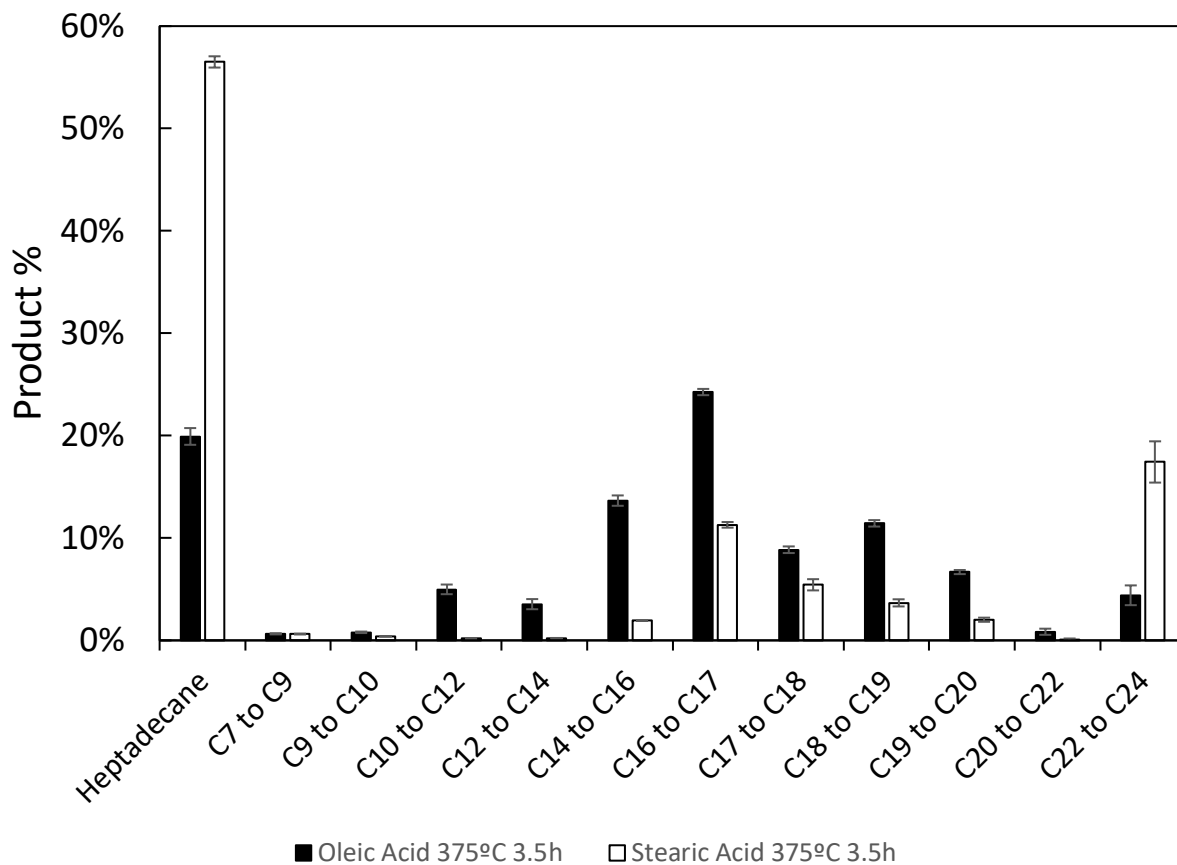


Figure 2.8 GC-FID fractions of oleic acid at 375°C and 3.5h res. time (black) and stearic acid at 375°C and 3.5 h res. time (white). The reaction time for both samples was 5 h.

GC-FID analysis was also conducted on the 8 h collection sample from stearic acid processed at a temperature of 375 °C with a residence time of 5 h. A comparison between this run and stearic acid processed at the same temperature and 3.5 h residence time can be seen in

Figure 2.9.

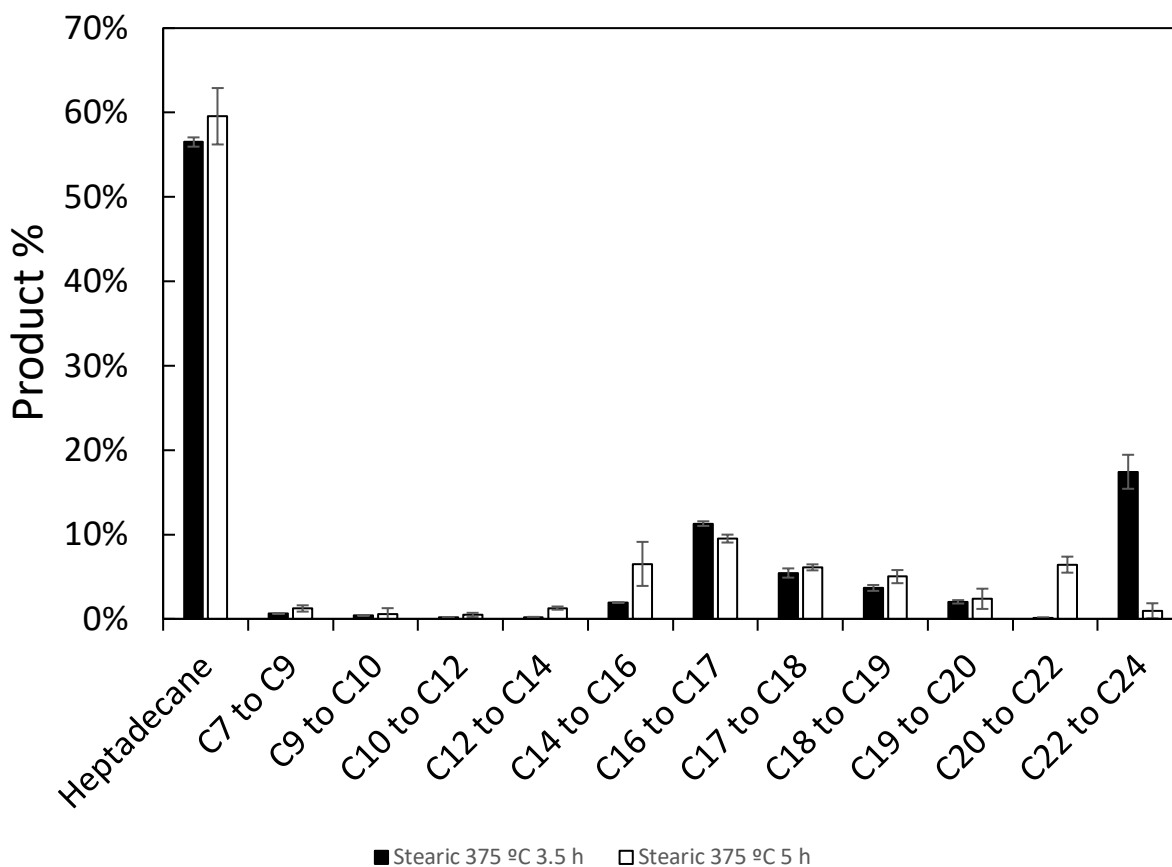


Figure 2.9 GC-FID fractions of stearic acid processed at 375 °C and 3.5 h res. time (black) and stearic acid at 375 °C and 5 h res. time (white).

5 h residence time was shown to have a sustained 90% decarboxylation over the course of the run, and this improvement in percent decarboxylation can be seen in the product fractions. Heptadecane comprises approximately 60% of the product and has a 16% less C<sub>22</sub> to C<sub>24</sub> products, which can be indicative of unconverted stearic acid. However, the 5 h residence time run appears to contain 6.4% C<sub>20</sub> to C<sub>22</sub> hydrocarbons where the 3.5 h residence time sample comprises effectively 0% C<sub>20</sub> to C<sub>22</sub> hydrocarbons. There is also 6.5% C<sub>14</sub> to C<sub>16</sub> hydrocarbons in 5 h compared to 2% in 3.5 h. There appears to be a larger spread of fractions larger and smaller than heptadecane in 5 h compared to 3.5 h, when lack of conversion in 3.5 h is taken into account. When compared to oleic acid at 375 °C and 3.5 h, the 5 h stearic acid products have larger amounts of C<sub>20</sub> to C<sub>22</sub> hydrocarbons (6% vs 1%). It is likely that 5 h is the necessary residence time to allow significant decarboxylation to occur at 375 °C.

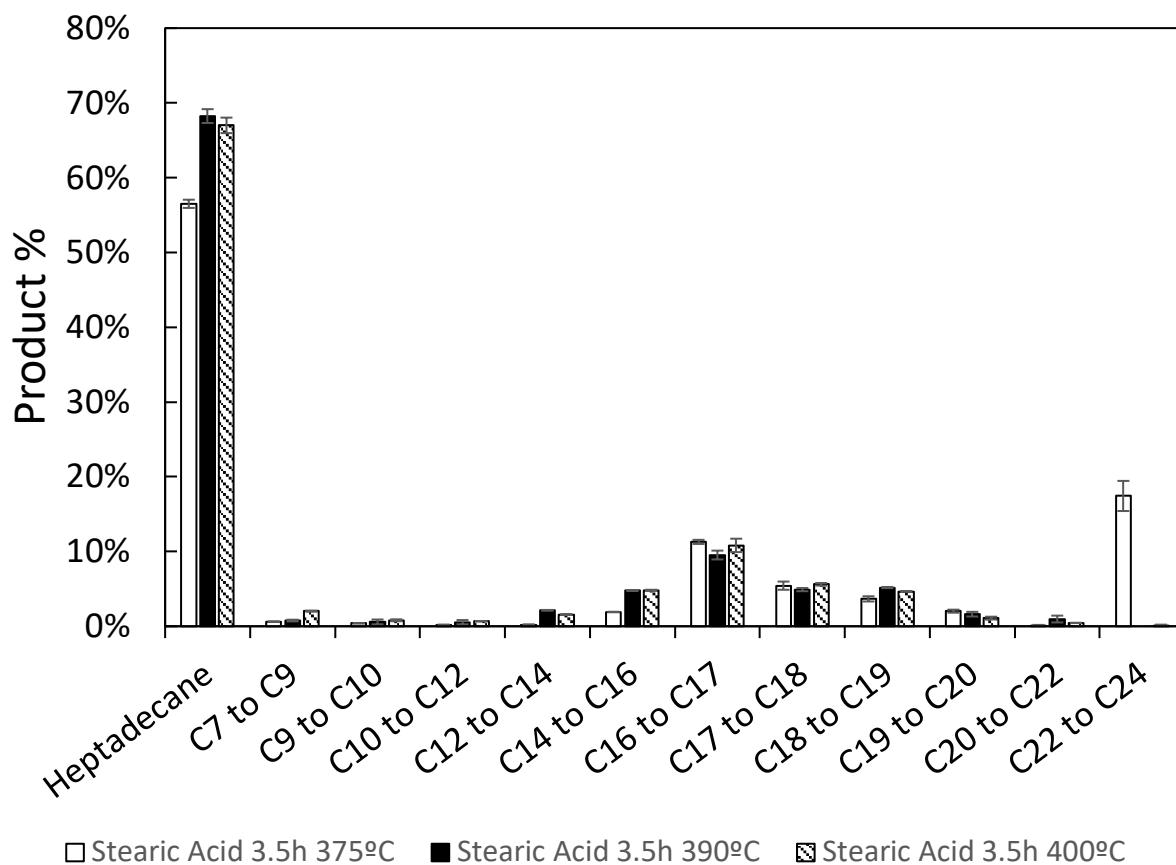


Figure 2.10 Product fractions of stearic acid at 375 °C (white), 390 °C (grey), and 400 °C (diagonal lines).

The product fractions of stearic acid catalyzed to deoxygenated products at residence times of 3.5 h and temperatures of 375 °C, 390 °C, and 400 °C can be seen in

Figure 2.10. There are larger percentages of smaller than heptadecane fractions in both 390 °C (15.0%) and 400 °C (17.8%) compared to 375 °C (13%). More heptadecane is produced with stearic acid at 390 °C (68.0%) and 400 °C (67.0%) than with oleic acid (19.9%). Even with increases in temperatures, oleic acid cracks more than stearic acid, producing a significant proportion of lower molecular weight hydrocarbon fractions.

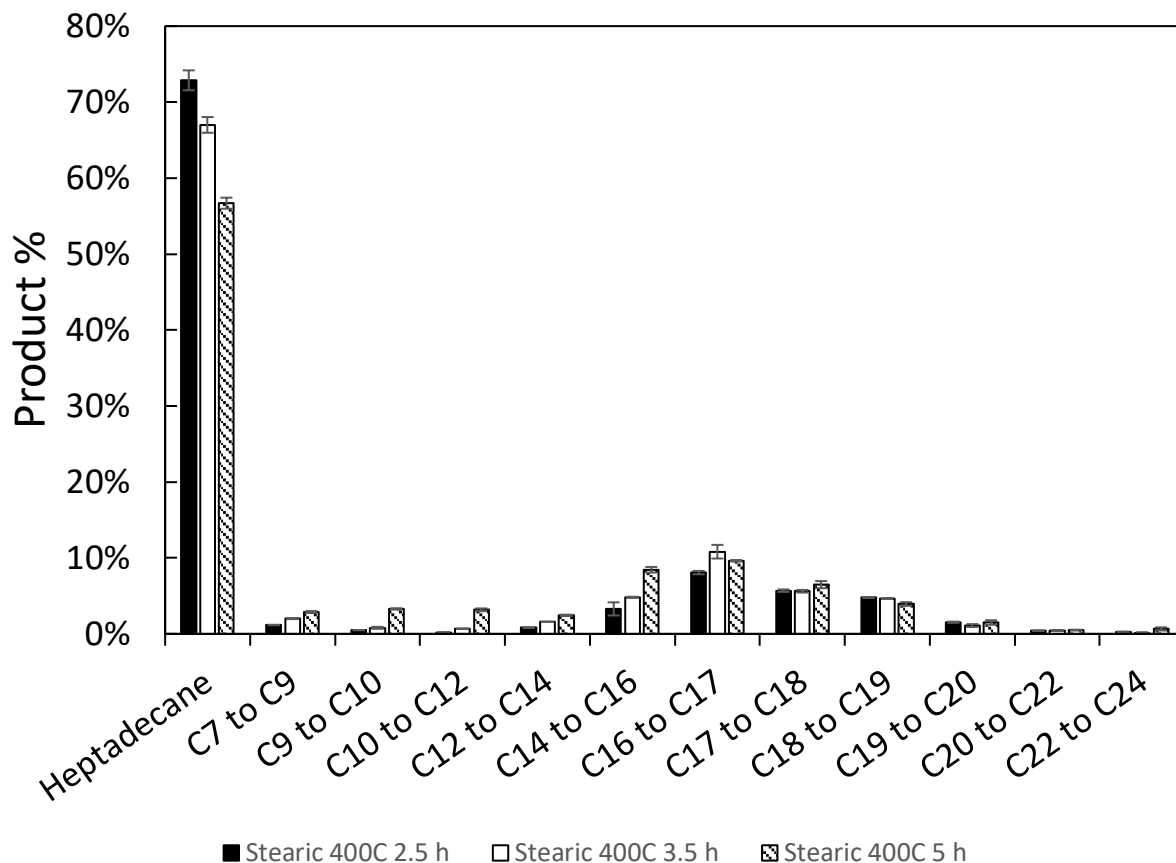


Figure 2.11 Product fractions of stearic acid processed at 400 °C at residence times of 2.5 h (black), 3.5 h (white), and 5 h (diagonal lines).

Product chain length of stearic acid run at 400 °C and 3 different residence times are compared in Figure 2.12. Percent heptadecane for 2.5 h, 3.5 h, and 5 h was found to be 72.9 %, 67.0 %, and 56.7 %, respectively. Product chain length appears to decrease with increasing residence times. Chain lengths lower than heptadecane comprise 12.0 % at 2.5 h, 17.8 % at 3.5 h, and 25.1 % at 5 h residence times. It appears that increasing residence time results in an increase of cracking and therefore lower chain products. This can be inefficient if the goal is decarboxylation to heptadecane.

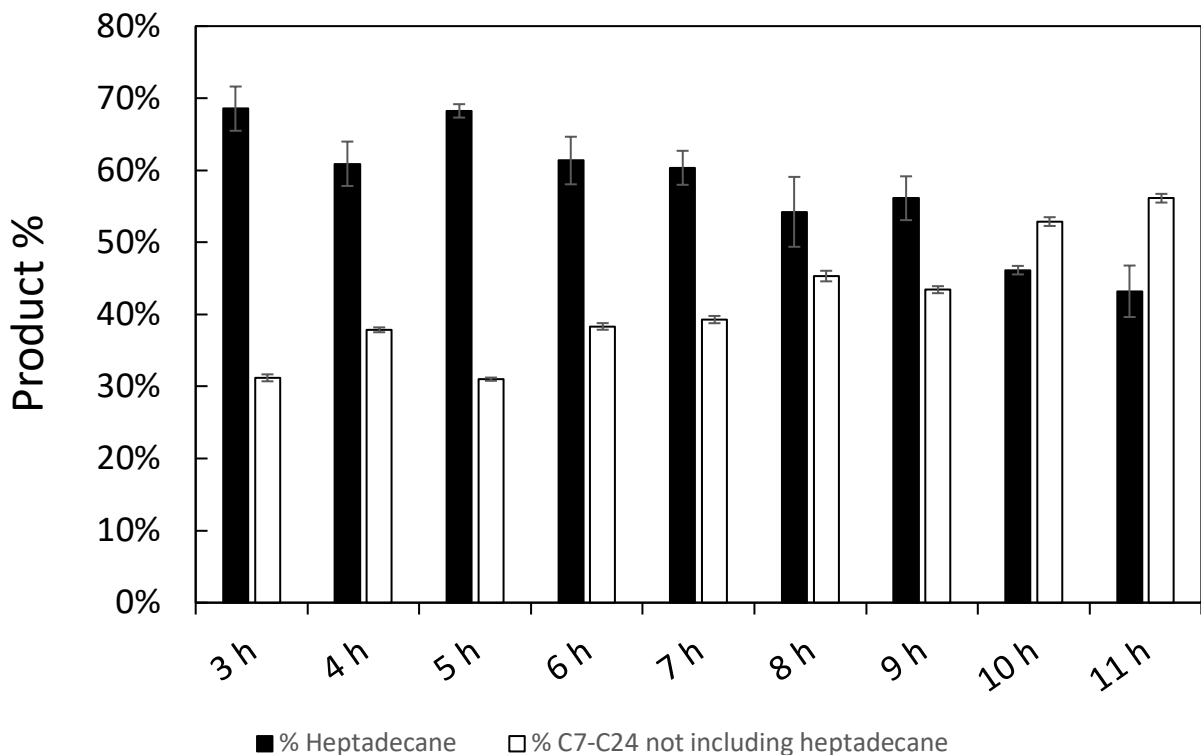


Figure 2.12 Stearic acid feed processed at 390 °C with a 3.5 h residence time, product quantities over time. Percent heptadecane in black and all other products not including heptadecane in white.

Figure 2.12 shows the product fractions over time during a run at 390 °C with a 3.5 h residence time. This reaction was run continuously for 11 h. Oil-feed was stopped at 8 h, and from 8 h until 11 h only water was added to the reactor to push out the remaining material. One can see increases in lower than C<sub>17</sub> fractions past the 7 h collection point, when new material was no longer being added. However, it takes 3.5 h for all material added to exit the reactor and therefore we would expect no large changes to occur until after 11 h. The composition of the product appears to change at the 8 h time-point, which results in increases of both lower and higher than C<sub>17</sub> products being formed. It is possible that the longer the reactor runs, the more accumulation occurs of product. This can result in longer chains accumulating within the reactor and undergoing additional cracking and combining. This will form shorter chain products from cracking. Cracked products may take the form of olefins and dienes (in an assorted number of chain lengths) of which can combine through diels-alder reactions and form longer products (Teeter et al., 1957). This may

be an explanation for why we see a reduction in the overall heptadecane yield and increases in both longer and shorter hydrocarbon chains over the course of the reaction.

From the product fraction profiles, it appears that one can tune the average hydrocarbon product weight by modifying the system's temperature and residence time. The highest heptadecane proportions were found for stearic acid processed at 400 °C at 2.5 h residence time (72.9%). If a mixture of products is desired, increasing the residence time will enhance cracking and create a larger distribution of product fractions. Changing the feed to oleic acid can also create a larger distribution of product fractions, with heptadecane comprising 19.9%.

## 2.4.4. Decarboxylation and Product Analysis by Alkene Content in Fatty Acids

Studying the decarboxylation of a mix of oleic and stearic acid was pursued for three purposes. One, oleic acid was shown to have good decarboxylation rates and preferable deactivation rates at lower temperatures and residence times than stearic acid. Two, that real feeds from waste oils and non-edible oils will almost always have some degree of unsaturation. Three, it was shown that decarboxylation rates increase with increasing cracking, and addition of oleic acid may reduce the temperature requirement for stearic acid. Based on these three observations, a series of experiments were conducted which measured the Percent decarboxylation over time in our continuous reactor with feeds of mixed stearic acid and oleic acid in proportions of 10:90 oleic:stearic acid to 50:50 oleic:stearic. All runs were conducted at 375°C and with a residence time of 3.5 h. The results of varying the saturation level of the feedstock can be seen in Figure 2.13

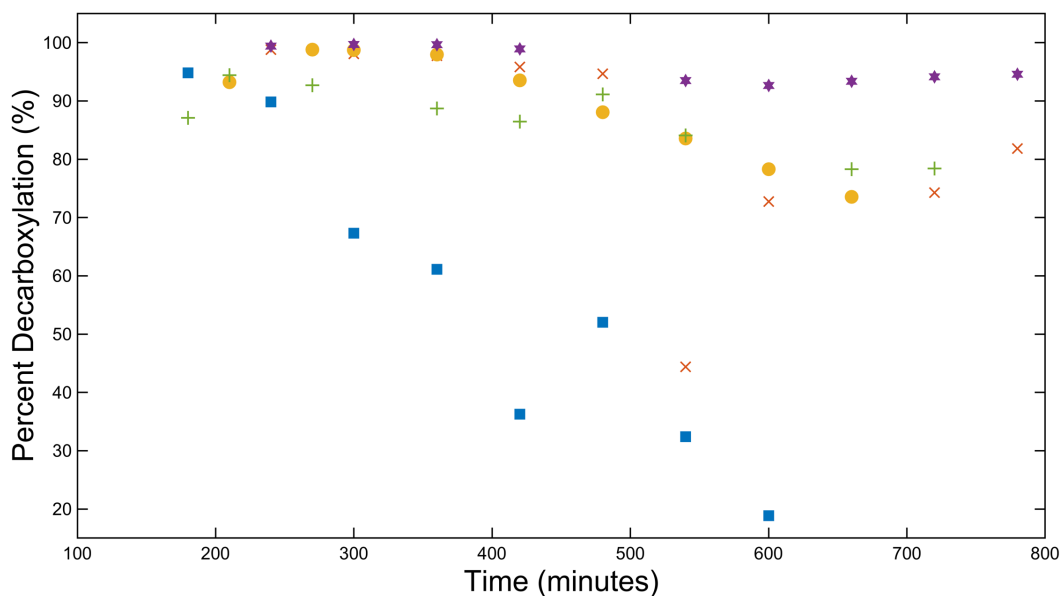


Figure 2.13 Decarboxylation of mixtures of oleic and stearic acid. 0:100 oleic:stearic (■), 10:90 (×), 25:75 (★), 50:50 (+), and 100:0 (●).

Only 10% oleic acid is needed to show improvement over the pure stearic acid feed. Minimum decarboxylation percent with 10:90 OA:SA as feed is observed to be 73%, (whereas the minimum for pure stearic acid is < 20% decarboxylation) at 540 min. The feed ratio with the best performance was found to be 25:75 (oleic:stearic) with all measured samples remaining above 90% decarboxylation. 100% oleic acid feed minimum decarboxylation was found to be 74%, and therefore had a lower performance than the 25:75 (oleic:stearic) feed. While the degree of decarboxylation was highest using the 25:75 feed mixture, it is imperative to know the hydrocarbon product weight fractions. The mass balance of 50:50 oleic stearic mixture is 87 % liquid yield, 10 % solids, and 3 % gas production.

Figure 2.14 demonstrates the product fractions formed by these feed mixtures and are analyzed by GC-FID.

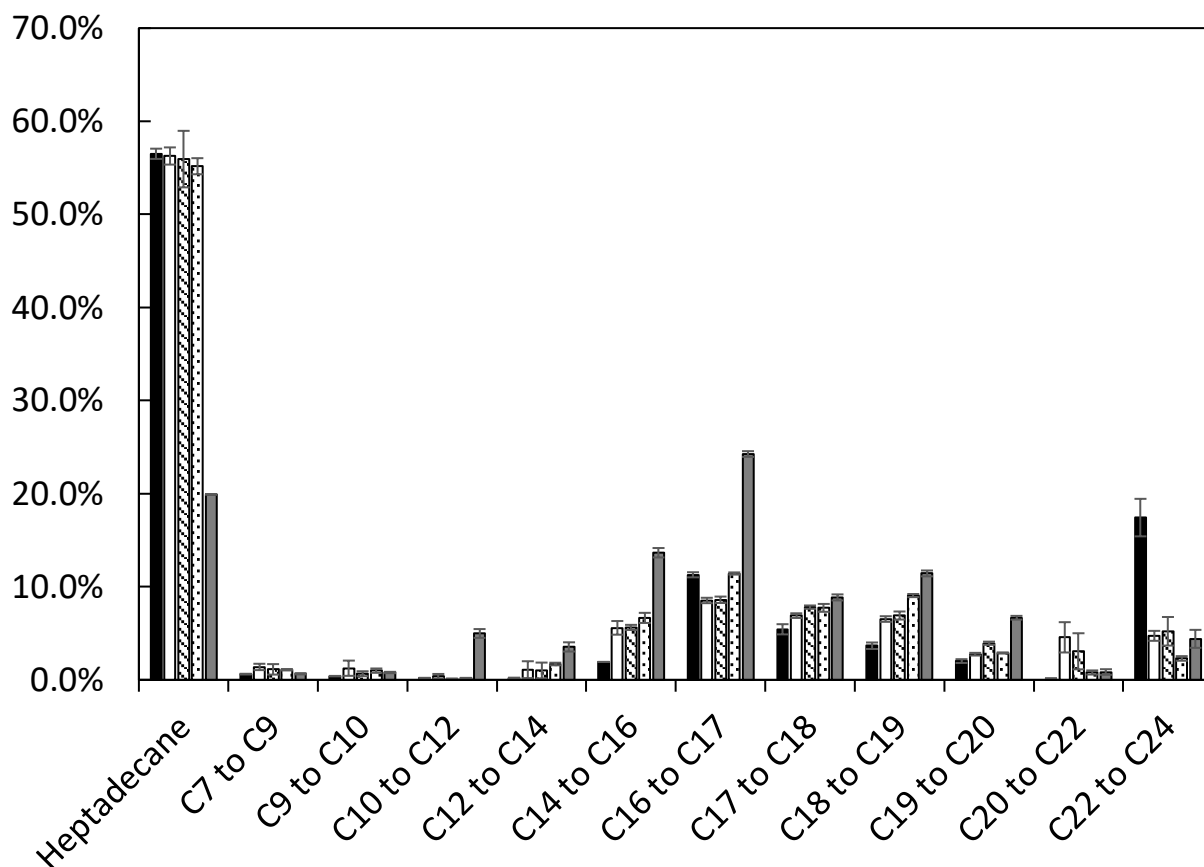


Figure 2.14 Product hydrocarbon fractions of mixtures of stearic and oleic acid. 0:100 oleic:stearic (grey), 10:90 (white), 25:75 (striped), 50:50 (dotted), and 100:0 (black).

It can be seen in Figure 2.14 that the overall heptadecane yield does not change in between any of the SA:OA mixtures and remains around 56.0%. Pure oleic acid results in 19.9% heptadecane and a larger proportion of C<sub>16</sub> to C<sub>17</sub> fractions (24%). 50:50 feed appears to have a slightly larger proportion of C<sub>16</sub> to C<sub>17</sub> fractions (1%) compared to 90:10 (9%) and 25:75 (9%) feed mixtures. This is likely due to the large ratio increase of oleic acid in the feed material. There is a significant decrease in the proportion of C<sub>22</sub> to C<sub>24</sub> fractions when oleic acid, in any proportion, is added to stearic acid as feed. This is because unconverted stearic acid elutes from the column in the same time frame as C<sub>22</sub> to C<sub>24</sub> fractions, as discovered from GC-FID analysis of pure stearic acid. The mixtures also appear to have higher selectivity to heptadecane than pure oleic acid feeds. These findings confirm that additional decarboxylation activity is gained when adding small amounts of oleic acid to stearic acid feeds.

The relevant literature (Fu, Lu, et al., 2011a) states that most catalysts facilitate the saturation reaction first, and then catalyze the decarboxylation reactions. Most literature that states this mechanism uses H<sub>2</sub> gas as an input in their processes. We have shown here that we can sacrifice small amounts of oleic acid to generate higher levels of heptadecane when mixing oleic and stearic acid together as a feed. We postulate that oleic acid is more likely to crack and produce hydrogen, protons, or some other form of hydrogen deposited on or interacting with the catalyst surface that will be referred to as “hydrogen equivalents”. These hydrogen equivalents may act to facilitate decarboxylation and/or enhance the reduction of the activation energy by the MoO<sub>x</sub>/Al<sub>2</sub>O<sub>3</sub> catalyst.

## 2.4.5. Decarboxylation of CDO

Contrary to the findings with Pt/C catalysts by Snare et al. (M. Snåre et al., 2008), we have found increases of reaction rates and resistance to deactivation with added unsaturation at 375 °C. In subcritical water and steam conditions, glycerol and ethanol are suggested to undergo aqueous phase and steam reforming (Luo, Fu, Cao, Xiao, & Edwards, 2008).

The decarboxylation of CDO, without any feed pre-treatments was investigated. It is thought that the steam reforming of glycerol and other natural by-products in CDO may aid in maintaining the catalyst's stability and active catalytic properties. Glycerol should be freed from the TGA via hydrolysis at these conditions in water, and will be allowed to participate in reforming (R. C. Archuleta, 1991). The result of these experiments can be seen in Figure 2.15.

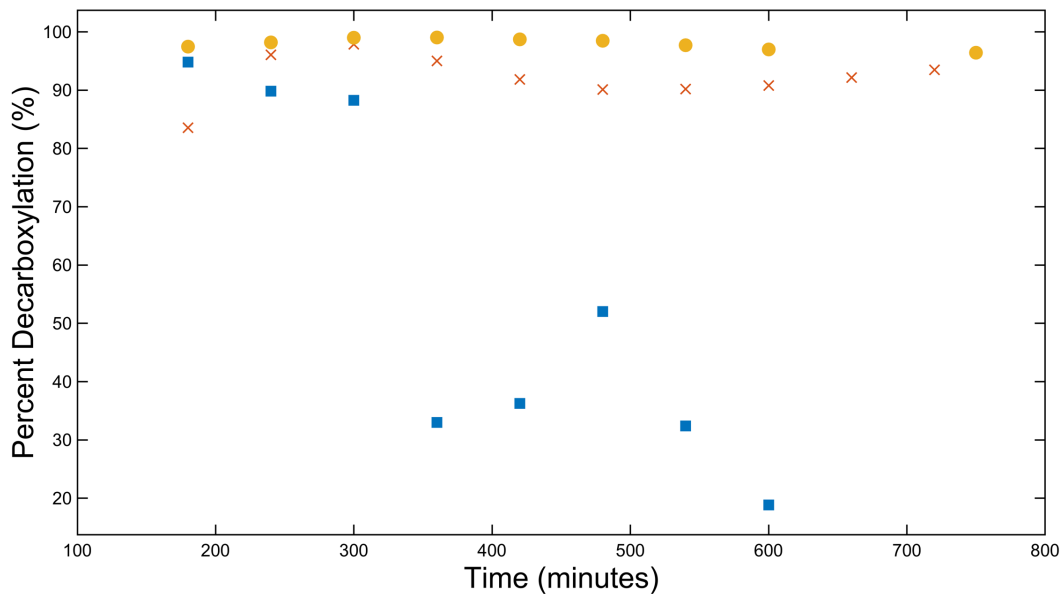


Figure 2.15 Percent decarboxylation over time of CDO at 375 °C in water (●), oleic acid in water at 375 °C (×), and stearic acid at 375 °C (■) all with residence times of 3.5 h.

This system requires no pre-treatment to process corn oil and leads to decarboxylation levels greater than achieved with stearic acid or oleic acid at the same temperature and residence

times (min: 96 % vs min 90 %). The natural unsaturated fatty acids and glycerol present within CDO appears to increase the percent decarboxylation and help to maintain catalyst activity over time.

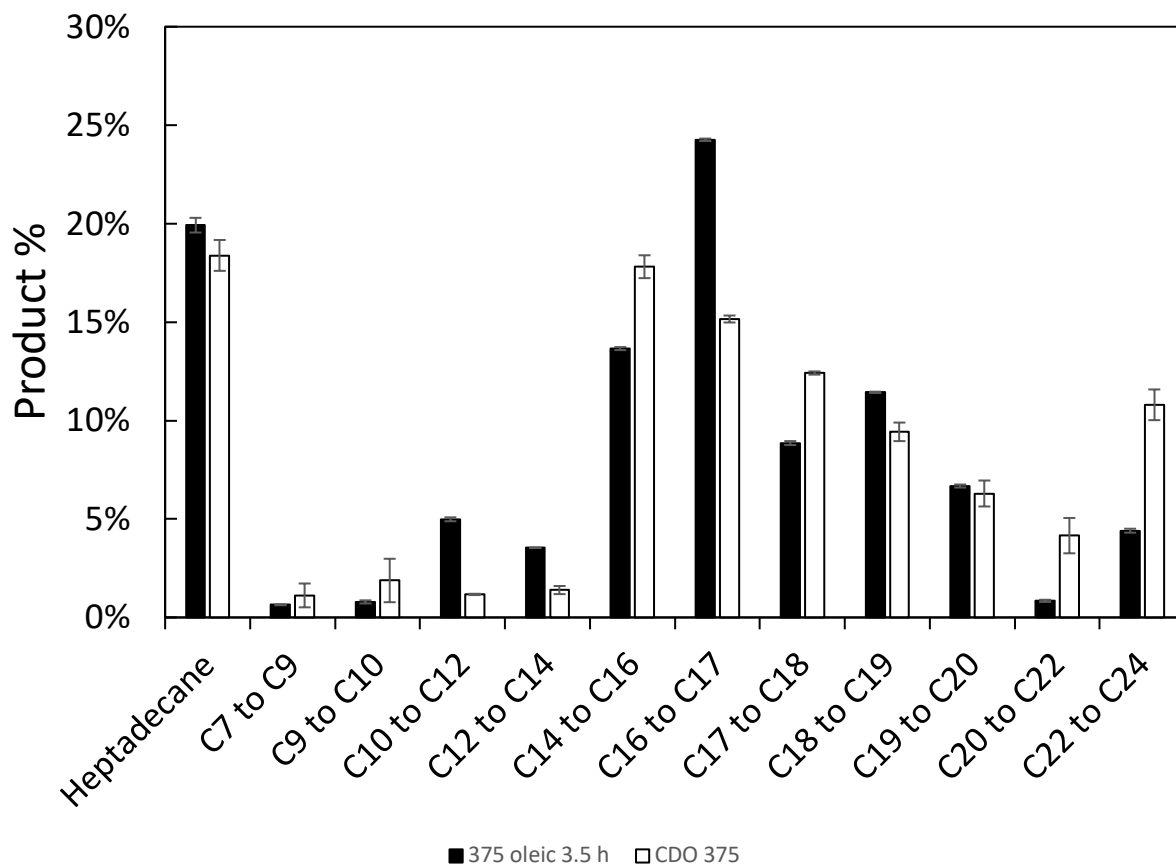


Figure 2.16 GC-FID fractions of products formed from oleic acid in water at 375 °C (black) and CDO in water at 375 °C (white). All experiments were run at 375 °C and 3.5 h residence time.

Figure 2.16 demonstrates the hydrocarbon product profiles of oleic acid and CDO processed at 375 °C with 3.5 h residence time in water. Oleic acid was chosen to compare against CDO as both feeds comprise mostly or only unsaturated fatty acids, as opposed to a saturated fatty acid such as stearic acid. Oleic acid product has a slightly higher proportion of heptadecane at 20 % than CDO product at 18 %. There is a large proportion of C<sub>22</sub> to C<sub>24</sub> in the CDO product (11 %) which is likely due to the cracking of di-unsaturated fatty acids such as linoleic acid after forming products through diels-alder polymerization (Teeter, Bell, O'Donnell, Danzig, & Cowan, 1958), or by radicals that are produced by cracking which then combine with other products. These

heavier types of hydrocarbons have lower fuel quality and can contribute to deactivation of the catalyst over time. Minimizing larger than  $C_{17}$  fractions is desirable. Oleic acid possesses a higher proportion of lighter-than-heptadecane products (48 %) than the CDO product (39 %). Considering that diesel fuel contains hydrocarbons of approximately  $C_{12}$ - $C_{20}$  in length and weight, the presence of larger than  $C_{20}$  fractions in the CDO product would negatively impact fuel quality. It may be necessary in the future to preprocess CDO by hydrogenation and saturation of alkene bonds to improve overall fuel quality by the decarboxylation process.

Third-party fuel quality analysis was carried out by InnoTech Alberta (Edmonton, Alberta) on the 5 h collection sample that was a CDO feed processed at 375 °C with a residence time of 3.5 h. The results from the testing can be observed in

Table 2.1.

Table 2.1 Third Party fuel quality testing on 5 h collection product. Run conditions were 3.5 h residence time and a temperature of 390 °C.

<i>Property</i>	<i>Value</i>	<i>Comments</i>
Cetane Index	65.5-78.4	Minimum Required for Diesel 40
Kinematic Viscosity @40 °C (cSt)	1.96	Typical Diesel 1.3 to 2.4
Oxygen (%)	0.75	Typical Diesel 0.8 (Represents a 93.5% deoxygenation yield vs free fatty acids)
Nitrogen (ppm)	6.3	In diesel fuel range
Carbon (%)	84.23	In diesel fuel range
Hydrogen (%)	13.95	In diesel fuel range
Flash Point (°C)	< -31	Due to the presence of products from decomposition of higher – MW hydrocarbons
10% Recovery (°C)	168.7	Within the range of typical diesel
50% Recovery (°C)	286.9	

Parameters tested for included cetane index (quality aspect of a diesel fuel, related to its density and volatility), kinematic viscosity, oxygen content, nitrogen content, carbon %, hydrogen %, and flash point. All values are within the ranges of a typical diesel fuel without further separation of fatty acid from the diesel-like product. The only parameter that would be desired to be improved is the flash point. It worthwhile to keep in mind that the flash point of Heptadecane is 149 °C, and an increase in heptadecane will result in higher flash points. This fuel may comprise of small chain hydrocarbons and/or substituted aromatics that have low flash points. Based on the GC-FID, CDO product comprises of 76.1% greater than C<sub>16</sub> fractions (does not include heptadecane). The solvent used for GC-FID was hexanes, which prevents the detection of any hexanes produced in the samples. Therefore, the fuel product from CDO is likely to either have large amounts of aromatics, or large amounts of undetectable fractions of C<sub>6</sub> and lower. Molybdenum oxide on alumina has been used as a reforming catalyst in the past, and it is possible that reforming could contribute to the formation of aromatics found in the product (Behnejad, Abdouss, & Tavasoli, 2019). The overall mass balance of the decarboxylation of CDO at 375 °C is 58.82 % liquid yield, 10.32 % solids yield, and 30.95 % gas yield.

It is possible that further distillation of this product can be performed to contour the flash point to be more suitable for diesel. The removal of lower flash point products may be used as a fuel similar to gasoline (flash point of gasoline = -42 °C (Anon, 1974)). It is possible that the removal of gasoline-range fuel molecules will create a diesel or jet fuel in the remaining product, and that the ratio of diesel to jet fuel may be controlled via distillation.

## 2.4.6. NMR of Products

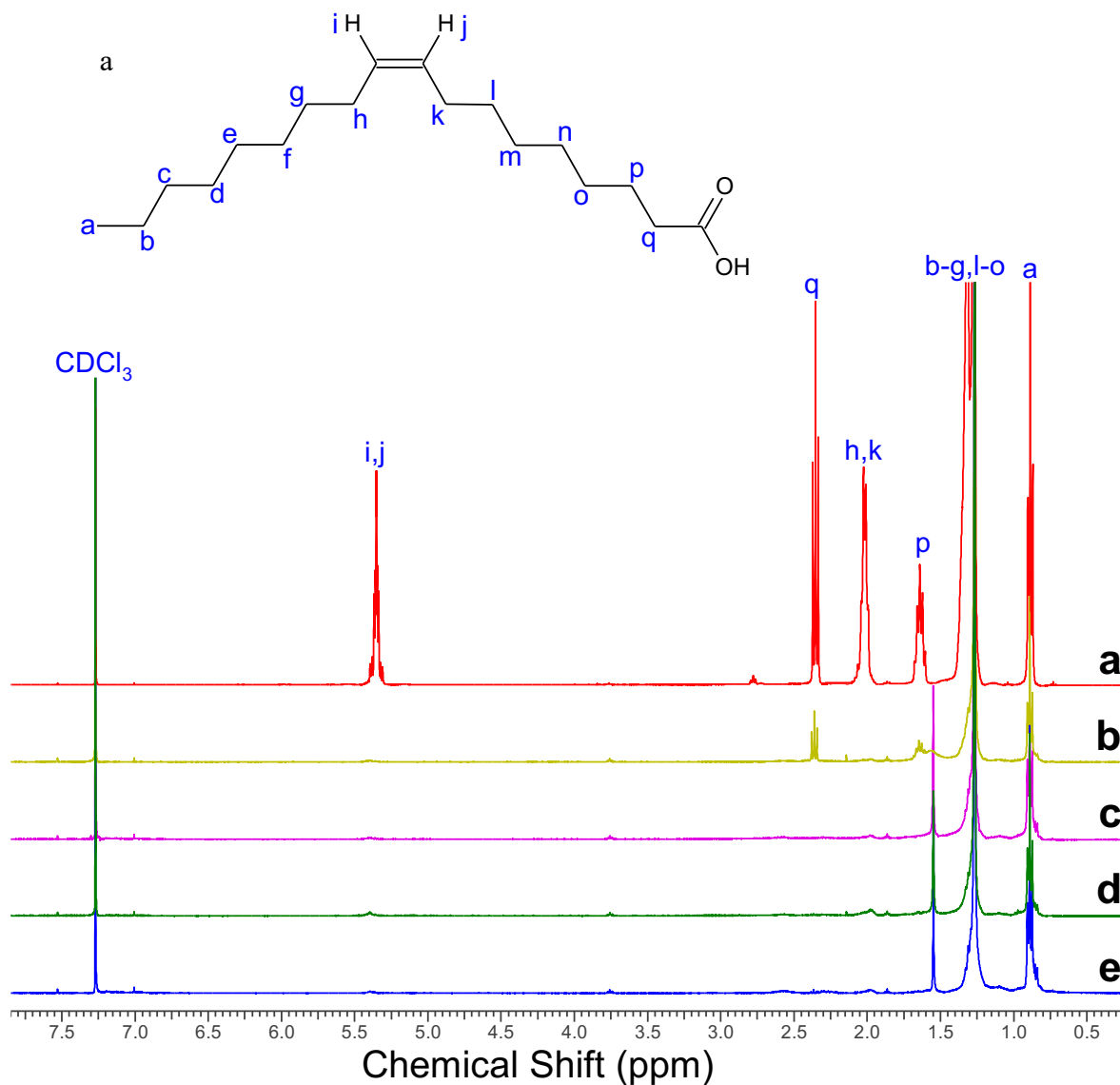


Figure 2.17  $^1\text{H}$  NMR spectra of (a) oleic acid, (b) stearic 375 °C 3.5h, (c) stearic 390 °C 3.5 h (4 h collection point), (d) stearic 390 °C 3.5 h (8 h collection point), (e) stearic 400 °C 3.5h.

Excess amounts of cracking may lead to products with extensive amounts of double bonds that may lead to less stable fuel products (Pereira & Pasa, 2006). These products may polymerize or oxidize over time, leading to gum formation in fuels. To better understand the conversion of alkenyl group and decarboxylation of oleic acid, stearic acid, and mixes of the two, the decarboxylated liquid products were further characterized by  $^1\text{H}$  NMR spectroscopies. Figure 2.17

compares the  $^1\text{H}$  NMR spectra of oleic acid and the formed liquid products. In the spectrum of oleic acid (Figure 2.16a), there are several proton peaks located at 10.74 (a broad peak, not shown), 5.35, 2.36, 2.04, 1.64, 1.30, and 0.89 ppm that can be attributed to protons adjacent and secondary to the carbonyl group (p, q), alkenyl protons (i,j,h,k), methylene (b-g l-o), and methyl (a) protons, respectively. In the spectrum of the formed products from stearic acid (d and e), there is a reduction of the peaks related to the carboxylic group (p,q) and a minimal quantity of alkenyl groups (i,j,h,k). In the spectrum of the formed products from stearic acid (Figure 2.15a), there is a reduction of the peaks related to the carboxylic group (p, q) and a minimal quantity of alkenyl groups (i,j,h,k), suggesting incomplete decarboxylation at 375 °C, but minimal carboxylic acid at temperatures greater than 375 °C. The presence of the alkenyl group (i,j,h,k) has been significantly diminished compared to the starting material, which indicates significant conversion of the alkenyl group. Therefore, all of these NMR results support the hypothesis that decarboxylation is occurring reaction under the selected reaction conditions. The NMR results are in good agreement with the FTIR results. During cracking, carbon-carbon single bonds release hydrogen to form alkene bonds. If extensive cracking is taking place to decarboxylate the fatty acids, the oleic acid product NMR spectrum should show large alkene peaks. There appears to be a slight production of alkene groups in all products, and possibly more alkene present in 390 °C at 8 h collection than 4 h collection. This ties into the GC-FID profile in which there are larger percentages of cracked product the longer the plug flow reactor is run.

## 2.4.7. Catalyst Characterization

According to literature, catalyst acidity is a predictor of catalyst activity (Fu et al., 2010; Hossain, Chowdhury, Jhavar, Xu, Biesinger, et al., 2018). Theoretically, catalyst activity and longevity should be improved if fully saturated feeds are used, as lower proportions of double bonds will result in less cracking by acidic catalysts (M. C. Kim & Kim, 1996) and result in less dimerized products (Den Otter, 1970). However, it is found in this study with mixtures of oleic and stearic acid that there is an optimal level of unsaturation that produces desired chain lengths and deoxygenated content. Fully saturated stearic acid has shown low degrees of decarboxylation, and 100% oleic acid results in a larger proportion of cracked products and larger amounts of high molecular weight products. It is hypothesized that the cracking reactions on the catalyst surface will lead to coking, which leads to reductions in surface area and pore size. These reductions in surface area and catalyst pore size lead to deactivation of the catalyst.

The effect of the composition variation on the textural properties of the fresh and spent catalyst was evaluated by N<sub>2</sub> physisorption. The main properties determined were surface area, pore volume, and pore size. The results of N<sub>2</sub> physisorption of various spent catalysts can be seen in *Table 2.2.2*.

All isotherms are type IVa according to the IUPAC classification, which is characteristic for mesoporous materials (Thommes et al., 2015). The isotherms can be found in the supporting information. The data show that the surface area and volume all reduced in the spent catalysts whereas pore size appears to remain unchanged or increased. The fresh catalyst has a surface area of 140.9 m<sup>2</sup>/g, a pore volume of 0.4 cm<sup>3</sup>/g, and a pore size of 116.4 Å. There is a greater reduction in area and volume when oleic acid is used as a feed and when stearic acid is processed below or above 390 °C. Stearic acid at 375 °C with both 3.5 h and 5 h residence times show decreases in surface area, and pore volume compared to fresh catalyst. It is also observed that surface area and pore volumes are slightly reduced at higher residence time (5 h compared with 3.5 h residence time). The GC-FID revealed that a larger degree of cracked products produced in 5 h, and cracked products may deposit on the catalyst and reduce activity as coke. It stands to reason that cracking produces more coke, which eventually will lead to catalyst deactivation. Stearic acid processed at 390 °C and at 3.5 h residence time showed the best properties out of any of the spent catalysts

examined, which indicates that this might be the best condition to prevent coke formation. The catalyst processed with 25:75 OA:SA feed at 3.5 h and 375 °C shows the highest reduction in surface area (41.7%) and pore volume (41.5%). The 25:75 OA:SA mixture had the greatest decarboxylation results of all the mixtures, but the worst surface area properties. The increase in decarboxylation activity is likely related to the activity of cracking and coke production, which reduces the surface properties. Surprisingly, CDO processed catalyst shows good surface area properties (SA = 97.25 m<sup>2</sup>/g, PV = 0.28 cm<sup>3</sup>/g) considering that it contains lots of unsaturated fatty acids and glycerol, which are thought to contribute to coking.

Table 2.2.2. Surface Areas, Pore Volumes, and Pore Sizes of Selected Catalysts

<b>Sample ID</b>	<b>BET Surface Area (m<sup>2</sup>/g)</b>	<b>Pore Volume (cm<sup>3</sup>/g)</b>	<b>Pore Size (Å)</b>
<b>Fresh Catalyst</b>	140.91	0.41	116.36
<b>Gamma alumina calcined</b>	145.22	0.46	126.46
<b>Spent Catalyst, stearic 3.5h at 375 °C</b>	100.88	0.29	114.17
<b>Spent Catalyst, stearic at 390 °C</b>	107.76	0.32	117.86
<b>Spent catalyst, stearic 3.5h at 400 °C</b>	98.74	0.29	118.26
<b>Spent Catalyst, stearic 5h at 375 °C</b>	94.16	0.28	117.96
<b>Spent catalyst, oleic 3.5 h at 375 °C</b>	86.41	0.26	120.74
<b>Spent catalyst, OA:SA 25:75 3.5 h at 375 °C</b>	82.21	0.24	117.16
<b>Spent catalyst, CDO 3.5 h at 375 °C</b>	97.25	0.28	113.74

Thermogravimetric analysis (TGA) under an air atmosphere was further used to compare the fresh and spent catalysts. An example TGA plot is shown in Figure 2.18 which is the TGA of spent catalyst processed with stearic acid at 390 °C with a residence time of 3.5 h.

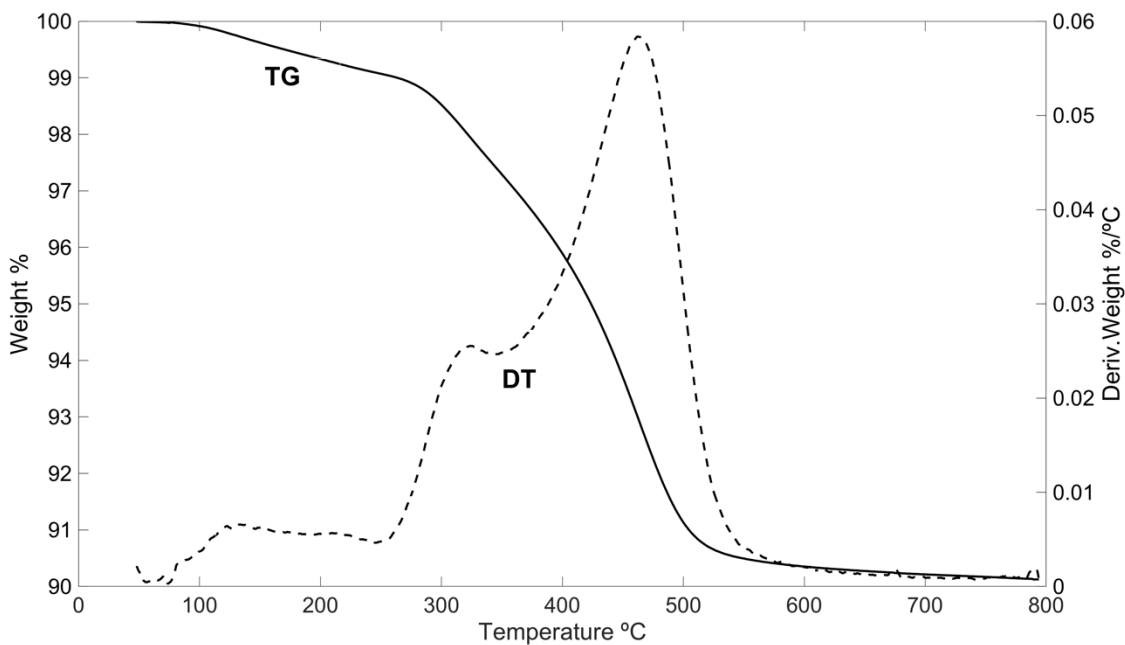


Figure 2.18 TGA analysis of spent catalyst processed with stearic acid feed under 390 °C and a residence time of 3.5 h. TGA (TG) signal corresponds to the left axis while the derivative of the TGA signal (DT) corresponds to the right axis.

Table 2.3 shows the relative percent weight of the catalyst that is water, volatiles, polymer/feed, and coke present on the surfaces of the catalysts tested. The weight losses observed in the TGA profiles at temperatures of less than 130 °C are assigned to the removal of adsorbed water. The weight loss associated with the fresh catalyst corresponds to the removal of adsorbed water. Weight losses at temperatures greater than 130 °C but less than 250 °C are attributed to low volatility carbonaceous species. The weight loss at temperatures between 250 °C and 400 °C are attributed to deposited feed products and similar diels-alder adduct species. Weight losses greater than 400 °C and lesser than 600 °C for the spent catalyst is due to the burning of amorphous carbon (coke) that was deposited on the catalyst's surface post-reaction. These deposited materials may contribute to the observed reduction in catalyst surface area of the spent catalyst as found by N<sub>2</sub> physisorption. Any weight losses occurring at greater than 600 °C are attributed to graphitic coke, and of which none were found.

TGA supports the findings of N<sub>2</sub> physisorption, as in spent catalysts that have reduced surface areas, there is more coke present (25:75 OA:SA, pure oleic, 375 °C 3.5 h SA, 375 °C 5 h SA). The 25:75 OA:SA feed also leaves a much larger amount of remaining feed material/polymer deposited on the catalyst surface. It appears that stearic acid processed at 390 °C at 3.5 h has some of the best activity combined with the least amount of deposited material with the least reduction in surface and pore size, as confirmed by TGA and N<sub>2</sub> Physisorption.

Table 2.3 Relative weights of products on catalyst surfaces measured by TGA

<b>Sample ID</b>	<b>% Water</b>	<b>%Low Volatile</b>	<b>%Polymer/feed</b>	<b>% Coke</b>
<b>Fresh catalyst</b>	1.80	1.26	0.00	0.00
<b>Spent Catalyst, stearic 3.5h at 375 °C</b>	0.77	0.79	4.39	7.21
<b>Spent Catalyst, stearic at 390 °C</b>	0.25	0.68	3.18	5.54

<b>Spent catalyst, stearic 2.5h at 400 °C</b>	0.65	0.55	3.15	5.04
<b>Spent Catalyst, stearic 5h at 375 °C</b>	0.86	0.63	2.95	6.94
<b>Spent Catalyst, oleic 3.5 h at 375 °C</b>	0.65	0.91	5.67	7.04
<b>Spent Catalyst, oleic 2.5 h at 375 °C</b>	0.34	0.40	2.60	5.03
<b>Spent catalyst, OA:SA 25:75 3.5 h at 375 °C</b>	0.39	0.99	6.06	6.97

Active metal dispersion is an important catalyst quality, as it gauges efficiency and access of reactant to the active site. Catalyst active metal dispersion was measured by O<sub>2</sub> pulse chemisorption. Sintering was found to occur between fresh and spent catalysts, with a drop in overall dispersion of 50%. O<sub>2</sub> pulse chemisorption profiles for fresh and spent catalyst can be found in the appendix.

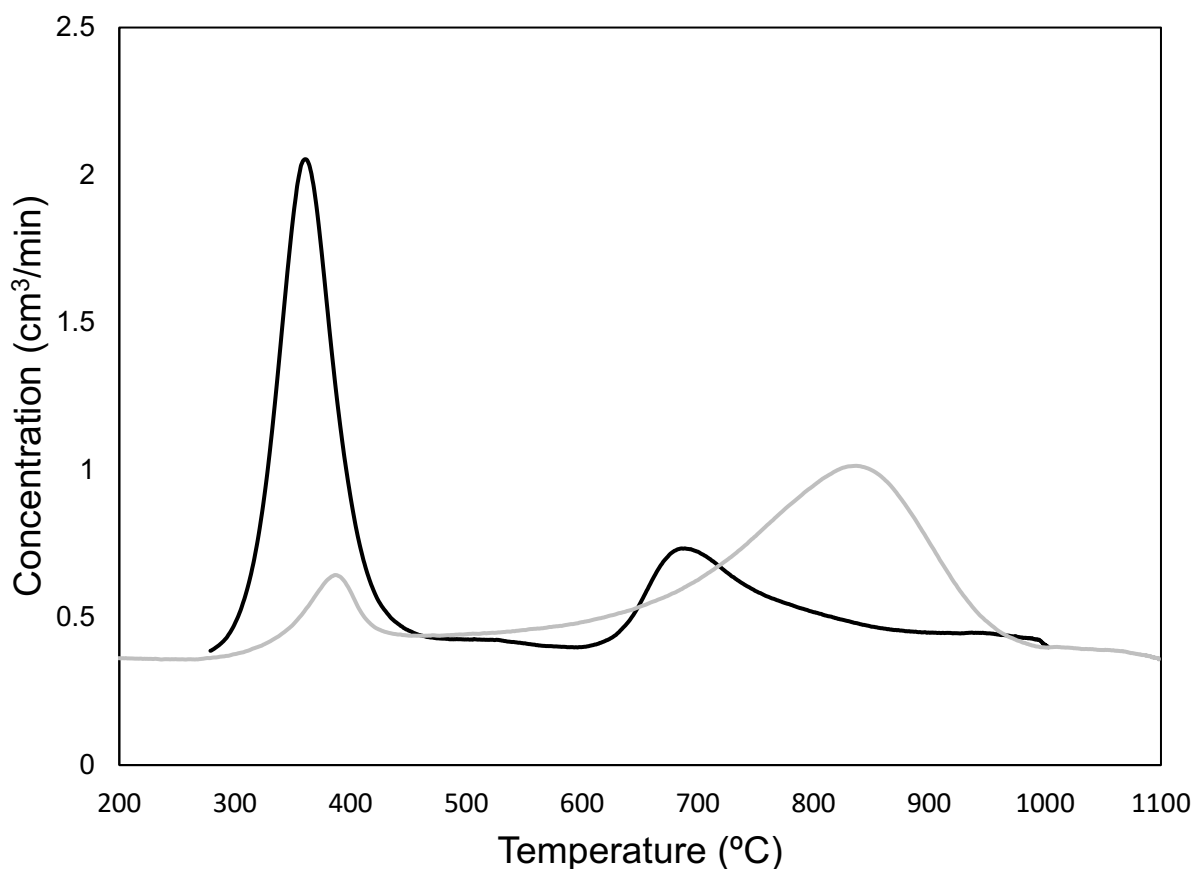


Figure 2.19 Temperature Programmed Reduction of fresh (grey) and spent (black)  $\text{MoO}_x/\text{Al}_2\text{O}_3$  catalysts.

$\text{H}_2$ -TPR experiments were conducted to determine the reduction temperatures of the fresh and spent catalysts.  $\text{H}_2$ -TPR profiles of fresh catalysts are shown in Figure 2.19. Two reduction peaks are observed in the fresh catalyst at 393 °C and 842 °C. It has been demonstrated that the reduction of Mo species is a two-step process, as the reduction progresses from  $\text{MoO}_3$  to  $\text{MoO}_2$  and then from  $\text{MoO}_2$  to Mo (Ma et al., 2015). Different reduction temperatures obtained in the TPR profile indicate two different Mo species present, which are confirmed by XPS to be Mo(VI) and Mo(V) in Figure 2.21. The TPR profile of spent catalyst indicates two peaks at 364 °C and 690 °C. The 364 °C peak in the spent catalyst is much larger than the 393 °C in the fresh catalyst, and could be related to an increase in that phase of Mo. An increase in Mo(V) and Mo(IV) can be seen in the XPS spectra of the spent catalyst in Figure 2.21.

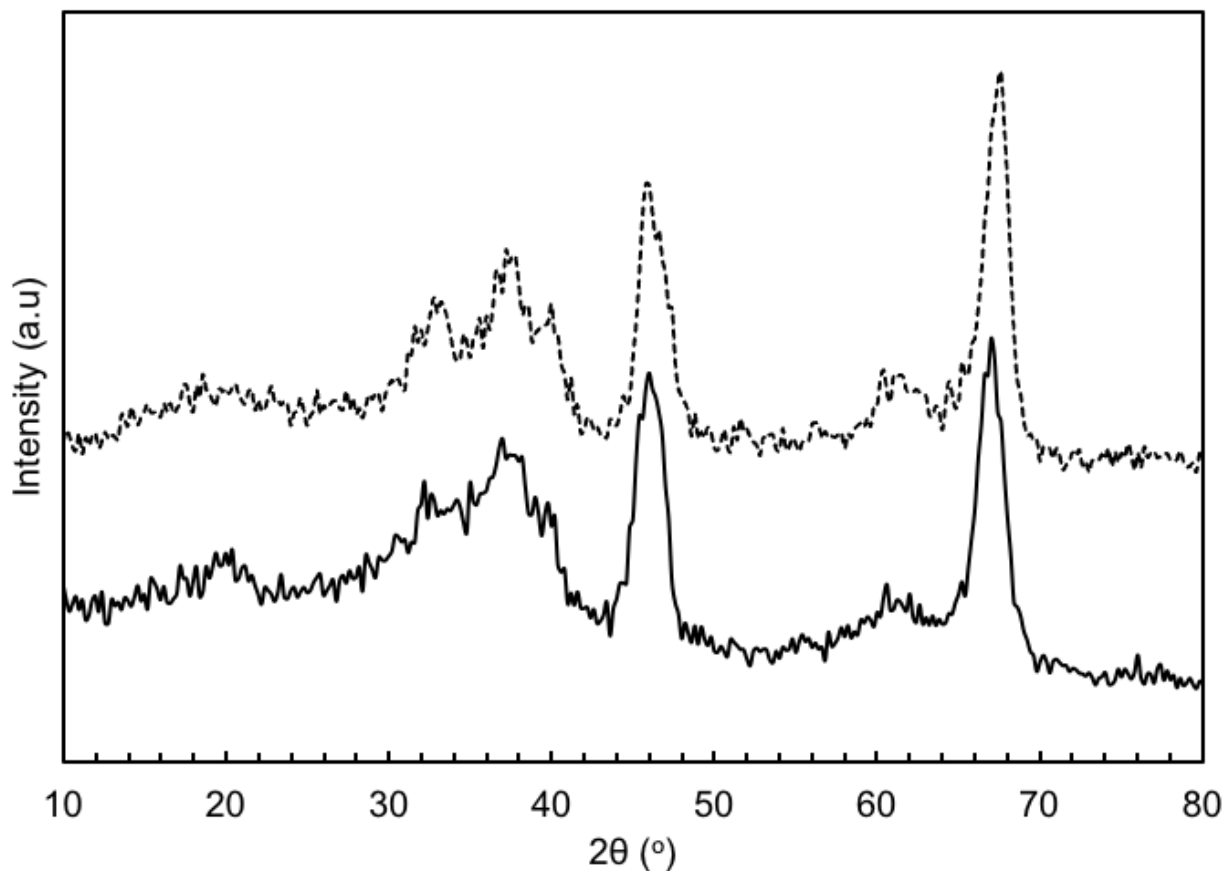


Figure 2.20 XRD spectra of fresh (solid line) and spent (dashed line)  $\text{MoO}_3$  catalysts. There is no indication of graphitic coke ( $14.8$  and  $28.6^\circ$ ) in the spent catalyst

Crystallinity of catalysts are typically measured by X-Ray powder diffraction (XRD). XRD pattern of fresh catalysts and support are shown in Figure 2.20. The peaks of pure  $\gamma\text{-Al}_2\text{O}_3$  phase can be seen at  $2\theta = 35.2, 47.2$  and  $67.6^\circ$  (Charisiou, Baklavaridis, Papadakis, & Goula, 2016). Very weak reflections of pure Mo can be seen at  $2\theta = 42$  and  $61^\circ$ , and other phases of molybdenum oxides are not readily visible in these spectra. No reflections for  $\theta\text{-Al}_2\text{O}_3$  ( $25.6$  and  $43.3^\circ$ ) or  $\alpha\text{-Al}_2\text{O}_3$  ( $31.2$  and  $36.6^\circ$ ) (Dou, Wang, Song, Chen, & Xu, 2014) were observed on the catalysts, indicating that no  $\theta\text{-Al}_2\text{O}_3$  was formed by calcination or reaction conditions. XRD is also used to probe for the presence of graphitic coke. No graphitic coke at  $14.8$  and  $28.6^\circ$  was observed in the spent catalysts (Hossain, Chowdhury, Jhavar, Xu, Biesinger, et al., 2018).

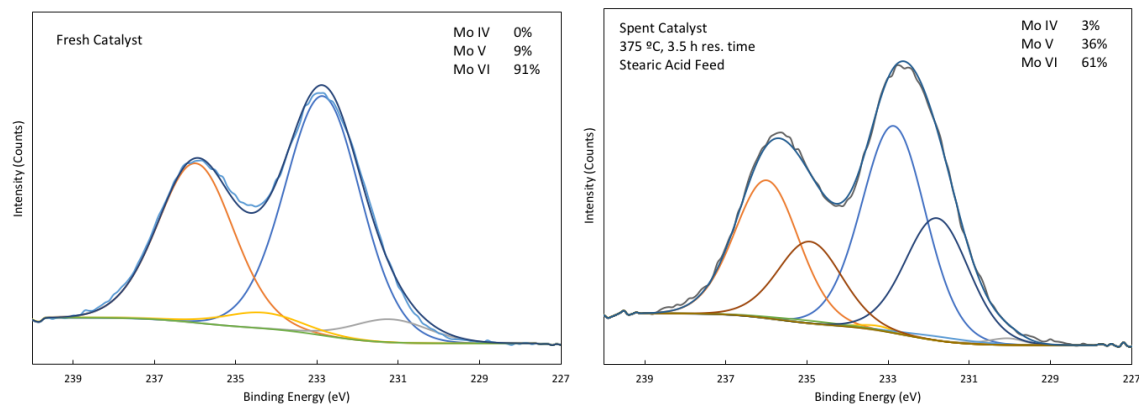


Figure 2.21 XPS spectra for Mo/Al<sub>2</sub>O<sub>3</sub> catalysts. Spectrum on the left is of a fresh catalyst, spectrum on the right is a spent catalyst that was used with stearic acid at 375 °C and 3.5 h residence time.

For a more detailed investigation of the surface structure, XPS spectra of a fresh and spent MoO<sub>x</sub>/Al<sub>2</sub>O<sub>3</sub> catalyst are presented in Figure 2.21. The spent catalyst is from the process using stearic acid as a feed at 375 °C with a residence time of 3.5 h. This catalyst was chosen as it had demonstrated some of the lowest conversion of fatty acid to deoxygenated product. The spectra were curve-fit using the screened and unscreened peak-fitting parameters peak positions, full width at half-maximum (fwhm), and area ratios for Mo(IV) as outlined by Scanlon et al. (Scanlon et al., 2010) There appears to be a large degree of change from Mo(VI) to Mo(V) between fresh and spent catalyst. There is a four-fold increase in proportion of Mo(V). This transition between Molybdenum oxidation states can also be seen in a study by Hossain et al. (Hossain, Chowdhury, Jhavar, Xu, Biesinger, et al., 2018) in which they also use a Molybdenum doped Alumina catalyst.

A Mo 3d<sub>5/2</sub>–Mo 3d<sub>3/2</sub> spin–orbit doublet for Mo(VI) was constrained to have an area ratio of 3:2, equal fwhms, a doublet spacing of 3.13 eV, and an Mo 3d<sub>5/2</sub> peak position ranging from 232.2 to 232.6 eV (Hossain, Chowdhury, Jhavar, Xu, Biesinger, et al., 2018). Peak fitting showed that a small component attributable to Mo(V) was also present. As such, a spin–orbit doublet, constrained to have a similar fwhm as that for the Mo(VI) component, was added with an Mo 3d<sub>5/2</sub> peak position ranging from 231.6 to 231.9 eV. (Spevack & McIntyre, 1992), (Clayton & Lu,

1989). The presence of Mo(V) may be due to the effect of the X-ray reduction of MoO<sub>3</sub> during XPS analysis (Baltrusaitis et al., 2015).

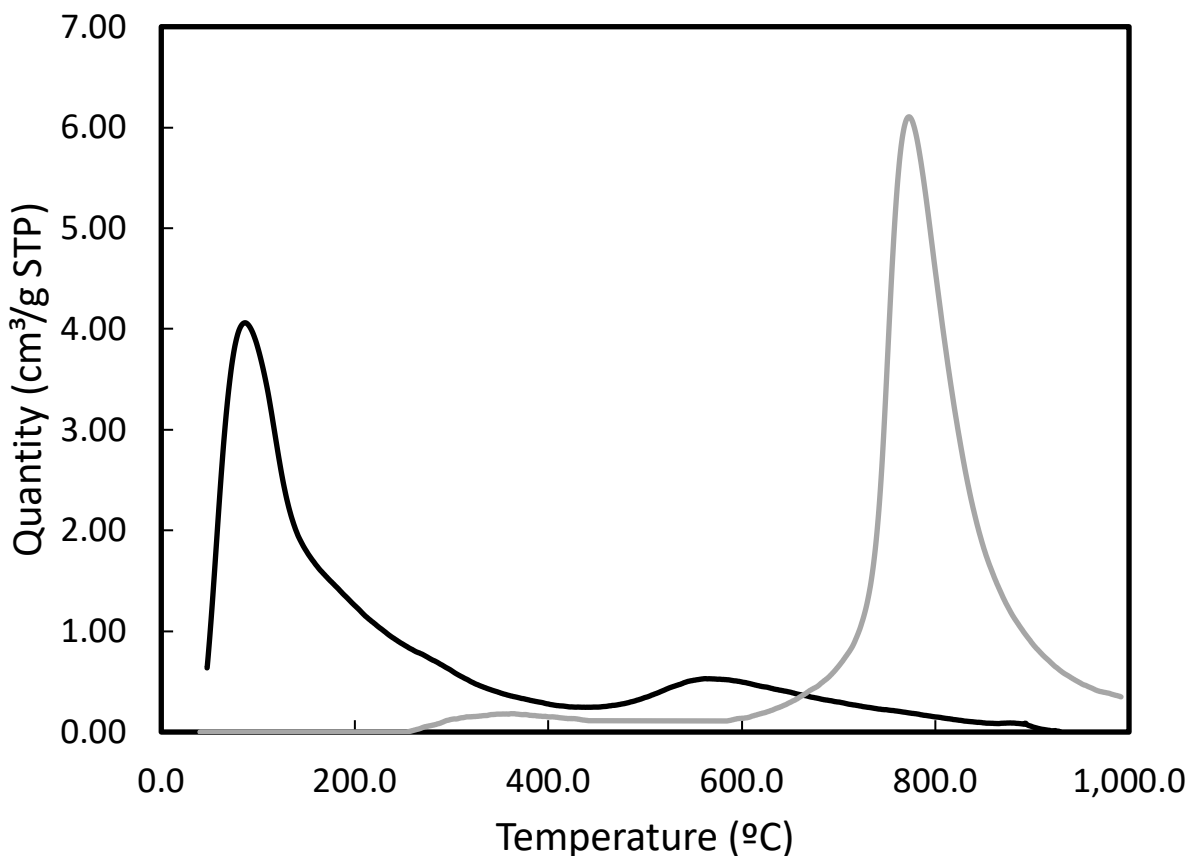


Figure 2.22 NH<sub>3</sub> TPD of spent (grey) and fresh (black) MoO<sub>x</sub>/Al<sub>2</sub>O<sub>3</sub> catalysts

Due to the heterogeneity of solid surfaces, materials can possess acidic and basic sites (Lewis or Brønsted types) of various strengths. Ammonia can interact with acidic sites through hydrogen bonding, and Hengst et al. (Hengst et al., 2015) found enhanced deoxygenation of free fatty acids using an acidic catalyst (Pd/Pural SB1-derived Al<sub>2</sub>O<sub>3</sub>). As acidic sites can correlate with activity, the catalyst was probed for acidic sites by the use of NH<sub>3</sub> Temperature Programmed Desorption (TPD). The sorption profiles of a spent and fresh MoO<sub>x</sub>/Al<sub>2</sub>O<sub>3</sub> can be seen in

Figure 2.22. More NH<sub>3</sub> is adsorbed onto the surface of the spent catalyst than the fresh (52.68 vs 19.11 cm<sup>3</sup>/g STP) but this larger amount of acid sites desorb at a temperature of 775 °C.

NH<sub>3</sub> molecules released at temperatures lower than 400 °C correspond to weak acidity, while sorption occurring past 400 °C is indicative of strong acid sites (Gonçalves, Faustino, Assaf, & Jaroniec, 2017).

It is theorized weak acid sites are the active sites of decarboxylation (H. Wang, Lin, Feng, Han, & Zheng, 2017) (Dos Anjos, De Araujo Gonzalez, Lam, & Frety, 1983) (Kirszensztejn, Przekop, Tolińska, & MaćKowska, 2009), and strong acid sites contribute to cracking and coking. The turnover number (TON) is defined as molecules reacting per catalyst active site (IUPAC, 2014). Turnover frequency (TOF) is the TON per unit time. The TON and TOF are convenient ways to express and compare catalytic activity of catalysts.

$$TON = \frac{\text{moles of reactant consumed}}{\text{moles of catalyst active sites}} \quad TOF = \frac{TON}{\text{reaction time}} \quad (2.4)$$

Based on the calculated moles of acid sites of the fresh catalyst (0.05 moles) and the number of moles of stearic acid converted at 390 °C with a residence time of 2.5 h (0.033 moles), the TON is 0.66 moles of product/moles of acid sites and the TOF is 0.0044 moles of product/moles of acid sites/minute. Since the turnover number is less than one, this suggests that MoO<sub>x</sub>/Al<sub>2</sub>O<sub>3</sub> may not be acting as a catalyst, instead maybe participating as a reactant (e.g. hydrogen on catalyst surface). It could also suggest that the site of catalysis for decarboxylation may not be acid sites.

The spent catalyst has an increase in the number of strong acid sites, and a reduction in weak sites. Peng et al. (J. Peng, Chen, Lou, & Zheng, 2009) confirm that strong acid sites are on HZSM-5 catalysts enhance the cracking of bio-oil. It is possible that over extended reaction time in a continuous reactor that cracking increases due to the increase of strong acid sites on the catalyst. We are increasing the strong acidity and therefore cracking, and this is evidently seen in Table A.5.1. Table A.5.1. shows that over the extent of time, selectivity to heptadecane decreases and the relative number of cracked fractions increases. This could lead to enhanced coking over time and therefore catalyst deactivation.

## 2.5. Conclusions

The scalable decarboxylation of corn distiller's oil, stearic acid, oleic acid, and mixtures of both under high temperature water conditions was demonstrated and examined in this work. Our study showed that it is possible to remove almost 100% of the carboxylic acid groups from oleic acid and stearic acid to produce distributions of hydrocarbons. Oleic acid decarboxylates more readily possibly due to its alkene bond being an oxidation site that facilitates cracking, adding hydrogen into the process that enhance decarboxylation. The removal of oxygen in the form of carboxylic acid was confirmed by ATR-FTIR spectroscopy and its accuracy validated by correlation to acid value titrations. We can selectively tune for heptadecane by changing the proportions of the feed content to have more stearic acid. Having a small proportion (10%) of oleic acid was found to decrease the temperature needed for the near-complete decarboxylation of stearic acid from 375 °C to 390 °C. We avoided the use of expensive noble metal catalyses, hydrogen gas, and used steam as a green solvent to build towards a green and inexpensive green diesel production process. A feedstock of 50:50 oleic:stearic acid processed at 375°C and 3.5 h residence time had a minimum decarboxylation of 90 % in all its samples, a selectivity to heptadecane of 55 % at 5 h collection, and a liquid yield of 86 %. The GC-FID indicated the 50:50 mix feed contained lower ratio of alkenes to alkanes as compared to pure oleic acid feeds, as confirmed by NMR spectroscopy. It was also found that the selectivity to heptadecane decreases as the process continues, with an increase of a distribution of products. A third-party fuel analysis was performed and found that our product formed from CDO was suitable as a diesel fuel in all qualities measured, except for flash point. The extremely low flash point (-31 °C) indicates that there may be a high proportion of small chain products, as confirmed by GC-FID.

## 2.6. References

- 11, A. D. –. (2011). Standard Test Method for Acidity in Aviation Turbine Fuel 1. *Annual Book of ASTM Standards*. <https://doi.org/10.1520/D3242-11>.This
- Abbas, J., Hussain, S., Iqbal, M. J., Nadeem, H., Qasim, M., Hina, S., & Hafeez, F. (2016). Oil industry waste: a potential feedstock for biodiesel production. *Environmental Technology (United Kingdom)*. <https://doi.org/10.1080/09593330.2016.1141997>
- Abdulkareem-Alsultan, G., Asikin-Mijan, N., Lee, H. V., Rashid, U., Islam, A., & Taufiq-Yap, Y. H. (2019). Review on thermal conversion of plant oil (Edible and inedible) into green fuel using carbon-based nanocatalyst. *Catalysts*. <https://doi.org/10.3390/catal9040350>
- Adroit Market Research. (2019). *Global Biodiesel Market Size 2019 by Feedstock (Vegetable Oil [Soybean oil, Canola oil, Other edible oils], Animal fats[Poultry, White grease, Tallow, Others]), by Application (Fuel[Automotive, Marines, Others], Power Generation, Others), by Region and Fo*. Dallas, TX.
- Afshar Taromi, A., & Kaliaguine, S. (2018). Hydrodeoxygenation of triglycerides over reduced mesostructured Ni/γ-alumina catalysts prepared via one-pot sol-gel route for green diesel production. *Applied Catalysis A: General*, 558(September), 140–149. <https://doi.org/10.1016/j.apcata.2018.03.030>
- Ahmadi, M., Macias, E. E., Jasinski, J. B., Ratnasamy, P., & Carreon, M. A. (2014). Decarboxylation and further transformation of oleic acid over bifunctional, Pt/SAPO-11 catalyst and Pt/chloride Al<sub>2</sub>O<sub>3</sub> catalysts. *Journal of Molecular Catalysis A: Chemical*. <https://doi.org/10.1016/j.molcata.2014.02.004>
- Al Alwan, B., Salley, S. O., & Ng, K. Y. S. (2015). Biofuels production from hydrothermal decarboxylation of oleic acid and soybean oil over Ni-based transition metal carbides supported on Al-SBA-15. *Applied Catalysis A: General*, 498, 32–40. <https://doi.org/10.1016/j.apcata.2015.03.012>
- Anon. (1974). FLAMMABLE AND COMBUSTIBLE LIQUIDS CODE 1973. *ANSI Stand.*

- Asomaning, J., Mussone, P., & Bressler, D. C. (2014). Thermal deoxygenation and pyrolysis of oleic acid. *Journal of Analytical and Applied Pyrolysis*. <https://doi.org/10.1016/j.jaap.2013.09.005>
- Babcock, B. A. (2012). The impact of US biofuel policies on agricultural price levels and volatility. *China Agricultural Economic Review*. <https://doi.org/10.1108/17561371211284786>
- Baltrusaitis, J., Mendoza-Sanchez, B., Fernandez, V., Veenstra, R., Dukstiene, N., Roberts, A., & Fairley, N. (2015). Generalized molybdenum oxide surface chemical state XPS determination via informed amorphous sample model. *Applied Surface Science*. <https://doi.org/10.1016/j.apsusc.2014.11.077>
- Behnejad, B., Abdouss, M., & Tavasoli, A. (2019). Comparison of performance of Ni–Mo/ $\gamma$ -alumina catalyst in HDS and HDN reactions of main distillate fractions. *Petroleum Science*. <https://doi.org/10.1007/s12182-019-0319-5>
- Bell, A. T., Gates, B. C., Ray, D., & Thompson, M. R. (2008). *Basic Research Needs: Catalysis for Energy*. <https://doi.org/10.2172/927492>
- Button, S. (2010). Biodiesel: Vehicle Fuel from Vegetable Oil. *Energy & Environment*. <https://doi.org/10.1260/0958-305x.20/21.8/1.1305>
- Castello, D., & Fiori, L. (2011). Supercritical water gasification of biomass: Thermodynamic constraints. *Bioresource Technology*. <https://doi.org/10.1016/j.biortech.2011.05.017>
- Centeno, A., Laurent, E., & Delmon, B. (1995). Influence of the support of CoMo sulfide catalysts and of the addition of potassium and platinum on the catalytic performances for the hydrodeoxygenation of carbonyl, carboxyl, and guaiacol-type molecules. *Journal of Catalysis*. <https://doi.org/10.1006/jcat.1995.1170>
- Chapman, L. (2007). Transport and climate change: a review. *Journal of Transport Geography*. <https://doi.org/10.1016/j.jtrangeo.2006.11.008>
- Charisiou, N. D., Baklavaridis, A., Papadakis, V. G., & Goula, M. A. (2016). Synthesis Gas Production via the Biogas Reforming Reaction Over Ni/MgO–Al<sub>2</sub>O<sub>3</sub> and Ni/CaO–Al<sub>2</sub>O<sub>3</sub>

- Catalysts. *Waste and Biomass Valorization*. <https://doi.org/10.1007/s12649-016-9627-9>
- Cheng, H. N., Dowd, M. K., Easson, M. W., & Condon, B. D. (2012). Hydrogenation of cottonseed oil with nickel, palladium and platinum catalysts. *JAOCs, Journal of the American Oil Chemists' Society*. <https://doi.org/10.1007/s11746-012-2036-8>
- Chou, C. C., Riviere, J. E., & Monteiro-Riviere, N. A. (2002). Differential relationship between the carbon chain length of jet fuel aliphatic hydrocarbons and their ability to induce cytotoxicity vs. interleukin-8 release in human epidermal keratinocytes. *Toxicological Sciences*. <https://doi.org/10.1093/toxsci/69.1.226>
- Choudhury, M. B. I., Ahmed, S., Shalabi, M. A., & Inui, T. (2006). Preferential methanation of CO in a syngas involving CO<sub>2</sub> at lower temperature range. *Applied Catalysis A: General*. <https://doi.org/10.1016/j.apcata.2006.08.008>
- Chowdhury, M. B. I., Hossain, M. M., & Charpentier, P. A. (2011). Effect of supercritical water gasification treatment on Ni/La 2O<sub>3</sub>-Al<sub>2</sub>O<sub>3</sub>-based catalysts. *Applied Catalysis A: General*. <https://doi.org/10.1016/j.apcata.2011.07.031>
- Clayton, C. R., & Lu, Y. C. (1989). Electrochemical and XPS evidence of the aqueous formation of Mo<sub>2</sub>O<sub>5</sub>. *Surface and Interface Analysis*. <https://doi.org/10.1002/sia.740140114>
- Coenen, J. W. E. (1986). Catalytic Hydrogenation of Fatty Oils. *Industrial and Engineering Chemistry Fundamentals*. <https://doi.org/10.1021/i100021a006>
- Condon, N., Klemick, H., & Wolverton, A. (2015). Impacts of ethanol policy on corn prices: A review and meta-analysis of recent evidence. *Food Policy*. <https://doi.org/10.1016/j.foodpol.2014.12.007>
- Corma, A., & Orchillés, A. V. (2000). Current views on the mechanism of catalytic cracking. *Microporous and Mesoporous Materials*. [https://doi.org/10.1016/S1387-1811\(99\)00205-X](https://doi.org/10.1016/S1387-1811(99)00205-X)
- Cruz, I. O., Ribeiro, N. F. P., Aranda, D. A. G., & Souza, M. M. V. M. (2008). Hydrogen production by aqueous-phase reforming of ethanol over nickel catalysts prepared from hydrotalcite precursors. *Catalysis Communications*.

<https://doi.org/10.1016/j.catcom.2008.07.031>

Demirbas, A. (2009). Political, economic and environmental impacts of biofuels: A review. *Applied Energy*. <https://doi.org/10.1016/j.apenergy.2009.04.036>

Demirbas, A. (2011). Biodiesel from oilgae, biofixation of carbon dioxide by microalgae: A solution to pollution problems. *Applied Energy*. <https://doi.org/10.1016/j.apenergy.2010.12.050>

Demirbas, A., & Fatih Demirbas, M. (2011). Importance of algae oil as a source of biodiesel. *Energy Conversion and Management*. <https://doi.org/10.1016/j.enconman.2010.06.055>

Den Otter, I. M. J. A. M. (1970). The Dimerization of Oleic Acid with a Montmorillonite Catalyst I: Important Process Parameters; Some Main Reactions. *Fette, Seifen, Anstrichmittel*. <https://doi.org/10.1002/lipi.19700720809>

Desikan, A. N., Huang, L., & Oyama, S. T. (1992). Structure and dispersion of molybdenum oxide supported on alumina and titania. *Journal of the Chemical Society, Faraday Transactions*. <https://doi.org/10.1039/FT9928803357>

Di Serio, M., Cozzolino, M., Giordano, M., Tesser, R., Patrono, P., & Santacesaria, E. (2007). From homogeneous to heterogeneous catalysts in biodiesel production. *Industrial and Engineering Chemistry Research*. <https://doi.org/10.1021/ie070663q>

Ding, R., Wu, Y., Chen, Y., Liang, J., Liu, J., & Yang, M. (2015). Effective hydrodeoxygenation of palmitic acid to diesel-like hydrocarbons over MoO<sub>2</sub>/CNTs catalyst. *Chemical Engineering Science*. <https://doi.org/10.1016/j.ces.2014.10.024>

Dinh, L. T. T., Guo, Y., & Sam Mannan, M. (2009). Sustainability evaluation of biodiesel production using multicriteria decision-making. *Environmental Progress and Sustainable Energy*. <https://doi.org/10.1002/ep.10335>

Dos Anjos, J. R. S., De Araujo Gonzalez, W., Lam, Y. L., & Frety, R. (1983). Catalytic decomposition of vegetable oil. *Applied Catalysis*. [https://doi.org/10.1016/0166-9834\(83\)80158-4](https://doi.org/10.1016/0166-9834(83)80158-4)

- Dou, B., Wang, C., Song, Y., Chen, H., & Xu, Y. (2014). Activity of Ni-Cu-Al based catalyst for renewable hydrogen production from steam reforming of glycerol. *Energy Conversion and Management*. <https://doi.org/10.1016/j.enconman.2013.10.067>
- Douette, A. M. D., Turn, S. Q., Wang, W., & Keffer, V. I. (2007). Experimental investigation of hydrogen production from glycerin reforming. *Energy and Fuels*. <https://doi.org/10.1021/ef060379w>
- Douvartzides, S. L., Charisiou, N. D., Papageridis, K. N., & Goula, M. A. (2019). Green Diesel: Biomass Feedstocks, Production Technologies, Catalytic Research, Fuel Properties and Performance in Compression Ignition Internal Combustion Engines. *Energies*. <https://doi.org/10.3390/en12050809>
- EPA. (2012). Chapter 3. Energy. In *Inventory of U.S. Greenhouse Gas Emissions and Sinks: 1990–2012*.
- Ford, J. P., Immer, J. G., & Lamb, H. H. (2012). Palladium catalysts for fatty acid deoxygenation: Influence of the support and fatty acid chain length on decarboxylation kinetics. *Topics in Catalysis*. <https://doi.org/10.1007/s11244-012-9786-2>
- Friedman, D., Masciangioli, T., & Olson, S. (2012). Replacing critical materials with abundant materials. In *The role of the chemical sciences in finding alternatives to critical resources - A workshop summary*.
- Fu, J., Lu, X., & Savage, P. E. (2010). Catalytic hydrothermal deoxygenation of palmitic acid. *Energy and Environmental Science*. <https://doi.org/10.1039/b923198f>
- Fu, J., Lu, X., & Savage, P. E. (2011a). Hydrothermal decarboxylation and hydrogenation of fatty acids over Pt/C. *ChemSusChem*. <https://doi.org/10.1002/cssc.201000370>
- Fu, J., Lu, X., & Savage, P. E. (2011b). Hydrothermal decarboxylation and hydrogenation of fatty acids over Pt/C. *ChemSusChem*, 4(4), 481–486. <https://doi.org/10.1002/cssc.201000370>
- Fu, J., Shi, F., Thompson, L. T., Lu, X., & Savage, P. E. (2011). Activated carbons for hydrothermal decarboxylation of fatty acids. *ACS Catalysis*.

<https://doi.org/10.1021/cs1001306>

Global EV Outlook 2020. (2020). In *Global EV Outlook 2020*. <https://doi.org/10.1787/d394399e-en>

Gollakota, A. R. K., Kishore, N., & Gu, S. (2018). A review on hydrothermal liquefaction of biomass. *Renewable and Sustainable Energy Reviews*. <https://doi.org/10.1016/j.rser.2017.05.178>

Gonçalves, A. A. S., Faustino, P. B., Assaf, J. M., & Jaroniec, M. (2017). One-Pot Synthesis of Mesoporous Ni-Ti-Al Ternary Oxides: Highly Active and Selective Catalysts for Steam Reforming of Ethanol. *ACS Applied Materials and Interfaces*. <https://doi.org/10.1021/acsami.6b15507>

Gorham, R. (2002). Air Pollution From Ground Transportation; An Assessment of Causes , Strategies and Tactics , and Proposed Actions for the International Community. In *The Global Initiative on Transport Emissions*.

Gosselink, R. W., Hollak, S. A. W., Chang, S. W., Van Haveren, J., De Jong, K. P., Bitter, J. H., & Van Es, D. S. (2013). Reaction pathways for the deoxygenation of vegetable oils and related model compounds. *ChemSusChem*. <https://doi.org/10.1002/cssc.201300370>

Gosselink, R. W., Stellwagen, D. R., & Bitter, J. H. (2013). Tungsten-based catalysts for selective deoxygenation. *Angewandte Chemie - International Edition*. <https://doi.org/10.1002/anie.201209809>

Guzman, A., Torres, J. E., Prada, L. P., & Nuñez, M. L. (2010). Hydroprocessing of crude palm oil at pilot plant scale. *Catalysis Today*. <https://doi.org/10.1016/j.cattod.2009.11.015>

Hengst, K., Arend, M., Pfützenreuter, R., & Hoelderich, W. F. (2015). Deoxygenation and cracking of free fatty acids over acidic catalysts by single step conversion for the production of diesel fuel and fuel blends. *Applied Catalysis B: Environmental*. <https://doi.org/10.1016/j.apcatb.2015.03.009>

Hoekman, S. K. (2009). Biofuels in the U.S. - Challenges and Opportunities. *Renewable Energy*.

<https://doi.org/10.1016/j.renene.2008.04.030>

Holliday, R. L., King, J. W., & List, G. R. (1997). Hydrolysis of Vegetable Oils in Sub- And Supercritical Water. *Industrial and Engineering Chemistry Research*.

<https://doi.org/10.1021/ie960668f>

Hossain, M. Z., Chowdhury, M. B. I., Jhavar, A. K., Xu, W. Z., Biesinger, M. C., & Charpentier, P. A. (2018). Continuous Hydrothermal Decarboxylation of Fatty Acids and Their Derivatives into Liquid Hydrocarbons Using Mo/Al<sub>2</sub>O<sub>3</sub> Catalyst. *ACS Omega*.

<https://doi.org/10.1021/acsomega.8b00562>

Hossain, M. Z., Chowdhury, M. B. I., Jhavar, A. K., Xu, W. Z., & Charpentier, P. A. (2018). Continuous low pressure decarboxylation of fatty acids to fuel-range hydrocarbons with in situ hydrogen production. *Fuel*. <https://doi.org/10.1016/j.fuel.2017.09.092>

Hossain, M. Z., Jhavar, A. K., Chowdhury, M. B. I., Xu, W. Z., Wu, W., Hiscott, D. V., & Charpentier, P. A. (2017). Using Subcritical Water for Decarboxylation of Oleic Acid into Fuel-Range Hydrocarbons. *Energy and Fuels*.

<https://doi.org/10.1021/acs.energyfuels.6b03418>

Huang, J., Jiang, Y., Marthala, V. R. R., Bressel, A., Frey, J., & Hunger, M. (2009). Effect of pore size and acidity on the coke formation during ethylbenzene conversion on zeolite catalysts. *Journal of Catalysis*. <https://doi.org/10.1016/j.jcat.2009.02.019>

Immer, J. G., Kelly, M. J., & Lamb, H. H. (2010). Catalytic reaction pathways in liquid-phase deoxygenation of C18 free fatty acids. *Applied Catalysis A: General*.

<https://doi.org/10.1016/j.apcata.2009.12.028>

India, B. (2014). *Millettia Pinnata*.

IPCC. (2013). Summary for policymakers. In *Climate Change 2014: Impacts, Adaptation, and Vulnerability. Part A: Global and Sectoral Aspects. Contribution of Working Group II to the Fifth Assessment Report of the Intergovernmental Panel on Climate Change*.

IPCC. (2014). Climate Change 2014: Summary for Policymakers. *Climate Change 2014: Impacts,*

*Adaptation and Vulnerability - Contributions of the Working Group II to the Fifth Assessment Report.* <https://doi.org/10.1016/j.renene.2009.11.012>

Itthibenchapong, V., Srifa, A., Kaewmeesri, R., Kidkhunthod, P., & Faungnawakij, K. (2017). Deoxygenation of palm kernel oil to jet fuel-like hydrocarbons using Ni-MoS<sub>2</sub>/γ-Al<sub>2</sub>O<sub>3</sub> catalysts. *Energy Conversion and Management.* <https://doi.org/10.1016/j.enconman.2016.12.034>

IUPAC. (2014). Compendium of Chemical Terminology 2nd ed. (the “Gold Book”). *Blackwell Scientific Publications, Oxford.* <https://doi.org/10.1351/goldbook.I03352>

Janampelli, S., & Darbha, S. (2018). Metal Oxide-Promoted Hydrodeoxygenation Activity of Platinum in Pt-MO<sub>x</sub>/Al<sub>2</sub>O<sub>3</sub> Catalysts for Green Diesel Production. *Energy and Fuels.* <https://doi.org/10.1021/acs.energyfuels.8b03588>

Janampelli, S., & Darbha, S. (2019). Highly efficient Pt-MoO<sub>x</sub>/ZrO<sub>2</sub> catalyst for green diesel production. *Catalysis Communications.* <https://doi.org/10.1016/j.catcom.2019.03.027>

Jęczmionek, Ł., & Porzycka-Semczuk, K. (2014). Hydrodeoxygenation, decarboxylation and decarbonylation reactions while co-processing vegetable oils over a NiMo hydrotreatment catalyst. Part I: Thermal effects - Theoretical considerations. *Fuel.* <https://doi.org/10.1016/j.fuel.2014.04.055>

Jeon, J. Y., Han, Y., Kim, Y. W., Lee, Y. W., Hong, S., & Hwang, I. T. (2019). Feasibility of unsaturated fatty acid feedstocks as green alternatives in bio-oil refinery. *Biofuels, Bioproducts and Biorefining.* <https://doi.org/10.1002/bbb.1979>

Jessop, P. G. (2011). Searching for green solvents. *Green Chemistry.* <https://doi.org/10.1039/c0gc00797h>

Jiménez-López, A., Jiménez-Morales, I., Santamaría-González, J., & Maireles-Torres, P. (2011). Biodiesel production from sunflower oil by tungsten oxide supported on zirconium doped MCM-41 silica. *Journal of Molecular Catalysis A: Chemical.* <https://doi.org/10.1016/j.molcata.2010.11.035>

- Jutz, F., Andanson, J. M., & Baiker, A. (2011). Ionic liquids and dense carbon dioxide: A beneficial biphasic system for catalysis. *Chemical Reviews*. <https://doi.org/10.1021/cr100194q>
- Katryniok, B., Paul, S., & Dumeignil, F. (2013). Recent developments in the field of catalytic dehydration of glycerol to acrolein. *ACS Catalysis*, 3(8), 1819–1834. <https://doi.org/10.1021/cs400354p>
- Kern, C., & Jess, A. (2005). Regeneration of coked catalysts - Modelling and verification of coke burn-off in single particles and fixed bed reactors. *Chemical Engineering Science*. <https://doi.org/10.1016/j.ces.2005.01.024>
- Kim, M. C., & Kim, K. L. (1996). A role of molybdenum and shape selectivity of catalysts in simultaneous reactions of hydrocracking and hydrodesulfurization. *Korean Journal of Chemical Engineering*. <https://doi.org/10.1007/BF02705881>
- Kim, M. Y., Kim, J. K., Lee, M. E., Lee, S., & Choi, M. (2017). Maximizing Biojet Fuel Production from Triglyceride: Importance of the Hydrocracking Catalyst and Separate Deoxygenation/Hydrocracking Steps. *ACS Catalysis*. <https://doi.org/10.1021/acscatal.7b01326>
- King, J. W., Holliday, R. L., & List, G. R. (1999). Hydrolysis of soybean oil: In a subcritical water flow reactor. *Green Chemistry*. <https://doi.org/10.1039/a908861j>
- Kirszenstejn, P., Przekop, R., Tolińska, A., & Maćkowska, E. (2009). Pyrolytic and catalytic conversion of rape oil into aromatic and aliphatic fractions in a fixed bed reactor on Al<sub>2</sub>O<sub>3</sub> and Al<sub>2</sub>O<sub>3</sub>/B<sub>2</sub>O<sub>3</sub> catalysts. *Chemical Papers*. <https://doi.org/10.2478/s11696-008-0104-1>
- Knothe, G. (2007). Some aspects of biodiesel oxidative stability. *Fuel Processing Technology*. <https://doi.org/10.1016/j.fuproc.2007.01.005>
- Kordouli, E., Sygellou, L., Kordulis, C., Bourikas, K., & Lycourghiotis, A. (2017). Probing the synergistic ratio of the NiMo/Γ-Al<sub>2</sub>O<sub>3</sub> reduced catalysts for the transformation of natural triglycerides into green diesel. *Applied Catalysis B: Environmental*, 209, 12–22. <https://doi.org/10.1016/j.apcatb.2017.02.045>

- Kubička, D., & Horáček, J. (2011). Deactivation of HDS catalysts in deoxygenation of vegetable oils. *Applied Catalysis A: General*. <https://doi.org/10.1016/j.apcata.2010.10.034>
- Kubička, D., & Kaluža, L. (2010). Deoxygenation of vegetable oils over sulfided Ni, Mo and NiMo catalysts. *Applied Catalysis A: General*. <https://doi.org/10.1016/j.apcata.2009.10.034>
- Lestari, S., Päivi, M. A., Bernas, H., Simakova, O., Sjöholm, R., Beltramini, J., ... Murzin, D. Y. (2009). Catalytic deoxygenation of stearic acid in a continuous reactor over a mesoporous carbon-supported pd catalyst. *Energy and Fuels*. <https://doi.org/10.1021/ef900110t>
- Lin, R., Zhu, Y., & Tavlarides, L. L. (2014). Effect of thermal decomposition on biodiesel viscosity and cold flow property. *Fuel*. <https://doi.org/10.1016/j.fuel.2013.10.034>
- Loe, R., Santillan-Jimenez, E., Morgan, T., Sewell, L., Ji, Y., Jones, S., ... Crocker, M. (2016). Effect of Cu and Sn promotion on the catalytic deoxygenation of model and algal lipids to fuel-like hydrocarbons over supported Ni catalysts. *Applied Catalysis B: Environmental*. <https://doi.org/10.1016/j.apcatb.2016.03.025>
- Luo, N., Fu, X., Cao, F., Xiao, T., & Edwards, P. P. (2008). Glycerol aqueous phase reforming for hydrogen generation over Pt catalyst - Effect of catalyst composition and reaction conditions. *Fuel*. <https://doi.org/10.1016/j.fuel.2008.06.021>
- Ma, X., Cui, K., Hao, W., Ma, R., Tian, Y., & Li, Y. (2015). Alumina supported molybdenum catalyst for lignin valorization: Effect of reduction temperature. *Bioresource Technology*. <https://doi.org/10.1016/j.biortech.2015.05.032>
- Madsen, A. T., Ahmed, E. H., Christensen, C. H., Fehrmann, R., & Riisager, A. (2011). Hydrodeoxygenation of waste fat for diesel production: Study on model feed with Pt/alumina catalyst. *Fuel*. <https://doi.org/10.1016/j.fuel.2011.06.005>
- Mäki-Arvela, P., Snåre, M., Eränen, K., Myllyoja, J., & Murzin, D. Y. (2008). Continuous decarboxylation of lauric acid over Pd/C catalyst. *Fuel*. <https://doi.org/10.1016/j.fuel.2008.07.004>
- Mäki-Arvela, Päivi, Kubickova, I., Snåre, M., Eränen, K., & Murzin, D. Y. (2007). Catalytic

- deoxygenation of fatty acids and their derivatives. *Energy and Fuels*.  
<https://doi.org/10.1021/ef060455v>
- Mäki-Arvela, Päivi, Rozmysłowicz, B., Lestari, S., Simakova, O., Eränen, K., Salmi, T., & Murzin, D. Y. (2011). Catalytic deoxygenation of tall oil fatty acid over palladium supported on mesoporous carbon. *Energy and Fuels*. <https://doi.org/10.1021/ef200380w>
- March, J. (2009). The decarboxylation of organic acid. *Journal of Chemical Education*, 40(4), 212.  
<https://doi.org/10.1021/ed040p212>
- Marquevich, M., Coll, R., & Montane, D. (2000). Steam Reforming of Sunflower Oil for Hydrogen Production. . *Industrial & Engineering Chemistry Research*.  
<https://doi.org/10.1021/ie9910874>
- Melero, J. A., Clavero, M. M., Calleja, G., García, A., Miravalles, R., & Galindo, T. (2010). Production of biofuels via the catalytic cracking of mixtures of crude vegetable oils and nonedible animal fats with vacuum gas oil. *Energy and Fuels*.  
<https://doi.org/10.1021/ef900914e>
- Miao, C., Marin-Flores, O., Davidson, S. D., Li, T., Dong, T., Gao, D., ... Chen, S. (2016). Hydrothermal catalytic deoxygenation of palmitic acid over nickel catalyst. *Fuel*.  
<https://doi.org/10.1016/j.fuel.2015.10.120>
- Miao, C., Marin-Flores, O., Dong, T., Gao, D., Wang, Y., Garcia-Pérez, M., & Chen, S. (2018). Hydrothermal Catalytic Deoxygenation of Fatty Acid and Bio-oil with in Situ H<sub>2</sub>. *ACS Sustainable Chemistry and Engineering*. <https://doi.org/10.1021/acssuschemeng.7b02226>
- Mo, N., & Savage, P. E. (2014). Hydrothermal catalytic cracking of fatty acids with HZSM-5. *ACS Sustainable Chemistry and Engineering*. <https://doi.org/10.1021/sc400368n>
- Mohite, S., Armbruster, U., Richter, M., & Martin, A. (2014). Impact of Chain Length of Saturated Fatty Acids during Their Heterogeneously Catalyzed Deoxygenation. *Journal of Sustainable Bioenergy Systems*. <https://doi.org/10.4236/jsbs.2014.43017>
- Müller-Langer, F., Majer, S., & O’Keeffe, S. (2014). Benchmarking biofuels—a comparison of

- technical, economic and environmental indicators. *Energy, Sustainability and Society*.  
<https://doi.org/10.1186/s13705-014-0020-x>
- Na, J. G., Yi, B. E., Kim, J. N., Yi, K. B., Park, S. Y., Park, J. H., ... Ko, C. H. (2010). Hydrocarbon production from decarboxylation of fatty acid without hydrogen. *Catalysis Today*.  
<https://doi.org/10.1016/j.cattod.2009.11.008>
- National Energy Board. (2016). Canada's Energy Future 2016 Energy Supply and Demand Projections to 2040.
- Ndubuisi, R. U., Sinichi, S., (Cathy) Chin, Y. H., & Diosady, L. L. (2019). Diesel Precursors Via Catalytic Hydrothermal Deoxygenation of Aqueous Canola Oil Emulsion. *JAACS, Journal of the American Oil Chemists' Society*. <https://doi.org/10.1002/aocs.12208>
- Nikolskaya, E., & Hiltunen, Y. (2018). Determination of Carbon Chain Lengths of Fatty Acid Mixtures by Time Domain NMR. *Applied Magnetic Resonance*.  
<https://doi.org/10.1007/s00723-017-0953-2>
- Olefin by-product may be carcinogenic. (2010). *Chemical & Engineering News*.  
<https://doi.org/10.1021/cen-v054n035.p008>
- Otera, J. (1993). Transesterification. *Chemical Reviews*. <https://doi.org/10.1021/cr00020a004>
- Paul Abishek, M., Patel, J., & Prem Rajan, A. (2014). Algae Oil: A Sustainable Renewable Fuel of Future. *Biotechnology Research International*. <https://doi.org/10.1155/2014/272814>
- Peng, B., Zhao, C., Kasakov, S., Foraita, S., & Lercher, J. A. (2013). Manipulating catalytic pathways: Deoxygenation of palmitic acid on multifunctional catalysts. *Chemistry - A European Journal*. <https://doi.org/10.1002/chem.201203110>
- Peng, J., Chen, P., Lou, H., & Zheng, X. (2009). Catalytic upgrading of bio-oil by HZSM-5 in sub- and super-critical ethanol. *Bioresource Technology*.  
<https://doi.org/10.1016/j.biortech.2009.02.007>
- Pereira, R. C. C., & Pasa, V. M. D. (2006). Effect of mono-olefins and diolefins on the stability of

automotive gasoline. *Fuel*. <https://doi.org/10.1016/j.fuel.2006.01.022>

Perrotin-Brunel, H., Buijs, W., Spronsen, J. Van, Roosmalen, M. J. E. V., Peters, C. J., Verpoorte, R., & Witkamp, G. J. (2011). Decarboxylation of  $\Delta^9$ -tetrahydrocannabinol: Kinetics and molecular modeling. *Journal of Molecular Structure*, 987(1–3), 67–73. <https://doi.org/10.1016/j.molstruc.2010.11.061>

Peterson, A. A., Vogel, F., Lachance, R. P., Fröling, M., Antal, M. J., & Tester, J. W. (2008). Thermochemical biofuel production in hydrothermal media: A review of sub- and supercritical water technologies. *Energy and Environmental Science*. <https://doi.org/10.1039/b810100k>

Pinto, J. S. S., & Lanças, F. M. (2006). Hydrolysis of corn oil using subcritical water. *Journal of the Brazilian Chemical Society*. <https://doi.org/10.1590/S0103-50532006000100013>

Popov, S., & Kumar, S. (2015). Rapid hydrothermal deoxygenation of oleic acid over activated carbon in a continuous flow process. *Energy and Fuels*. <https://doi.org/10.1021/acs.energyfuels.5b00308>

R. C. Archuleta. (1991). Non catalytic steam hydrolysis of fats and oils. *Montana State University*.

Ramadhias, A. S., Jayaraj, S., & Muraleedharan, C. (2005). Biodiesel production from high FFA rubber seed oil. *Fuel*. <https://doi.org/10.1016/j.fuel.2004.09.016>

Ravenelle, R. M., Copeland, J. R., Kim, W. G., Crittenden, J. C., & Sievers, C. (2011). Structural Changes of  $\gamma$ -Al<sub>2</sub>O<sub>3</sub>-Supported Catalysts in Hot Liquid Water. *ACS Catalysis*. <https://doi.org/10.1021/cs1001515>

Remón, J., Randall, J., Budarin, V. L., & Clark, J. H. (2019). Production of bio-fuels and chemicals by microwave-assisted, catalytic, hydrothermal liquefaction (MAC-HTL) of a mixture of pine and spruce biomass. *Green Chemistry*. <https://doi.org/10.1039/c8gc03244k>

Robin, T., Jones, J. M., & Ross, A. B. (2017). Catalytic hydrothermal processing of lipids using metal doped zeolites. *Biomass and Bioenergy*. <https://doi.org/10.1016/j.biombioe.2017.01.012>

- Rostrup-Nielsen, J. R., Christensen, T. S., & Dybkjaer, I. (1998). Steam reforming of liquid hydrocarbons. *Studies in Surface Science and Catalysis*. [https://doi.org/10.1016/s0167-2991\(98\)80277-2](https://doi.org/10.1016/s0167-2991(98)80277-2)
- Rozmysłowicz, B., Mäki-Arvela, P., Tokarev, A., Leino, A. R., Eränen, K., & Murzin, D. Y. (2012). Influence of hydrogen in catalytic deoxygenation of fatty acids and their derivatives over Pd/C. *Industrial and Engineering Chemistry Research*. <https://doi.org/10.1021/ie202421x>
- Sahoo, P. K., Das, L. M., Babu, M. K. G., & Naik, S. N. (2007). Biodiesel development from high acid value polanga seed oil and performance evaluation in a CI engine. *Fuel*. <https://doi.org/10.1016/j.fuel.2006.07.025>
- Sakata, Y., Tamaura, Y., Imamura, H., & Watanabe, M. (2006). Preparation of a new type of CaSiO<sub>3</sub> with high surface area and property as a catalyst support. In *Studies in Surface Science and Catalysis*. [https://doi.org/10.1016/S0167-2991\(06\)80924-9](https://doi.org/10.1016/S0167-2991(06)80924-9)
- Santillan-Jimenez, E., & Crocker, M. (2012). Catalytic deoxygenation of fatty acids and their derivatives to hydrocarbon fuels via decarboxylation/decarbonylation. *Journal of Chemical Technology and Biotechnology*. <https://doi.org/10.1002/jctb.3775>
- Savchenko, V. I., & Makaryan, I. A. (1999). Palladium catalyst for the production of pure margarine: Catalyst and new non-filtration technology improve production and quality. *Platinum Metals Review*.
- Sawangkeaw, R., & Ngamprasertsith, S. (2013). A review of lipid-based biomasses as feedstocks for biofuels production. *Renewable and Sustainable Energy Reviews*. <https://doi.org/10.1016/j.rser.2013.04.007>
- Scanlon, D. O., Watson, G. W., Payne, D. J., Atkinson, G. R., Egdell, R. G., & Law, D. S. L. (2010). Theoretical and experimental study of the electronic structures of MoO<sub>3</sub> and MoO<sub>2</sub>. *Journal of Physical Chemistry C*. <https://doi.org/10.1021/jp9093172>
- Shay, E. G. (1993). Diesel fuel from vegetable oils: Status and opportunities. *Biomass and*

*Bioenergy*. [https://doi.org/10.1016/0961-9534\(93\)90080-N](https://doi.org/10.1016/0961-9534(93)90080-N)

- Smits, G. (1976). Measurement of the diffusion coefficient of free fatty acid in groundnut oil by the capillary-cell method. *Journal of the American Oil Chemists' Society*, 53(4), 122–124. <https://doi.org/10.1007/BF02586347>
- Snåre, M., Kubičková, I., Mäki-Arvela, P., Chichova, D., Eränen, K., & Murzin, D. Y. (2008). Catalytic deoxygenation of unsaturated renewable feedstocks for production of diesel fuel hydrocarbons. *Fuel*, 87(6), 933–945. <https://doi.org/10.1016/j.fuel.2007.06.006>
- Snåre, M., Mäki-Arvela, P., Simakova, I. L., Myllyoja, J., & Murzin, D. Y. (2009). Overview of catalytic methods for production of next generation biodiesel from natural oils and fats. *Russian Journal of Physical Chemistry B*. <https://doi.org/10.1134/S1990793109070021>
- Snåre, Mathias, Kubičková, I., Mäki-Arvela, P., Eränen, K., & Murzin, D. Y. (2006). Heterogeneous catalytic deoxygenation of stearic acid for production of biodiesel. *Industrial and Engineering Chemistry Research*. <https://doi.org/10.1021/ie060334i>
- Somerville, C., Youngs, H., Taylor, C., Davis, S. C., & Long, S. P. (2010). Feedstocks for lignocellulosic biofuels. *Science*. <https://doi.org/10.1126/science.1189268>
- Song, C., Nihonmatsu, T., & Nomura, M. (1991). Effect of Pore Structure of Ni–Mo/Al<sub>2</sub>O<sub>3</sub> Catalysts in Hydrocracking of Coal Derived and Oil Sand Derived Asphaltenes. *Industrial and Engineering Chemistry Research*. <https://doi.org/10.1021/ie00056a008>
- Spevack, P. A., & McIntyre, N. S. (1992). Thermal reduction of molybdenum trioxide. *The Journal of Physical Chemistry*. <https://doi.org/10.1021/j100201a062>
- Srifa, A., Faungnawakij, K., Itthibenchapong, V., Viriya-empikul, N., Charinpanitkul, T., & Assabumrungrat, S. (2014). Production of bio-hydrogenated diesel by catalytic hydrotreating of palm oil over NiMoS<sub>2</sub>/γ-Al<sub>2</sub>O<sub>3</sub> catalyst. *Bioresource Technology*. <https://doi.org/10.1016/j.biortech.2014.01.100>
- Steinberg, M., & Cheng, H. C. (1989). Modern and prospective technologies for hydrogen production from fossil fuels. *International Journal of Hydrogen Energy*.

[https://doi.org/10.1016/0360-3199\(89\)90018-9](https://doi.org/10.1016/0360-3199(89)90018-9)

- Swick, D., Jaques, A., Walker, J. C., & Estreicher, H. (2014). Gasoline toxicology: Overview of regulatory and product stewardship programs. *Regulatory Toxicology and Pharmacology*. <https://doi.org/10.1016/j.yrtph.2014.06.016>
- Talebian-Kiakalaieh, A., Amin, N. A. S., & Hezaveh, H. (2014). Glycerol for renewable acrolein production by catalytic dehydration. *Renewable and Sustainable Energy Reviews*. <https://doi.org/10.1016/j.rser.2014.07.168>
- Teeter, H. M., Bell, E. W., O'Donnell, J. L., Danzig, M. J., & Cowan, J. C. (1958). Reactions of conjugated fatty acids. VI. Selenium catalysis, a method for preparing diels-alder adducts from cis,trans-octadecadienoic acid. *Journal of the American Oil Chemists' Society*, 35(5), 238–240. <https://doi.org/10.1007/BF02639835>
- Teeter, H. M., O'Donnell, J. L., Schneider, W. J., Gast, L. E., & Danzig, M. J. (1957). Reactions of Conjugated Fatty Acids. IV. Diels-Alder Adducts of 9,11-Octadecadienoic Acid. *Journal of Organic Chemistry*, 22(5), 512–514. <https://doi.org/10.1021/jo01356a010>
- Thommes, M., Kaneko, K., Neimark, A. V., Olivier, J. P., Rodriguez-Reinoso, F., Rouquerol, J., & Sing, K. S. W. (2015). Physisorption of gases, with special reference to the evaluation of surface area and pore size distribution (IUPAC Technical Report). *Pure and Applied Chemistry*. <https://doi.org/10.1515/pac-2014-1117>
- Thornton, T. D., & Savage, P. E. (1990). Phenol oxidation in supercritical water. *The Journal of Supercritical Fluids*. [https://doi.org/10.1016/0896-8446\(90\)90029-L](https://doi.org/10.1016/0896-8446(90)90029-L)
- Tian, Q., Zhang, Z., Zhou, F., Chen, K., Fu, J., Lu, X., & Ouyang, P. (2017). Role of Solvent in Catalytic Conversion of Oleic Acid to Aviation Biofuels. *Energy and Fuels*. <https://doi.org/10.1021/acs.energyfuels.7b00586>
- Toba, M., Abe, Y., Kuramochi, H., Osako, M., Mochizuki, T., & Yoshimura, Y. (2011). Hydrodeoxygenation of waste vegetable oil over sulfide catalysts. *Catalysis Today*. <https://doi.org/10.1016/j.cattod.2010.11.049>

- Topsøe, H., Clausen, B. S., & Massoth, F. E. (2012). Hydrotreating Catalysis. In *Catalysis*. [https://doi.org/10.1007/978-3-642-61040-0\\_1](https://doi.org/10.1007/978-3-642-61040-0_1)
- W. Scaroni, A., Jenkins, R. G., & Walker, P. L. (1985). Coke deposition on Co-Mo/Al<sub>2</sub>O<sub>3</sub> and Co-Mo/C catalysts. *Applied Catalysis*. [https://doi.org/10.1016/S0166-9834\(00\)84353-5](https://doi.org/10.1016/S0166-9834(00)84353-5)
- Wan, J., Cao, Y. D., Ran, R., Li, M., Xiao, Y., Wu, X. D., & Weng, D. (2016). Regeneration of sintered Rh/ZrO<sub>2</sub> catalysts via Rh re-dispersion and Rh–ZrO<sub>2</sub> interaction. *Science China Technological Sciences*. <https://doi.org/10.1007/s11431-016-6052-z>
- Wan Omar, W. N. N., & Saidina Amin, N. A. (2011). Optimization of heterogeneous biodiesel production from waste cooking palm oil via response surface methodology. *Biomass and Bioenergy*. <https://doi.org/10.1016/j.biombioe.2010.12.049>
- Wang, H., Lin, H., Feng, P., Han, X., & Zheng, Y. (2017). Integration of catalytic cracking and hydrotreating technology for triglyceride deoxygenation. *Catalysis Today*. <https://doi.org/10.1016/j.cattod.2016.12.009>
- Wang, W. C., & Tao, L. (2016). Bio-jet fuel conversion technologies. *Renewable and Sustainable Energy Reviews*, 53, 801–822. <https://doi.org/10.1016/j.rser.2015.09.016>
- Watanabe, M., Iida, T., & Inomata, H. (2006). Decomposition of a long chain saturated fatty acid with some additives in hot compressed water. *Energy Conversion and Management*. <https://doi.org/10.1016/j.enconman.2006.01.009>
- Wen, G., Xu, Y., Ma, H., Xu, Z., & Tian, Z. (2008). Production of hydrogen by aqueous-phase reforming of glycerol. *International Journal of Hydrogen Energy*. <https://doi.org/10.1016/j.ijhydene.2008.07.072>
- Westacott, R. E., Johnston, K. P., & Rossky, P. J. (2001). Stability of ionic and radical molecular dissociation pathways for reaction in supercritical water. *Journal of Physical Chemistry B*. <https://doi.org/10.1021/jp010005y>
- WHO. (2016). WHO | Air pollution. *World Health Organization*.

- Wu, J., Shi, J., Fu, J., Leidl, J. A., Hou, Z., & Lu, X. (2016). Catalytic decarboxylation of fatty acids to aviation fuels over nickel supported on activated carbon. *Scientific Reports*. <https://doi.org/10.1038/srep27820>
- Yang, J., Xu, M., Zhang, X., Hu, Q., Sommerfeld, M., & Chen, Y. (2011). Life-cycle analysis on biodiesel production from microalgae: Water footprint and nutrients balance. *Bioresource Technology*. <https://doi.org/10.1016/j.biortech.2010.07.017>
- Yang, L., Ruess, G. L., & Carreon, M. A. (2015). Cu, Al and Ga based metal organic framework catalysts for the decarboxylation of oleic acid. *Catalysis Science and Technology*. <https://doi.org/10.1039/c4cy01609b>
- Yang, Liqiu, & Carreon, M. A. (2017a). Deoxygenation of Palmitic and Lauric Acids over Pt/ZIF-67 Membrane/Zeolite 5A Bead Catalysts. *ACS Applied Materials and Interfaces*. <https://doi.org/10.1021/acsami.7b11638>
- Yang, Liqiu, & Carreon, M. A. (2017b). Effect of reaction parameters on the decarboxylation of oleic acid over Pt/ZIF-67membrane/zeolite 5A bead catalysts. *Journal of Chemical Technology and Biotechnology*. <https://doi.org/10.1002/jctb.5112>
- Yang, Liqiu, Tate, K. L., Jasinski, J. B., & Carreon, M. A. (2015). Decarboxylation of Oleic Acid to Heptadecane over Pt Supported on Zeolite 5A Beads. *ACS Catalysis*. <https://doi.org/10.1021/acscatal.5b01913>
- Yeh, T. M., Hockstad, R. L., Linic, S., & Savage, P. E. (2015). Hydrothermal decarboxylation of unsaturated fatty acids over PtSn<sub>x</sub>/C catalysts. *Fuel*. <https://doi.org/10.1016/j.fuel.2015.04.039>
- Yu, J., & Savage, P. E. (2001). Catalyst activity, stability, and transformations during oxidation in supercritical water. *Applied Catalysis B: Environmental*. [https://doi.org/10.1016/S0926-3373\(00\)00273-3](https://doi.org/10.1016/S0926-3373(00)00273-3)
- Zhang, Jing, Huo, X., Li, Y., & Strathmann, T. J. (2019). Catalytic Hydrothermal Decarboxylation and Cracking of Fatty Acids and Lipids over Ru/C. *ACS Sustainable Chemistry and*

*Engineering*. <https://doi.org/10.1021/acssuschemeng.9b00215>

Zhang, Junhua, Chen, S., Yang, R., & Yan, Y. (2010). Biodiesel production from vegetable oil using heterogenous acid and alkali catalyst. *Fuel*. <https://doi.org/10.1016/j.fuel.2010.05.009>

Zhao, C., Brück, T., & Lercher, J. A. (2013). Catalytic deoxygenation of microalgae oil to green hydrocarbons. *Green Chemistry*, *15*(7), 1720–1739. <https://doi.org/10.1039/c3gc40558c>

Zhou, C.-H., Xia, X., Lin, C.-X., Tong, D.-S., & Beltramini, J. (2011). Catalytic conversion of lignocellulosic biomass to fine chemicals and fuels. *Chemical Society Reviews*. <https://doi.org/10.1039/c1cs15124j>

## Chapter 3

### 3. Effects of Reaction Solvent and Added Hydrogen Donor to the Continuous Thermo-catalytic Decarboxylation of Fatty Acids into Liquid Hydrocarbons

#### 3.1. Abstract

Hydrogen gas-free decarboxylation of fatty acids with inexpensive transition metal catalysts is a possible promising alternative route to produce economically green diesel. This study demonstrates continuous production of oxygen free straight chain liquid hydrocarbons from stearic and oleic acid assisted by steam phase reforming of ethanol or glycerol using a  $\text{MoO}_x/\gamma\text{-Al}_2\text{O}_3$  catalyst. Temperatures of 375 °C – 400 °C, residence times of 2.5 h - 5 h, and the presence of reforming species were tested for their effect on decarboxylation. Diesel-like product mainly composed of heptadecane was obtained via decarboxylation of oleic acid and stearic acid without adding any hydrogen gas. The addition of ethanol and glycerol to oleic acid or stearic acid processes did not significantly increase selectivity to heptadecane. Solvent systems of toluene and no solvent were also tested. Greatest selectivity (70 %) to heptadecane was found with stearic acid feed processed at 375 °C with a toluene solvent. It was demonstrated that the necessary reaction temperature for the complete decarboxylation of stearic acid could be reduced from 390 °C to 375 °C by the addition of the reforming species, glycerol and ethanol. The regenerated catalyst demonstrates similar activity to that of fresh catalyst, while having a far lower number of acid sites and possessing a turnover number of less than one. This indicates that acid sites may not be the active sites of the  $\text{MoO}_x/\gamma\text{-Al}_2\text{O}_3$  catalyst, which what was previously thought.

## 3.2. Introduction

Hydrothermal liquefaction is of interest in recent literature as a bio-oil production process. Hydrothermal liquefaction produces a bio-oil sufficiently similar to fossil crude oil from biomass waste such as sewage sludge, manure, wood, compost etc. (Remón, Randall, Budarin, & Clark, 2019). While this technique is feedstock flexible, (Gollakota, Kishore, & Gu, 2018) it results in viscous products that contain significant quantities of oxygen (Ndubuisi, Sinichi, (Cathy) Chin, & Diosady, 2019) that result in high freezing points and low energy densities (Kordouli, Sygellou, Kordulis, Bourikas, & Lycourghiotis, 2017). Therefore, fuels with high oxygen content are unsuitable as transportation fuels and needs further processing downstream.

Fats oils, and greases (containing triglycerides (TGA) and fatty acids (FA)) are common renewable feedstocks used to produce transportation fuels. TGAs and FAs are upgraded either through transesterification, where additional paraffinic groups are added to the oxygen containing side of the molecule or are upgraded via deoxygenation where oxygen containing groups are removed from the molecule. This deoxygenation typically occurs by decarbonylation, decarboxylation, and/or hydrodeoxygenation. Hydrodeoxygenation requires three moles of H<sub>2</sub> per fatty acid, decarbonylation requires one mole of H<sub>2</sub> per fatty acid, while decarboxylation requires no H<sub>2</sub> in order to produce a paraffinic fuel molecule. For stearic acid undergoing decarboxylation at 300 °C, the reaction is slightly endothermic ( $\Delta H = 9.2$  kJ/mol) while decarbonylation is much more endothermic ( $\Delta H = 179.1$  kJ/mol) (Popov & Kumar, 2015). The addition of H<sub>2</sub> gas can reduce the endothermic requirements of decarbonylation ( $\Delta H = 48.1$  kJ/mol) (Popov & Kumar, 2015). Experimentally, it has been found that the addition of H<sub>2</sub> gas into most deoxygenation processes have been found to increase fuel/paraffin yields overall (Rozmysłowicz et al., 2012), (Gosselink, Stellwagen, et al., 2013). However, H<sub>2</sub> gas is an expensive input for a process with already incredibly tight economic margins.

Various supported monometallic catalysts such as Pd, Pt, Ru, Mo, Ni, Rh, Ir and Os have been used for deoxygenation/decarboxylation of fatty acids and their esters. These metals have been supported on activated carbon, Al<sub>2</sub>O<sub>3</sub>, ZrO<sub>2</sub>, SiO<sub>2</sub>, and Zeolites (Hossain, Chowdhury, Jhavar, Xu, & Charpentier, 2018; Madsen, Ahmed, Christensen, Fehrmann, & Riisager, 2011), (Fu, Lu, et al., 2011b; M. Snåre et al., 2009). Hengst et al. (Hengst et al., 2015) and Fu et al. (Fu

et al., 2010) demonstrated that catalyst activity for decarboxylation goes according to acidity. Noble metal catalysts have some of the highest published deoxygenation yields, but they are expensive and require expensive H<sub>2</sub> gas (Fu, Lu, et al., 2011b), (M. Snåre et al., 2008). Peng et al. (B. Peng et al., 2013) performed deoxygenation of palmitic acid under H<sub>2</sub> and inert environments and concluded that for monometallic catalysts, a source for disassociated hydrogen protons on the catalyst surface is required to provide adequate results. An inexpensive MoO<sub>x</sub> catalyst supported on  $\gamma$ -Al<sub>2</sub>O<sub>3</sub> was demonstrated by the Charpentier group (Hossain, Chowdhury, Jhawar, Xu, Biesinger, et al., 2018) to have good decarboxylation rates without the costly input of hydrogen.

The main deoxygenation reaction by the Mo/Al<sub>2</sub>O<sub>3</sub> catalyst in water was shown by Hossain et al. (Hossain, Chowdhury, Jhawar, Xu, Biesinger, et al., 2018) to be decarboxylation. In Chapter 2's studies with a MoO<sub>x</sub> catalyst, it was found that oleic acid cracks and decarboxylates more readily and to a higher degree than stearic acid. Testing mixes of oleic and stearic acid were found to increase the decarboxylation of stearic acid while reducing total cracked products. However, there resulted in larger proportions of deposited species on the catalyst surface. These species are thought to be the result of oleic acid undergoing reforming to provide in-situ hydrogen, or 'hydrogen equivalents' to the catalyst (Fu, Lu, et al., 2011b). This is problematic as oleic acid is a high value material and real-world green diesel feeds will have significant unsaturated fatty acids that will undergo cracking.

The use of small amounts (5-10% by oil weight) of ethanol or glycerol may replace the role of oleic acid or other unsaturated fatty acids as sacrificial hydrogen/proton sources (Miao et al., 2018) to improve the degree of decarboxylation and increase the percentage of heptadecane. Miao et al. (Miao et al., 2018) demonstrated a 10 mL minibatch reactor subcritical water hydrothermal catalytic deoxygenation approach that produced hydrocarbons from fatty acids and bio-oil with Ni-ZrO<sub>2</sub> catalyst with in-situ self-sustaining H<sub>2</sub>. Using stearic acid and oleic acid as model compounds they achieved differing paraffin yields (63.59% from SA and 47% from OA). Glycerol was chosen as it occurs naturally in feeds such as algal oils and CDO and is a by-product of the hydrolysis of triglycerides and the biodiesel process. Ethanol is industrially produced as a gasoline additive by the fermentation of corn sugars, and the by-product of its production is CDO. Low-cost ethanol could be added to the on-site decarboxylation of the corn distiller's oil (CDO)

to improve the product quality of the green diesel produced without having to pay for cost of transport for either product.

Hydrothermal processing utilizes water as the reaction medium and benefits from the increased hydronium ions, hydroxide ions, and fatty acid solubility under subcritical water conditions (Peterson et al., 2008). These solvent properties create a highly reactive environment for decarboxylation and reforming (Douette, Turn, Wang, & Keffer, 2007). However, Yu et al. 114, (Yu & Savage, 2001) demonstrated a more than 20-fold reduction in specific surface area of metal oxide catalysts supported on  $\gamma$ -Al<sub>2</sub>O<sub>3</sub> when exposed to supercritical water conditions. We are using Mo/ $\gamma$ -Al<sub>2</sub>O<sub>3</sub> due to its low cost compared to noble metals, its high catalytic activity despite the lack of hydrogen, and the acidity of the alumina support to effect better decarboxylation rates (Hengst et al., 2015). Based on Yu et al.'s (Thornton & Savage, 1990)(Yu & Savage, 2001) work and results indicated in other studies, we suspect that our MoO<sub>x</sub>/ $\gamma$ -Al<sub>2</sub>O<sub>3</sub> will eventually deactivate during continuous processing due to surface area collapse if exposed to subcritical water conditions. Because of this, most conditions of this study have been run with high temperature water at autogenous conditions instead of supercritical water conditions.

Tian et al. (Tian et al., 2017) investigated the role of solvents (solvent-free, water, and dodecane) in a microbatch system (1.67 cm<sup>3</sup> volume) for the conversion of oleic acid at 350 °C over Pt/C. The solvent-free system was found to be superior to the water and dodecane systems. This is because dodecane competes for the active sites of Pt/C. In the hydrothermal reaction system, H<sup>+</sup> released from water and hydrogen bonding inhibited the ionization of carboxyl groups which played a large role in the slower decarboxylation and aromatization rates.

In the previous chapter we showed that oleic acid underwent cracking and reforming to effect better decarboxylation of stearic acid. This chapters seeks to continue the exploration of in-situ hydrogen production by ethanol and glycerol to effect increased decarboxylation of stearic and oleic acid, and the impact of solvents (steam, toluene, and no solvent) on the decarboxylation process. In order to further close the gap between laboratory processes and pilot plant scale, this work utilized a larger scale continuous fixed bed PFR (reactor 24" in length, 0.532" in diameter) as opposed to mini- or micro-batch reactors, and the use of a comparatively cheap and effective MoO<sub>x</sub>/ $\gamma$ -Al<sub>2</sub>O<sub>3</sub> catalyst as opposed to using expensive noble metal catalysts.

Characterization of fresh and spent catalysts was conducted using several physicochemical techniques including N<sub>2</sub>- physisorption Brunauer–Emmett–Teller (BET) surface area and Barrett–Joyner–Halenda (BJH) pore size distribution, NH<sub>3</sub> temperature-programmed desorption (NH<sub>3</sub>-TPD), X-ray diffraction (XRD), H<sub>2</sub> temperature-programmed reduction (H<sub>2</sub>-TPR), CO pulse chemisorption, X-ray photoelectron spectroscopy (XPS), transmission electron microscopy (TEM), and scanning electron microscopy (SEM). Product quality was determined with FTIR for percent remaining carboxylic acid, and the method compared to values determined from acid value titrations. Product fractions were determined by GC-FID.

### 3.3. Materials and Methods

See section 2.3 for materials and methods section for this study.

## 3.4. Results and Discussion

### 3.4.1. Addition of Ethanol and Glycerol into Decarboxylation Process

It is desirable to remove oxygen from fatty acids to produce paraffins as oxygen decreases the freezing point of the fuel, reduces the energy density, increases fuel acidity, and reduces the oxidative stability of the fuel. The oxygen-containing functional group in fatty acids is a carboxylic acid, which shows a strong response in Fourier transform infrared spectroscopy (FTIR) at approximately  $1700\text{ cm}^{-1}$ . As fatty acids convert to paraffins, the  $1700\text{ cm}^{-1}$  peak will decrease and correlate to the area under this peak. Therefore, % removal can be calculated by equation 2.1.

Work in section 2.4.1 validated this method by correlating to the values obtained from acid value titrations performed according to ASTM D3242 - Standard Test Method for Acidity in Aviation Turbine Fuel (11, 2011). All decarboxylation values calculated in this study was performed by this FTIR method.

Temperature and residence time are the two main parameters that impact decarboxylation rate and catalyst longevity. The reactor used was a continuous plug flow reactor (PFR) with a fixed bed of 7.5 wt% Mo/Al<sub>2</sub>O<sub>3</sub> catalyst. The degree of decarboxylation was assessed at different temperatures (Temp = 375 to 400°C) with the addition of glycerol or ethanol to stearic or oleic acid. The process used 60 g of the 7.5 wt% Mo/Al<sub>2</sub>O<sub>3</sub> catalyst. All reactions were run so as to process 38 mL of feedstock regardless of residence time.

The decarboxylation of stearic with and without ethanol or glycerol added (5-10% by stearic acid weight) at a temperature of 375°C and a residence time of 3.5 h is shown in Figure 3.1. Without the added oxygenated species (ethanol or glycerol), the catalyst quickly deactivated with the minimum percent decarboxylation at less than 20%. The addition of ethanol or glycerol at the same temperatures and residence times resulted in minimum percent decarboxylation of 73-86 %. Higher decarboxylation rates and reduced catalyst deactivation were achieved with addition of

10% ethanol or 10% glycerol. It is obvious that the small addition of either glycerol or ethanol increases the degree of decarboxylation of stearic acid.

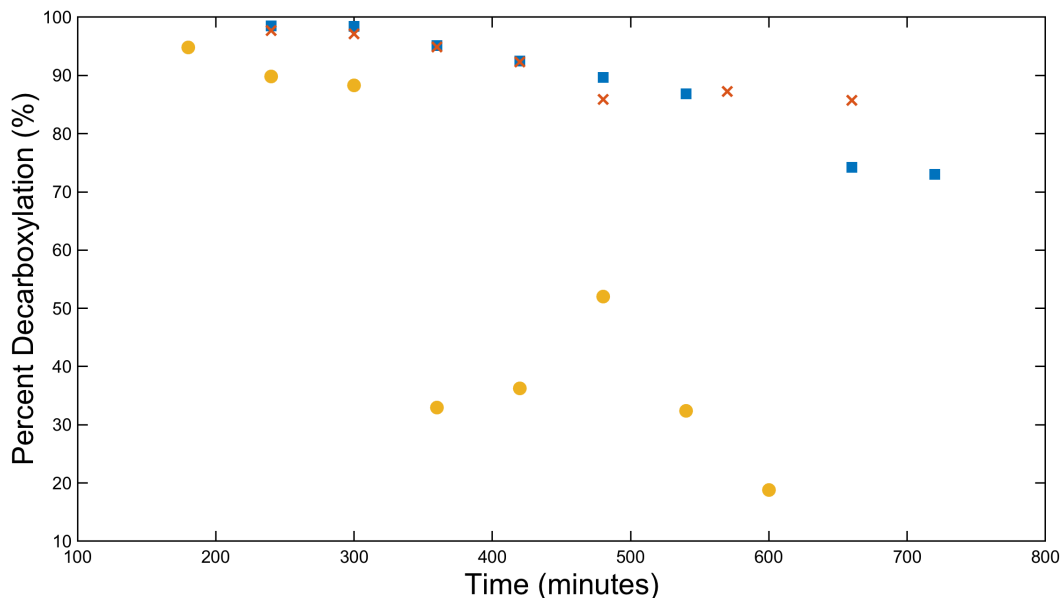


Figure 3.1 Percent decarboxylation over time in a PFR of stearic acid at 375°C with a residence time of 3.5 h (●). The impact of added glycerol (×) or ethanol (■) at the same conditions

Figure 3.2 demonstrates the decarboxylation degree over time of stearic acid processed with 3.5 h residence time and at 390 °C. The impact of added ethanol and glycerol is shown to be minimal compared to the improvements seen at 375 °C. The difference of minimum decarboxylation samples between stearic acid with and without glycerol/ethanol at 390 °C is 1 %, whereas the difference with and without glycerol/ethanol at 375 °C is 53 %. This is perhaps due to cracking being enhanced past temperatures of 390 °C, and which may create some form of hydrogen/H<sup>+</sup>. Hydrogen gas and in situ produced hydrogen has been demonstrated to assist in the decarboxylation reaction (Fu et al., 2010), and may provide an explanation for ethanol and glycerol's ability to decrease reaction temperatures from 390 °C to 375 °C for stearic acid.

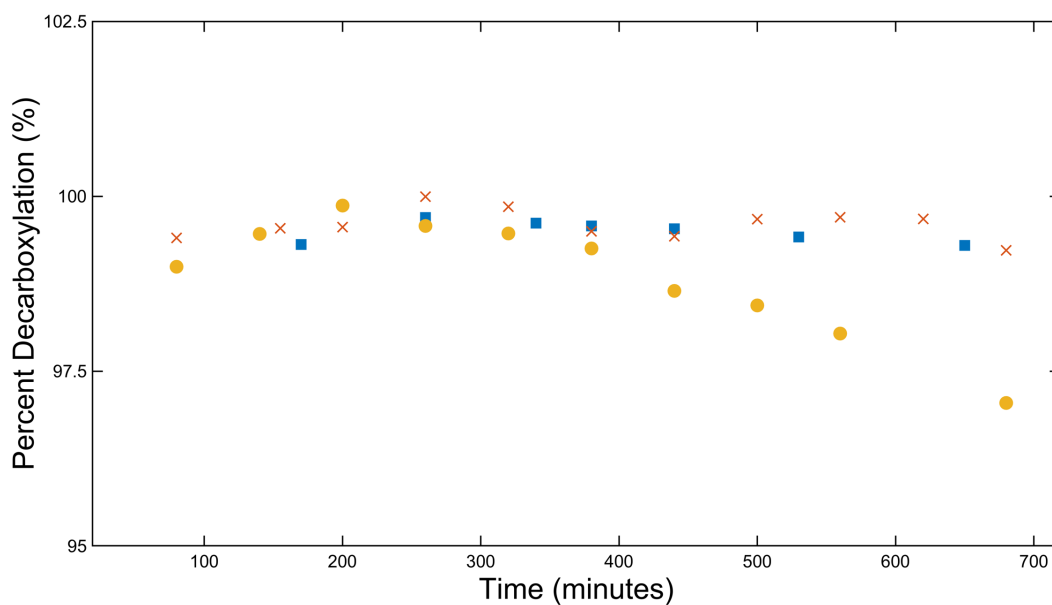


Figure 3.2 Percent decarboxylation over time in a PFR of stearic acid at 390 °C (●) and a residence time of 3.5 h. The impact of additions of ethanol (■) and glycerol (×) are shown

Stearic acid decarboxylation with and without ethanol was performed at 400 °C with a residence time of 3.5 h, and the results of this reaction can be seen in Figure 3.3. There is likely no difference between additions at 400 °C (1 %), which is the same phenomena observed at 390 °C. These findings confirm that the addition of ethanol or glycerol at 10 % weight by fatty acid

does not have any further benefit on increasing decarboxylation % past temperatures of 375 °C.

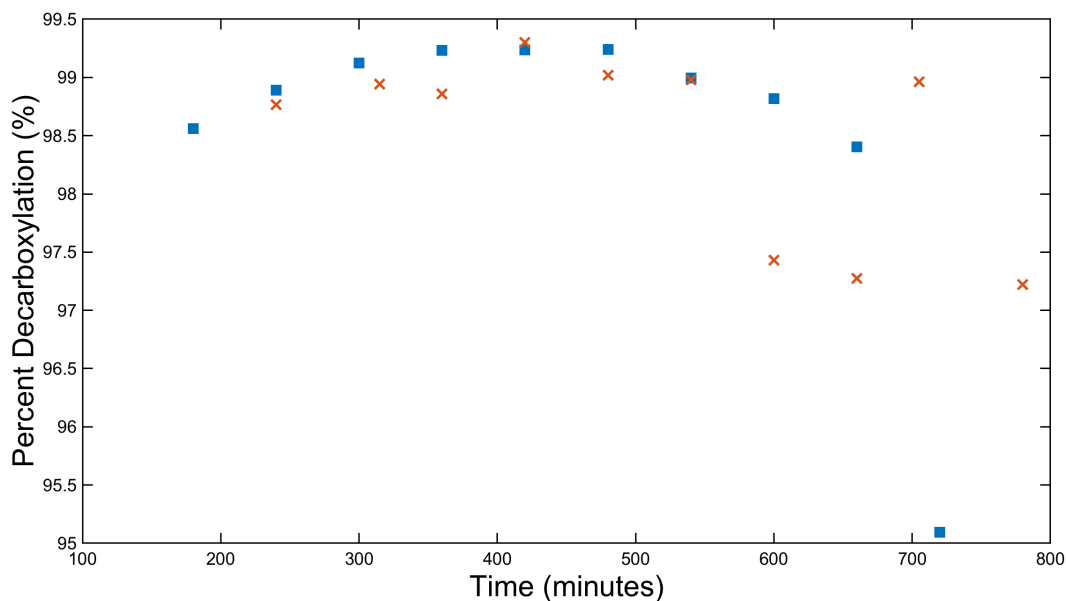


Figure 3.3 Percent decarboxylation over time in a PFR of stearic acid at 400 °C (×) and a residence time of 3.5 h. The impact of the additions of ethanol (■) is shown

In the previous chapter, it was postulated that decarboxylation can be enhanced by the hydrogen produced as a by-product of the cracking of fatty acids, and this is supported by other authors as well (Yeh et al., 2015), (Mo & Savage, 2014). This hydrogen is referred to as hydrogen equivalents as the exact structure or nature of the participating hydrogen is not directly known. Here, the impact of added ethanol to oleic acid processed continuously at 375 °C with a residence time of 3.5 h was assessed for the degree of decarboxylation over time. The results of these experiments are shown in Figure 3.4. Oleic acid processed with added ethanol appears to show no additional degree of decarboxylation (min: 83%, max: 99%) over oleic acid processed without added ethanol (min: 84%, max: 98%). There is a dip in the decarboxylation of oleic acid with and without ethanol at about 300 minutes and 360 minutes, respectively. It appears steady state is not reached, but then activity gains towards the end of the reaction. A possible explanation for this is that a change occurs in the chemical structure of the catalyst throughout the course of the reaction, which modifies the mechanism of decarboxylation. This is supported by the change in the catalyst's properties ( $\text{NH}_3$  TPD,  $\text{H}_2$  TPR, and XPS) from fresh to spent. GC-FID confirms the

product profile of the products collected from the reactor will change over the course of the continuous reaction.

Increasing the reaction temperature from 375 °C to 390 °C or 400 °C seems to increase the percent decarboxylation more than the addition of glycerol or oleic acid at 375 °C or changing the feed material to 100% oleic acid at 375 °C. However, these experiments were all conducted with the use of water/steam as the process solvent. It was desirable to investigate how different solvent systems impact decarboxylation, and if water is also ineffective in a  $\text{MoO}_x/\text{Al}_2\text{O}_3$  catalyst.

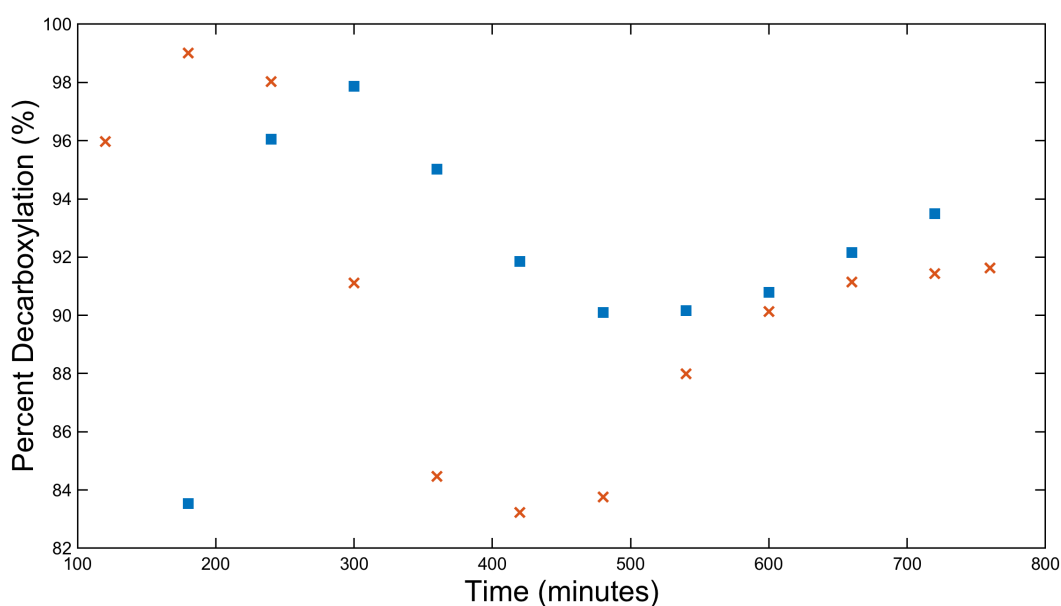


Figure 3.4 Percent decarboxylation over time in a PFR of oleic acid at 375 °C (■) and a residence time of 3.5 h. The impact of the addition of ethanol (×) is shown

### 3.4.2. Solvent Comparisons

According to Tian et al.(Tian et al., 2017) the use of water on Pt/C catalysts for decarboxylation of oleic acid is ineffective due to H<sup>+</sup> released from water and hydrogen bonding, which inhibits the ionization of carboxyl groups and therefore decarboxylation. Comparisons are still necessary between hydrocarbon solvent systems and solvent-free systems on a larger-scale process. Figure 1.6 demonstrates the percent decarboxylation of oleic acid processed at 375 °C with 3.5 h residence time in water, water with added 10% ethanol, toluene, and with no added solvent. Before FTIR and GC-FID measurements, samples processed with toluene were separated from toluene via distillation. The presence of toluene was probed by FTIR, and if the spectrum of toluene was present, spectral subtraction was performed before percent decarboxylation was calculated.

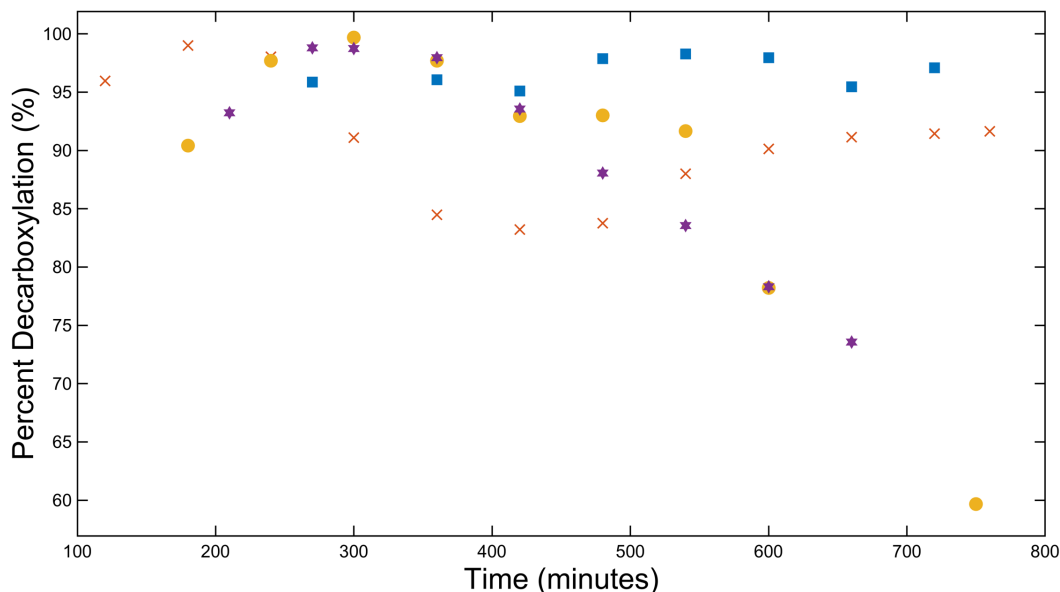


Figure 3.5 Percent decarboxylation over time in a PFR of oleic acid at 375 °C in water (★), in water with ethanol (x), in toluene (■) and oleic acid processed with no solvent (●) all with residence times of 3.5 h.

Some of the highest degrees of consistent decarboxylation occurred in the no solvent system and in the toluene solvent system. Decarboxylation does not apparently require a solvent

to progress. GC-MS was performed on a blank run with only toluene, and it was found that toluene did not degrade in this system. In order to maintain comparable flowrates and residence times with the no solvent system, far more mass was processed with the solvent free run (136 g vs 34 g in other solvents). Deactivation in the no solvent system did not start to occur until the addition of water at 8 h sampling time. The decrease in decarboxylation could be due to the expansion of water pushing the oleic acid out of the reactor, effectively decreasing its residence time at 8 h to 12 h. Water is not required for this reaction and can still act as a mobile phase, but it may alter the chemistry and properties of the final product and the catalyst itself. Toluene was found to produce product with a minimum value of 95.1 % decarboxylated product and a maximum of 98.3 % decarboxylated product. The addition of ethanol prevents the deactivation shown in the later stages of the process seen in the water only process.

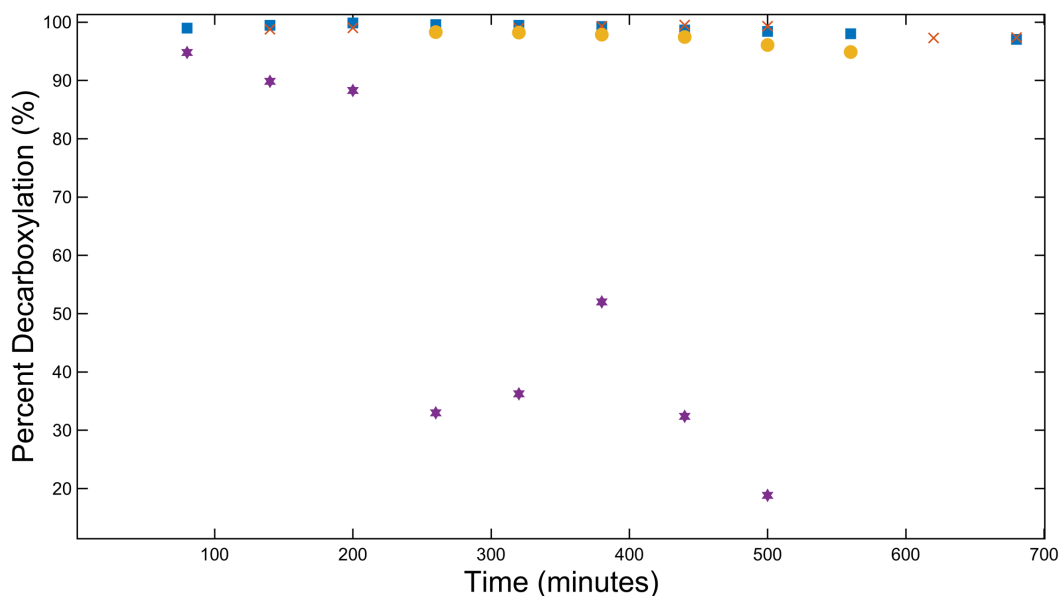


Figure 3.6 Percent decarboxylation over time in a PFR of stearic acid at 375 °C in water (★), in toluene as a solvent at 375 °C (×), stearic acid at 390 °C in water (■), and in toluene as a solvent at 390 °C (●) all with residence times of 3.5 h.

Figure 3.6 compares the deoxygenation of stearic acid at 375 °C with a residence time of 3.5 h in water and in toluene at 375 °C and 390 °C. Using toluene as a solvent boasts great increases

in minimum percent decarboxylation over 10 – 12 h of run time. The minimum decarboxylation of stearic acid in water is 19%, whereas the minimum for the same process conditions with a toluene solvent is 97%. The minimum decarboxylation when using toluene as a solvent at 390 °C is 95%. No significant catalyst deactivation is observed when toluene is used as a solvent, whereas deactivation and low activity is readily apparent when using water as a solvent at 375 °C.

### 3.4.3. GC-FID

Hydrocarbon size and chain length is a main determining factor of fuel quality and fuel type (Nikolskaya & Hiltunen, 2018). The hydrocarbons of gasoline are usually C<sub>4</sub>-C<sub>12</sub> with boiling range between 30 and 210 °C (Chou et al., 2002), whereas diesel fuel contains hydrocarbons with approximately C<sub>12</sub>-C<sub>20</sub> with a boiling range is between 170 and 360 °C. Aliphatic hydrocarbons are the main components (81%) of jet fuels, and exhibit ranges of carbon chain length of mainly C<sub>10</sub>-C<sub>14</sub> (Chou et al., 2002). GC-FID was employed to investigate hydrocarbon chain length of the products formed from the various systems investigated.

The product fractions of stearic acid, stearic acid with 10 % glycerol, and stearic acid with 10 % ethanol processed at 375 °C and 3.5 h residence time can be observed in Figure 3.7. The stearic acid product has lower decarboxylation rates, and remaining stearic acid elutes from the column in the same region as C<sub>22</sub> to C<sub>24</sub> fractions. For clarification, C<sub>9</sub> to C<sub>10</sub> fractions would contain nonane up to but not including decane fractions. This is the pattern maintained among all GC-FID figures. In the figures, the heptadecane percent is separate from the C<sub>17-18</sub> category in the figures, as heptadecane is the main product from decarboxylation. This is useful for understanding cracking and combining reactions. Using glycerol and ethanol, heptadecane increases by 8% and 7% respectively compared to stearic acid only products. There appears to be no significant differences in product fractions between added ethanol or added glycerol.

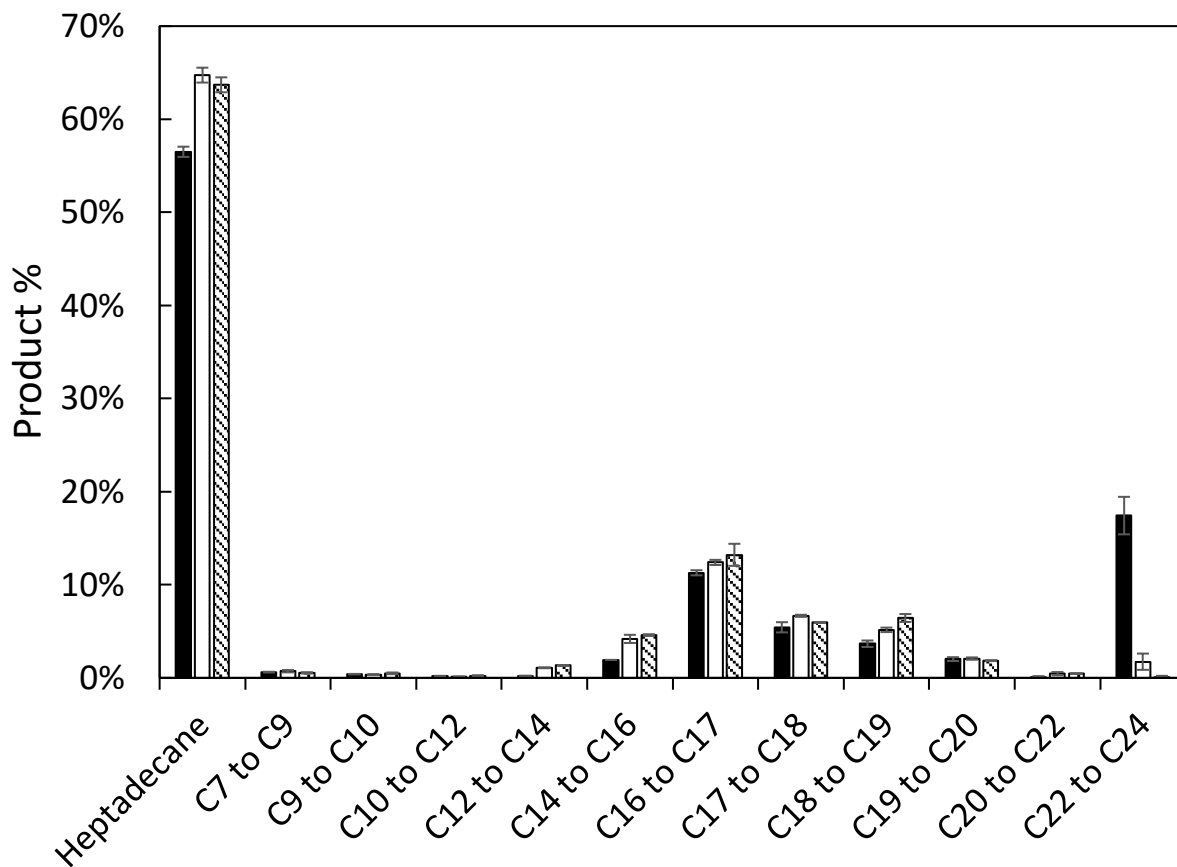


Figure 3.7 GC-FID fractions of products formed from stearic acid (black), stearic acid with 10 % w/w glycerol (white), and stearic acid with 10 % w/w ethanol (striped). All experiments were run at 375 °C and 3.5 h res. time.

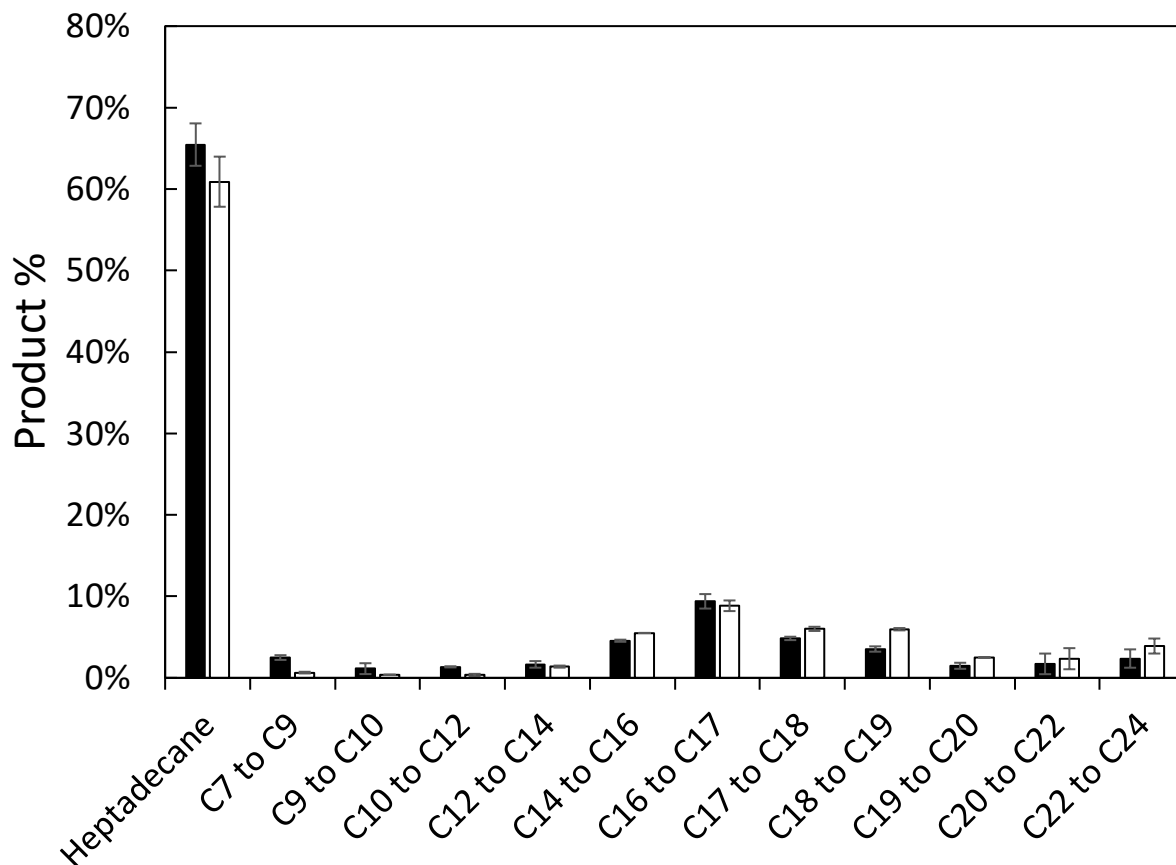


Figure 3.8 GC-FID fractions of products formed from stearic acid with 10 % w/w ethanol (black) and stearic acid without any added ethanol (white). All experiments were run at 390 °C and 3.5h res. time.

The product fractions of stearic acid with and without 10 % glycerol at 390 °C and 3.5 h residence time can be observed in Figure 3.8. The samples analyzed were collected at the 4 h mark in each experiment. An increase in heptadecane (65 %) is observed when ethanol is added to the reaction as opposed to no ethanol added (61 %). There appears to be more heavier-than-heptadecane fractions in stearic acid only product (21 %) vs ethanol added (14 %). The addition of ethanol appears to slightly increase fractions lighter than heptadecane (21 % vs 17 %).

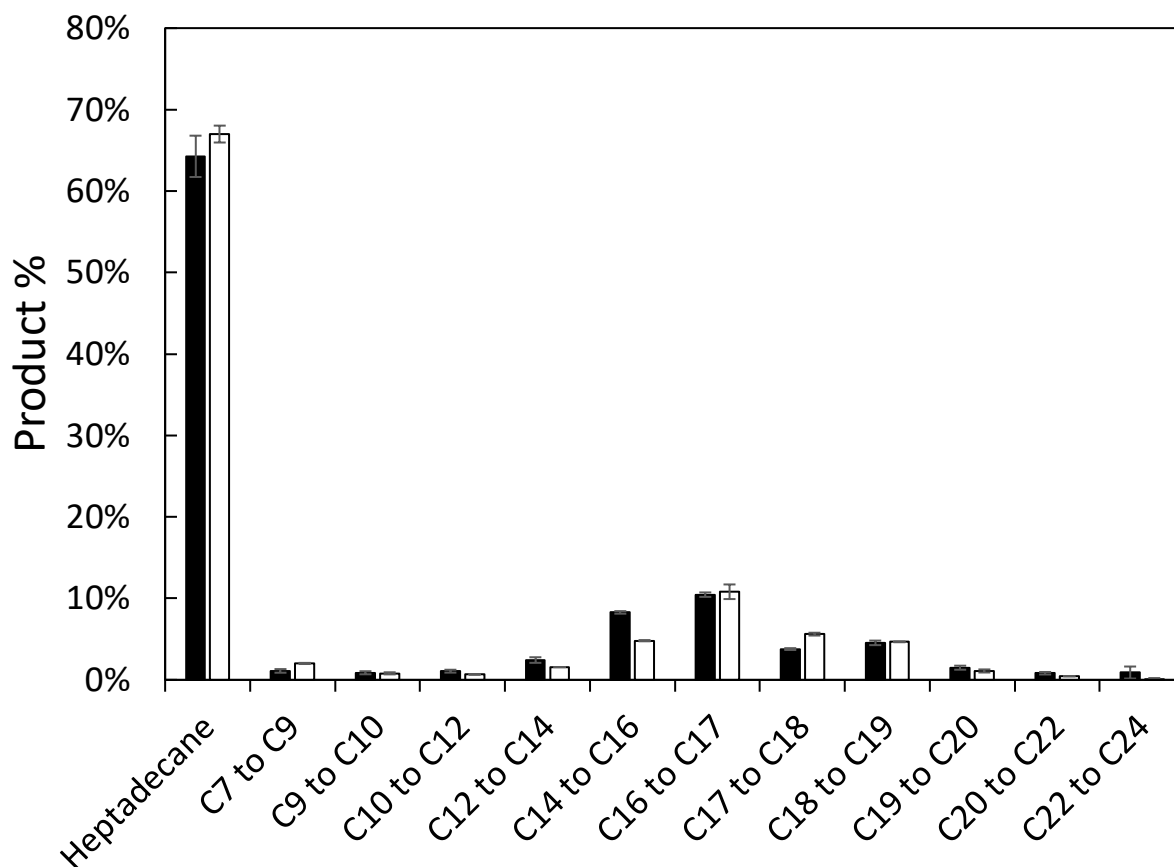


Figure 3.9 GC-FID fractions of products formed from stearic Acid with 10 % w/w ethanol (black) and stearic acid without any added ethanol (white). All experiments were run at 400 °C and 3.5 h res. time.

The product fractions of stearic acid and stearic acid processed with 10 % ethanol at 400 °C and 3.5 h residence time can be observed in Figure 3.9. The samples analyzed were also collected at the 4 h mark in each experiment. There appears to be a decrease in heptadecane (64 %) when ethanol is added to the reaction as opposed to no ethanol added (67 %). There appears to be negligibly more heavier-than-heptadecane fractions in stearic acid only product (12 %) vs ethanol added (12 %). The opposite was found in lighter than heptadecane fractions. The addition of ethanol appears to slightly increase fractions lighter than heptadecane (24 % vs 21 %).

Previous studies conducted by and Miao et al (Miao et al., 2018) showed differing paraffin yields and hydrocarbon lengths and weights. The product fractions of oleic acid processed at 375 °C and 3.5 h residence time were investigated by addition of ethanol. If addition of ethanol

increases the degree of decarboxylation in stearic acid at 375 °C then it might also be possible that the product quality of oleic acid processed at these conditions is changed in some capacity. The hydrocarbon fraction profile generated by GC-FID for oleic acid processed with and without ethanol at 375 °C and 3.5 h residence time is shown in Figure 3.10.

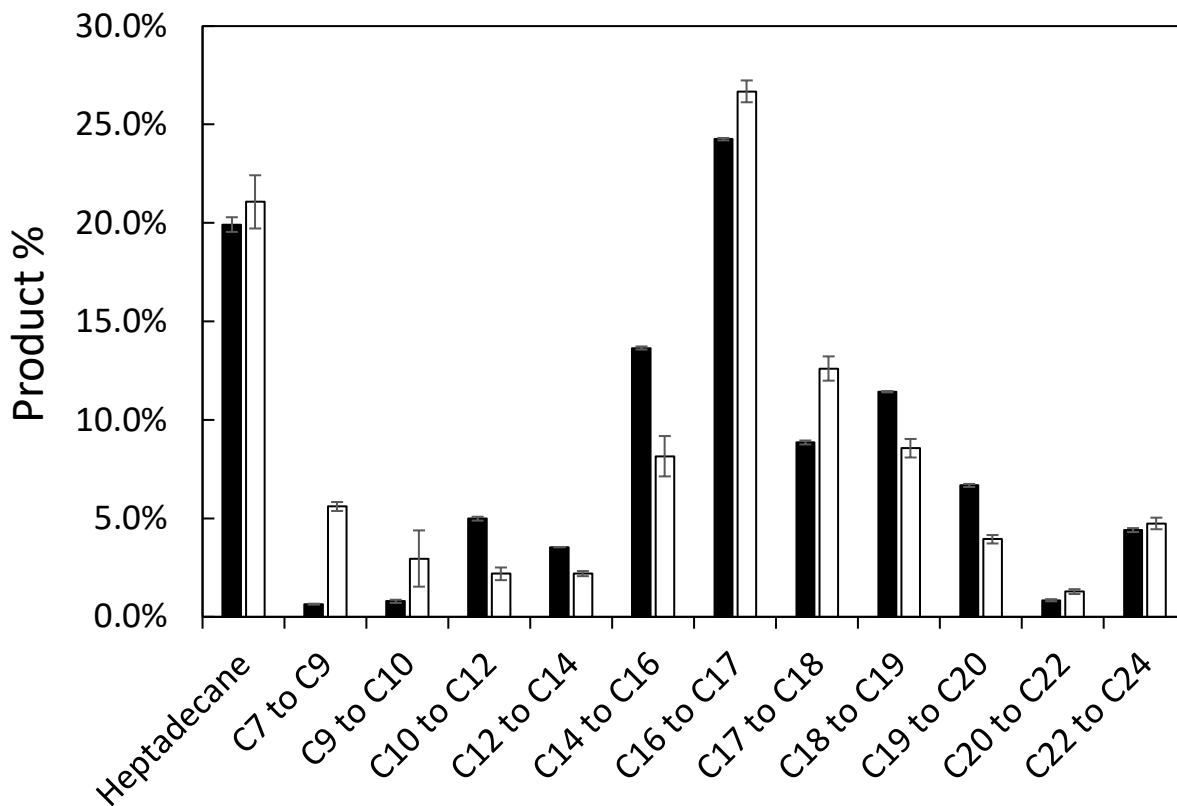


Figure 3.10 GC-FID fractions of products formed from oleic acid with 10 % w/w ethanol (white) and oleic acid without any added ethanol (black). All experiments were run at 375 °C and 3.5 h res. time.

The product fractions of oleic acid product and oleic acid processed with 10 % glycerol at 375 °C and 3.5 h residence time can be observed in Figure 3.10. The samples analyzed were collected at the 4 h mark in each experiment. There is a slight increase in heptadecane (21 %) when ethanol is added to the reaction as opposed to no ethanol added (20 %). No significant variation is

observed in heavier-than-heptadecane fractions (32 % oleic acid only product vs 31% ethanol added product). The addition of ethanol does not change the relative percent of fractions lighter than heptadecane (48 % vs 48 %). Overall, the addition of ethanol appears to not only provide little change in the degree of decarboxylation over time, but also does not appear to provide any change in the product profile when using oleic acid as a feedstock in water. It is possible that ethanol will not compete for the same catalyst sites that crack oleic acid, and any hydrogen equivalents generated by the reforming of ethanol do not appear to increase hydrogenation and heptadecane yields. The largest proportion of heptadecane produced in a water solvent system was stearic acid with no added ethanol at 400 °C (67 %).

In the previous section, water and toluene as solvents and no solvent were tested for their impacts on decarboxylation. It was found that the degree of decarboxylation among water solvent systems was generally lower than that of the toluene solvent and no solvent systems. What is also of interest is how the solvent impacts the product fractions produced.

Figure 3.11 demonstrates the hydrocarbon product profiles of oleic acid processed at 375 °C with 3.5 h residence time in water, toluene, and no solvent. Oleic acid processed in a toluene environment produced products with the highest proportion of heptadecane at 28 %. Proportion of heptadecane was found to be 19 % and 20 % in the no solvent and water solvent systems, respectively. The toluene system had the lowest amount of less than heptadecane fractions at 39 %, while the no solvent and water solvent systems both comprised 48 % of hydrocarbon weights less than heptadecane. Toluene had the largest proportion of fractions greater than heptadecane at 35 %. No solvent had 31.0 % greater than heptadecane while the water solvent system had 32 %. A lower proportion of heptadecane may indicate more cracking of heavier components and therefore more activity overall, or it may just indicate a lack of specificity for decarboxylation among other reactions.

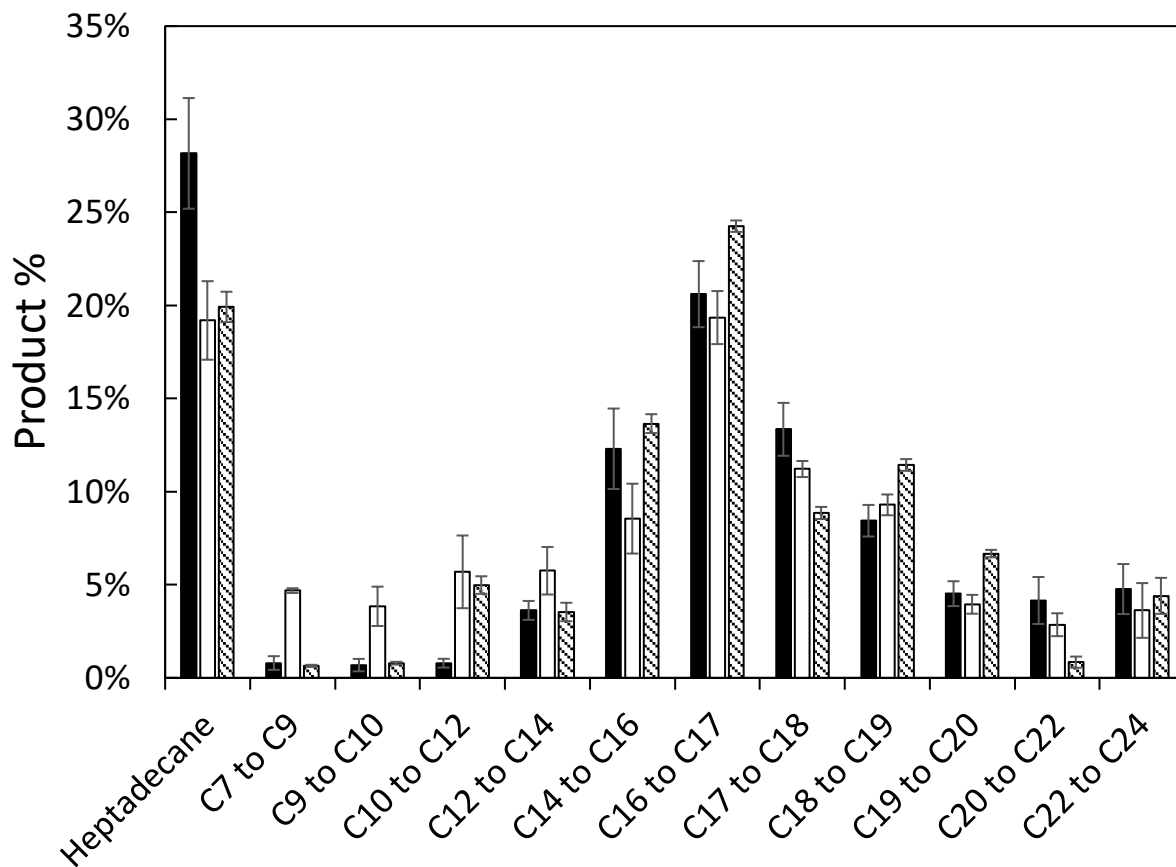


Figure 3.11 GC-FID fractions of products formed from oleic acid in toluene at 375 °C (black), oleic acid with no added solvent (white), and oleic acid processed in water (striped). All experiments were run at 375 °C and 3.5 h res. time.

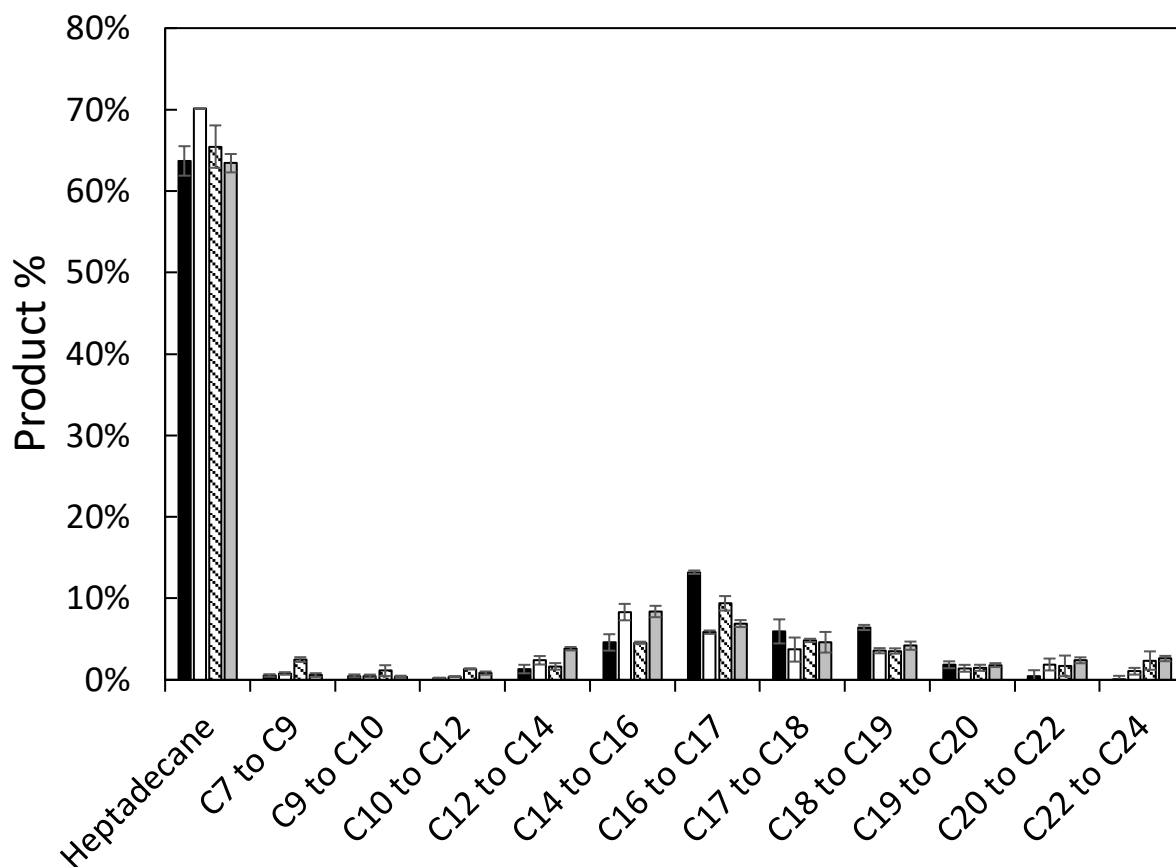


Figure 3.12 GC-FID fractions of products formed; stearic acid processed in water with 10 % ethanol at 375 °C (black), stearic acid in toluene at 375 °C (white), stearic acid processed in water with 10 % ethanol at 390 °C (striped), and stearic acid processed in toluene at 390 °C. All experiments were run with 3.5 h res. time.

Figure 3.12 demonstrates the hydrocarbon product profiles of stearic acid processed at 375 and 390 °C with 3.5 h residence time in water and toluene. Stearic acid processed in a toluene environment at 375 °C produced products with the highest proportion of heptadecane at 70 %. The product obtained from processing stearic acid at 375 °C with 10 % ethanol gives 64 % proportion of heptadecane and the highest proportion of lighter-than-heptadecane fractions at 22 % total. The highest proportion of heavier-than-heptadecane was found in toluene solvent processed at 390 °C. Overall, relative proportions of the heptadecane and the heavier and lighter fractions do not differ

more than 7 % from the four different conditions. It appears that the implementation of a hydrocarbon solvent like toluene has the largest impact on oleic acid when processed at 375 °C.

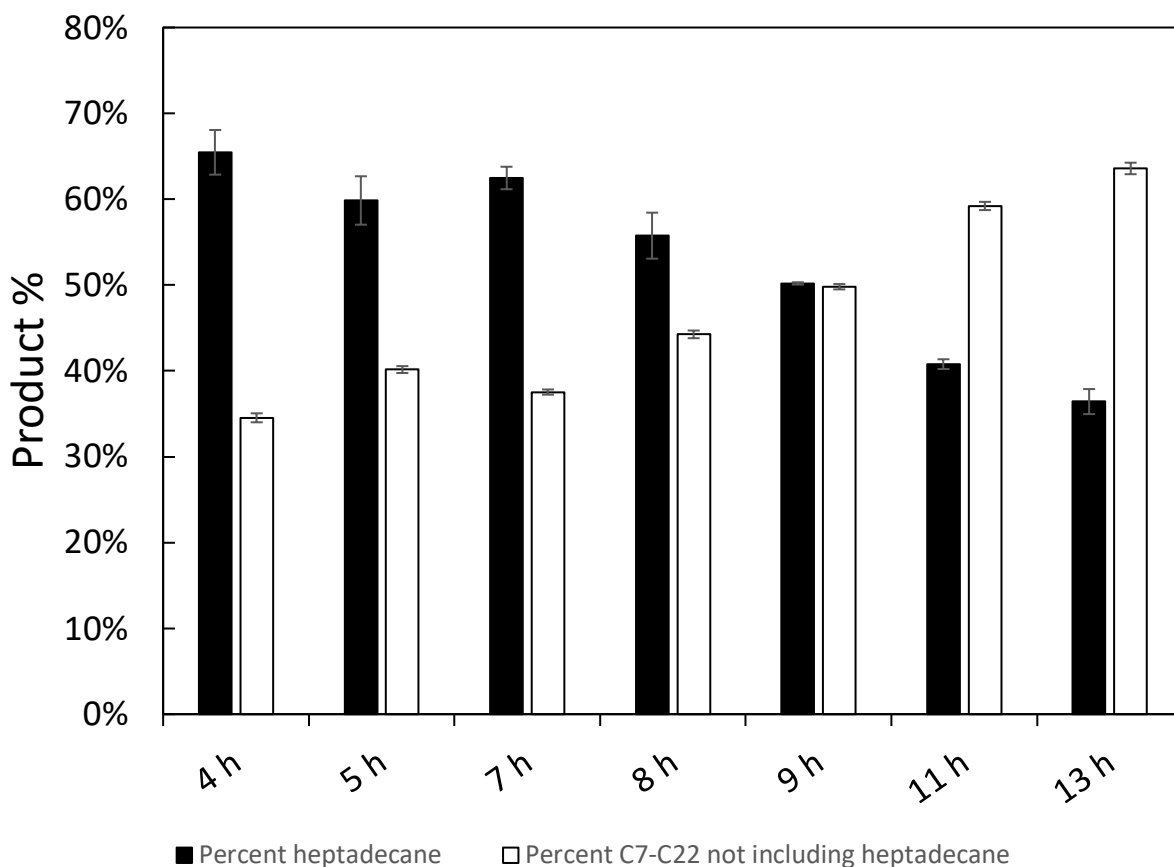


Figure 3.13 Stearic acid feed processed at 390 °C with a 3.5 h residence time, product quantities over time. Percent heptadecane in black and all other products not including heptadecane in white.

Figure 3.13 shows the product fractions over time during a run at 390 °C with a 3.5 h residence time. This reaction was run continuously for 11 h with a stearic acid feed with 10 % ethanol added. Oil-feed was stopped at 8 h, and from 8 h until 13 h only water was passed through the reactor to push out the remaining material. The proportion of heptadecane starts at the highest relative proportions at 4 h (66 %) and declines over time until 13 h (36 %). One can see that lighter than and heavier than C<sub>17</sub> fractions increases past the 7 h collection point, when new material was no longer being added. However, it takes 3.5 h for all material added to exit the reactor and therefore we would expect no large changes to occur until after 11 h. The composition of the

product appears to change at the 8 h time-point, which results in increases of both lower and higher than C<sub>17</sub> products being formed. It is possible that the longer the reactor runs, the more accumulation occurs of product. This can result in longer chains accumulating within the reactor and undergoing additional cracking and combining. This will form shorter products from cracking and longer products from diels-alder adducts over time (Teeter et al., 1958). This is an explanation for why we see a reduction in the overall heptadecane yield and increases in both longer and shorter hydrocarbon chains over the course of the reaction.

### 3.4.4. NMR of products

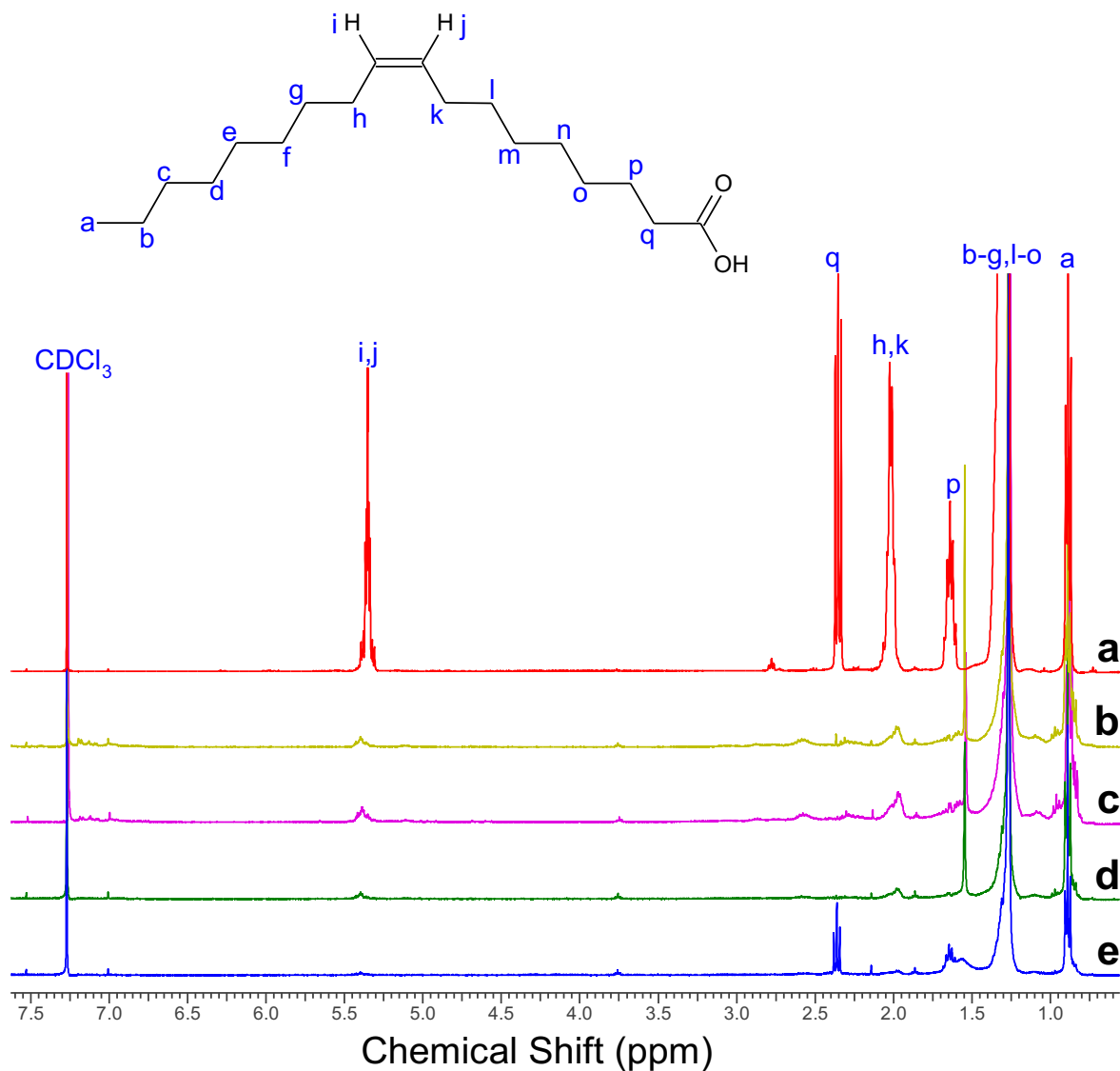


Figure 3.14 <sup>1</sup>H NMR spectra of (a) oleic acid, (b) oleic acid 375 °C 3.5 h 10% ethanol, (c) oleic acid 375 °C 3.5 h, (d) stearic 375 °C 3.5 h 10% glycerol, and (e) stearic 375 °C 3.5 h.

Excess amounts of cracking may lead to products with extensive amounts of double bonds that may lead to less stable fuel products (Pereira & Pasa, 2006). These products may polymerize or oxidize over time, leading to gum formation in fuels. To better understand the conversion of

alkenyl group and decarboxylation of oleic acid, stearic acid, and mixes of the two, the decarboxylated liquid products were further characterized by  $^1\text{H}$  NMR spectroscopies. Figure 3.14 compares the  $^1\text{H}$  NMR spectra of oleic acid and the formed liquid products. In the spectrum of oleic acid (Figure 1.16a), there are several proton peaks located at 10.74 (a broad peak, not shown), 5.35, 2.36, 2.04, 1.64, 1.30, and 0.89 ppm that can be attributed to protons adjacent and secondary to carboxylic acid (p, q), alkenyl protons (i,j,h,k), methylene (b-g, l-o), and methyl (a) protons, respectively. In the spectrum of the formed products from stearic acid (d and e), there is a reduction of the peaks related to the carboxylic group (p,q) and a minimal quantity of alkenyl groups (i,j,h,k). However, stearic acid at 375 °C shows remaining carboxylic acid which suggests incomplete decarboxylation. The addition of glycerol to stearic acid at 375 °C has a slight production of alkene groups and minimal carboxylic acid. In the product formed from oleic acid at 375 °C and 3.5 h residence time, the peaks related to the carboxylic group (p,q) disappear, indicating complete decarboxylation. The presence of the alkenyl group (i,j,h,k) has been significantly diminished compared to the starting material, which indicates significant conversion of the alkenyl group. Therefore, all of these NMR results can confirm the conversion of the carboxylic after the decarboxylation reaction under the selected reaction conditions, in good agreement with the FTIR results. During cracking, carbon-carbon single bonds release hydrogen to form alkene bonds. If extensive cracking is taking place to decarboxylate the fatty acids, the oleic acid product NMR spectrum might show an increase in alkene peaks. As these alkene peaks are reduced, there appears to be a mechanism of saturation or replacement of alkene bonds with aliphatic bonds, as there is a reduction in alkenes from oleic acid.

### 3.4.5. Regenerated Catalyst

Catalyst regeneration was tested via an in-situ method. The catalyst was heated at 650 °C inside the reactor under 50 mL/min of air to burn off coke and other carbonaceous species. This form of regeneration was conducted because the TGA profiles in Table 3.2 support the hypothesis that coke is produced as a byproduct of decarboxylation. Figure 3.19 indicates the lack of graphitic coke on the catalyst surface, indicating that the catalyst can be regenerated via burning of coke under air. This catalyst then processed a feedstock of CDO with a residence time of 3.5 h. The results of the decarboxylation can be seen in Figure 3.15.

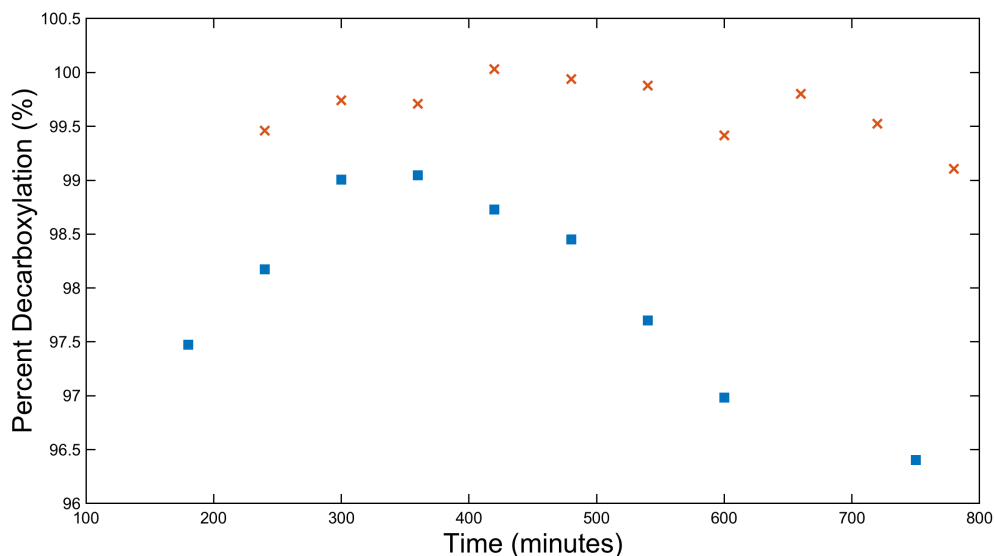


Figure 3.15 Decarboxylation over time of CDO with a fresh catalyst (■) and CDO processed with in-situ regenerated catalyst (×)

From the decarboxylation plot, one can see that the regenerated catalyst is able to regain decarboxylation activity. This regained activity is similar to that of the fresh catalyst.

### 3.4.6. Catalyst Characterization

The effect of the composition variation on the textural properties of the fresh and spent catalyst was evaluated by N<sub>2</sub> physisorption. The main properties determined were surface area, pore volume, and pore size. The results of N<sub>2</sub> physisorption of various spent catalysts can be seen in Table 3.1.

All isotherms are type IVa according to the IUPAC classification, which is characteristic for mesoporous materials (Thommes et al., 2015). Example isotherms can be found in the supporting information. The data show that the surface area and pore volume all reduce in the spent catalysts whereas pore size appears to remain unchanged or increase. The fresh catalyst has a surface area of 140.9 m<sup>2</sup>/g, a pore volume of 0.4 cm<sup>3</sup>/g, and a pore size of 116.4 Å.

Table 3.1 N<sub>2</sub> Physisorption of Catalyst surface properties

Sample ID	BET Surface Area (m <sup>2</sup> /g)	Pore Volume (cm <sup>3</sup> /g)	Pore Size (Å)
Fresh Catalyst	140.91	0.41	116.36
Gamma alumina calcined	145.22	0.46	126.46
Spent catalyst, stearic 3.5h at 375 °C	100.88	0.29	114.17
Spent catalyst, stearic 3.5 h at 375 °C with glycerol	87.68	0.29	130.64
Spent catalyst, stearic 3.5 h at 375 °C with ethanol	107.96	0.31	113.98
Spent catalyst, stearic 3.5 h at 390°C	107.76	0.32	117.86
Spent catalyst, stearic 3.5h at 390 °C, with glycerol	109.98	0.32	115.72
Spent catalyst, stearic 3.5 h at 390 °C in Toluene	79.56	0.22	108.73
Spent catalyst, oleic 3.5 h at 375 °C	86.41	0.26	120.74
Spent catalyst, oleic 3.5 h at 375 °C, with ethanol	117.84	0.33	111.9
Spent catalyst, oleic 3.5 h at 375 °C in Toluene	61.48	0.20	133.26
Spent catalyst, oleic only 3.5 h at 375 °C	57.61	0.21	144.86
Fresh regenerated catalyst	92.44	0.33	142.68

There are decreases in catalyst surface area and pore volume regardless of the reaction conditions. The fresh catalyst has a surface area of 140.91 m<sup>2</sup>/g and a pore volume of 0.41 cm<sup>3</sup>/g. The largest decline in catalyst surface properties were found in the spent catalyst exposed to

conditions of oleic acid feed with no solvent at 375 °C and 3.5 h residence time, with a surface area of 57.6 m<sup>2</sup>/g and pore volume of 0.21 cm<sup>3</sup>/g. The next largest decrease in properties is oleic acid processed in toluene at 375 °C and 3.5 h residence time (SA = 61.48 m<sup>2</sup>/g, PV = 0.20 cm<sup>3</sup>/g). The catalyst that appeared to have the smallest drop in surface properties was oleic acid processed at 375 °C with ethanol added into the process. It might be theorized that having extra carbonaceous species within the process would produce more coke and reduce surface properties, but this is not seen with ethanol. 390 °C with a stearic acid feed appears to have similar, if not better properties when glycerol is added to the process. However, the addition of glycerol at 375 °C with stearic acid does not show the same trend, as the addition of glycerol shows surface area decline from 100.88 to 87.68 m<sup>2</sup>/g, and no change in pore volume (PV = 0.29 cm<sup>3</sup>/g). Ethanol with stearic acid at 375 °C shows less reduction in surface area and pore volume than with the use of glycerol. It is theorized that this occurs because under these conditions with an acidic catalyst, glycerol will form acrolein (Talebian-Kiakalaieh, Amin, & Hezaveh, 2014). Acrolein will readily self-polymerize, and this polymer could deposit on the catalyst surface and form coke, which would reduce surface areas. Acrolein is not likely to form with ethanol use, leading to less reductions in surface area and pore volume.

The use of toluene as a solvent appears to significantly reduce surface area and pore volume in both stearic acid at 390 °C (79.56 m<sup>2</sup>/g, 0.22 cm<sup>3</sup>/g) and oleic acid at 375 °C (61.48 m<sup>2</sup>/g, 0.2 cm<sup>3</sup>/g). It is likely that toluene and no solvent systems promote higher activities as solvents than water, as proven by Tian et al. (Tian et al., 2017). The reaction conditions tested for toluene solvent and no solvent systems are likely too high in temperature and residence time, which increases cracking, which increases total coke production.

Thermogravimetric analysis (TGA) was further used to compare the fresh and spent catalysts. Table 3.2 shows the relative percent weight of the catalyst that is water, volatiles, polymer/feed, and coke present on the surfaces of the catalysts tested. Temperature was ramped at 10 °C/min starting at 50 °C up to 800 °C under air. The highest proportion of coke formed on the catalyst surface was found oleic and stearic acid processed in toluene, 11.18 % and 10.87 % respectively. This is in agreement with BET that our conditions tested may be too intense in toluene and no solvent systems, which enhances cracking. The catalyst that processed oleic acid without any solvent at 375 °C had a large percentage of coke (9.53 %) but also had the largest percent of

remaining feed/polymer at 6.05 %. Stearic acid processed at 390 °C shows less coke than when processed at 375 °C (5.54 % vs 7.21 %). The addition of ethanol and glycerol do not appear to greatly alter the proportion of coke at 390 °C, but a 2 % reduction in coke is visible when using glycerol and ethanol at 375 °C. The catalyst with the lowest remaining material on the surface is oleic acid processed with 10% ethanol at 375 °C and stearic acid processed at 390 °C with 10% ethanol. These positive results are confirmed by the surface properties measured by BET.

Table 3.2 Table of Thermogravimetric analysis data of spent catalysts, quantified based on combustion and evaporation temperatures.

Sample ID	%			
	% Water	Volatile	%Polymer/feed	%Coke
Fresh catalyst	1.80	1.26	0.00	0.00
Stearic acid 375 °C 3.5 h	0.77	0.79	4.39	7.21
Stearic acid 390 °C 3.5 h	0.25	0.68	3.18	5.54
Oleic acid 375 °C 3.5 h	0.65	0.91	5.67	7.04
Stearic acid 375 °C 3.5 h, 10 % glycerol	0.73	0.62	3.96	5.56
Stearic acid 390 °C 3.5 h, 10 % glycerol	0.85	0.61	2.60	6.28
Stearic acid 390 °C 3.5 h, 10 % ethanol	0.71	0.70	2.62	5.60
Stearic acid 375 °C 3.5 h, 10 % ethanol	0.81	0.93	3.07	5.88
Stearic acid 375 °C 3.5 h, in toluene	0.58	0.61	4.65	11.18
Oleic acid 375 °C 3.5 h, 10 % ethanol	0.93	0.48	1.58	4.72
Oleic acid 375 °C 3.5 h, no solvent	0.39	0.61	6.05	9.53
Oleic acid 375 °C 3.5 h, in toluene	0.21	0.45	3.29	10.87

Due to the heterogeneity of solid surfaces, materials can possess acidic and basic sites (Lewis or Brønsted types) of various strengths. Ammonia can interact with acidic sites through hydrogen bonding, and Hengst et al. (Hengst et al., 2015) found enhanced deoxygenation of free fatty acids using an acidic catalyst (Pd/Pural SB1-derived Al<sub>2</sub>O<sub>3</sub>). As acidic sites can correlate with activity, the catalyst was probed for acidic sites by the use of NH<sub>3</sub> Temperature Programmed

Desorption (TPD). The sorption profiles of a spent and fresh  $\text{MoO}_x/\text{Al}_2\text{O}_3$  can be seen in Figure 3.16. More  $\text{NH}_3$  is adsorbed onto the surface of the spent catalyst than the fresh ( $52.68$  vs  $19.11$   $\text{cm}^3/\text{g}$  STP) but this larger amount of acid sites desorb at a temperature of  $775$   $^\circ\text{C}$ .  $\text{NH}_3$  molecules released at temperatures lower than  $400$   $^\circ\text{C}$  correspond to weak acidity, while sorption occurring past  $400$   $^\circ\text{C}$  is indicative of strong acid sites (Gonçalves et al., 2017).

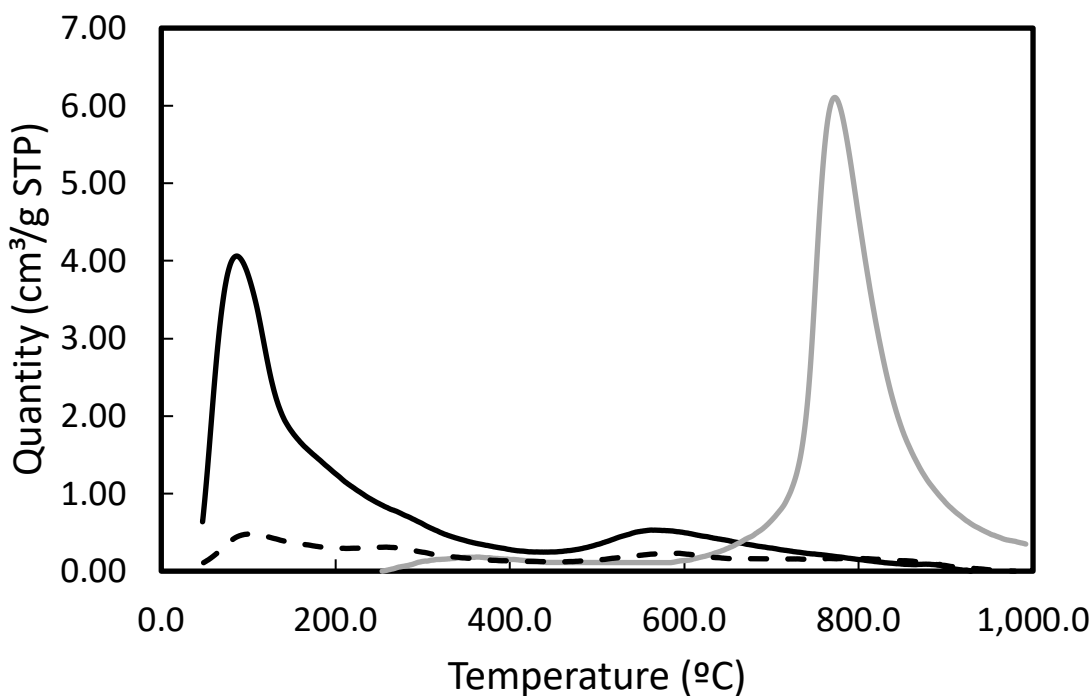


Figure 3.16  $\text{NH}_3$  TPD of  $\text{MoO}_3/\text{Al}_2\text{O}_3$  Catalysts. In situ regenerated fresh catalyst (dashed), spent catalyst (grey), and freshly prepared catalyst (black).

The fresh catalyst's main desorption peak centers at  $96$   $^\circ\text{C}$ , and has a much smaller peak at  $576$   $^\circ\text{C}$ . The most striking  $\text{NH}_3$  profile is that of the regenerated catalyst. The regenerated catalyst has 3 peaks at  $110$   $^\circ\text{C}$ ,  $275$   $^\circ\text{C}$ , and  $585$   $^\circ\text{C}$ . This is a large increase in weak acid sites from the spent catalyst, and a profile different than that of fresh catalyst. Total acid sites are measured to be  $10.95$   $\text{cm}^3/\text{g}$  STP. This is far fewer acid sites than can be seen on the fresh catalyst. Due to a reduction in weak acid sites, we might expect lower activities. Figure 3.15 displayed the decarboxylation of CDO by a fresh catalyst, and then a catalyst regenerated in-situ by burning under air. There is not a large difference in decarboxylation found between the fresh and regenerated catalyst. More

experimentation is required to determine why a reduction in acid sites has not resulted in a reduction in activity.

It is thought weak acid sites are the active sites of decarboxylation (H. Wang et al., 2017) (Dos Anjos et al., 1983) (Kirszensztejn et al., 2009), and strong acid sites contribute to cracking and coking. TON and TOF were calculated for the regenerated catalyst reaction of CDO at 375 °C with 3.5h residence time based on equation 2.4. The regenerated catalyst has 0.029 moles of total acid sites and the moles of fatty acids within CDO converted at the specified conditions was 0.049 moles. The TON for the regenerated catalyst at this condition is 1.69 moles of product/moles of acid sites. The TOF is 0.008 moles of product/moles of weak acid sites/minute. Fresh catalyst processing the same feed under the same conditions has a TON of 0.98 moles of product/moles of acid sites and a TOF of 0.0047 moles of product/moles of weak acid sites/minute. This suggests that the regenerated catalyst has a better activity than the fresh catalyst. XPS, TPR, and XRD are further utilized to determine possible reasons for the increase in activity.

The spent catalyst has an increase in the number of strong acid sites, and a reduction in weak sites. Peng et al. (J. Peng et al., 2009) confirm that strong acid sites are on HZSM-5 catalysts enhance the cracking of bio-oil. It is possible that over extended reaction time in a continuous reactor that cracking increases due to the increase of strong acid sites on the catalyst. We are increasing the strong acidity and therefore cracking, and this is evidently seen in shows that over the extent of time, selectivity to heptadecane decreases and the relative amount of cracked fractions increases. This could lead to enhanced coking over time and therefore catalyst deactivation.

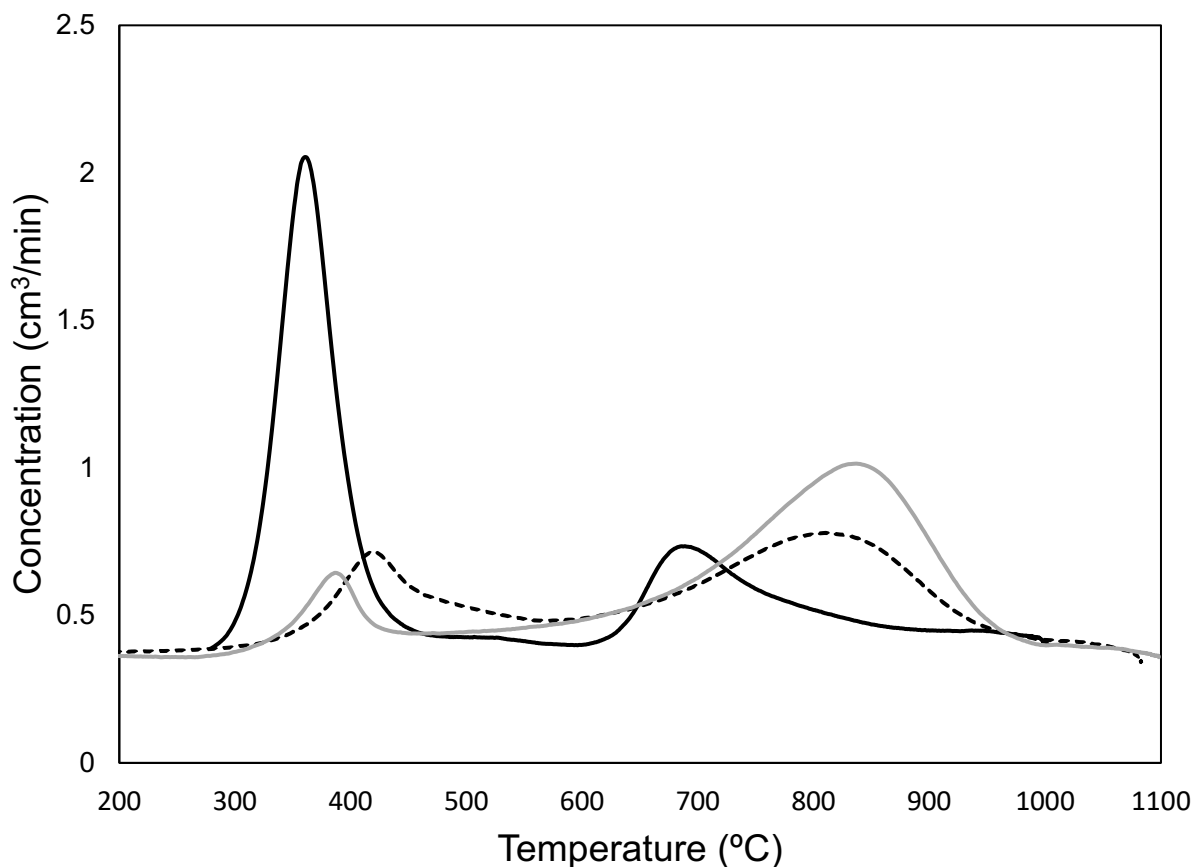


Figure 3.17 H<sub>2</sub> TPR profile of fresh (grey), spent (black), and regenerated (dashed) MoO<sub>x</sub>/Al<sub>2</sub>O<sub>3</sub> catalysts

H<sub>2</sub>-TPR experiments were conducted to determine the reduction temperatures of the fresh and spent catalysts. H<sub>2</sub>-TPR profiles of fresh catalysts are shown in Figure 3.17. Two reduction peaks are observed in the fresh catalyst at 393 °C and 842 °C. It has been reported that the reduction of Mo species is a two-step process such as MoO<sub>3</sub> to MoO<sub>2</sub> and then MoO<sub>2</sub> to Mo (Ma et al., 2015). Different reduction temperatures obtained in the TPR profile indicate two different Mo species present, which are confirmed by XPS to be Mo(VI) and Mo(V) in Figure 3.18. The TPR profile of spent catalyst indicates two peaks at 364 °C and 690 °C. The 364 °C peak in the spent catalyst is much larger than the 393 °C in the fresh catalyst, and could be related to an increase in that phase of Mo. An increase in Mo(V) and Mo(IV) can be seen in the XPS spectra of the spent catalyst in

Figure 3.18. The regenerated catalyst also shows two peaks at 411 °C and 816 °C, very similar to fresh catalyst. XPS confirm the oxidation state similarities between fresh and regenerated as the two catalysts have roughly the same percentages of Mo(VI) and Mo(V). The regenerated catalyst's peak at 411 °C is higher than the fresh catalyst's peak at 393 °C. This indicates that the regenerated catalyst reduces from MoO<sub>3</sub> to MoO<sub>2</sub> at higher temperatures than the fresh catalyst. Hossain et al. (Hossain, Chowdhury, Jhavar, Xu, Biesinger, et al., 2018) found that when using their MoO<sub>x</sub>/Al<sub>2</sub>O<sub>3</sub> catalyst that MoO<sub>3</sub> was likely the active metal. Based on this, we hypothesize that the regenerated catalyst may be more likely to resist reduction and maintain the active MoO<sub>3</sub> phase, possibly being a better catalyst overall.

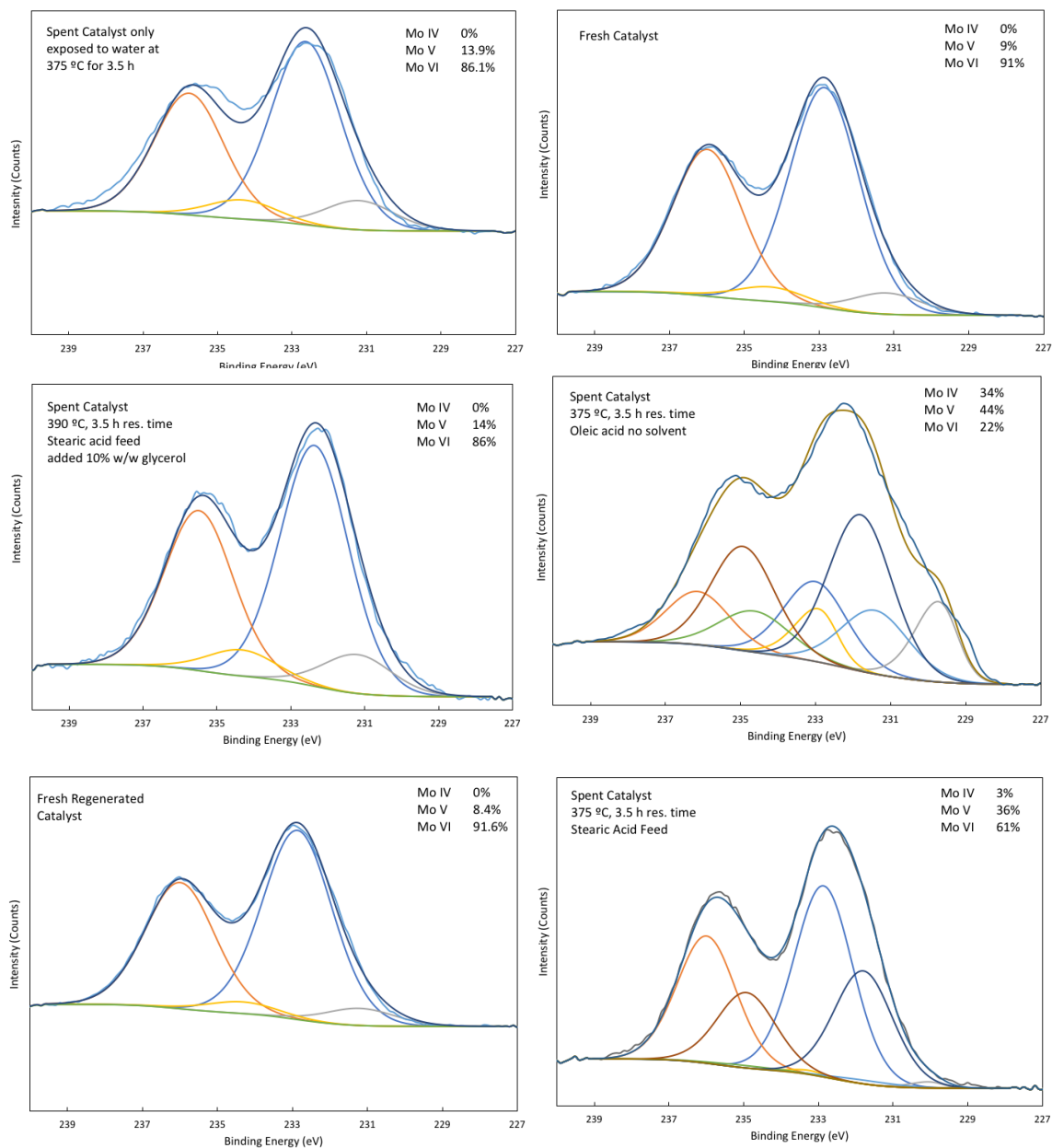


Figure 3.18 XPS spectra for Mo/Al<sub>2</sub>O<sub>3</sub> catalysts. Details for each catalyst conditions can be found in each spectrum

For a more detailed investigation of the surface structure, XPS spectra of a fresh and spent MoO<sub>x</sub>/Al<sub>2</sub>O<sub>3</sub> catalyst are presented in Figure 3.18. The spent catalyst is from the process using stearic acid as a feed at 375 °C with a residence time of 3.5 h. This catalyst was chosen as it had demonstrated some of the lowest conversion of fatty acid to deoxygenated product. The spectra

were curve-fit using the screened and unscreened peak-fitting parameters peak positions, full width at half-maximum (fwhm), and area ratios for Mo(IV) as outlined by Scanlon et al. (Scanlon et al., 2010) A Mo 3d<sub>5/2</sub>–Mo 3d<sub>3/2</sub> spin–orbit doublet for Mo(VI) was constrained to have an area ratio of 3:2, equal fwhms, a doublet spacing of 3.13 eV, and an Mo 3d<sub>5/2</sub> peak position ranging from 232.2 to 232.6 eV. Mo(V) may be present because of the X-ray reduction of MoO<sub>3</sub> during the analysis (Baltrusaitis et al., 2015).

There appears to be a small degree of change from Mo(VI) to Mo(V) between fresh and stearic acid with 10 % ethanol spent catalyst. This exact same degree of change is also observed in the catalyst that was only exposed to water at 375 °C. However, the catalyst that did not have ethanol added to stearic acid at 375 °C has a large decrease in Mo(VI) (91 % to 61 %) and large increase in Mo(V) (8 % to 36 %) and the presence of Mo(IV) (0 % vs 3 %). The transition between Molybdenum VI to V from fresh to spent catalyst can also be seen in a study by Hossain et al. (Hossain, Chowdhury, Jhawar, Xu, Biesinger, et al., 2018) in which they also use a Molybdenum doped Alumina catalyst. This catalyst used in these conditions had some of the worst activity found in this study. It may be that Mo(VI) is the most active phase and ethanol allows for regeneration of the Mo(VI) oxidation state. The catalyst from the experiment from oleic acid processed at 375 °C with no solvent was also analyzed with XPS. This catalyst had produced products with high degrees of decarboxylation from 3 h to 8 h, and then lost this activity when the product was flushed from the system with water. This catalyst shows the lowest amount of Mo(VI) (22 %) and the highest amount of Mo(IV) (34 %). No broad conclusions can be taken from this, but more must be investigated as to the relationship between solvent use, decarboxylation, and molybdenum oxidation states. The in-situ regenerated catalyst shows no large difference in oxidation states between itself and fresh catalyst.

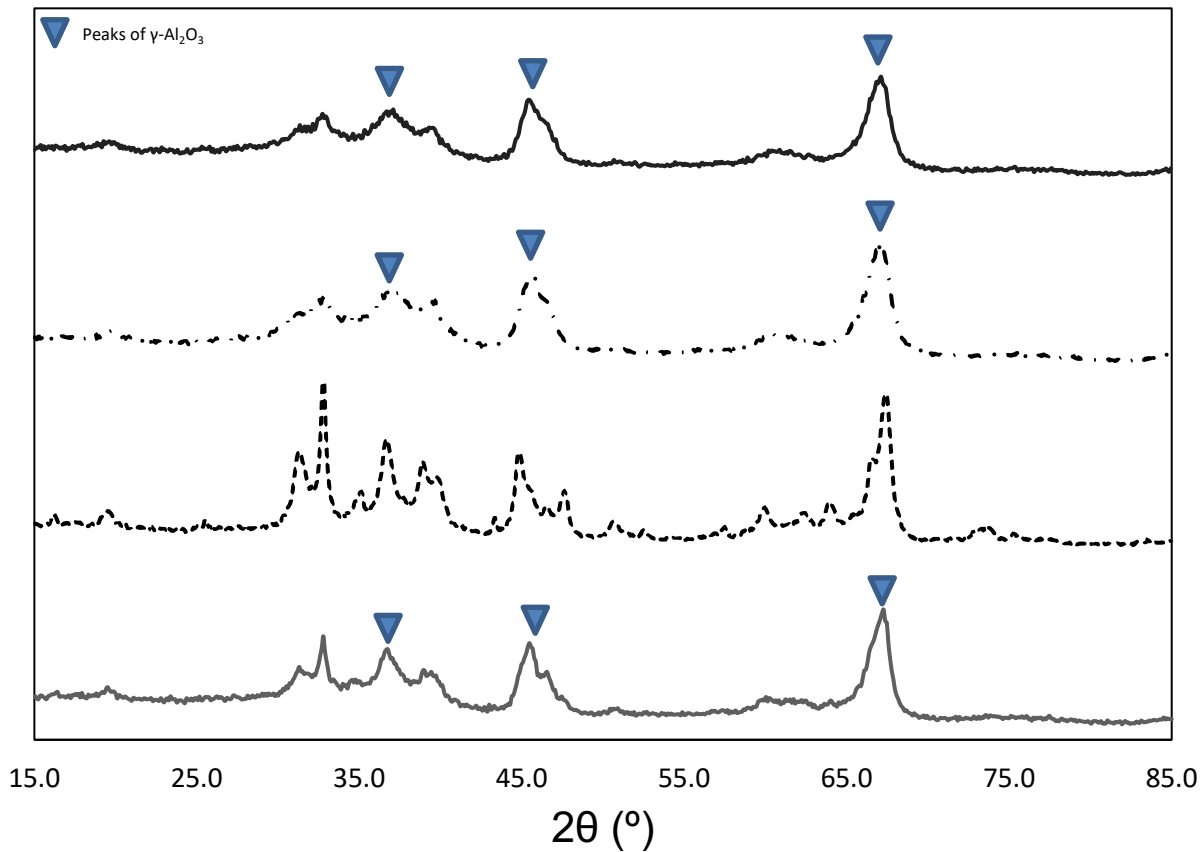


Figure 3.19 XRD spectra of fresh gamma alumina  $\text{MoO}_x$  catalyst (solid line), calcined gamma alumina (dashed and dotted line), regenerated gamma alumina  $\text{MoO}_x$  catalyst (grey), and calcined theta alumina (dashed).

Crystallinity of catalysts are typically measured by X-Ray diffraction (XRD). XRD pattern of fresh catalyst, calcined gamma alumina, calcined theta alumina, and regenerated  $\text{MoO}_x$  catalysts are shown in Figure 3.19. The peaks of pure  $\gamma\text{-Al}_2\text{O}_3$  phase can be seen at  $2\theta = 35.2, 47.2$  and  $67.6^\circ$  (Charisiou et al., 2016). Very weak reflections of pure Mo cannot be seen at  $2\theta = 42$  and  $61^\circ$ , and other phases of molybdenum oxides are not readily visible in these spectra. The XRD in Figure 3.19 suggests that the regenerated catalyst possesses both theta and gamma alumina. Theta alumina doped with Mo was tested as a catalyst and prepared in the same manner as gamma alumina. The theta alumina doped  $\text{MoO}_x$  catalyst was found to have no catalytic ability. It is suggested that phase changes within the catalyst act to form defects in the catalyst leading to interruptions in the lattice and therefore an increase in active sites. The increase in the number of

sites is confirmed by TPD and O<sub>2</sub> chemisorption. Active metal dispersion is an important catalyst quality, as it gauges efficiency and access of reactant to the active site. Catalyst active metal dispersion was measured by O<sub>2</sub> pulse chemisorption. Sintering was found to occur between fresh and spent catalysts, with a drop in overall dispersion of 50%. O<sub>2</sub> pulse chemisorption profiles for fresh and spent catalyst can be found in the supporting information. The active metal dispersion of the regenerated catalyst was found to have twice the active metal dispersion of the fresh catalyst. The increase in active metal dispersion could be due to the in-situ regeneration process reversing sintering. This phenomenon was also found by Wan et al. (Wan et al., 2016) in which O<sub>2</sub> was used to re-disperse Rh supported on ZrO<sub>2</sub>. This redispersion helps to elevate the regenerated catalyst's activity.

### 3.5. Conclusions

This work investigated the impact of added glycerol and ethanol to the continuous decarboxylation of stearic and oleic acid. It was found that added glycerol and ethanol can reduce the necessary reaction temperature conditions (from 390 °C to 375 °C) to achieve near-complete decarboxylation of stearic acid with a main product of heptadecane. The impact of solvent (steam, toluene, and no solvent) was investigated. It was found that toluene and no solvent systems have higher activity than the steam system. GC-FID results showed a high selectivity to heptadecane conversion (67 %) with stearic acid as a feed, whereas products formed from oleic acid show low heptadecane proportions (20 %) and a high proportion of cracked products. The selectivity for heptadecane (70 %) obtained at maximized reaction conditions were with stearic acid feed in toluene solvent at 375 °C. In-situ regenerated catalyst was found to be able to decarboxylate CDO after being subjected to a continuous stream of air and temperatures of 600 °C. The NH<sub>3</sub> TPD found that the decarboxylation process reduces the number of weak acid sites on the catalyst and increases the number of strong acid sites. The regenerated catalyst loses both strong and weak acid sites, yet still has comparable decarboxylation rates compared to fresh catalyst. The turnover frequency for the regenerated catalyst was greater than the fresh catalyst, 0.008 vs 0.0047 moles of product/moles of weak acid sites/minute, respectively.

### 3.6. References

- 11, A. D. –. (2011). Standard Test Method for Acidity in Aviation Turbine Fuel 1. *Annual Book of ASTM Standards*. <https://doi.org/10.1520/D3242-11>.This
- Abbas, J., Hussain, S., Iqbal, M. J., Nadeem, H., Qasim, M., Hina, S., & Hafeez, F. (2016). Oil industry waste: a potential feedstock for biodiesel production. *Environmental Technology (United Kingdom)*. <https://doi.org/10.1080/09593330.2016.1141997>
- Abdulkareem-Alsultan, G., Asikin-Mijan, N., Lee, H. V., Rashid, U., Islam, A., & Taufiq-Yap, Y. H. (2019). Review on thermal conversion of plant oil (Edible and inedible) into green fuel using carbon-based nanocatalyst. *Catalysts*. <https://doi.org/10.3390/catal9040350>
- Adroit Market Research. (2019). *Global Biodiesel Market Size 2019 by Feedstock (Vegetable Oil [Soybean oil, Canola oil, Other edible oils], Animal fats[Poultry, White grease, Tallow, Others]), by Application (Fuel[Automotive, Marines, Others], Power Generation, Others), by Region and Fo*. Dallas, TX.
- Afshar Taromi, A., & Kaliaguine, S. (2018). Hydrodeoxygenation of triglycerides over reduced mesostructured Ni/γ-alumina catalysts prepared via one-pot sol-gel route for green diesel production. *Applied Catalysis A: General*, 558(September), 140–149. <https://doi.org/10.1016/j.apcata.2018.03.030>
- Ahmadi, M., Macias, E. E., Jasinski, J. B., Ratnasamy, P., & Carreon, M. A. (2014). Decarboxylation and further transformation of oleic acid over bifunctional, Pt/SAPO-11 catalyst and Pt/chloride Al<sub>2</sub>O<sub>3</sub> catalysts. *Journal of Molecular Catalysis A: Chemical*. <https://doi.org/10.1016/j.molcata.2014.02.004>
- Al Alwan, B., Salley, S. O., & Ng, K. Y. S. (2015). Biofuels production from hydrothermal decarboxylation of oleic acid and soybean oil over Ni-based transition metal carbides supported on Al-SBA-15. *Applied Catalysis A: General*, 498, 32–40. <https://doi.org/10.1016/j.apcata.2015.03.012>
- Anon. (1974). FLAMMABLE AND COMBUSTIBLE LIQUIDS CODE 1973. *ANSI Stand.*

- Asomaning, J., Mussone, P., & Bressler, D. C. (2014). Thermal deoxygenation and pyrolysis of oleic acid. *Journal of Analytical and Applied Pyrolysis*. <https://doi.org/10.1016/j.jaap.2013.09.005>
- Babcock, B. A. (2012). The impact of US biofuel policies on agricultural price levels and volatility. *China Agricultural Economic Review*. <https://doi.org/10.1108/17561371211284786>
- Baltrusaitis, J., Mendoza-Sanchez, B., Fernandez, V., Veenstra, R., Dukstiene, N., Roberts, A., & Fairley, N. (2015). Generalized molybdenum oxide surface chemical state XPS determination via informed amorphous sample model. *Applied Surface Science*. <https://doi.org/10.1016/j.apsusc.2014.11.077>
- Behnejad, B., Abdouss, M., & Tavasoli, A. (2019). Comparison of performance of Ni–Mo/ $\gamma$ -alumina catalyst in HDS and HDN reactions of main distillate fractions. *Petroleum Science*. <https://doi.org/10.1007/s12182-019-0319-5>
- Bell, A. T., Gates, B. C., Ray, D., & Thompson, M. R. (2008). *Basic Research Needs: Catalysis for Energy*. <https://doi.org/10.2172/927492>
- Button, S. (2010). Biodiesel: Vehicle Fuel from Vegetable Oil. *Energy & Environment*. <https://doi.org/10.1260/0958-305x.20/21.8/1.1305>
- Castello, D., & Fiori, L. (2011). Supercritical water gasification of biomass: Thermodynamic constraints. *Bioresource Technology*. <https://doi.org/10.1016/j.biortech.2011.05.017>
- Centeno, A., Laurent, E., & Delmon, B. (1995). Influence of the support of CoMo sulfide catalysts and of the addition of potassium and platinum on the catalytic performances for the hydrodeoxygenation of carbonyl, carboxyl, and guaiacol-type molecules. *Journal of Catalysis*. <https://doi.org/10.1006/jcat.1995.1170>
- Chapman, L. (2007). Transport and climate change: a review. *Journal of Transport Geography*. <https://doi.org/10.1016/j.jtrangeo.2006.11.008>
- Charisiou, N. D., Baklavaridis, A., Papadakis, V. G., & Goula, M. A. (2016). Synthesis Gas Production via the Biogas Reforming Reaction Over Ni/MgO–Al<sub>2</sub>O<sub>3</sub> and Ni/CaO–Al<sub>2</sub>O<sub>3</sub>

- Catalysts. *Waste and Biomass Valorization*. <https://doi.org/10.1007/s12649-016-9627-9>
- Cheng, H. N., Dowd, M. K., Easson, M. W., & Condon, B. D. (2012). Hydrogenation of cottonseed oil with nickel, palladium and platinum catalysts. *JAOCs, Journal of the American Oil Chemists' Society*. <https://doi.org/10.1007/s11746-012-2036-8>
- Chou, C. C., Riviere, J. E., & Monteiro-Riviere, N. A. (2002). Differential relationship between the carbon chain length of jet fuel aliphatic hydrocarbons and their ability to induce cytotoxicity vs. interleukin-8 release in human epidermal keratinocytes. *Toxicological Sciences*. <https://doi.org/10.1093/toxsci/69.1.226>
- Choudhury, M. B. I., Ahmed, S., Shalabi, M. A., & Inui, T. (2006). Preferential methanation of CO in a syngas involving CO<sub>2</sub> at lower temperature range. *Applied Catalysis A: General*. <https://doi.org/10.1016/j.apcata.2006.08.008>
- Chowdhury, M. B. I., Hossain, M. M., & Charpentier, P. A. (2011). Effect of supercritical water gasification treatment on Ni/La 2O<sub>3</sub>-Al<sub>2</sub>O<sub>3</sub>-based catalysts. *Applied Catalysis A: General*. <https://doi.org/10.1016/j.apcata.2011.07.031>
- Clayton, C. R., & Lu, Y. C. (1989). Electrochemical and XPS evidence of the aqueous formation of Mo<sub>2</sub>O<sub>5</sub>. *Surface and Interface Analysis*. <https://doi.org/10.1002/sia.740140114>
- Coenen, J. W. E. (1986). Catalytic Hydrogenation of Fatty Oils. *Industrial and Engineering Chemistry Fundamentals*. <https://doi.org/10.1021/i100021a006>
- Condon, N., Klemick, H., & Wolverton, A. (2015). Impacts of ethanol policy on corn prices: A review and meta-analysis of recent evidence. *Food Policy*. <https://doi.org/10.1016/j.foodpol.2014.12.007>
- Corma, A., & Orchillés, A. V. (2000). Current views on the mechanism of catalytic cracking. *Microporous and Mesoporous Materials*. [https://doi.org/10.1016/S1387-1811\(99\)00205-X](https://doi.org/10.1016/S1387-1811(99)00205-X)
- Cruz, I. O., Ribeiro, N. F. P., Aranda, D. A. G., & Souza, M. M. V. M. (2008). Hydrogen production by aqueous-phase reforming of ethanol over nickel catalysts prepared from hydrotalcite precursors. *Catalysis Communications*.

<https://doi.org/10.1016/j.catcom.2008.07.031>

Demirbas, A. (2009). Political, economic and environmental impacts of biofuels: A review. *Applied Energy*. <https://doi.org/10.1016/j.apenergy.2009.04.036>

Demirbas, A. (2011). Biodiesel from oilgae, biofixation of carbon dioxide by microalgae: A solution to pollution problems. *Applied Energy*. <https://doi.org/10.1016/j.apenergy.2010.12.050>

Demirbas, A., & Fatih Demirbas, M. (2011). Importance of algae oil as a source of biodiesel. *Energy Conversion and Management*. <https://doi.org/10.1016/j.enconman.2010.06.055>

Den Otter, I. M. J. A. M. (1970). The Dimerization of Oleic Acid with a Montmorillonite Catalyst I: Important Process Parameters; Some Main Reactions. *Fette, Seifen, Anstrichmittel*. <https://doi.org/10.1002/lipi.19700720809>

Desikan, A. N., Huang, L., & Oyama, S. T. (1992). Structure and dispersion of molybdenum oxide supported on alumina and titania. *Journal of the Chemical Society, Faraday Transactions*. <https://doi.org/10.1039/FT9928803357>

Di Serio, M., Cozzolino, M., Giordano, M., Tesser, R., Patrono, P., & Santacesaria, E. (2007). From homogeneous to heterogeneous catalysts in biodiesel production. *Industrial and Engineering Chemistry Research*. <https://doi.org/10.1021/ie070663q>

Ding, R., Wu, Y., Chen, Y., Liang, J., Liu, J., & Yang, M. (2015). Effective hydrodeoxygenation of palmitic acid to diesel-like hydrocarbons over MoO<sub>2</sub>/CNTs catalyst. *Chemical Engineering Science*. <https://doi.org/10.1016/j.ces.2014.10.024>

Dinh, L. T. T., Guo, Y., & Sam Mannan, M. (2009). Sustainability evaluation of biodiesel production using multicriteria decision-making. *Environmental Progress and Sustainable Energy*. <https://doi.org/10.1002/ep.10335>

Dos Anjos, J. R. S., De Araujo Gonzalez, W., Lam, Y. L., & Frety, R. (1983). Catalytic decomposition of vegetable oil. *Applied Catalysis*. [https://doi.org/10.1016/0166-9834\(83\)80158-4](https://doi.org/10.1016/0166-9834(83)80158-4)

- Dou, B., Wang, C., Song, Y., Chen, H., & Xu, Y. (2014). Activity of Ni-Cu-Al based catalyst for renewable hydrogen production from steam reforming of glycerol. *Energy Conversion and Management*. <https://doi.org/10.1016/j.enconman.2013.10.067>
- Douette, A. M. D., Turn, S. Q., Wang, W., & Keffer, V. I. (2007). Experimental investigation of hydrogen production from glycerin reforming. *Energy and Fuels*. <https://doi.org/10.1021/ef060379w>
- Douvartzides, S. L., Charisiou, N. D., Papageridis, K. N., & Goula, M. A. (2019). Green Diesel: Biomass Feedstocks, Production Technologies, Catalytic Research, Fuel Properties and Performance in Compression Ignition Internal Combustion Engines. *Energies*. <https://doi.org/10.3390/en12050809>
- EPA. (2012). Chapter 3. Energy. In *Inventory of U.S. Greenhouse Gas Emissions and Sinks: 1990–2012*.
- Ford, J. P., Immer, J. G., & Lamb, H. H. (2012). Palladium catalysts for fatty acid deoxygenation: Influence of the support and fatty acid chain length on decarboxylation kinetics. *Topics in Catalysis*. <https://doi.org/10.1007/s11244-012-9786-2>
- Friedman, D., Masciangioli, T., & Olson, S. (2012). Replacing critical materials with abundant materials. In *The role of the chemical sciences in finding alternatives to critical resources - A workshop summary*.
- Fu, J., Lu, X., & Savage, P. E. (2010). Catalytic hydrothermal deoxygenation of palmitic acid. *Energy and Environmental Science*. <https://doi.org/10.1039/b923198f>
- Fu, J., Lu, X., & Savage, P. E. (2011a). Hydrothermal decarboxylation and hydrogenation of fatty acids over Pt/C. *ChemSusChem*. <https://doi.org/10.1002/cssc.201000370>
- Fu, J., Lu, X., & Savage, P. E. (2011b). Hydrothermal decarboxylation and hydrogenation of fatty acids over Pt/C. *ChemSusChem*, 4(4), 481–486. <https://doi.org/10.1002/cssc.201000370>
- Fu, J., Shi, F., Thompson, L. T., Lu, X., & Savage, P. E. (2011). Activated carbons for hydrothermal decarboxylation of fatty acids. *ACS Catalysis*.

<https://doi.org/10.1021/cs1001306>

Global EV Outlook 2020. (2020). In *Global EV Outlook 2020*. <https://doi.org/10.1787/d394399e-en>

Gollakota, A. R. K., Kishore, N., & Gu, S. (2018). A review on hydrothermal liquefaction of biomass. *Renewable and Sustainable Energy Reviews*. <https://doi.org/10.1016/j.rser.2017.05.178>

Gonçalves, A. A. S., Faustino, P. B., Assaf, J. M., & Jaroniec, M. (2017). One-Pot Synthesis of Mesoporous Ni-Ti-Al Ternary Oxides: Highly Active and Selective Catalysts for Steam Reforming of Ethanol. *ACS Applied Materials and Interfaces*. <https://doi.org/10.1021/acsami.6b15507>

Gorham, R. (2002). Air Pollution From Ground Transportation; An Assessment of Causes , Strategies and Tactics , and Proposed Actions for the International Community. In *The Global Initiative on Transport Emissions*.

Gosselink, R. W., Hollak, S. A. W., Chang, S. W., Van Haveren, J., De Jong, K. P., Bitter, J. H., & Van Es, D. S. (2013). Reaction pathways for the deoxygenation of vegetable oils and related model compounds. *ChemSusChem*. <https://doi.org/10.1002/cssc.201300370>

Gosselink, R. W., Stellwagen, D. R., & Bitter, J. H. (2013). Tungsten-based catalysts for selective deoxygenation. *Angewandte Chemie - International Edition*. <https://doi.org/10.1002/anie.201209809>

Guzman, A., Torres, J. E., Prada, L. P., & Nuñez, M. L. (2010). Hydroprocessing of crude palm oil at pilot plant scale. *Catalysis Today*. <https://doi.org/10.1016/j.cattod.2009.11.015>

Hengst, K., Arend, M., Pfützenreuter, R., & Hoelderich, W. F. (2015). Deoxygenation and cracking of free fatty acids over acidic catalysts by single step conversion for the production of diesel fuel and fuel blends. *Applied Catalysis B: Environmental*. <https://doi.org/10.1016/j.apcatb.2015.03.009>

Hoekman, S. K. (2009). Biofuels in the U.S. - Challenges and Opportunities. *Renewable Energy*.

<https://doi.org/10.1016/j.renene.2008.04.030>

Holliday, R. L., King, J. W., & List, G. R. (1997). Hydrolysis of Vegetable Oils in Sub- And Supercritical Water. *Industrial and Engineering Chemistry Research*.

<https://doi.org/10.1021/ie960668f>

Hossain, M. Z., Chowdhury, M. B. I., Jhavar, A. K., Xu, W. Z., Biesinger, M. C., & Charpentier, P. A. (2018). Continuous Hydrothermal Decarboxylation of Fatty Acids and Their Derivatives into Liquid Hydrocarbons Using Mo/Al<sub>2</sub>O<sub>3</sub> Catalyst. *ACS Omega*.

<https://doi.org/10.1021/acsomega.8b00562>

Hossain, M. Z., Chowdhury, M. B. I., Jhavar, A. K., Xu, W. Z., & Charpentier, P. A. (2018). Continuous low pressure decarboxylation of fatty acids to fuel-range hydrocarbons with in situ hydrogen production. *Fuel*. <https://doi.org/10.1016/j.fuel.2017.09.092>

Hossain, M. Z., Jhavar, A. K., Chowdhury, M. B. I., Xu, W. Z., Wu, W., Hiscott, D. V., & Charpentier, P. A. (2017). Using Subcritical Water for Decarboxylation of Oleic Acid into Fuel-Range Hydrocarbons. *Energy and Fuels*.

<https://doi.org/10.1021/acs.energyfuels.6b03418>

Huang, J., Jiang, Y., Marthala, V. R. R., Bressel, A., Frey, J., & Hunger, M. (2009). Effect of pore size and acidity on the coke formation during ethylbenzene conversion on zeolite catalysts. *Journal of Catalysis*. <https://doi.org/10.1016/j.jcat.2009.02.019>

Immer, J. G., Kelly, M. J., & Lamb, H. H. (2010). Catalytic reaction pathways in liquid-phase deoxygenation of C18 free fatty acids. *Applied Catalysis A: General*.

<https://doi.org/10.1016/j.apcata.2009.12.028>

India, B. (2014). *Millettia Pinnata*.

IPCC. (2013). Summary for policymakers. In *Climate Change 2014: Impacts, Adaptation, and Vulnerability. Part A: Global and Sectoral Aspects. Contribution of Working Group II to the Fifth Assessment Report of the Intergovernmental Panel on Climate Change*.

IPCC. (2014). Climate Change 2014: Summary for Policymakers. *Climate Change 2014: Impacts,*

*Adaptation and Vulnerability - Contributions of the Working Group II to the Fifth Assessment Report.* <https://doi.org/10.1016/j.renene.2009.11.012>

Itthibenchapong, V., Srifa, A., Kaewmeesri, R., Kidkhunthod, P., & Faungnawakij, K. (2017). Deoxygenation of palm kernel oil to jet fuel-like hydrocarbons using Ni-MoS<sub>2</sub>/γ-Al<sub>2</sub>O<sub>3</sub> catalysts. *Energy Conversion and Management.* <https://doi.org/10.1016/j.enconman.2016.12.034>

IUPAC. (2014). Compendium of Chemical Terminology 2nd ed. (the “Gold Book”). *Blackwell Scientific Publications, Oxford.* <https://doi.org/10.1351/goldbook.I03352>

Janampelli, S., & Darbha, S. (2018). Metal Oxide-Promoted Hydrodeoxygenation Activity of Platinum in Pt-MO<sub>x</sub>/Al<sub>2</sub>O<sub>3</sub> Catalysts for Green Diesel Production. *Energy and Fuels.* <https://doi.org/10.1021/acs.energyfuels.8b03588>

Janampelli, S., & Darbha, S. (2019). Highly efficient Pt-MoO<sub>x</sub>/ZrO<sub>2</sub> catalyst for green diesel production. *Catalysis Communications.* <https://doi.org/10.1016/j.catcom.2019.03.027>

Jęczmionek, Ł., & Porzycka-Semczuk, K. (2014). Hydrodeoxygenation, decarboxylation and decarbonylation reactions while co-processing vegetable oils over a NiMo hydrotreatment catalyst. Part I: Thermal effects - Theoretical considerations. *Fuel.* <https://doi.org/10.1016/j.fuel.2014.04.055>

Jeon, J. Y., Han, Y., Kim, Y. W., Lee, Y. W., Hong, S., & Hwang, I. T. (2019). Feasibility of unsaturated fatty acid feedstocks as green alternatives in bio-oil refinery. *Biofuels, Bioproducts and Biorefining.* <https://doi.org/10.1002/bbb.1979>

Jessop, P. G. (2011). Searching for green solvents. *Green Chemistry.* <https://doi.org/10.1039/c0gc00797h>

Jiménez-López, A., Jiménez-Morales, I., Santamaría-González, J., & Maireles-Torres, P. (2011). Biodiesel production from sunflower oil by tungsten oxide supported on zirconium doped MCM-41 silica. *Journal of Molecular Catalysis A: Chemical.* <https://doi.org/10.1016/j.molcata.2010.11.035>

- Jutz, F., Andanson, J. M., & Baiker, A. (2011). Ionic liquids and dense carbon dioxide: A beneficial biphasic system for catalysis. *Chemical Reviews*. <https://doi.org/10.1021/cr100194q>
- Katryniok, B., Paul, S., & Dumeignil, F. (2013). Recent developments in the field of catalytic dehydration of glycerol to acrolein. *ACS Catalysis*, 3(8), 1819–1834. <https://doi.org/10.1021/cs400354p>
- Kern, C., & Jess, A. (2005). Regeneration of coked catalysts - Modelling and verification of coke burn-off in single particles and fixed bed reactors. *Chemical Engineering Science*. <https://doi.org/10.1016/j.ces.2005.01.024>
- Kim, M. C., & Kim, K. L. (1996). A role of molybdenum and shape selectivity of catalysts in simultaneous reactions of hydrocracking and hydrodesulfurization. *Korean Journal of Chemical Engineering*. <https://doi.org/10.1007/BF02705881>
- Kim, M. Y., Kim, J. K., Lee, M. E., Lee, S., & Choi, M. (2017). Maximizing Biojet Fuel Production from Triglyceride: Importance of the Hydrocracking Catalyst and Separate Deoxygenation/Hydrocracking Steps. *ACS Catalysis*. <https://doi.org/10.1021/acscatal.7b01326>
- King, J. W., Holliday, R. L., & List, G. R. (1999). Hydrolysis of soybean oil: In a subcritical water flow reactor. *Green Chemistry*. <https://doi.org/10.1039/a908861j>
- Kirszensztejn, P., Przekop, R., Tolińska, A., & Maćkowska, E. (2009). Pyrolytic and catalytic conversion of rape oil into aromatic and aliphatic fractions in a fixed bed reactor on Al<sub>2</sub>O<sub>3</sub> and Al<sub>2</sub>O<sub>3</sub>/B<sub>2</sub>O<sub>3</sub> catalysts. *Chemical Papers*. <https://doi.org/10.2478/s11696-008-0104-1>
- Knothe, G. (2007). Some aspects of biodiesel oxidative stability. *Fuel Processing Technology*. <https://doi.org/10.1016/j.fuproc.2007.01.005>
- Kordouli, E., Sygellou, L., Kordulis, C., Bourikas, K., & Lycourghiotis, A. (2017). Probing the synergistic ratio of the NiMo/Γ-Al<sub>2</sub>O<sub>3</sub> reduced catalysts for the transformation of natural triglycerides into green diesel. *Applied Catalysis B: Environmental*, 209, 12–22. <https://doi.org/10.1016/j.apcatb.2017.02.045>

- Kubička, D., & Horáček, J. (2011). Deactivation of HDS catalysts in deoxygenation of vegetable oils. *Applied Catalysis A: General*. <https://doi.org/10.1016/j.apcata.2010.10.034>
- Kubička, D., & Kaluža, L. (2010). Deoxygenation of vegetable oils over sulfided Ni, Mo and NiMo catalysts. *Applied Catalysis A: General*. <https://doi.org/10.1016/j.apcata.2009.10.034>
- Lestari, S., Päivi, M. A., Bernas, H., Simakova, O., Sjöholm, R., Beltramini, J., ... Murzin, D. Y. (2009). Catalytic deoxygenation of stearic acid in a continuous reactor over a mesoporous carbon-supported pd catalyst. *Energy and Fuels*. <https://doi.org/10.1021/ef900110t>
- Lin, R., Zhu, Y., & Tavlarides, L. L. (2014). Effect of thermal decomposition on biodiesel viscosity and cold flow property. *Fuel*. <https://doi.org/10.1016/j.fuel.2013.10.034>
- Loe, R., Santillan-Jimenez, E., Morgan, T., Sewell, L., Ji, Y., Jones, S., ... Crocker, M. (2016). Effect of Cu and Sn promotion on the catalytic deoxygenation of model and algal lipids to fuel-like hydrocarbons over supported Ni catalysts. *Applied Catalysis B: Environmental*. <https://doi.org/10.1016/j.apcatb.2016.03.025>
- Luo, N., Fu, X., Cao, F., Xiao, T., & Edwards, P. P. (2008). Glycerol aqueous phase reforming for hydrogen generation over Pt catalyst - Effect of catalyst composition and reaction conditions. *Fuel*. <https://doi.org/10.1016/j.fuel.2008.06.021>
- Ma, X., Cui, K., Hao, W., Ma, R., Tian, Y., & Li, Y. (2015). Alumina supported molybdenum catalyst for lignin valorization: Effect of reduction temperature. *Bioresource Technology*. <https://doi.org/10.1016/j.biortech.2015.05.032>
- Madsen, A. T., Ahmed, E. H., Christensen, C. H., Fehrmann, R., & Riisager, A. (2011). Hydrodeoxygenation of waste fat for diesel production: Study on model feed with Pt/alumina catalyst. *Fuel*. <https://doi.org/10.1016/j.fuel.2011.06.005>
- Mäki-Arvela, P., Snåre, M., Eränen, K., Myllyoja, J., & Murzin, D. Y. (2008). Continuous decarboxylation of lauric acid over Pd/C catalyst. *Fuel*. <https://doi.org/10.1016/j.fuel.2008.07.004>
- Mäki-Arvela, Päivi, Kubickova, I., Snåre, M., Eränen, K., & Murzin, D. Y. (2007). Catalytic

- deoxygenation of fatty acids and their derivatives. *Energy and Fuels*. <https://doi.org/10.1021/ef060455v>
- Mäki-Arvela, Päivi, Rozmysłowicz, B., Lestari, S., Simakova, O., Eränen, K., Salmi, T., & Murzin, D. Y. (2011). Catalytic deoxygenation of tall oil fatty acid over palladium supported on mesoporous carbon. *Energy and Fuels*. <https://doi.org/10.1021/ef200380w>
- March, J. (2009). The decarboxylation of organic acid. *Journal of Chemical Education*, 40(4), 212. <https://doi.org/10.1021/ed040p212>
- Marquevich, M., Coll, R., & Montane, D. (2000). Steam Reforming of Sunflower Oil for Hydrogen Production. . *Industrial & Engineering Chemistry Research*. <https://doi.org/10.1021/ie9910874>
- Melero, J. A., Clavero, M. M., Calleja, G., García, A., Miravalles, R., & Galindo, T. (2010). Production of biofuels via the catalytic cracking of mixtures of crude vegetable oils and nonedible animal fats with vacuum gas oil. *Energy and Fuels*. <https://doi.org/10.1021/ef900914e>
- Miao, C., Marin-Flores, O., Davidson, S. D., Li, T., Dong, T., Gao, D., ... Chen, S. (2016). Hydrothermal catalytic deoxygenation of palmitic acid over nickel catalyst. *Fuel*. <https://doi.org/10.1016/j.fuel.2015.10.120>
- Miao, C., Marin-Flores, O., Dong, T., Gao, D., Wang, Y., Garcia-Pérez, M., & Chen, S. (2018). Hydrothermal Catalytic Deoxygenation of Fatty Acid and Bio-oil with in Situ H<sub>2</sub>. *ACS Sustainable Chemistry and Engineering*. <https://doi.org/10.1021/acssuschemeng.7b02226>
- Mo, N., & Savage, P. E. (2014). Hydrothermal catalytic cracking of fatty acids with HZSM-5. *ACS Sustainable Chemistry and Engineering*. <https://doi.org/10.1021/sc400368n>
- Mohite, S., Armbruster, U., Richter, M., & Martin, A. (2014). Impact of Chain Length of Saturated Fatty Acids during Their Heterogeneously Catalyzed Deoxygenation. *Journal of Sustainable Bioenergy Systems*. <https://doi.org/10.4236/jsbs.2014.43017>
- Müller-Langer, F., Majer, S., & O’Keeffe, S. (2014). Benchmarking biofuels—a comparison of

- technical, economic and environmental indicators. *Energy, Sustainability and Society*.  
<https://doi.org/10.1186/s13705-014-0020-x>
- Na, J. G., Yi, B. E., Kim, J. N., Yi, K. B., Park, S. Y., Park, J. H., ... Ko, C. H. (2010). Hydrocarbon production from decarboxylation of fatty acid without hydrogen. *Catalysis Today*.  
<https://doi.org/10.1016/j.cattod.2009.11.008>
- National Energy Board. (2016). Canada's Energy Future 2016 Energy Supply and Demand Projections to 2040.
- Ndubuisi, R. U., Sinichi, S., (Cathy) Chin, Y. H., & Diosady, L. L. (2019). Diesel Precursors Via Catalytic Hydrothermal Deoxygenation of Aqueous Canola Oil Emulsion. *JAACS, Journal of the American Oil Chemists' Society*. <https://doi.org/10.1002/aocs.12208>
- Nikolskaya, E., & Hiltunen, Y. (2018). Determination of Carbon Chain Lengths of Fatty Acid Mixtures by Time Domain NMR. *Applied Magnetic Resonance*.  
<https://doi.org/10.1007/s00723-017-0953-2>
- Olefin by-product may be carcinogenic. (2010). *Chemical & Engineering News*.  
<https://doi.org/10.1021/cen-v054n035.p008>
- Otera, J. (1993). Transesterification. *Chemical Reviews*. <https://doi.org/10.1021/cr00020a004>
- Paul Abishek, M., Patel, J., & Prem Rajan, A. (2014). Algae Oil: A Sustainable Renewable Fuel of Future. *Biotechnology Research International*. <https://doi.org/10.1155/2014/272814>
- Peng, B., Zhao, C., Kasakov, S., Foraita, S., & Lercher, J. A. (2013). Manipulating catalytic pathways: Deoxygenation of palmitic acid on multifunctional catalysts. *Chemistry - A European Journal*. <https://doi.org/10.1002/chem.201203110>
- Peng, J., Chen, P., Lou, H., & Zheng, X. (2009). Catalytic upgrading of bio-oil by HZSM-5 in sub- and super-critical ethanol. *Bioresource Technology*.  
<https://doi.org/10.1016/j.biortech.2009.02.007>
- Pereira, R. C. C., & Pasa, V. M. D. (2006). Effect of mono-olefins and diolefins on the stability of

automotive gasoline. *Fuel*. <https://doi.org/10.1016/j.fuel.2006.01.022>

Perrotin-Brunel, H., Buijs, W., Spronsen, J. Van, Roosmalen, M. J. E. V., Peters, C. J., Verpoorte, R., & Witkamp, G. J. (2011). Decarboxylation of  $\Delta^9$ -tetrahydrocannabinol: Kinetics and molecular modeling. *Journal of Molecular Structure*, 987(1–3), 67–73. <https://doi.org/10.1016/j.molstruc.2010.11.061>

Peterson, A. A., Vogel, F., Lachance, R. P., Fröling, M., Antal, M. J., & Tester, J. W. (2008). Thermochemical biofuel production in hydrothermal media: A review of sub- and supercritical water technologies. *Energy and Environmental Science*. <https://doi.org/10.1039/b810100k>

Pinto, J. S. S., & Lanças, F. M. (2006). Hydrolysis of corn oil using subcritical water. *Journal of the Brazilian Chemical Society*. <https://doi.org/10.1590/S0103-50532006000100013>

Popov, S., & Kumar, S. (2015). Rapid hydrothermal deoxygenation of oleic acid over activated carbon in a continuous flow process. *Energy and Fuels*. <https://doi.org/10.1021/acs.energyfuels.5b00308>

R. C. Archuleta. (1991). Non catalytic steam hydrolysis of fats and oils. *Montana State University*.

Ramadhias, A. S., Jayaraj, S., & Muraleedharan, C. (2005). Biodiesel production from high FFA rubber seed oil. *Fuel*. <https://doi.org/10.1016/j.fuel.2004.09.016>

Ravenelle, R. M., Copeland, J. R., Kim, W. G., Crittenden, J. C., & Sievers, C. (2011). Structural Changes of  $\gamma$ -Al<sub>2</sub>O<sub>3</sub>-Supported Catalysts in Hot Liquid Water. *ACS Catalysis*. <https://doi.org/10.1021/cs1001515>

Remón, J., Randall, J., Budarin, V. L., & Clark, J. H. (2019). Production of bio-fuels and chemicals by microwave-assisted, catalytic, hydrothermal liquefaction (MAC-HTL) of a mixture of pine and spruce biomass. *Green Chemistry*. <https://doi.org/10.1039/c8gc03244k>

Robin, T., Jones, J. M., & Ross, A. B. (2017). Catalytic hydrothermal processing of lipids using metal doped zeolites. *Biomass and Bioenergy*. <https://doi.org/10.1016/j.biombioe.2017.01.012>

- Rostrup-Nielsen, J. R., Christensen, T. S., & Dybkjaer, I. (1998). Steam reforming of liquid hydrocarbons. *Studies in Surface Science and Catalysis*. [https://doi.org/10.1016/s0167-2991\(98\)80277-2](https://doi.org/10.1016/s0167-2991(98)80277-2)
- Rozmysłowicz, B., Mäki-Arvela, P., Tokarev, A., Leino, A. R., Eränen, K., & Murzin, D. Y. (2012). Influence of hydrogen in catalytic deoxygenation of fatty acids and their derivatives over Pd/C. *Industrial and Engineering Chemistry Research*. <https://doi.org/10.1021/ie202421x>
- Sahoo, P. K., Das, L. M., Babu, M. K. G., & Naik, S. N. (2007). Biodiesel development from high acid value polanga seed oil and performance evaluation in a CI engine. *Fuel*. <https://doi.org/10.1016/j.fuel.2006.07.025>
- Sakata, Y., Tamaura, Y., Imamura, H., & Watanabe, M. (2006). Preparation of a new type of CaSiO<sub>3</sub> with high surface area and property as a catalyst support. In *Studies in Surface Science and Catalysis*. [https://doi.org/10.1016/S0167-2991\(06\)80924-9](https://doi.org/10.1016/S0167-2991(06)80924-9)
- Santillan-Jimenez, E., & Crocker, M. (2012). Catalytic deoxygenation of fatty acids and their derivatives to hydrocarbon fuels via decarboxylation/decarbonylation. *Journal of Chemical Technology and Biotechnology*. <https://doi.org/10.1002/jctb.3775>
- Savchenko, V. I., & Makaryan, I. A. (1999). Palladium catalyst for the production of pure margarine: Catalyst and new non-filtration technology improve production and quality. *Platinum Metals Review*.
- Sawangkeaw, R., & Ngamprasertsith, S. (2013). A review of lipid-based biomasses as feedstocks for biofuels production. *Renewable and Sustainable Energy Reviews*. <https://doi.org/10.1016/j.rser.2013.04.007>
- Scanlon, D. O., Watson, G. W., Payne, D. J., Atkinson, G. R., Egdell, R. G., & Law, D. S. L. (2010). Theoretical and experimental study of the electronic structures of MoO<sub>3</sub> and MoO<sub>2</sub>. *Journal of Physical Chemistry C*. <https://doi.org/10.1021/jp9093172>
- Shay, E. G. (1993). Diesel fuel from vegetable oils: Status and opportunities. *Biomass and*

*Bioenergy*. [https://doi.org/10.1016/0961-9534\(93\)90080-N](https://doi.org/10.1016/0961-9534(93)90080-N)

- Smits, G. (1976). Measurement of the diffusion coefficient of free fatty acid in groundnut oil by the capillary-cell method. *Journal of the American Oil Chemists' Society*, 53(4), 122–124. <https://doi.org/10.1007/BF02586347>
- Snåre, M., Kubičková, I., Mäki-Arvela, P., Chichova, D., Eränen, K., & Murzin, D. Y. (2008). Catalytic deoxygenation of unsaturated renewable feedstocks for production of diesel fuel hydrocarbons. *Fuel*, 87(6), 933–945. <https://doi.org/10.1016/j.fuel.2007.06.006>
- Snåre, M., Mäki-Arvela, P., Simakova, I. L., Myllyoja, J., & Murzin, D. Y. (2009). Overview of catalytic methods for production of next generation biodiesel from natural oils and fats. *Russian Journal of Physical Chemistry B*. <https://doi.org/10.1134/S1990793109070021>
- Snåre, Mathias, Kubičková, I., Mäki-Arvela, P., Eränen, K., & Murzin, D. Y. (2006). Heterogeneous catalytic deoxygenation of stearic acid for production of biodiesel. *Industrial and Engineering Chemistry Research*. <https://doi.org/10.1021/ie060334i>
- Somerville, C., Youngs, H., Taylor, C., Davis, S. C., & Long, S. P. (2010). Feedstocks for lignocellulosic biofuels. *Science*. <https://doi.org/10.1126/science.1189268>
- Song, C., Nihonmatsu, T., & Nomura, M. (1991). Effect of Pore Structure of Ni–Mo/Al<sub>2</sub>O<sub>3</sub> Catalysts in Hydrocracking of Coal Derived and Oil Sand Derived Asphaltenes. *Industrial and Engineering Chemistry Research*. <https://doi.org/10.1021/ie00056a008>
- Spevack, P. A., & McIntyre, N. S. (1992). Thermal reduction of molybdenum trioxide. *The Journal of Physical Chemistry*. <https://doi.org/10.1021/j100201a062>
- Srifa, A., Faungnawakij, K., Itthibenchapong, V., Viriya-empikul, N., Charinpanitkul, T., & Assabumrungrat, S. (2014). Production of bio-hydrogenated diesel by catalytic hydrotreating of palm oil over NiMoS<sub>2</sub>/γ-Al<sub>2</sub>O<sub>3</sub> catalyst. *Bioresource Technology*. <https://doi.org/10.1016/j.biortech.2014.01.100>
- Steinberg, M., & Cheng, H. C. (1989). Modern and prospective technologies for hydrogen production from fossil fuels. *International Journal of Hydrogen Energy*.

[https://doi.org/10.1016/0360-3199\(89\)90018-9](https://doi.org/10.1016/0360-3199(89)90018-9)

- Swick, D., Jaques, A., Walker, J. C., & Estreicher, H. (2014). Gasoline toxicology: Overview of regulatory and product stewardship programs. *Regulatory Toxicology and Pharmacology*. <https://doi.org/10.1016/j.yrtph.2014.06.016>
- Talebian-Kiakalaieh, A., Amin, N. A. S., & Hezaveh, H. (2014). Glycerol for renewable acrolein production by catalytic dehydration. *Renewable and Sustainable Energy Reviews*. <https://doi.org/10.1016/j.rser.2014.07.168>
- Teeter, H. M., Bell, E. W., O'Donnell, J. L., Danzig, M. J., & Cowan, J. C. (1958). Reactions of conjugated fatty acids. VI. Selenium catalysis, a method for preparing diels-alder adducts from cis,trans-octadecadienoic acid. *Journal of the American Oil Chemists' Society*, 35(5), 238–240. <https://doi.org/10.1007/BF02639835>
- Teeter, H. M., O'Donnell, J. L., Schneider, W. J., Gast, L. E., & Danzig, M. J. (1957). Reactions of Conjugated Fatty Acids. IV. Diels-Alder Adducts of 9,11-Octadecadienoic Acid. *Journal of Organic Chemistry*, 22(5), 512–514. <https://doi.org/10.1021/jo01356a010>
- Thommes, M., Kaneko, K., Neimark, A. V., Olivier, J. P., Rodriguez-Reinoso, F., Rouquerol, J., & Sing, K. S. W. (2015). Physisorption of gases, with special reference to the evaluation of surface area and pore size distribution (IUPAC Technical Report). *Pure and Applied Chemistry*. <https://doi.org/10.1515/pac-2014-1117>
- Thornton, T. D., & Savage, P. E. (1990). Phenol oxidation in supercritical water. *The Journal of Supercritical Fluids*. [https://doi.org/10.1016/0896-8446\(90\)90029-L](https://doi.org/10.1016/0896-8446(90)90029-L)
- Tian, Q., Zhang, Z., Zhou, F., Chen, K., Fu, J., Lu, X., & Ouyang, P. (2017). Role of Solvent in Catalytic Conversion of Oleic Acid to Aviation Biofuels. *Energy and Fuels*. <https://doi.org/10.1021/acs.energyfuels.7b00586>
- Toba, M., Abe, Y., Kuramochi, H., Osako, M., Mochizuki, T., & Yoshimura, Y. (2011). Hydrodeoxygenation of waste vegetable oil over sulfide catalysts. *Catalysis Today*. <https://doi.org/10.1016/j.cattod.2010.11.049>

- Topsøe, H., Clausen, B. S., & Massoth, F. E. (2012). Hydrotreating Catalysis. In *Catalysis*. [https://doi.org/10.1007/978-3-642-61040-0\\_1](https://doi.org/10.1007/978-3-642-61040-0_1)
- W. Scaroni, A., Jenkins, R. G., & Walker, P. L. (1985). Coke deposition on Co-Mo/Al<sub>2</sub>O<sub>3</sub> and Co-Mo/C catalysts. *Applied Catalysis*. [https://doi.org/10.1016/S0166-9834\(00\)84353-5](https://doi.org/10.1016/S0166-9834(00)84353-5)
- Wan, J., Cao, Y. D., Ran, R., Li, M., Xiao, Y., Wu, X. D., & Weng, D. (2016). Regeneration of sintered Rh/ZrO<sub>2</sub> catalysts via Rh re-dispersion and Rh–ZrO<sub>2</sub> interaction. *Science China Technological Sciences*. <https://doi.org/10.1007/s11431-016-6052-z>
- Wan Omar, W. N. N., & Saidina Amin, N. A. (2011). Optimization of heterogeneous biodiesel production from waste cooking palm oil via response surface methodology. *Biomass and Bioenergy*. <https://doi.org/10.1016/j.biombioe.2010.12.049>
- Wang, H., Lin, H., Feng, P., Han, X., & Zheng, Y. (2017). Integration of catalytic cracking and hydrotreating technology for triglyceride deoxygenation. *Catalysis Today*. <https://doi.org/10.1016/j.cattod.2016.12.009>
- Wang, W. C., & Tao, L. (2016). Bio-jet fuel conversion technologies. *Renewable and Sustainable Energy Reviews*, 53, 801–822. <https://doi.org/10.1016/j.rser.2015.09.016>
- Watanabe, M., Iida, T., & Inomata, H. (2006). Decomposition of a long chain saturated fatty acid with some additives in hot compressed water. *Energy Conversion and Management*. <https://doi.org/10.1016/j.enconman.2006.01.009>
- Wen, G., Xu, Y., Ma, H., Xu, Z., & Tian, Z. (2008). Production of hydrogen by aqueous-phase reforming of glycerol. *International Journal of Hydrogen Energy*. <https://doi.org/10.1016/j.ijhydene.2008.07.072>
- Westacott, R. E., Johnston, K. P., & Rossky, P. J. (2001). Stability of ionic and radical molecular dissociation pathways for reaction in supercritical water. *Journal of Physical Chemistry B*. <https://doi.org/10.1021/jp010005y>
- WHO. (2016). WHO | Air pollution. *World Health Organization*.

- Wu, J., Shi, J., Fu, J., Leidl, J. A., Hou, Z., & Lu, X. (2016). Catalytic decarboxylation of fatty acids to aviation fuels over nickel supported on activated carbon. *Scientific Reports*. <https://doi.org/10.1038/srep27820>
- Yang, J., Xu, M., Zhang, X., Hu, Q., Sommerfeld, M., & Chen, Y. (2011). Life-cycle analysis on biodiesel production from microalgae: Water footprint and nutrients balance. *Bioresource Technology*. <https://doi.org/10.1016/j.biortech.2010.07.017>
- Yang, L., Ruess, G. L., & Carreon, M. A. (2015). Cu, Al and Ga based metal organic framework catalysts for the decarboxylation of oleic acid. *Catalysis Science and Technology*. <https://doi.org/10.1039/c4cy01609b>
- Yang, Liqiu, & Carreon, M. A. (2017a). Deoxygenation of Palmitic and Lauric Acids over Pt/ZIF-67 Membrane/Zeolite 5A Bead Catalysts. *ACS Applied Materials and Interfaces*. <https://doi.org/10.1021/acsami.7b11638>
- Yang, Liqiu, & Carreon, M. A. (2017b). Effect of reaction parameters on the decarboxylation of oleic acid over Pt/ZIF-67membrane/zeolite 5A bead catalysts. *Journal of Chemical Technology and Biotechnology*. <https://doi.org/10.1002/jctb.5112>
- Yang, Liqiu, Tate, K. L., Jasinski, J. B., & Carreon, M. A. (2015). Decarboxylation of Oleic Acid to Heptadecane over Pt Supported on Zeolite 5A Beads. *ACS Catalysis*. <https://doi.org/10.1021/acscatal.5b01913>
- Yeh, T. M., Hockstad, R. L., Linic, S., & Savage, P. E. (2015). Hydrothermal decarboxylation of unsaturated fatty acids over PtSn<sub>x</sub>/C catalysts. *Fuel*. <https://doi.org/10.1016/j.fuel.2015.04.039>
- Yu, J., & Savage, P. E. (2001). Catalyst activity, stability, and transformations during oxidation in supercritical water. *Applied Catalysis B: Environmental*. [https://doi.org/10.1016/S0926-3373\(00\)00273-3](https://doi.org/10.1016/S0926-3373(00)00273-3)
- Zhang, Jing, Huo, X., Li, Y., & Strathmann, T. J. (2019). Catalytic Hydrothermal Decarboxylation and Cracking of Fatty Acids and Lipids over Ru/C. *ACS Sustainable Chemistry and*

*Engineering*. <https://doi.org/10.1021/acssuschemeng.9b00215>

Zhang, Junhua, Chen, S., Yang, R., & Yan, Y. (2010). Biodiesel production from vegetable oil using heterogenous acid and alkali catalyst. *Fuel*. <https://doi.org/10.1016/j.fuel.2010.05.009>

Zhao, C., Brück, T., & Lercher, J. A. (2013). Catalytic deoxygenation of microalgae oil to green hydrocarbons. *Green Chemistry*, *15*(7), 1720–1739. <https://doi.org/10.1039/c3gc40558c>

Zhou, C.-H., Xia, X., Lin, C.-X., Tong, D.-S., & Beltramini, J. (2011). Catalytic conversion of lignocellulosic biomass to fine chemicals and fuels. *Chemical Society Reviews*. <https://doi.org/10.1039/c1cs15124j>

## Chapter 4

### 4. Catalyst-Free Hydrogenation of Fatty Acids and Corn Distiller's Oil in Subcritical Water and Subsequent Decarboxylation to form Liquid Hydrocarbons

#### 4.1. Abstract

Green diesel can be produced through decarboxylation of fatty acids feed streams. This study explores the catalyst-free hydrothermal hydrogenation of oleic acid and corn distiller's oil (CDO) via aqueous phase reforming. Temperatures of 330 °C – 360 °C and residence times of 2.5 h - 5 h were tested for their impact on hydrogenation of oleic acid. 64 % saturated CDO, as measured by NMR, was from conditions of 350 °C, 3.5 h residence times, and an oil:water ratio of 1:5. The saturated CDO was then decarboxylated with a MoO<sub>x</sub> doped gamma alumina catalyst to produce green diesel and the percent decarboxylation measured by FTIR. Decarboxylation up to 97 % was achieved with 81 % liquid yield, 7 % solids, and a 12 % gas yield.

## 4.2. Introduction

In the previous chapters of this thesis, it was found that the presence of an alkene bond within a fatty acid impacts the degree of decarboxylation and distribution of the chain lengths of the product. It was theorized that the alkene bond is more likely to crack and add hydrogen or protons, thus reducing the thermodynamic requirement for decarboxylation (Popov & Kumar, 2015). It was found that the addition of glycerol or ethanol to the decarboxylation process can lower the process conditions for the decarboxylation of stearic acid from 390 °C to 375 °C. However, the addition of glycerol and ethanol to the decarboxylation of oleic acid did not improve selectivity to heptadecane or increase reaction rates. In order to reduce coke formation on the catalyst, the amount of cracking must be minimized. Coke formation is undesirable as it leads to reductions in surface area and volume. Catalyst surface area and pore volume are important in mass transport of material to heterogeneous catalyst active sites. Based on work in the previous chapters, it was found that saturation of natural feedstocks should be performed as pre-processing in order to maximize heptadecane yields. Corn distiller's oil (CDO), algal oil, and other natural feedstocks will contain an abundance of unsaturated fatty acids (Jeon et al., 2019). Saturation/hydrogenation is performed with a nickel, platinum, or palladium catalyst and under a reducing ( $H_2$ ) environment (Cheng et al., 2012; Coenen, 1986). It is desirable to reduce the usage of  $H_2$  in green diesel production processes as  $H_2$  is a costly input to this low margin process.

There is significant literature on the production of  $H_2$  via aqueous phase reforming of natural compounds such as glycerol (Al Alwan, Salley, & Ng, 2015; Fu, Lu, et al., 2011a; Miao et al., 2018). Although it has been postulated in previous studies, there is a lack of evidence using subcritical water aqueous phase reforming of glycerol to hydrogenate unsaturated fatty acids. Using a waste material such as glycerol, this study investigated the ability to hydrogenate fatty acids without the use of a catalyst. Glycerol was chosen as a waste material because; (1) there is already literature on the reforming of glycerol in subcritical water, (2) glycerol is a waste material from the biodiesel process, and (3) it is the molecule that links fatty acid chains together within triglycerides that make up potential real-world feedstocks for green diesel production. Glycerol can be easily separated from fatty acids in the triglyceride via hydrolysis of ester bonds. Hydrolysis

can be done in subcritical water (Holliday et al., 1997; King, Holliday, & List, 1999; Pinto & Lanças, 2006).

A parametric study of the subcritical water saturation of oleic acid with the addition of glycerol was conducted with various temperatures (330 – 360 °C) and residence time (1 h – 3 h) and the product saturation content was measured by  $^1\text{H}$  NMR. CDO was saturated in a continuous PFR system to produce a feed that would be used for decarboxylation into green diesel. The decarboxylation of this feed was measured by FTIR.

### 4.3. Materials and Methods

Product Analysis: Infrared spectra ( $600\text{--}4000\text{ cm}^{-1}$  with a resolution of  $8\text{ cm}^{-1}$  over 32 scans) of feed and liquid products were collected using an ATR-FTIR spectroscope (Nicolet 6700 FTIR, Thermo Scientific).  $^1\text{H}$  nuclear magnetic resonance (NMR) spectra of reactant and product samples were recorded using a Varian Inova 400 spectrometer. Samples were dissolved in  $\text{CDCl}_3$  and the chemical shifts were referenced to  $\text{CDCl}_3$  (7.26 ppm). Corn distiller's oil was comprised of 12 % free fatty acids. When hydrolyzed, the total free fatty acids that make up the triglycerides is as follows; 12% palmitic acid, 29 % oleic acid, 56 % linoleic acid, 1 % linolenic acid, and 2% stearic acid

Testing Conditions: Three different reactor setups were used for this study. A 200 mL stainless steel batch reactor (Autoclave Engineers, Erie, PA) was used for the parametric investigation of the saturation of oleic acid. The reactor was heated with a 1.2 kW electric furnace that surrounded its main body and was manufactured by Industrial Heater Corp., (Cheshire, CT). Prior to any experiments, the reactor was washed with hexanes, THF, and water. In a given experiment, water, oleic acid, and glycerol would be added to the reactor, then purged with  $\text{N}_2$  to remove air from the system. Then desired reactions conditions of temperature and pressure would be reached via heating of the system.

Saturation of CDO was performed in a continuous reactor (The main reactor body was 24 inches long and has a 0.532" ID). The reactor was filled with 1/8" ball bearings to increase heat transfer. Decarboxylation was conducted in a reactor with the same dimensions. 38 mL of feed material was added to the heated oil pump in the reactor setup. Flowrates of water and oil were calculated to use 38 mL of oil material in 8 h with a residence time of 3.5 h. The main reactor body was 24 inches long and 0.532" ID, it was filled with 68 g of (1/8") ball bearings in the first phase of the reactor. The ball bearings were used as a pre-mixing and heating zone because the furnace used has an effective heating length of about 12". The second half of the reactor, separated from the first half by quartz wool as a filter, was filled with 60 g of  $\text{MoO}_x$  catalyst. From there, the product would exit the reactor and enter condensers/separators cooled to  $7\text{ }^\circ\text{C}$  by a chiller. If products in the condensers were solid, the condensers would be heated using a water bath to  $45\text{ }^\circ\text{C}$

and a heat gun, so as to recover the product. The product would then be contained in vials and/or centrifuge tubes awaiting analysis.

See section 2.3 for catalyst production and testing methods.

## 4.4. Results and Discussion

### 4.4.1. NMR Studies

<sup>1</sup>H NMR was used as the analytical tool to determine the ratio between alkene bonds and carbonyl bonds. The areas under the 5.3 ppm and 2.3 ppm corresponded to the number of alkenic protons and carbonyl adjacent protons, respectively. Figure 4.1 is an <sup>1</sup>H NMR spectrum of CDO and Figure 4.2 is of a saturated corn oil product. The saturated corn oil product was generated by subjecting CDO to a catalyst-free subcritical water system at 325 °C with a 2.5 h residence time with a water to oil ratio of 1:5. It can be readily seen that there is a reduction of the glycerolic protons (~4.2 ppm), and a reduction in the ratio of alkene protons to carbonyl adjacent protons (1:1.33 to 1:0.48). The removal of glycerol is through hydrolysis. The presence of acetone at 2.2 ppm is a residue from the NMR tube washing procedure. For the oleic acid parametric studies, the ratio of alkene protons to carbonyl adjacent protons was used as a measure of alkene bonds per fatty acid. To find the percent saturation of the feed material (oleic acid or corn distiller's oil), equation 4.1 is used. The ratio of alkene protons to carbonyl protons from the feed material is subtracted by the ratio found in the product subjected to the subcritical water system, and then divided by the ratio of the feed material.

*% saturation =*

$$\frac{\frac{\text{Feed material carbonyl 2.3 ppm peak area}}{\text{Feed material alkene 5.3 ppm peak area}} - \frac{\text{Product carbonyl 2.3 ppm peak area}}{\text{Product alkene 5.3 ppm peak area}}}{\frac{\text{Feed material carbonyl 2.3 ppm peak area}}{\text{Feed material alkene 5.3 ppm peak area}}} \times 100 \quad (4.1)$$

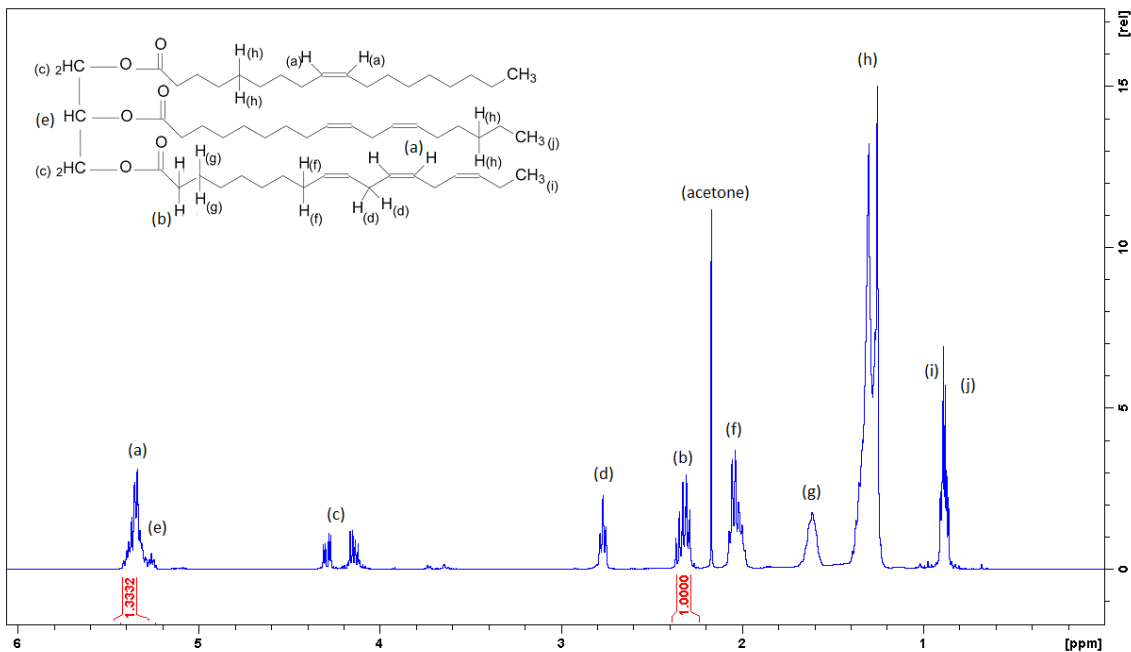


Figure 4.1 NMR spectrum of corn distiller's oil

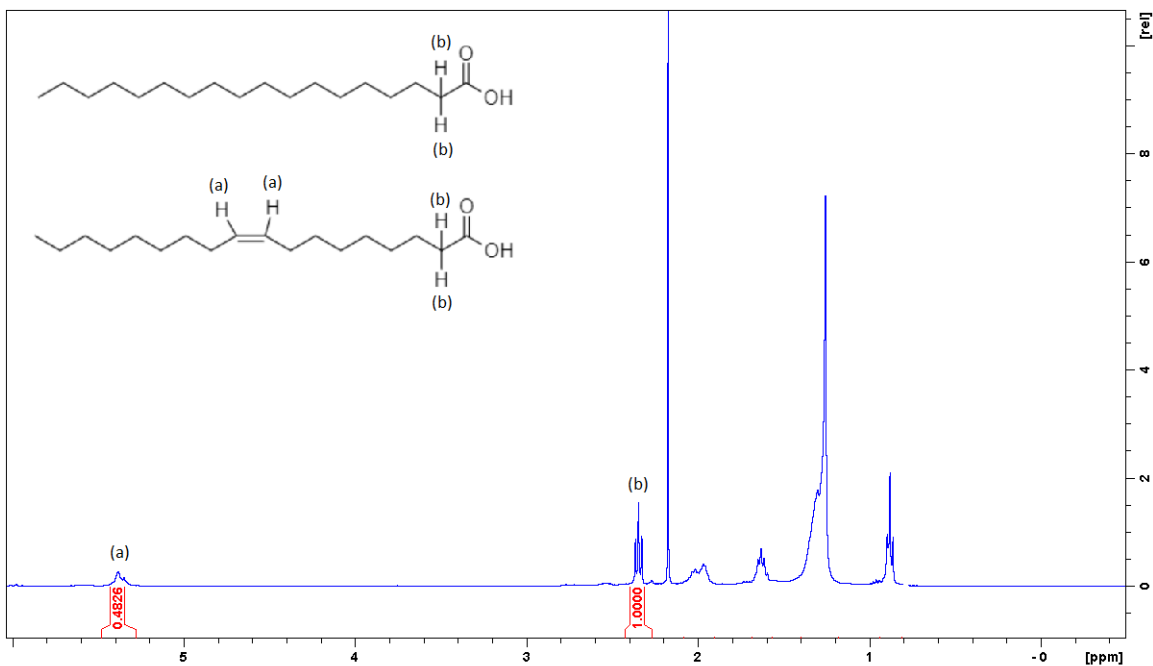


Figure 4.2 <sup>1</sup>H NMR spectrum of corn distiller's oil processed under subcritical water conditions of 325 °C with a 2.5 h residence time with a water to oil ratio of 1:5.

Table 4.1 Parametric study conditions and results of the saturation of oleic acid with subcritical water

Temperature (°C)	Pressure (psi)	Residence time	Feedstock Mass (g)	Water Volume (mL)	Glycerol mass (g)	Solids Mass (g)	Liquid Yield	Percent Saturation
330	2000	2 h	5.87	180	0.62	0	92%	18%
330	1966	3 h	4.97	190	0.51	0.0086	89%	11%
330	2000	4 h	5.1	190	0.47	0.2223	90%	21%
350	2680	2 h	5.11	180	0.55	0.4321	77%	26%
350	2350	2 h	5.07	170	0.54	0.2425	90%	25%
350	2600	2 h	4.91	185	0.46	0.0242	89%	18%
350	2600	3 h	4.94	180	0.5	0.0105	88%	13%
350	2820	4 h	4.86	170	0	0	NA	30%
350	2700	4 h	4.7	170	0.36	0	100%	25%
360	500	15 min	4.89	160	1.03	0	62%	19%
360	2800	2 h	5.03	160	0.48	0.7747	86%	15%
360	2780	3 h	5.08	160	0.53	0	91%	18%
360	2770	4 h	5.01	160	0.58	0.0036	99%	19%
375	2680	4 h	5.26	35	0.57	0.1924	90%	21%
380	3200	3 h	5.06	117	0.5	0.186	79%	23%
330	2000	4 h	5.1	190	0.47	0.2223	90%	21%

Table 4.1 is arranged by ascending temperature and ascending residence time. Saturation is not finely correlated to temperature as 350 °C has the highest degrees of saturation. Residence time does not also show a linear relationship.

It is readily apparent in Figure 4.3 that there is no strong linear kinetic relationship between temperature, residence time, pressure, or glycerol mass and hydrogenation yield. At 3 h residence times at 330 °C and 350 °C, saturation degree appears to dip and has a lower degree than both 2 h and 4 h conditions. This is not found at experiments run at 360 °C. More replicates of these runs must be performed, and further experiments should be conducted.

The largest reduction in the alkene peak in the NMR spectra is found at 350 °C, 4 h residence time, and no glycerol added. There is a possibility of a competing reaction of cracking under these conditions. However, based on literature, subcritical water cracking of fatty acids occur with a HZSM-5 catalyst at temperatures of at least 400 °C (Mo & Savage, 2014). Since only partial cracking occurs at 400 °C with the presence of HZSM-5 catalyst, it is unlikely that cracking can occur at this study's reaction conditions, which operates without the presence of a catalyst.

Further investigations should be conducted, as it is surprising that no added glycerol product has higher rates of alkene reduction than experiments performed with the addition of glycerol. GC-FID of the fatty acid products should be performed to ensure that cracking and other possible reactions are not possible explanations for the removal of alkene bonds in the product.

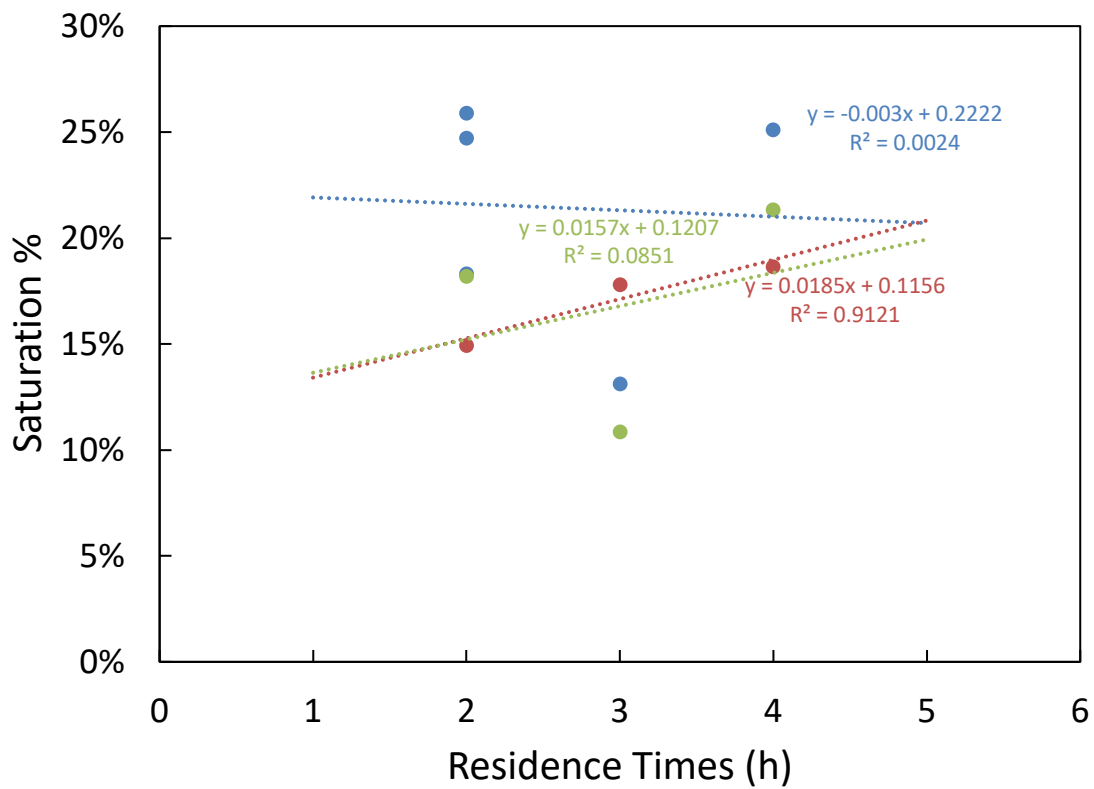


Figure 4.3 Plot of saturation yield by residence time for oleic acid processed under temperatures of 330 °C (green), 350 °C (blue), and 360 °C (red).

## 4.4.2. FTIR Decarboxylation Studies

Saturation of CDO was performed in a continuous PFR to generate feedstock for decarboxylation reactions. A temperature of 350 °C, space time of 2.5 h, and an oil:water ratio of 1:5 was used to produce large quantities of saturated CDO product (40 g per run). Based on the NMR of the product, it was ascertained that CDO had been saturated by 64 %. Best conditions for CDO decarboxylation was used based on the work in previous chapters.

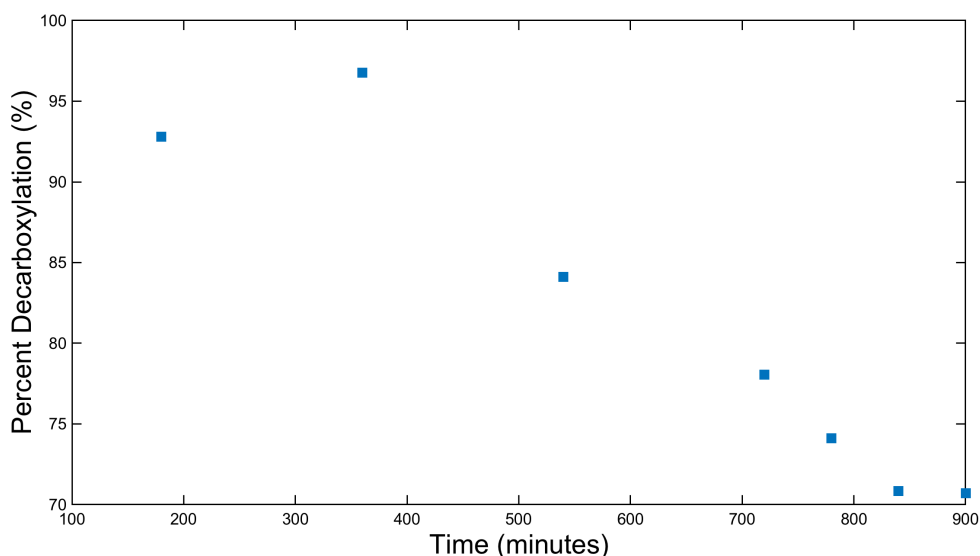


Figure 4.4 Decarboxylation of saturated CDO feed at 375 °C, 500 psi and 3.5 h space time

Decarboxylation maxed out at 97 % and the catalyst slowly deactivated over time to 71 %. 87 % was the average decarboxylation with 81% liquid yield, 6.53% solids, and a 12.36% gas yield. This decarboxylation is poorer than that found with unprocessed CDO in Chapter 2. Catalyst characterization should be performed to determine whether there are any advantages to using this saturation processed feed over CDO unprocessed. Pressures of 500 psi were also used instead of autogenous pressure, which could make comparison difficult between CDO and processed CDO feed.

The impact of reactor orientation for decarboxylation was also studied. The results of horizontal vs vertical decarboxylation reaction setups can be observed in Figure 4.5.

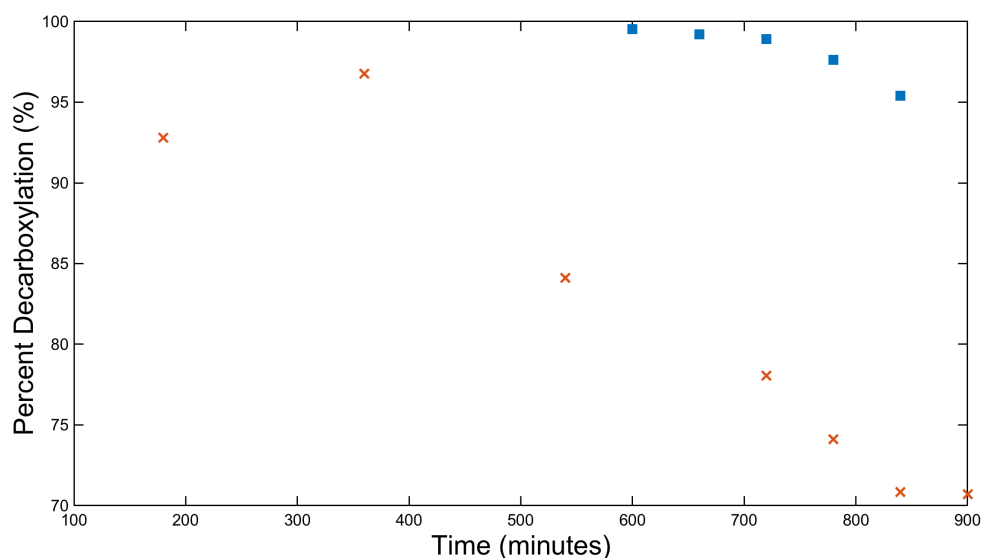


Figure 4.5 Horizontal (■) vs vertical (x) decarboxylation at 375 °C, 500 psi, and 3.5 h space times.

The horizontal reactor produced inconsistent time collection fractions. The horizontal flow product only being released from the reactor at hour 10, even though space time was aimed to be 3.5 h based on pump flow rates. It is not surprising that the horizontal orientation produced more decarboxylated product, as the true residence time was much greater. It would be expected that the catalyst surface properties would be poor in comparison to the vertical orientation. Vertical is assumed superior due to its predictability in collection times even though there is a larger degree of decarboxylation.

## 4.5. Conclusions

This work investigated the impact of added glycerol on the saturation of oleic acid in subcritical water and the subsequent decarboxylation of the saturated oleic acid product. Measurement of hydrogenation and decarboxylation were performed by  $^1\text{H}$  NMR and FTIR, respectively. It was found that higher temperatures can result in higher hydrogenation yields, but no direct linear relationship was found. The amount of glycerol added to the system also did not seem to have an impact, as the highest hydrogenation rate came from an experiment that had no glycerol added. The best percent saturation of 64% was obtained when a real-world feed of CDO was used. This saturated CDO product was then decarboxylated in a continuous fixed bed reactor with a  $\text{MoO}_x$  catalyst to produce green diesel. Decarboxylation maxed out at 97 % and slowly deactivated over time to 71 %. 86.95 % was the average decarboxylation with 81.11% liquid yield, 6.53% solids, and a 12.36% gas yield. More work is needed, as there could be other possible reactions that cause a reduction in alkene bonds that are not saturation but possibly cracking. Exploration with gas chromatography is suggested to discover longer chain polymer products and short chain cracked products.

## 4.6. References

- 11, A. D. –. (2011). Standard Test Method for Acidity in Aviation Turbine Fuel 1. *Annual Book of ASTM Standards*. <https://doi.org/10.1520/D3242-11>.This
- Abbas, J., Hussain, S., Iqbal, M. J., Nadeem, H., Qasim, M., Hina, S., & Hafeez, F. (2016). Oil industry waste: a potential feedstock for biodiesel production. *Environmental Technology (United Kingdom)*. <https://doi.org/10.1080/09593330.2016.1141997>
- Abdulkareem-Alsultan, G., Asikin-Mijan, N., Lee, H. V., Rashid, U., Islam, A., & Taufiq-Yap, Y. H. (2019). Review on thermal conversion of plant oil (Edible and inedible) into green fuel using carbon-based nanocatalyst. *Catalysts*. <https://doi.org/10.3390/catal9040350>
- Adroit Market Research. (2019). *Global Biodiesel Market Size 2019 by Feedstock (Vegetable Oil [Soybean oil, Canola oil, Other edible oils], Animal fats[Poultry, White grease, Tallow, Others]), by Application (Fuel[Automotive, Marines, Others], Power Generation, Others), by Region and Fo*. Dallas, TX.
- Afshar Taromi, A., & Kaliaguine, S. (2018). Hydrodeoxygenation of triglycerides over reduced mesostructured Ni/γ-alumina catalysts prepared via one-pot sol-gel route for green diesel production. *Applied Catalysis A: General*, 558(September), 140–149. <https://doi.org/10.1016/j.apcata.2018.03.030>
- Ahmadi, M., Macias, E. E., Jasinski, J. B., Ratnasamy, P., & Carreon, M. A. (2014). Decarboxylation and further transformation of oleic acid over bifunctional, Pt/SAPO-11 catalyst and Pt/chloride Al<sub>2</sub>O<sub>3</sub> catalysts. *Journal of Molecular Catalysis A: Chemical*. <https://doi.org/10.1016/j.molcata.2014.02.004>
- Al Alwan, B., Salley, S. O., & Ng, K. Y. S. (2015). Biofuels production from hydrothermal decarboxylation of oleic acid and soybean oil over Ni-based transition metal carbides supported on Al-SBA-15. *Applied Catalysis A: General*, 498, 32–40. <https://doi.org/10.1016/j.apcata.2015.03.012>

- Anon. (1974). FLAMMABLE AND COMBUSTIBLE LIQUIDS CODE 1973. *ANSI Stand.*
- Asomaning, J., Mussone, P., & Bressler, D. C. (2014). Thermal deoxygenation and pyrolysis of oleic acid. *Journal of Analytical and Applied Pyrolysis*. <https://doi.org/10.1016/j.jaap.2013.09.005>
- Babcock, B. A. (2012). The impact of US biofuel policies on agricultural price levels and volatility. *China Agricultural Economic Review*. <https://doi.org/10.1108/17561371211284786>
- Baltrusaitis, J., Mendoza-Sanchez, B., Fernandez, V., Veenstra, R., Dukstiene, N., Roberts, A., & Fairley, N. (2015). Generalized molybdenum oxide surface chemical state XPS determination via informed amorphous sample model. *Applied Surface Science*. <https://doi.org/10.1016/j.apsusc.2014.11.077>
- Behnejad, B., Abdouss, M., & Tavasoli, A. (2019). Comparison of performance of Ni–Mo/ $\gamma$ -alumina catalyst in HDS and HDN reactions of main distillate fractions. *Petroleum Science*. <https://doi.org/10.1007/s12182-019-0319-5>
- Bell, A. T., Gates, B. C., Ray, D., & Thompson, M. R. (2008). *Basic Research Needs: Catalysis for Energy*. <https://doi.org/10.2172/927492>
- Button, S. (2010). Biodiesel: Vehicle Fuel from Vegetable Oil. *Energy & Environment*. <https://doi.org/10.1260/0958-305x.20/21.8/1.1305>
- Castello, D., & Fiori, L. (2011). Supercritical water gasification of biomass: Thermodynamic constraints. *Bioresource Technology*. <https://doi.org/10.1016/j.biortech.2011.05.017>
- Centeno, A., Laurent, E., & Delmon, B. (1995). Influence of the support of CoMo sulfide catalysts and of the addition of potassium and platinum on the catalytic performances for the hydrodeoxygenation of carbonyl, carboxyl, and guaiacol-type molecules. *Journal of Catalysis*. <https://doi.org/10.1006/jcat.1995.1170>
- Chapman, L. (2007). Transport and climate change: a review. *Journal of Transport Geography*. <https://doi.org/10.1016/j.jtrangeo.2006.11.008>
- Charisiou, N. D., Baklavaridis, A., Papadakis, V. G., & Goula, M. A. (2016). Synthesis Gas Production

- via the Biogas Reforming Reaction Over Ni/MgO–Al<sub>2</sub>O<sub>3</sub> and Ni/CaO–Al<sub>2</sub>O<sub>3</sub> Catalysts. *Waste and Biomass Valorization*. <https://doi.org/10.1007/s12649-016-9627-9>
- Cheng, H. N., Dowd, M. K., Easson, M. W., & Condon, B. D. (2012). Hydrogenation of cottonseed oil with nickel, palladium and platinum catalysts. *JAOCS, Journal of the American Oil Chemists' Society*. <https://doi.org/10.1007/s11746-012-2036-8>
- Chou, C. C., Riviere, J. E., & Monteiro-Riviere, N. A. (2002). Differential relationship between the carbon chain length of jet fuel aliphatic hydrocarbons and their ability to induce cytotoxicity vs. interleukin-8 release in human epidermal keratinocytes. *Toxicological Sciences*. <https://doi.org/10.1093/toxsci/69.1.226>
- Choudhury, M. B. I., Ahmed, S., Shalabi, M. A., & Inui, T. (2006). Preferential methanation of CO in a syngas involving CO<sub>2</sub> at lower temperature range. *Applied Catalysis A: General*. <https://doi.org/10.1016/j.apcata.2006.08.008>
- Chowdhury, M. B. I., Hossain, M. M., & Charpentier, P. A. (2011). Effect of supercritical water gasification treatment on Ni/La<sub>2</sub>O<sub>3</sub>-Al<sub>2</sub>O<sub>3</sub>-based catalysts. *Applied Catalysis A: General*. <https://doi.org/10.1016/j.apcata.2011.07.031>
- Clayton, C. R., & Lu, Y. C. (1989). Electrochemical and XPS evidence of the aqueous formation of Mo<sub>2</sub>O<sub>5</sub>. *Surface and Interface Analysis*. <https://doi.org/10.1002/sia.740140114>
- Coenen, J. W. E. (1986). Catalytic Hydrogenation of Fatty Oils. *Industrial and Engineering Chemistry Fundamentals*. <https://doi.org/10.1021/i100021a006>
- Condon, N., Klemick, H., & Wolverton, A. (2015). Impacts of ethanol policy on corn prices: A review and meta-analysis of recent evidence. *Food Policy*. <https://doi.org/10.1016/j.foodpol.2014.12.007>
- Corma, A., & Orchillés, A. V. (2000). Current views on the mechanism of catalytic cracking. *Microporous and Mesoporous Materials*. [https://doi.org/10.1016/S1387-1811\(99\)00205-X](https://doi.org/10.1016/S1387-1811(99)00205-X)
- Cruz, I. O., Ribeiro, N. F. P., Aranda, D. A. G., & Souza, M. M. V. M. (2008). Hydrogen production

- by aqueous-phase reforming of ethanol over nickel catalysts prepared from hydrotalcite precursors. *Catalysis Communications*. <https://doi.org/10.1016/j.catcom.2008.07.031>
- Demirbas, A. (2009). Political, economic and environmental impacts of biofuels: A review. *Applied Energy*. <https://doi.org/10.1016/j.apenergy.2009.04.036>
- Demirbas, A. (2011). Biodiesel from oilgae, biofixation of carbon dioxide by microalgae: A solution to pollution problems. *Applied Energy*. <https://doi.org/10.1016/j.apenergy.2010.12.050>
- Demirbas, A., & Fatih Demirbas, M. (2011). Importance of algae oil as a source of biodiesel. *Energy Conversion and Management*. <https://doi.org/10.1016/j.enconman.2010.06.055>
- Den Otter, I. M. J. A. M. (1970). The Dimerization of Oleic Acid with a Montmorillonite Catalyst I: Important Process Parameters; Some Main Reactions. *Fette, Seifen, Anstrichmittel*. <https://doi.org/10.1002/lipi.19700720809>
- Desikan, A. N., Huang, L., & Oyama, S. T. (1992). Structure and dispersion of molybdenum oxide supported on alumina and titania. *Journal of the Chemical Society, Faraday Transactions*. <https://doi.org/10.1039/FT9928803357>
- Di Serio, M., Cozzolino, M., Giordano, M., Tesser, R., Patrono, P., & Santacesaria, E. (2007). From homogeneous to heterogeneous catalysts in biodiesel production. *Industrial and Engineering Chemistry Research*. <https://doi.org/10.1021/ie070663q>
- Ding, R., Wu, Y., Chen, Y., Liang, J., Liu, J., & Yang, M. (2015). Effective hydrodeoxygenation of palmitic acid to diesel-like hydrocarbons over MoO<sub>2</sub>/CNTs catalyst. *Chemical Engineering Science*. <https://doi.org/10.1016/j.ces.2014.10.024>
- Dinh, L. T. T., Guo, Y., & Sam Mannan, M. (2009). Sustainability evaluation of biodiesel production using multicriteria decision-making. *Environmental Progress and Sustainable Energy*. <https://doi.org/10.1002/ep.10335>
- Dos Anjos, J. R. S., De Araujo Gonzalez, W., Lam, Y. L., & Frety, R. (1983). Catalytic decomposition of vegetable oil. *Applied Catalysis*. [https://doi.org/10.1016/0166-9834\(83\)80158-4](https://doi.org/10.1016/0166-9834(83)80158-4)

- Dou, B., Wang, C., Song, Y., Chen, H., & Xu, Y. (2014). Activity of Ni-Cu-Al based catalyst for renewable hydrogen production from steam reforming of glycerol. *Energy Conversion and Management*. <https://doi.org/10.1016/j.enconman.2013.10.067>
- Douette, A. M. D., Turn, S. Q., Wang, W., & Keffer, V. I. (2007). Experimental investigation of hydrogen production from glycerin reforming. *Energy and Fuels*. <https://doi.org/10.1021/ef060379w>
- Douvartzides, S. L., Charisiou, N. D., Papageridis, K. N., & Goula, M. A. (2019). Green Diesel: Biomass Feedstocks, Production Technologies, Catalytic Research, Fuel Properties and Performance in Compression Ignition Internal Combustion Engines. *Energies*. <https://doi.org/10.3390/en12050809>
- EPA. (2012). Chapter 3. Energy. In *Inventory of U.S. Greenhouse Gas Emissions and Sinks: 1990–2012*.
- Ford, J. P., Immer, J. G., & Lamb, H. H. (2012). Palladium catalysts for fatty acid deoxygenation: Influence of the support and fatty acid chain length on decarboxylation kinetics. *Topics in Catalysis*. <https://doi.org/10.1007/s11244-012-9786-2>
- Friedman, D., Masciangioli, T., & Olson, S. (2012). Replacing critical materials with abundant materials. In *The role of the chemical sciences in finding alternatives to critical resources - A workshop summary*.
- Fu, J., Lu, X., & Savage, P. E. (2010). Catalytic hydrothermal deoxygenation of palmitic acid. *Energy and Environmental Science*. <https://doi.org/10.1039/b923198f>
- Fu, J., Lu, X., & Savage, P. E. (2011a). Hydrothermal decarboxylation and hydrogenation of fatty acids over Pt/C. *ChemSusChem*. <https://doi.org/10.1002/cssc.201000370>
- Fu, J., Lu, X., & Savage, P. E. (2011b). Hydrothermal decarboxylation and hydrogenation of fatty acids over Pt/C. *ChemSusChem*, 4(4), 481–486. <https://doi.org/10.1002/cssc.201000370>
- Fu, J., Shi, F., Thompson, L. T., Lu, X., & Savage, P. E. (2011). Activated carbons for hydrothermal

- decarboxylation of fatty acids. *ACS Catalysis*. <https://doi.org/10.1021/cs1001306>
- Global EV Outlook 2020. (2020). In *Global EV Outlook 2020*. <https://doi.org/10.1787/d394399e-en>
- Gollakota, A. R. K., Kishore, N., & Gu, S. (2018). A review on hydrothermal liquefaction of biomass. *Renewable and Sustainable Energy Reviews*. <https://doi.org/10.1016/j.rser.2017.05.178>
- Gonçalves, A. A. S., Faustino, P. B., Assaf, J. M., & Jaroniec, M. (2017). One-Pot Synthesis of Mesoporous Ni-Ti-Al Ternary Oxides: Highly Active and Selective Catalysts for Steam Reforming of Ethanol. *ACS Applied Materials and Interfaces*. <https://doi.org/10.1021/acsami.6b15507>
- Gorham, R. (2002). Air Pollution From Ground Transportation; An Assessment of Causes , Strategies and Tactics , and Proposed Actions for the International Community. In *The Global Initiative on Transport Emissions*.
- Gosselink, R. W., Hollak, S. A. W., Chang, S. W., Van Haveren, J., De Jong, K. P., Bitter, J. H., & Van Es, D. S. (2013). Reaction pathways for the deoxygenation of vegetable oils and related model compounds. *ChemSusChem*. <https://doi.org/10.1002/cssc.201300370>
- Gosselink, R. W., Stellwagen, D. R., & Bitter, J. H. (2013). Tungsten-based catalysts for selective deoxygenation. *Angewandte Chemie - International Edition*. <https://doi.org/10.1002/anie.201209809>
- Guzman, A., Torres, J. E., Prada, L. P., & Nuñez, M. L. (2010). Hydroprocessing of crude palm oil at pilot plant scale. *Catalysis Today*. <https://doi.org/10.1016/j.cattod.2009.11.015>
- Hengst, K., Arend, M., Pfützenreuter, R., & Hoelderich, W. F. (2015). Deoxygenation and cracking of free fatty acids over acidic catalysts by single step conversion for the production of diesel fuel and fuel blends. *Applied Catalysis B: Environmental*. <https://doi.org/10.1016/j.apcatb.2015.03.009>
- Hoekman, S. K. (2009). Biofuels in the U.S. - Challenges and Opportunities. *Renewable Energy*. <https://doi.org/10.1016/j.renene.2008.04.030>

- Holliday, R. L., King, J. W., & List, G. R. (1997). Hydrolysis of Vegetable Oils in Sub- And Supercritical Water. *Industrial and Engineering Chemistry Research*. <https://doi.org/10.1021/ie960668f>
- Hossain, M. Z., Chowdhury, M. B. I., Jhavar, A. K., Xu, W. Z., Biesinger, M. C., & Charpentier, P. A. (2018). Continuous Hydrothermal Decarboxylation of Fatty Acids and Their Derivatives into Liquid Hydrocarbons Using Mo/Al<sub>2</sub>O<sub>3</sub> Catalyst. *ACS Omega*. <https://doi.org/10.1021/acsomega.8b00562>
- Hossain, M. Z., Chowdhury, M. B. I., Jhavar, A. K., Xu, W. Z., & Charpentier, P. A. (2018). Continuous low pressure decarboxylation of fatty acids to fuel-range hydrocarbons with in situ hydrogen production. *Fuel*. <https://doi.org/10.1016/j.fuel.2017.09.092>
- Hossain, M. Z., Jhavar, A. K., Chowdhury, M. B. I., Xu, W. Z., Wu, W., Hiscott, D. V., & Charpentier, P. A. (2017). Using Subcritical Water for Decarboxylation of Oleic Acid into Fuel-Range Hydrocarbons. *Energy and Fuels*. <https://doi.org/10.1021/acs.energyfuels.6b03418>
- Huang, J., Jiang, Y., Marthala, V. R. R., Bressel, A., Frey, J., & Hunger, M. (2009). Effect of pore size and acidity on the coke formation during ethylbenzene conversion on zeolite catalysts. *Journal of Catalysis*. <https://doi.org/10.1016/j.jcat.2009.02.019>
- Immer, J. G., Kelly, M. J., & Lamb, H. H. (2010). Catalytic reaction pathways in liquid-phase deoxygenation of C18 free fatty acids. *Applied Catalysis A: General*. <https://doi.org/10.1016/j.apcata.2009.12.028>
- India, B. (2014). *Millettia Pinnata*.
- IPCC. (2013). Summary for policymakers. In *Climate Change 2014: Impacts, Adaptation, and Vulnerability. Part A: Global and Sectoral Aspects. Contribution of Working Group II to the Fifth Assessment Report of the Intergovernmental Panel on Climate Change*.
- IPCC. (2014). Climate Change 2014: Summary for Policymakers. *Climate Change 2014: Impacts, Adaptation and Vulnerability - Contributions of the Working Group II to the Fifth Assessment Report*. <https://doi.org/10.1016/j.renene.2009.11.012>

- Itthibenchapong, V., Srifa, A., Kaewmeesri, R., Kidkhunthod, P., & Faungnawakij, K. (2017). Deoxygenation of palm kernel oil to jet fuel-like hydrocarbons using Ni-MoS<sub>2</sub>/γ-Al<sub>2</sub>O<sub>3</sub> catalysts. *Energy Conversion and Management*. <https://doi.org/10.1016/j.enconman.2016.12.034>
- IUPAC. (2014). Compendium of Chemical Terminology 2nd ed. (the “Gold Book”). *Blackwell Scientific Publications, Oxford*. <https://doi.org/10.1351/goldbook.I03352>
- Janampelli, S., & Darbha, S. (2018). Metal Oxide-Promoted Hydrodeoxygenation Activity of Platinum in Pt-MO<sub>x</sub>/Al<sub>2</sub>O<sub>3</sub> Catalysts for Green Diesel Production. *Energy and Fuels*. <https://doi.org/10.1021/acs.energyfuels.8b03588>
- Janampelli, S., & Darbha, S. (2019). Highly efficient Pt-MoO<sub>x</sub>/ZrO<sub>2</sub> catalyst for green diesel production. *Catalysis Communications*. <https://doi.org/10.1016/j.catcom.2019.03.027>
- Jęczmionek, Ł., & Porzycka-Semczuk, K. (2014). Hydrodeoxygenation, decarboxylation and decarbonylation reactions while co-processing vegetable oils over a NiMo hydrotreatment catalyst. Part I: Thermal effects - Theoretical considerations. *Fuel*. <https://doi.org/10.1016/j.fuel.2014.04.055>
- Jeon, J. Y., Han, Y., Kim, Y. W., Lee, Y. W., Hong, S., & Hwang, I. T. (2019). Feasibility of unsaturated fatty acid feedstocks as green alternatives in bio-oil refinery. *Biofuels, Bioproducts and Biorefining*. <https://doi.org/10.1002/bbb.1979>
- Jessop, P. G. (2011). Searching for green solvents. *Green Chemistry*. <https://doi.org/10.1039/c0gc00797h>
- Jiménez-López, A., Jiménez-Morales, I., Santamaría-González, J., & Maireles-Torres, P. (2011). Biodiesel production from sunflower oil by tungsten oxide supported on zirconium doped MCM-41 silica. *Journal of Molecular Catalysis A: Chemical*. <https://doi.org/10.1016/j.molcata.2010.11.035>
- Jutz, F., Andanson, J. M., & Baiker, A. (2011). Ionic liquids and dense carbon dioxide: A beneficial biphasic system for catalysis. *Chemical Reviews*. <https://doi.org/10.1021/cr100194q>

- Katryniok, B., Paul, S., & Dumeignil, F. (2013). Recent developments in the field of catalytic dehydration of glycerol to acrolein. *ACS Catalysis*, 3(8), 1819–1834. <https://doi.org/10.1021/cs400354p>
- Kern, C., & Jess, A. (2005). Regeneration of coked catalysts - Modelling and verification of coke burn-off in single particles and fixed bed reactors. *Chemical Engineering Science*. <https://doi.org/10.1016/j.ces.2005.01.024>
- Kim, M. C., & Kim, K. L. (1996). A role of molybdenum and shape selectivity of catalysts in simultaneous reactions of hydrocracking and hydrodesulfurization. *Korean Journal of Chemical Engineering*. <https://doi.org/10.1007/BF02705881>
- Kim, M. Y., Kim, J. K., Lee, M. E., Lee, S., & Choi, M. (2017). Maximizing Biojet Fuel Production from Triglyceride: Importance of the Hydrocracking Catalyst and Separate Deoxygenation/Hydrocracking Steps. *ACS Catalysis*. <https://doi.org/10.1021/acscatal.7b01326>
- King, J. W., Holliday, R. L., & List, G. R. (1999). Hydrolysis of soybean oil: In a subcritical water flow reactor. *Green Chemistry*. <https://doi.org/10.1039/a908861j>
- Kirszensztejn, P., Przekop, R., Tolińska, A., & MaćKowska, E. (2009). Pyrolytic and catalytic conversion of rape oil into aromatic and aliphatic fractions in a fixed bed reactor on Al<sub>2</sub>O<sub>3</sub> and Al<sub>2</sub>O<sub>3</sub>/B<sub>2</sub>O<sub>3</sub> catalysts. *Chemical Papers*. <https://doi.org/10.2478/s11696-008-0104-1>
- Knothe, G. (2007). Some aspects of biodiesel oxidative stability. *Fuel Processing Technology*. <https://doi.org/10.1016/j.fuproc.2007.01.005>
- Kordouli, E., Sygellou, L., Kordulis, C., Bourikas, K., & Lycourghiotis, A. (2017). Probing the synergistic ratio of the NiMo/Γ-Al<sub>2</sub>O<sub>3</sub> reduced catalysts for the transformation of natural triglycerides into green diesel. *Applied Catalysis B: Environmental*, 209, 12–22. <https://doi.org/10.1016/j.apcatb.2017.02.045>
- Kubička, D., & Horáček, J. (2011). Deactivation of HDS catalysts in deoxygenation of vegetable oils. *Applied Catalysis A: General*. <https://doi.org/10.1016/j.apcata.2010.10.034>

- Kubička, D., & Kaluža, L. (2010). Deoxygenation of vegetable oils over sulfided Ni, Mo and NiMo catalysts. *Applied Catalysis A: General*. <https://doi.org/10.1016/j.apcata.2009.10.034>
- Lestari, S., Päivi, M. A., Bernas, H., Simakova, O., Sjöholm, R., Beltramini, J., ... Murzin, D. Y. (2009). Catalytic deoxygenation of stearic acid in a continuous reactor over a mesoporous carbon-supported Pd catalyst. *Energy and Fuels*. <https://doi.org/10.1021/ef900110t>
- Lin, R., Zhu, Y., & Tavlarides, L. L. (2014). Effect of thermal decomposition on biodiesel viscosity and cold flow property. *Fuel*. <https://doi.org/10.1016/j.fuel.2013.10.034>
- Loe, R., Santillan-Jimenez, E., Morgan, T., Sewell, L., Ji, Y., Jones, S., ... Crocker, M. (2016). Effect of Cu and Sn promotion on the catalytic deoxygenation of model and algal lipids to fuel-like hydrocarbons over supported Ni catalysts. *Applied Catalysis B: Environmental*. <https://doi.org/10.1016/j.apcatb.2016.03.025>
- Luo, N., Fu, X., Cao, F., Xiao, T., & Edwards, P. P. (2008). Glycerol aqueous phase reforming for hydrogen generation over Pt catalyst - Effect of catalyst composition and reaction conditions. *Fuel*. <https://doi.org/10.1016/j.fuel.2008.06.021>
- Ma, X., Cui, K., Hao, W., Ma, R., Tian, Y., & Li, Y. (2015). Alumina supported molybdenum catalyst for lignin valorization: Effect of reduction temperature. *Bioresource Technology*. <https://doi.org/10.1016/j.biortech.2015.05.032>
- Madsen, A. T., Ahmed, E. H., Christensen, C. H., Fehrmann, R., & Riisager, A. (2011). Hydrodeoxygenation of waste fat for diesel production: Study on model feed with Pt/alumina catalyst. *Fuel*. <https://doi.org/10.1016/j.fuel.2011.06.005>
- Mäki-Arvela, P., Snåre, M., Eränen, K., Myllyoja, J., & Murzin, D. Y. (2008). Continuous decarboxylation of lauric acid over Pd/C catalyst. *Fuel*. <https://doi.org/10.1016/j.fuel.2008.07.004>
- Mäki-Arvela, Päivi, Kubickova, I., Snåre, M., Eränen, K., & Murzin, D. Y. (2007). Catalytic deoxygenation of fatty acids and their derivatives. *Energy and Fuels*. <https://doi.org/10.1021/ef060455v>

- Mäki-Arvela, Päivi, Rozmysłowicz, B., Lestari, S., Simakova, O., Eränen, K., Salmi, T., & Murzin, D. Y. (2011). Catalytic deoxygenation of tall oil fatty acid over palladium supported on mesoporous carbon. *Energy and Fuels*. <https://doi.org/10.1021/ef200380w>
- March, J. (2009). The decarboxylation of organic acid. *Journal of Chemical Education*, 40(4), 212. <https://doi.org/10.1021/ed040p212>
- Marquevich, M., Coll, R., & Montane, D. (2000). Steam Reforming of Sunflower Oil for Hydrogen Production. *Industrial & Engineering Chemistry Research*. <https://doi.org/10.1021/ie9910874>
- Melero, J. A., Clavero, M. M., Calleja, G., García, A., Miravalles, R., & Galindo, T. (2010). Production of biofuels via the catalytic cracking of mixtures of crude vegetable oils and nonedible animal fats with vacuum gas oil. *Energy and Fuels*. <https://doi.org/10.1021/ef900914e>
- Miao, C., Marin-Flores, O., Davidson, S. D., Li, T., Dong, T., Gao, D., ... Chen, S. (2016). Hydrothermal catalytic deoxygenation of palmitic acid over nickel catalyst. *Fuel*. <https://doi.org/10.1016/j.fuel.2015.10.120>
- Miao, C., Marin-Flores, O., Dong, T., Gao, D., Wang, Y., Garcia-Pérez, M., & Chen, S. (2018). Hydrothermal Catalytic Deoxygenation of Fatty Acid and Bio-oil with in Situ H<sub>2</sub>. *ACS Sustainable Chemistry and Engineering*. <https://doi.org/10.1021/acssuschemeng.7b02226>
- Mo, N., & Savage, P. E. (2014). Hydrothermal catalytic cracking of fatty acids with HZSM-5. *ACS Sustainable Chemistry and Engineering*. <https://doi.org/10.1021/sc400368n>
- Mohite, S., Armbruster, U., Richter, M., & Martin, A. (2014). Impact of Chain Length of Saturated Fatty Acids during Their Heterogeneously Catalyzed Deoxygenation. *Journal of Sustainable Bioenergy Systems*. <https://doi.org/10.4236/jsbs.2014.43017>
- Müller-Langer, F., Majer, S., & O’Keeffe, S. (2014). Benchmarking biofuels—a comparison of technical, economic and environmental indicators. *Energy, Sustainability and Society*. <https://doi.org/10.1186/s13705-014-0020-x>
- Na, J. G., Yi, B. E., Kim, J. N., Yi, K. B., Park, S. Y., Park, J. H., ... Ko, C. H. (2010). Hydrocarbon

production from decarboxylation of fatty acid without hydrogen. *Catalysis Today*.  
<https://doi.org/10.1016/j.cattod.2009.11.008>

National Energy Board. (2016). Canada's Energy Future 2016 Energy Supply and Demand Projections to 2040.

Ndubuisi, R. U., Sinichi, S., (Cathy) Chin, Y. H., & Diosady, L. L. (2019). Diesel Precursors Via Catalytic Hydrothermal Deoxygenation of Aqueous Canola Oil Emulsion. *JAACS, Journal of the American Oil Chemists' Society*. <https://doi.org/10.1002/aocs.12208>

Nikolskaya, E., & Hiltunen, Y. (2018). Determination of Carbon Chain Lengths of Fatty Acid Mixtures by Time Domain NMR. *Applied Magnetic Resonance*. <https://doi.org/10.1007/s00723-017-0953-2>

Olefin by-product may be carcinogenic. (2010). *Chemical & Engineering News*.  
<https://doi.org/10.1021/cen-v054n035.p008>

Otera, J. (1993). Transesterification. *Chemical Reviews*. <https://doi.org/10.1021/cr00020a004>

Paul Abishek, M., Patel, J., & Prem Rajan, A. (2014). Algae Oil: A Sustainable Renewable Fuel of Future. *Biotechnology Research International*. <https://doi.org/10.1155/2014/272814>

Peng, B., Zhao, C., Kasakov, S., Foraita, S., & Lercher, J. A. (2013). Manipulating catalytic pathways: Deoxygenation of palmitic acid on multifunctional catalysts. *Chemistry - A European Journal*.  
<https://doi.org/10.1002/chem.201203110>

Peng, J., Chen, P., Lou, H., & Zheng, X. (2009). Catalytic upgrading of bio-oil by HZSM-5 in sub- and super-critical ethanol. *Bioresource Technology*.  
<https://doi.org/10.1016/j.biortech.2009.02.007>

Pereira, R. C. C., & Pasa, V. M. D. (2006). Effect of mono-olefins and diolefins on the stability of automotive gasoline. *Fuel*. <https://doi.org/10.1016/j.fuel.2006.01.022>

Perrotin-Brunel, H., Buijs, W., Spronsen, J. Van, Roosmalen, M. J. E. V., Peters, C. J., Verpoorte, R., & Witkamp, G. J. (2011). Decarboxylation of  $\Delta^9$ -tetrahydrocannabinol: Kinetics and molecular  
204

modeling. *Journal of Molecular Structure*, 987(1–3), 67–73.  
<https://doi.org/10.1016/j.molstruc.2010.11.061>

Peterson, A. A., Vogel, F., Lachance, R. P., Fröling, M., Antal, M. J., & Tester, J. W. (2008). Thermochemical biofuel production in hydrothermal media: A review of sub- and supercritical water technologies. *Energy and Environmental Science*. <https://doi.org/10.1039/b810100k>

Pinto, J. S. S., & Lanças, F. M. (2006). Hydrolysis of corn oil using subcritical water. *Journal of the Brazilian Chemical Society*. <https://doi.org/10.1590/S0103-50532006000100013>

Popov, S., & Kumar, S. (2015). Rapid hydrothermal deoxygenation of oleic acid over activated carbon in a continuous flow process. *Energy and Fuels*. <https://doi.org/10.1021/acs.energyfuels.5b00308>

R. C. Archuleta. (1991). Non catalytic steam hydrolysis of fats and oils. *Montana State University*.

Ramadhas, A. S., Jayaraj, S., & Muraleedharan, C. (2005). Biodiesel production from high FFA rubber seed oil. *Fuel*. <https://doi.org/10.1016/j.fuel.2004.09.016>

Ravenelle, R. M., Copeland, J. R., Kim, W. G., Crittenden, J. C., & Sievers, C. (2011). Structural Changes of  $\gamma$ -Al<sub>2</sub>O<sub>3</sub>-Supported Catalysts in Hot Liquid Water. *ACS Catalysis*. <https://doi.org/10.1021/cs1001515>

Remón, J., Randall, J., Budarin, V. L., & Clark, J. H. (2019). Production of bio-fuels and chemicals by microwave-assisted, catalytic, hydrothermal liquefaction (MAC-HTL) of a mixture of pine and spruce biomass. *Green Chemistry*. <https://doi.org/10.1039/c8gc03244k>

Robin, T., Jones, J. M., & Ross, A. B. (2017). Catalytic hydrothermal processing of lipids using metal doped zeolites. *Biomass and Bioenergy*. <https://doi.org/10.1016/j.biombioe.2017.01.012>

Rostrup-Nielsen, J. R., Christensen, T. S., & Dybkjaer, I. (1998). Steam reforming of liquid hydrocarbons. *Studies in Surface Science and Catalysis*. [https://doi.org/10.1016/s0167-2991\(98\)80277-2](https://doi.org/10.1016/s0167-2991(98)80277-2)

Rozmysłowicz, B., Mäki-Arvela, P., Tokarev, A., Leino, A. R., Eränen, K., & Murzin, D. Y. (2012). Influence of hydrogen in catalytic deoxygenation of fatty acids and their derivatives over Pd/C.

*Industrial and Engineering Chemistry Research*. <https://doi.org/10.1021/ie202421x>

- Sahoo, P. K., Das, L. M., Babu, M. K. G., & Naik, S. N. (2007). Biodiesel development from high acid value polanga seed oil and performance evaluation in a CI engine. *Fuel*. <https://doi.org/10.1016/j.fuel.2006.07.025>
- Sakata, Y., Tamaura, Y., Imamura, H., & Watanabe, M. (2006). Preparation of a new type of CaSiO<sub>3</sub> with high surface area and property as a catalyst support. In *Studies in Surface Science and Catalysis*. [https://doi.org/10.1016/S0167-2991\(06\)80924-9](https://doi.org/10.1016/S0167-2991(06)80924-9)
- Santillan-Jimenez, E., & Crocker, M. (2012). Catalytic deoxygenation of fatty acids and their derivatives to hydrocarbon fuels via decarboxylation/decarbonylation. *Journal of Chemical Technology and Biotechnology*. <https://doi.org/10.1002/jctb.3775>
- Savchenko, V. I., & Makaryan, I. A. (1999). Palladium catalyst for the production of pure margarine: Catalyst and new non-filtration technology improve production and quality. *Platinum Metals Review*.
- Sawangkeaw, R., & Ngamprasertsith, S. (2013). A review of lipid-based biomasses as feedstocks for biofuels production. *Renewable and Sustainable Energy Reviews*. <https://doi.org/10.1016/j.rser.2013.04.007>
- Scanlon, D. O., Watson, G. W., Payne, D. J., Atkinson, G. R., Egdell, R. G., & Law, D. S. L. (2010). Theoretical and experimental study of the electronic structures of MoO<sub>3</sub> and MoO<sub>2</sub>. *Journal of Physical Chemistry C*. <https://doi.org/10.1021/jp9093172>
- Shay, E. G. (1993). Diesel fuel from vegetable oils: Status and opportunities. *Biomass and Bioenergy*. [https://doi.org/10.1016/0961-9534\(93\)90080-N](https://doi.org/10.1016/0961-9534(93)90080-N)
- Smits, G. (1976). Measurement of the diffusion coefficient of free fatty acid in groundnut oil by the capillary-cell method. *Journal of the American Oil Chemists' Society*, 53(4), 122–124. <https://doi.org/10.1007/BF02586347>
- Snåre, M., Kubičková, I., Mäki-Arvela, P., Chichova, D., Eränen, K., & Murzin, D. Y. (2008).

- Catalytic deoxygenation of unsaturated renewable feedstocks for production of diesel fuel hydrocarbons. *Fuel*, 87(6), 933–945. <https://doi.org/10.1016/j.fuel.2007.06.006>
- Snåre, M., Mäki-Arvela, P., Simakova, I. L., Myllyoja, J., & Murzin, D. Y. (2009). Overview of catalytic methods for production of next generation biodiesel from natural oils and fats. *Russian Journal of Physical Chemistry B*. <https://doi.org/10.1134/S1990793109070021>
- Snåre, Mathias, Kubičková, I., Mäki-Arvela, P., Eränen, K., & Murzin, D. Y. (2006). Heterogeneous catalytic deoxygenation of stearic acid for production of biodiesel. *Industrial and Engineering Chemistry Research*. <https://doi.org/10.1021/ie060334i>
- Somerville, C., Youngs, H., Taylor, C., Davis, S. C., & Long, S. P. (2010). Feedstocks for lignocellulosic biofuels. *Science*. <https://doi.org/10.1126/science.1189268>
- Song, C., Nihonmatsu, T., & Nomura, M. (1991). Effect of Pore Structure of Ni–Mo/Al<sub>2</sub>O<sub>3</sub> Catalysts in Hydrocracking of Coal Derived and Oil Sand Derived Asphaltenes. *Industrial and Engineering Chemistry Research*. <https://doi.org/10.1021/ie00056a008>
- Spevack, P. A., & McIntyre, N. S. (1992). Thermal reduction of molybdenum trioxide. *The Journal of Physical Chemistry*. <https://doi.org/10.1021/j100201a062>
- Srifa, A., Faungnawakij, K., Itthibenchapong, V., Viriya-empikul, N., Charinpanitkul, T., & Assabumrungrat, S. (2014). Production of bio-hydrogenated diesel by catalytic hydrotreating of palm oil over NiMoS<sub>2</sub>/γ-Al<sub>2</sub>O<sub>3</sub> catalyst. *Bioresource Technology*. <https://doi.org/10.1016/j.biortech.2014.01.100>
- Steinberg, M., & Cheng, H. C. (1989). Modern and prospective technologies for hydrogen production from fossil fuels. *International Journal of Hydrogen Energy*. [https://doi.org/10.1016/0360-3199\(89\)90018-9](https://doi.org/10.1016/0360-3199(89)90018-9)
- Swick, D., Jaques, A., Walker, J. C., & Estreicher, H. (2014). Gasoline toxicology: Overview of regulatory and product stewardship programs. *Regulatory Toxicology and Pharmacology*. <https://doi.org/10.1016/j.yrtph.2014.06.016>

- Talebian-Kiakalaieh, A., Amin, N. A. S., & Hezaveh, H. (2014). Glycerol for renewable acrolein production by catalytic dehydration. *Renewable and Sustainable Energy Reviews*. <https://doi.org/10.1016/j.rser.2014.07.168>
- Teeter, H. M., Bell, E. W., O'Donnell, J. L., Danzig, M. J., & Cowan, J. C. (1958). Reactions of conjugated fatty acids. VI. Selenium catalysis, a method for preparing diels-alder adducts from cis,trans-octadecadienoic acid. *Journal of the American Oil Chemists' Society*, 35(5), 238–240. <https://doi.org/10.1007/BF02639835>
- Teeter, H. M., O'Donnell, J. L., Schneider, W. J., Gast, L. E., & Danzig, M. J. (1957). Reactions of Conjugated Fatty Acids. IV. Diels-Alder Adducts of 9,11-Octadecadienoic Acid. *Journal of Organic Chemistry*, 22(5), 512–514. <https://doi.org/10.1021/jo01356a010>
- Thommes, M., Kaneko, K., Neimark, A. V., Olivier, J. P., Rodriguez-Reinoso, F., Rouquerol, J., & Sing, K. S. W. (2015). Physisorption of gases, with special reference to the evaluation of surface area and pore size distribution (IUPAC Technical Report). *Pure and Applied Chemistry*. <https://doi.org/10.1515/pac-2014-1117>
- Thornton, T. D., & Savage, P. E. (1990). Phenol oxidation in supercritical water. *The Journal of Supercritical Fluids*. [https://doi.org/10.1016/0896-8446\(90\)90029-L](https://doi.org/10.1016/0896-8446(90)90029-L)
- Tian, Q., Zhang, Z., Zhou, F., Chen, K., Fu, J., Lu, X., & Ouyang, P. (2017). Role of Solvent in Catalytic Conversion of Oleic Acid to Aviation Biofuels. *Energy and Fuels*. <https://doi.org/10.1021/acs.energyfuels.7b00586>
- Toba, M., Abe, Y., Kuramochi, H., Osako, M., Mochizuki, T., & Yoshimura, Y. (2011). Hydrodeoxygenation of waste vegetable oil over sulfide catalysts. *Catalysis Today*. <https://doi.org/10.1016/j.cattod.2010.11.049>
- Topsøe, H., Clausen, B. S., & Massoth, F. E. (2012). Hydrotreating Catalysis. In *Catalysis*. [https://doi.org/10.1007/978-3-642-61040-0\\_1](https://doi.org/10.1007/978-3-642-61040-0_1)
- W. Scaroni, A., Jenkins, R. G., & Walker, P. L. (1985). Coke deposition on Co-Mo/Al<sub>2</sub>O<sub>3</sub> and Co-Mo/C catalysts. *Applied Catalysis*. [https://doi.org/10.1016/S0166-9834\(00\)84353-5](https://doi.org/10.1016/S0166-9834(00)84353-5)

- Wan, J., Cao, Y. D., Ran, R., Li, M., Xiao, Y., Wu, X. D., & Weng, D. (2016). Regeneration of sintered Rh/ZrO<sub>2</sub> catalysts via Rh re-dispersion and Rh–ZrO<sub>2</sub> interaction. *Science China Technological Sciences*. <https://doi.org/10.1007/s11431-016-6052-z>
- Wan Omar, W. N. N., & Saidina Amin, N. A. (2011). Optimization of heterogeneous biodiesel production from waste cooking palm oil via response surface methodology. *Biomass and Bioenergy*. <https://doi.org/10.1016/j.biombioe.2010.12.049>
- Wang, H., Lin, H., Feng, P., Han, X., & Zheng, Y. (2017). Integration of catalytic cracking and hydrotreating technology for triglyceride deoxygenation. *Catalysis Today*. <https://doi.org/10.1016/j.cattod.2016.12.009>
- Wang, W. C., & Tao, L. (2016). Bio-jet fuel conversion technologies. *Renewable and Sustainable Energy Reviews*, 53, 801–822. <https://doi.org/10.1016/j.rser.2015.09.016>
- Watanabe, M., Iida, T., & Inomata, H. (2006). Decomposition of a long chain saturated fatty acid with some additives in hot compressed water. *Energy Conversion and Management*. <https://doi.org/10.1016/j.enconman.2006.01.009>
- Wen, G., Xu, Y., Ma, H., Xu, Z., & Tian, Z. (2008). Production of hydrogen by aqueous-phase reforming of glycerol. *International Journal of Hydrogen Energy*. <https://doi.org/10.1016/j.ijhydene.2008.07.072>
- Westacott, R. E., Johnston, K. P., & Rossky, P. J. (2001). Stability of ionic and radical molecular dissociation pathways for reaction in supercritical water. *Journal of Physical Chemistry B*. <https://doi.org/10.1021/jp010005y>
- WHO. (2016). WHO | Air pollution. *World Health Organization*.
- Wu, J., Shi, J., Fu, J., Leidl, J. A., Hou, Z., & Lu, X. (2016). Catalytic decarboxylation of fatty acids to aviation fuels over nickel supported on activated carbon. *Scientific Reports*. <https://doi.org/10.1038/srep27820>
- Yang, J., Xu, M., Zhang, X., Hu, Q., Sommerfeld, M., & Chen, Y. (2011). Life-cycle analysis on

- biodiesel production from microalgae: Water footprint and nutrients balance. *Bioresource Technology*. <https://doi.org/10.1016/j.biortech.2010.07.017>
- Yang, L., Ruess, G. L., & Carreon, M. A. (2015). Cu, Al and Ga based metal organic framework catalysts for the decarboxylation of oleic acid. *Catalysis Science and Technology*. <https://doi.org/10.1039/c4cy01609b>
- Yang, Liqiu, & Carreon, M. A. (2017a). Deoxygenation of Palmitic and Lauric Acids over Pt/ZIF-67 Membrane/Zeolite 5A Bead Catalysts. *ACS Applied Materials and Interfaces*. <https://doi.org/10.1021/acsami.7b11638>
- Yang, Liqiu, & Carreon, M. A. (2017b). Effect of reaction parameters on the decarboxylation of oleic acid over Pt/ZIF-67membrane/zeolite 5A bead catalysts. *Journal of Chemical Technology and Biotechnology*. <https://doi.org/10.1002/jctb.5112>
- Yang, Liqiu, Tate, K. L., Jasinski, J. B., & Carreon, M. A. (2015). Decarboxylation of Oleic Acid to Heptadecane over Pt Supported on Zeolite 5A Beads. *ACS Catalysis*. <https://doi.org/10.1021/acscatal.5b01913>
- Yeh, T. M., Hockstad, R. L., Linic, S., & Savage, P. E. (2015). Hydrothermal decarboxylation of unsaturated fatty acids over PtSn<sub>x</sub>/C catalysts. *Fuel*. <https://doi.org/10.1016/j.fuel.2015.04.039>
- Yu, J., & Savage, P. E. (2001). Catalyst activity, stability, and transformations during oxidation in supercritical water. *Applied Catalysis B: Environmental*. [https://doi.org/10.1016/S0926-3373\(00\)00273-3](https://doi.org/10.1016/S0926-3373(00)00273-3)
- Zhang, Jing, Huo, X., Li, Y., & Strathmann, T. J. (2019). Catalytic Hydrothermal Decarboxylation and Cracking of Fatty Acids and Lipids over Ru/C. *ACS Sustainable Chemistry and Engineering*. <https://doi.org/10.1021/acssuschemeng.9b00215>
- Zhang, Junhua, Chen, S., Yang, R., & Yan, Y. (2010). Biodiesel production from vegetable oil using heterogenous acid and alkali catalyst. *Fuel*. <https://doi.org/10.1016/j.fuel.2010.05.009>

Zhao, C., Brück, T., & Lercher, J. A. (2013). Catalytic deoxygenation of microalgae oil to green hydrocarbons. *Green Chemistry*, *15*(7), 1720–1739. <https://doi.org/10.1039/c3gc40558c>

Zhou, C.-H., Xia, X., Lin, C.-X., Tong, D.-S., & Beltramini, J. (2011). Catalytic conversion of lignocellulosic biomass to fine chemicals and fuels. *Chemical Society Reviews*. <https://doi.org/10.1039/c1cs15124j>

## 5. Conclusions and Recommendations

### 5.1. General Conclusions

Almost 100% removal of oxygen with 68% selectivity to heptadecane was achieved during the continuous thermocatalytic decarboxylation of stearic acid in the presence of  $\text{MoO}_x/\text{Al}_2\text{O}_3$  as a catalyst. It was found that oleic acid decarboxylates at lower temperatures than stearic acid, and the addition of 10 % oleic acid to stearic acid in the feed decreased the necessary reaction temperature from 390 °C to 375 °C. Since many of the physical properties of stearic and oleic acid are similar, it is thought that the cracking of oleic acid may release hydrogen into the system and this hydrogen helps to decarboxylate stearic acid. The addition of glycerol or ethanol to stearic acid also had a similar effect as oleic acid, as the necessary reaction temperature was dropped from 390 °C to 375 °C.

Despite being a real-world feed, corn distiller's oil (12% palmitic acid, 29 % oleic acid, 56 % linoleic acid, 1 % linolenic acid, and 2% stearic acid) was ca. 99 % decarboxylated at 375 °C and 3.5 h residence time. The decarboxylated liquid product of corn distiller's oil obtained from the continuous reactor system has a similar cetane index value, viscosity, oxygen content, and nitrogen content to diesel. However, the flash point is much lower than diesel and this is confirmed by the GC-FID chromatogram. Distillation on the product may be performed to obtain a range of products.

In-situ regenerated  $\text{MoO}_x/\text{Al}_2\text{O}_3$  catalyst shows similar activities to that of fresh catalyst. XPS indicates no oxidation state changes of molybdenum between fresh and regenerated catalyst.  $\text{NH}_3$  TPD indicates a marked decrease in acid sites, and this reduction in acid sites should reduce activity since acid sites are considered the active sites of the catalyst. The turnover number is also less than one, so more must be explored as to the mechanism of decarboxylation and the active sites of the  $\text{MoO}_x$  catalyst.

## 5.2. Recommendations and Future Work

The following recommendations can be made based on this thesis.

While it has been demonstrated in this thesis that model compounds and real-world feedstocks can be decarboxylated in a continuous system to produce diesel-like products, the conditions are energy intensive and reducing thermal energy inputs is important for commercial viability. While no hydrogen input was needed for this process and thus decreases the cost of the process, current residence times of 3 hours or more are unrealistic. Solutions may be found with the catalyst. Increasing the active metal dispersion will increase the number of active sites, which will reduce residence times and total catalyst mass necessary for this process. Understanding the active sites of the catalyst will allow for more intelligent catalyst design, hopefully reducing activation energies and reducing heating costs. Exploration of a bimetallic Pt or Pd catalyst with a transition metal catalyst may be of interest. Darbha et al. (Janampelli & Darbha, 2018) have shown that promotion of hydrodeoxygenation by Pt/Alumina catalysts is improved with the addition of  $\text{MoO}_x/\text{Al}_2\text{O}_3$ . It should be explored whether decarboxylation can be performed without  $\text{H}_2$  gas with this catalyst. Additional studies using glycerol or ethanol as in situ sources of  $\text{H}_2$  may help reduce temperature requirements needed for the process.

More parametric studies must be conducted with the  $\text{MoO}_x/\text{Al}_2\text{O}_3$  catalyst in different solvents. It was shown that toluene has higher activities than water with both stearic and oleic acid. Oleic acid processed without a catalyst showed better activities than water as well. The addition of ethanol and glycerol was shown to increase the degree of decarboxylation of stearic acid at lower temperatures. It should be explored whether this phenomenon can occur without water, both in a hydrocarbon solvent or no solvent systems. The goal should be to decrease the necessary reaction temperature.

Real-world feeds such as corn distiller's oil (CDO) will contain significant unsaturated fatty acids and this quality contributes to coking and other undesired reaction pathways. However, fully saturated fatty acids do not readily undergo decarboxylation and the presence of at least 10 % unsaturated fatty acids increases the total decarboxylation of the saturated fatty acids. The exploration of real-world feed pre-processing should be investigated as to the optimal amount of glycerol, saturated fatty acids, and unsaturated fatty acids that will lead to the best decarboxylation, liquid yields, and least amount of solids deposition.

The reaction mechanism of the decarboxylation of fatty acids via the  $\text{MoO}_x$  catalyst should be explored. Acid sites are thought to be the catalyst active sites. The regenerated catalyst showed much lower acidity than the fresh catalyst, and still had comparable degrees of decarboxylation. More studies should be performed with the regenerated catalyst to evaluate how many times that catalyst can be regenerated and product quality must be analyzed to determine whether a different reaction mechanism occurs for the regenerated catalyst.

Finally, the study on the in-situ saturation of fatty acids in subcritical water should be expanded. GC-FID must be performed on the products to determine whether cracking is occurring instead of saturation. More parametric studies must be performed to elucidate the impact of temperature, residence time, and glycerol content on reaction rates.



## Appendix A

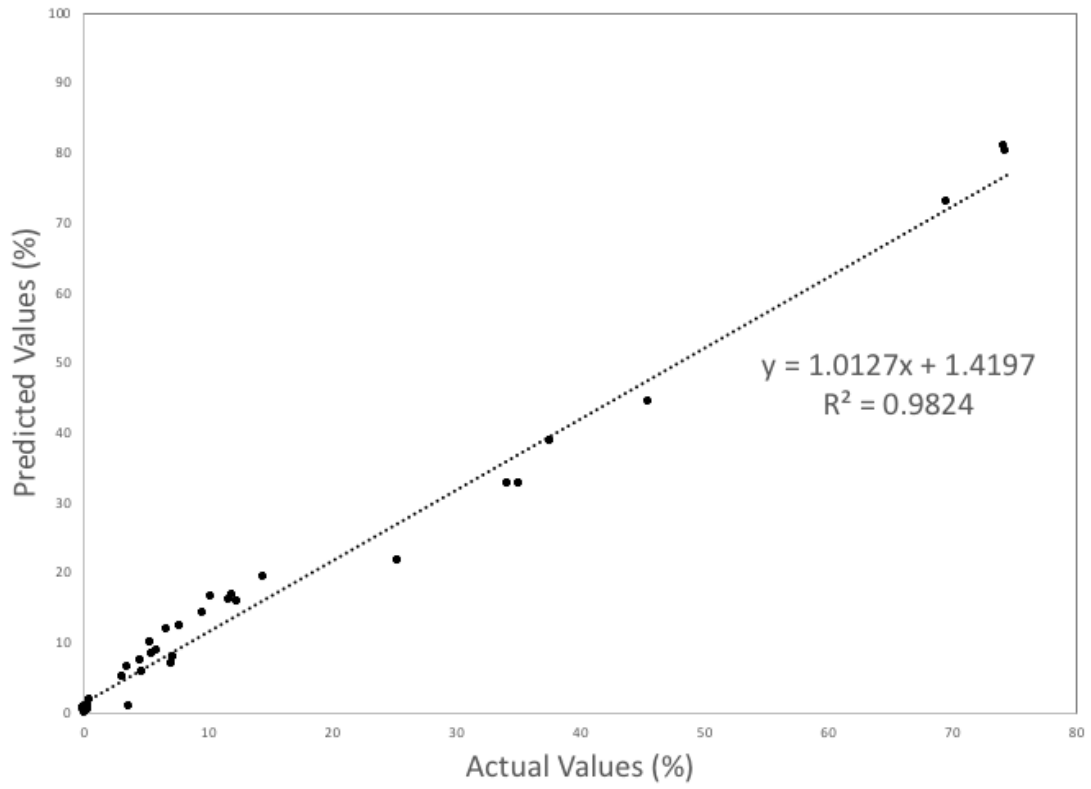


Figure A1 1: Predicted values by FTIR method vs Actual values by acid Value Titration

Table A.5.1 Stearic acid feed processed at 390 °C with a 3.5 h residence time, product quantities over time

Time	Heptadecane %	C <sub>7</sub> to C <sub>9</sub> %	C <sub>9</sub> to C <sub>10</sub> %	C <sub>10</sub> to C <sub>12</sub> %	C <sub>12</sub> to C <sub>14</sub> %	C <sub>14</sub> to C <sub>16</sub> %	C <sub>16</sub> to C <sub>17</sub> %	C <sub>17</sub> to C <sub>18</sub> %	C <sub>18</sub> to C <sub>19</sub> %	C <sub>19</sub> to C <sub>20</sub> %	C <sub>20</sub> to C <sub>22</sub> %	C <sub>22</sub> to C <sub>24</sub> %
3 h	68.55	0.76	0.36	0.32	1.08	5.57	8.56	5.44	5.39	1.52	0.63	1.57
Std. Dev	3.07	0.05	0.15	0.15	0.12	0.35	0.58	1.37	0.60	0.31	0.51	1.12
4 h	60.90	0.65	0.38	0.34	1.38	5.51	8.85	6.01	5.97	2.51	2.35	3.91
Std. Dev	3.08	0.10	0.03	0.15	0.13	0.01	0.65	0.26	0.14	0.04	1.30	0.92
5 h	68.24	0.77	0.58	0.55	2.13	4.78	9.53	4.90	5.18	1.62	0.97	0.00
Std. Dev	0.93	0.11	0.32	0.28	0.05	0.05	0.59	0.21	0.08	0.31	0.46	0.00
6 h	61.35	0.83	0.53	0.54	1.33	5.52	10.50	6.40	5.31	2.27	1.78	3.32
Std. Dev	3.30	0.13	0.11	0.08	0.37	0.40	0.37	0.20	0.14	0.19	1.46	1.61
7 h	60.34	0.89	0.41	0.52	1.76	6.31	12.11	5.94	5.36	2.07	1.02	2.89
Std. Dev	2.36	0.06	0.04	0.12	0.23	0.21	1.13	0.63	0.48	0.39	0.60	1.66

8 h	54.23	1.95	1.02	1.32	1.91	6.54	11.50	6.31	5.47	2.28	2.67	4.35
Std. Dev	4.85	0.22	0.81	0.50	0.24	0.85	0.71	0.38	0.37	0.38	1.31	2.29
9 h	56.12	2.13	1.32	1.82	1.90	5.74	9.64	5.93	5.83	2.43	1.77	4.92
Std. Dev	3.04	0.36	0.71	0.19	0.17	0.54	0.19	0.21	0.23	0.19	1.29	1.26
10 h	46.14	4.45	1.51	2.38	2.58	7.66	5.61	5.87	5.17	4.46	6.22	6.97
Std. Dev	0.59	0.09	0.05	0.43	0.46	0.36	0.84	0.70	0.49	0.36	2.16	0.75
11 h	43.21	3.80	2.63	1.95	2.33	5.97	7.20	9.07	7.77	4.19	4.38	6.83
Std. Dev	3.57	0.14	0.13	0.51	0.13	0.73	0.15	1.51	0.31	0.56	1.57	0.91

Table A.5.2 Stearic acid feed processed at 390 °C with 10 % glycerol and a 3.5 h residence time, product quantities over time

Time	Heptadecane %	C7 to C9 %	C9 to C10 %	C10 to C12 %	C12 to C14 %	C14 to C16 %	C16 to C17 %	C17 to C18 %	C18 to C19 %	C19 to C20 %	C20 to C22 %	C22 to C24 %
4 h	65.46	2.49	1.13	1.35	1.65	4.56	9.4	4.84	3.54	1.48	1.72	2.37
Std. Dev	2.6	0.29	0.67	0.07	0.4	0.13	0.89	0.21	0.33	0.37	1.27	1.13
5 h	59.85	2.49	0.9	1.45	1.8	6.12	8.31	6.78	6.17	2.29	1.27	2.57
Std. Dev	2.82	0.34	0.44	0.27	0.18	0.1	0.53	0.37	0.03	0.2	0.81	1.13
7 h	62.47	1.41	0.18	0.83	1.68	6.55	9.78	6.5	7.18	2	0.72	0.7
Std. Dev	1.31	0.05	0.24	0.14	0.02	0.95	0.6	0.48	0.33	0.17	0.11	0.22
8 h	55.75	1.95	0.56	1.19	1.74	7.17	9.88	6.24	7.28	2.74	2.02	3.48
Std. Dev	2.68	0.32	0.03	0.28	0.49	0.73	0.72	0.27	0.25	0.1	0.96	0.77
9 h	50.19	2.69	1.38	1.8	1.78	6.26	10.1	6.92	8.06	2.7	3.39	4.72
Std. Dev	0.13	0.25	0.39	0.17	0.17	0.2	0.79	0.36	0.04	0.33	0.56	0.14
11 h	40.78	3.16	2.28	1.72	1.79	6.43	8.83	10.69	10.13	3.73	3.97	6.48

Std. Dev	0.57	0.48	1.1	0.4	0.21	0.18	0.5	0.37	0.54	0.13	0.78	0.59
13 h	36.42	4.31	2.8	2.51	2.46	6.95	7.7	10.89	8.91	4.04	5.32	7.69
Std. Dev	1.46	0.57	0.85	0.21	0.57	0.77	0.38	0.64	0.53	0.18	1.65	1.03

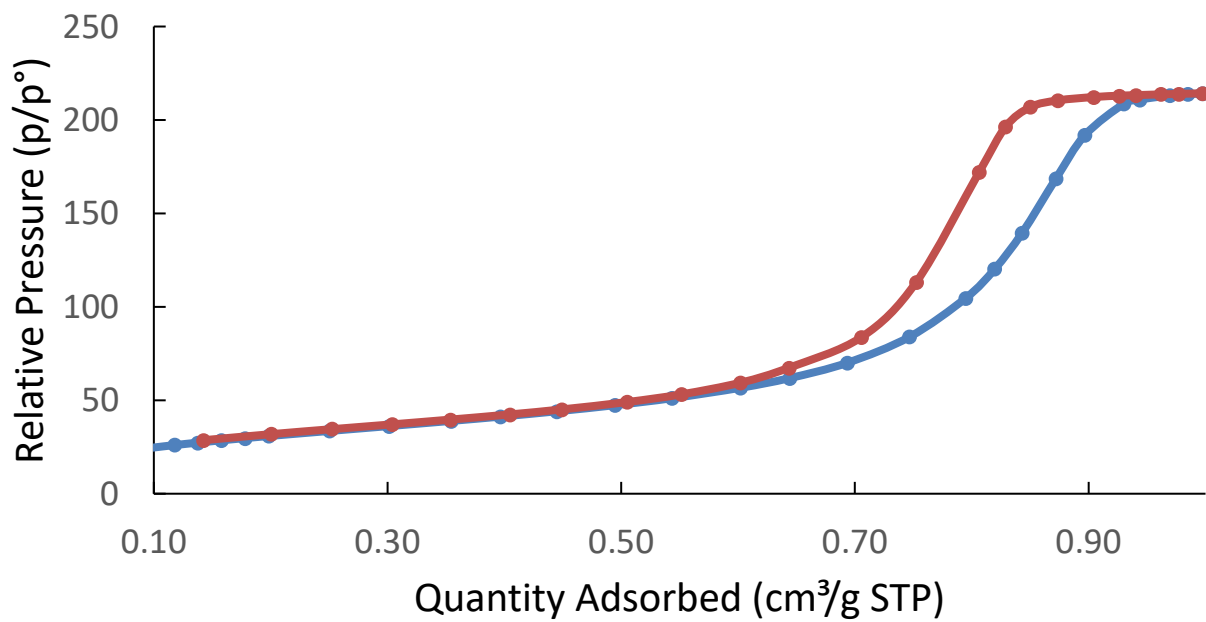


Figure A1 2: Example BET result of a spent catalyst. The blue line represents the absorption isotherm, and the red line the desorption

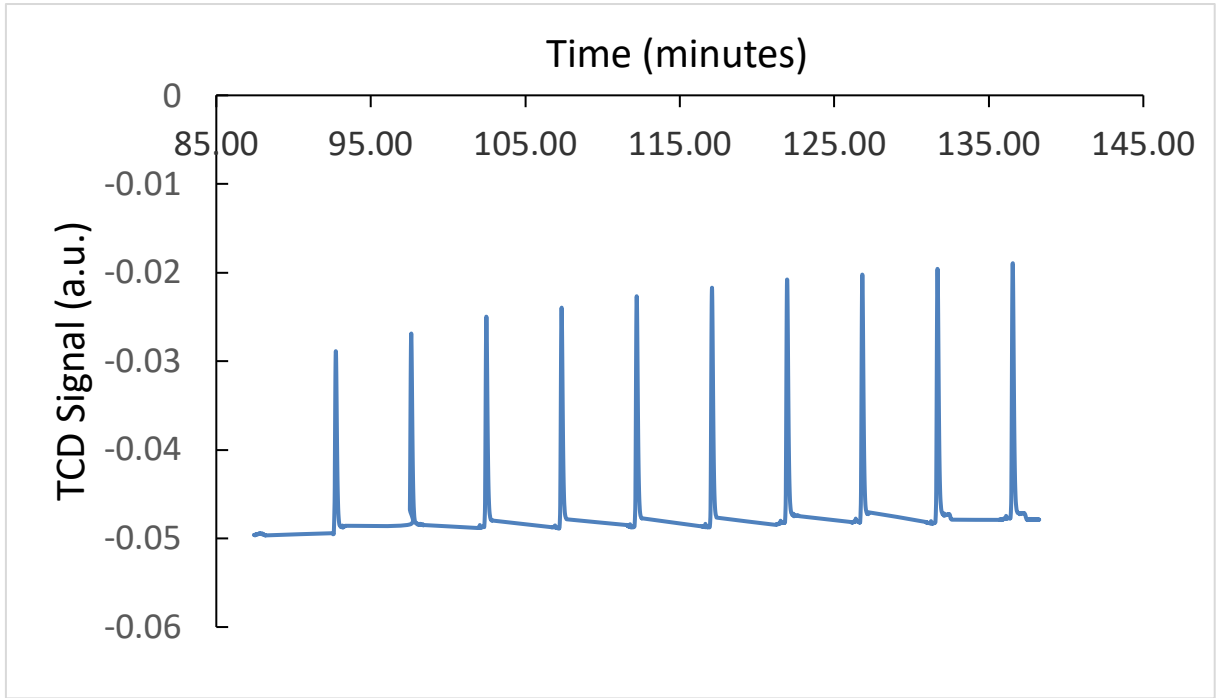


Figure A1 3: O<sub>2</sub> pulse chemisorption result for fresh MoO<sub>x</sub> catalyst.

## Curriculum Vitae

**Name:** Shaun Fraser

**Post-secondary Education and Degrees:** University of Waterloo  
Waterloo, Ontario, Canada  
2012-2017 Hon. B.Sc

The University of Western Ontario  
London, Ontario, Canada  
2018-2020 M.E.Sc

**Honours and Awards:** Waterloo Merit Scholarship  
2012

**Related Work Experience**

Applications Scientist  
Tornado Spectral Systems  
2017-2018

Teaching Assistant for courses:  
CBE 4417 PRINCIPLES OF HETEROGENEOUS CATALYSIS,  
CBE 9190 ADVANCED STATISTICAL PROCESS CONTROL,  
ENGSCI 9501 BUSINESS FOR ENGINEERS  
The University of Western Ontario  
2018-2020

Research Technician  
Tornado Spectral Systems  
2016

Biology Research Assistant  
Public Health Agency of Canada  
2014

**Publications:**